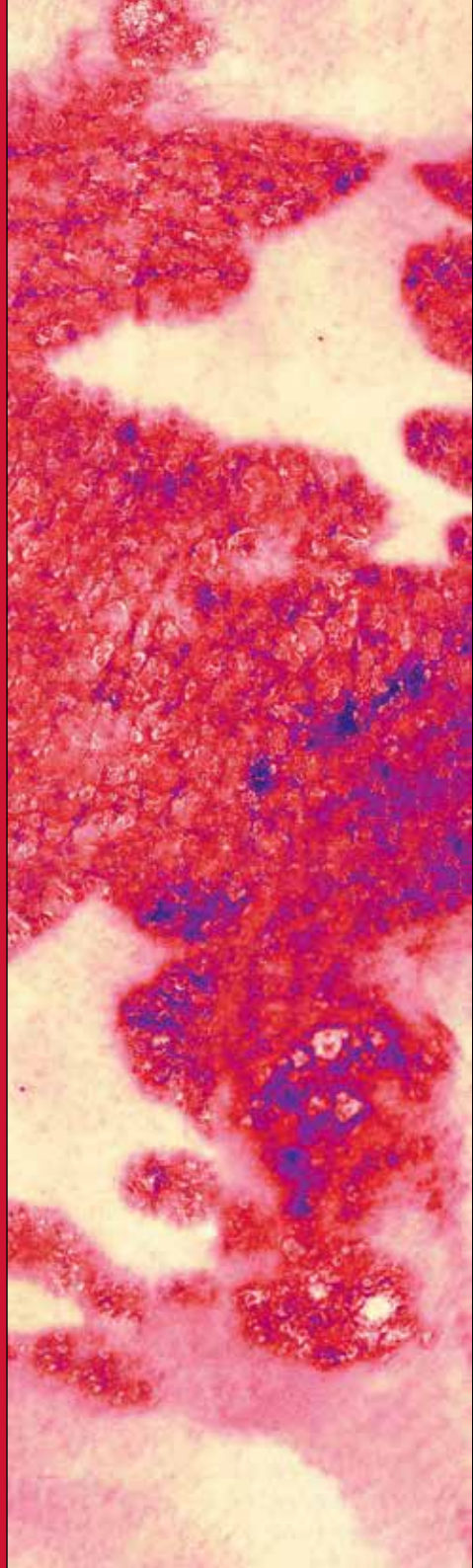


NON-INVASIVE  
BIOMARKERS FOR  
INFLAMMATORY  
SKIN DISEASES:  
TOWARDS SYSTEMS  
DERMATOLOGY

JANNIK ROUSEL



## GLOSSARY

*Some recurring terms are explained here so that they can be quickly looked up as they pass by.*

**Atopic dermatitis:** commonly called eczema and also referred to as atopic eczema.

**Biologics:** therapeutic antibodies with a specific mechanism of action.

**Biomarker:** an indicator of a biological process from which the condition of an individual can (partly) be derived.

**Biosimilars:** cheaper copies of drugs that are currently on the market.

**Ceramide composition:** the overall ratio between different classes of ceramide.

**Ceramides:** a group of molecules that make up a large part of the lipids in the stratum corneum. The specific classes of ceramides are often named with a letter code such as “Cer[NS]”.

**Early phase clinical trials:** the first steps in investigating the safety and efficacy of new drugs in small groups of healthy volunteers or patients.

**Endotypes:** different types of the same disease characterized by differences in pathophysiology.

**Guselkumab:** an effective treatment for psoriasis.

**Human skin equivalents:** pieces of skin artificially grown in the laboratory.

**Malassezia:** a yeast that occurs on the oily areas of the skin and contributes to the disease Seborrheic Dermatitis.

**Microbiome:** all microorganisms such as yeasts and bacteria that live together in one place.

**Multimodal:** an approach from different aspects.

*(Glossary continues on the inside of the back cover)*

# NON-INVASIVE BIOMARKERS FOR INFLAMMATORY SKIN DISEASES: TOWARDS SYSTEMS DERMATOLOGY

Proefschrift

ter verkrijging van  
de graad van doctor aan de Universiteit Leiden,  
op gezag van rector magnificus prof. dr. ir. H. Bijl,  
volgens besluit van het college voor promoties  
te verdedigen op donderdag 24 oktober 2024  
klokke 14.30 uur

door  
Jannik Rousel



**COPYRIGHT** - 2024 by Jannik Rousel. This thesis and associated publications are licensed under Creative Commons Attribution 4.0 International, unless otherwise noted.

**DESIGN** - Caroline de Lint, Den Haag  
**COVER IMAGE** - Katie Kimber, Lausanne

*Publication of this thesis was financially supported by the Foundation Centre for Human Drug Research (CHDR), Leiden, the Netherlands.*

**Promotores:**

Prof.dr. R. Rissmann  
Prof.dr. J.A. Bouwstra

**Copromotor:**

Dr. M.B.A. van Doorn (*Erasmus MC*)

**Promotiecommissie:**

Prof.dr. H. Irth  
Prof.dr. E.C.M. de Lange  
Prof.dr. I. Bot  
Prof.dr. M.S. de Bruin-Weller (*UMC Utrecht*)  
Prof.dr. E.M.G.J. de Jong (*Radboud UMC*)  
Prof.dr. S. Weidinger (*University Hospital Schleswig-Holstein*)

**17 CHAPTER 1** Introduction

**SECTION 1 MULTIMODAL CHARACTERIZATION OF THE SKIN OF SEBORRHEIC DERMATITIS PATIENTS**

**25 CHAPTER 2** Lesional skin of seborrheic dermatitis patients is characterized by skin barrier dysfunction and correlating alterations in the stratum corneum ceramide composition

**55 CHAPTER 3** Treatment with the topical antimicrobial peptide omiganan in mild-to-moderate facial seborrheic dermatitis versus ketoconazole and placebo: results of a randomized controlled proof-of-concept trial

**SECTION 2 ENABLING THE POTENTIAL OF MILD PSORIASIS PATIENTS FOR CLINICAL RESEARCH USING A MULTIMODAL IMAGING APPROACH**

**81 CHAPTER 4** Guselkumab induction therapy demonstrates long-lasting efficacy in patients with mild psoriasis: results from a randomized, placebo-controlled exploratory clinical trial

**95 CHAPTER 5** Mild psoriasis patients are suitable alternatives for moderate-to-severe psoriasis patients in early-phase clinical trials: results of a randomized controlled trial with guselkumab

**SECTION 3 THE STRATUM CORNEUM CERAMIDE PROFILE AS BIOMARKER AND THERAPEUTIC TARGET**

**131 CHAPTER 6** Similar alterations of the stratum corneum ceramide profile in atopic dermatitis, psoriasis, ichthyosis and other dermatoses, results from a systematic review and meta-analysis

**161 CHAPTER 7** Guselkumab treatment alleviates barrier dysfunction and normalizes the altered stratum corneum ceramide profile in lesional psoriasis: results of a randomized, placebo-controlled trial

**195 CHAPTER 8** Improved organotypic skin model with reduced quantity of monounsaturated ceramides by inhibiting stearyl-coa desaturase-1

**227 CHAPTER 9** Summary and perspectives

**APPENDICES**

**242** Nederlandse samenvatting

**265** Curriculum vitae

**266** List of publications

CHAPTER 1

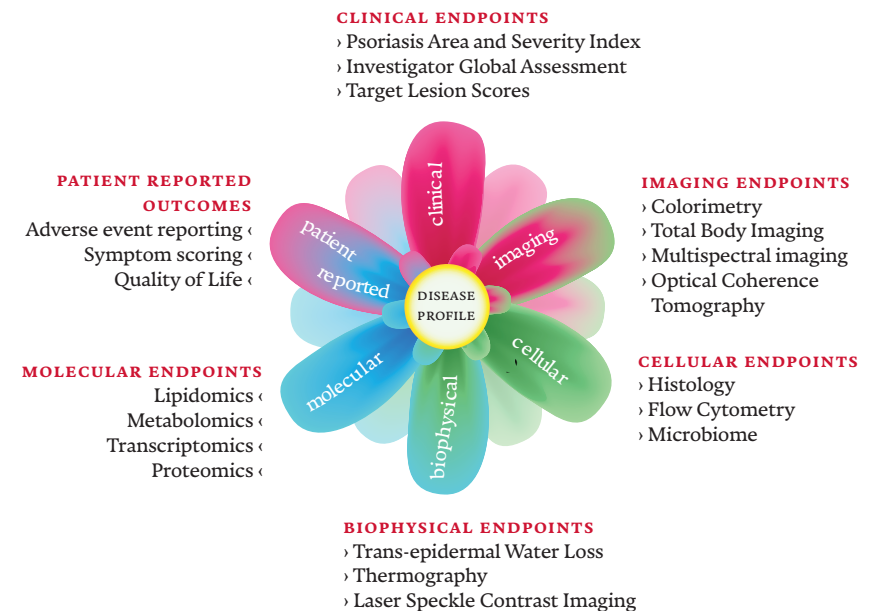
INTRODUCTION

Chronic inflammatory skin diseases are mediated by aberrant activation of the immune system and comprises diseases such as psoriasis, seborrheic dermatitis, atopic dermatitis, acne vulgaris, cutaneous lupus erythematosus and chronic urticaria.<sup>1</sup> Besides the evident involvement of the immune system, a variety of different factors seem to contribute to these diseases such as microbial dysbiosis, skin barrier dysfunction, genetics and the exposome.<sup>2-4</sup> Despite a limited mortality rate, inflammatory skin diseases constitute a considerable burden with over 20% of the world's population affected by atopic dermatitis, acne vulgaris, alopecia, psoriasis, rosacea or vitiligo. This amounts to a total of 18 million years lived with disability in Europe alone.<sup>5,6</sup> These chronic and relapsing disorders are associated with persistent physical burden from sore, itchy or bleeding skin which, combined with the psychological and social burden relating the appearance of lesions, converge into a major impact on the daily life of affected patients.<sup>7</sup>

Even though the management of most inflammatory skin diseases has improved considerably in the last decades, a medical need still remains as current treatments are sometimes insufficiently effective or associated with adverse effect. Therefore, substantial treatment dissatisfaction persists which not only impacts patients, but might also increase the (financial) strain on the healthcare system and therefore society in general.<sup>8</sup> To overcome this, new drugs are continuously being developed and evaluated in clinical trials. Unfortunately, drug development is associated with a high rate of attrition among drug candidates that might be partly attributed to a lack of rational and informed decision making.<sup>9,10</sup> Additionally, research in inflammatory skin diseases has been shown to be underfunded which further complicates the development of new drugs.<sup>11</sup> In order to boost the success rate of candidates entering the clinical stage of development and reduce the associated costs, this thesis entails the evaluation and application of non-invasive multimodal technology that enables rational decision making during early-stage clinical development. By first characterizing patients extensively through different domains, a holistic view can be obtained that integrates important modalities for disease such as the patient's personal predisposition, phenotype, microbiome and immune profile, and links this to disease (figure 1). Thereafter, this deep phenotyping approach can be applied to clinical trials where the effect of drugs and drug candidates can be characterized in detail, leading to clues on the mechanisms behind their clinical response or non-response.<sup>10</sup> In clinical practice, this systems dermatology approach

might support precision medicine where the patient's individual phenotype, or determination of the disease endotype, rather than a general treatment plan informs clinicians in selecting the most suitable treatment.<sup>12,13</sup>

**Figure 1** Schematic depiction of the multiple modalities that can be exploited in a systems dermatology approach. The different modalities are accompanied by a listing of assessments that can facilitate the deep-phenotyping approach and determination of disease endotypes.



## CURRENT PRACTICE IN CLINICAL DERMATOLOGY

In general clinical practice patients are prescribed different treatments based on the severity of disease, efficacy of their current treatment or the occurrence of adverse events during treatment.<sup>14</sup> Classification of disease severity in dermatology is often based on clinical scoring systems that evaluate the intensity and extent of symptoms throughout the body.<sup>15</sup> Depending on these scores, patients are classified as having mild, moderate or severe disease.<sup>16,17</sup> The mainstay of treatment for mild patients with limited skin involvement generally entails emollients in combination with corticosteroids or other

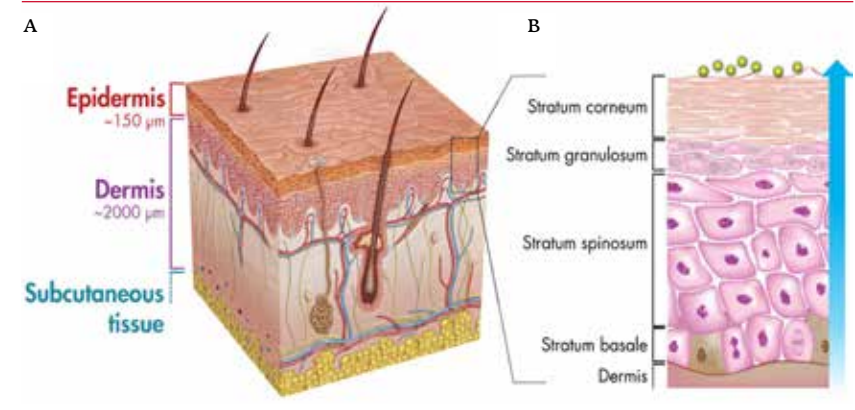
immunosuppressive agents such as calcineurin inhibitors that can be topically applied.<sup>18</sup> Even though general practitioners can prescribe more potent alternatives when topical treatment is insufficiently effective, long-term and continuous use of topical corticosteroids is contraindicated due to side effects such as skin atrophy and the development of striae as well as adverse effects relating to systemic exposure.<sup>18,19</sup> For more severe cases, when topical treatment results in insufficient response or upon the development of tachyphylaxis (resistance to therapy after prolonged exposure), oral immunosuppressants such as methotrexate and cyclosporin constitute effective alternatives. Nevertheless, the use of these general immunosuppressants is also limited by adverse reactions that might necessitate the cessation of therapy even when proven effective.<sup>20,21</sup> For atopic dermatitis and plaque psoriasis, biologic therapies have recently become available which demonstrate high efficacy with a favourable safety profile.<sup>22,23</sup> However, cessation of treatment still leads to relapse indicating that patients will remain dependent on chronic medication use.<sup>24,25</sup> Even though biologic therapy has demonstrated the ability to effectively treat atopic dermatitis and psoriasis, a medical need persists outside these two indications and in patients that do neither qualify for biologic or systemic therapy, nor respond to topical treatment, nor respond adequately to biologics.<sup>26,27</sup> Therefore, the development of new therapies throughout dermatology, including atopic dermatitis and psoriasis, remains warranted.

### THE HUMAN SKIN IN HEALTH AND INFLAMMATORY DISEASE

The skin is the organ at the interface between the body and external environment. It protects the body from external insults, pathogens, chemicals and radiation but also limits water loss and maintains homeostasis.<sup>28</sup> From within, the skin can be divided in the subcutaneous, dermal and epidermal compartments. Subcutaneous tissue contains mostly fat and connective tissue (figure 2). It underlies the highly perfused dermis where sebaceous glands, hair follicles and nerve endings are spread throughout. This layer functions as a scaffold for the more superficial epidermis. The epidermis contains a basal layer of proliferating keratinocytes. After keratinocytes escape from this layer, they undergo terminal differentiation in a process called cornification during which they migrate to the skin surface and transform into highly crosslinked, impermeable and flattened corneocytes.<sup>29</sup> Ultimately, these corneocytes form a thin layer at the skin surface called the stratum corneum

where cells are gradually released from the skin surface. Simultaneously, their loss is continuously compensated with newly differentiated keratinocytes at the interface between the viable epidermis and stratum corneum. The stratum corneum is responsible for much of the intact skin barrier function.<sup>28,29</sup>

**Figure 2** Schematic overview of the morphology of the skin (A) and a more detailed overview of the healthy epidermis (B). Blue arrow represents the inside-out barrier and direction of the trans-epidermal water loss. Adapted from van Smeden *et al.* (2013).



Representing the physical barrier to the outside world, the epidermis is one of the first points of contact where infectious agents can be tackled before spreading throughout the body. Many immune cells reside in and below the viable epidermis where they, in combination with keratinocytes, react to the presence of exogenous entities. Upon activation, immune cells and keratinocytes can readily produce pro-inflammatory cytokines and chemokines which instigate an immune cascade that prompt the recruitment of additional peripheral immune cells to the skin.<sup>30</sup> This contributes to the effective clearance of pathogens from the skin and prevents infection.

In chronic inflammatory skin diseases, this process has become deregulated and immune reactions are aberrantly evoked. Apart from exacerbating the initial aberrant response, the presence of pro-inflammatory mediators can result in changes to normal skin functioning such as increases in blood-flow and associated erythema, epidermal hyperproliferation and epidermal acanthosis leading to the formation of cutaneous lesions.<sup>31</sup> Although

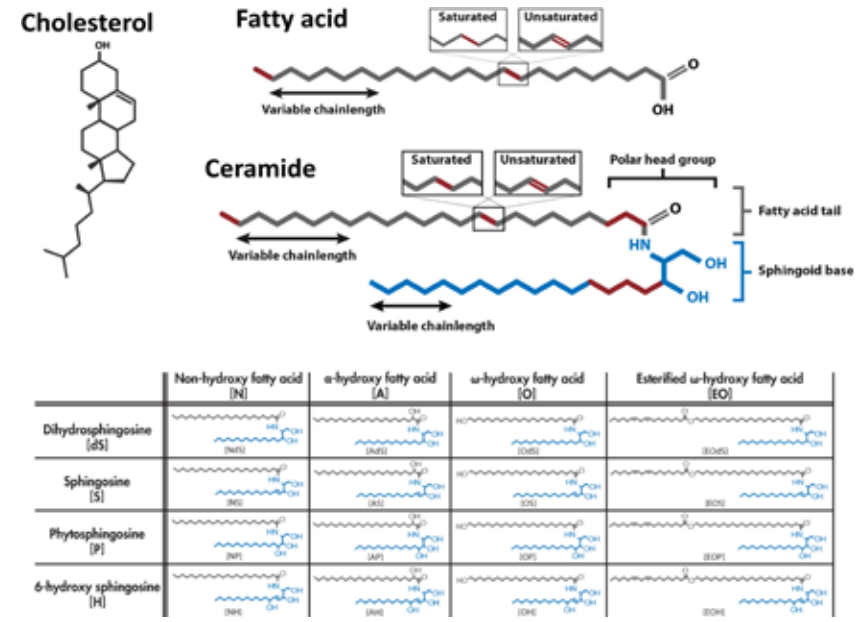
the triggers responsible for these reactions have been identified in certain diseases, such as metals in contact dermatitis or heat in inducible chronic urticaria, they remain unknown for many other indications.<sup>32-34</sup> Taking atopic dermatitis and psoriasis as two examples of inflammatory skin diseases, it becomes evident that these are associated with different genetic backgrounds and driven by different immune axis. In psoriasis, a dominant role for the T-helper 17 (TH17) cell has been established. In contrast, atopic dermatitis appears to be a TH2 dominant disease.<sup>35</sup> Elucidation of these key drivers behind the aberrant immune response have allowed for the development of targeted biologic therapies that are able to interfere with selected processes in the immune system and have demonstrated to be highly efficacious with a favourable safety profile.<sup>36,37</sup> However, the well-defined mode of action of biologics prevents their use in indications characterized by different immunological backgrounds.

### THE SKIN BARRIER AS AN ESSENTIAL PART OF LIFE

Although the immune system in the skin represents an effective mechanism to prevent infections from penetrating deeper into the body, the primary line of defence remains the skin's passive barrier function. This barrier function is heavily dependent on the stratum corneum lipid matrix.<sup>38</sup> During cornification, a vast amount of lipids is extruded to the extracellular space where they form tight and organized layers around the corneocytes. This matrix is of high importance to the barrier function, as it represents the only continuous pathway through the intact skin into the body.<sup>39</sup>

This lipid matrix is mainly comprised of cholesterol, fatty acids and ceramides in a roughly equimolar ratio (figure 3).<sup>38</sup> Fatty acids and ceramides form two heterogenous groups of lipids. Fatty acids consist of a single carbon chain which can vary in carbon chain length and degree of unsaturation. Ceramides are more complex and are composed of a fatty acid tail linked to a sphingoid base. Similar to fatty acids, ceramides demonstrate variation in carbon chain length and unsaturation but they are subjected to further chemical modifications after coupling of the fatty acid and sphingoid moiety, resulting in differences in their headgroup architecture.<sup>40</sup> Taken together, this allows for their classification in various subclasses of which 25 have been identified in human stratum corneum.<sup>41</sup> Of importance, the ceramide fraction CER[EO], with an additional fatty acid terminally bound to the fatty acid tail, can be covalently attached to corneocytes, anchoring the lipid matrix in place.<sup>42</sup>

**Figure 3** Overview of the structures of cholesterol, fatty acids and ceramides with possible alterations highlighted. Additionally, an overview of the structural variety in ceramides subclasses is shown. Only those discussed in this thesis are shown. Note that in this table, variation in carbon chain length and unsaturation are not shown. Adapted from Janssens *et al.* (2012)



The permeation of substances through the intact skin barrier is related to the composition and concurrent organization of the stratum corneum lipid matrix.<sup>43</sup> The skin barrier function can be assessed by monitoring the amount of water that evaporates through the skin, the trans-epidermal water loss (TEWL) or by monitoring the passive diffusion of more lipophilic compounds through the stratum corneum.<sup>44,45</sup> Synthetic models of the stratum corneum lipid matrix have shown that altering various lipid properties affects permeation. Indeed, incorporation of more unsaturated lipids, decreased carbon chain lengths and disproportionate fractions of subclass CER[NS] resulted in an altered organization and a poorer lipid barrier function.<sup>46-51</sup> This is substantiated by the barrier impairment observed in more complex *in vitro* cultured human skin equivalents. These fully differentiated models are derived from isolated human skin cells and bear a high resemblance to native



skin but demonstrate an impaired barrier function with concomitant alterations in the stratum corneum lipid profile and organization; an increase in short-chain fatty acids, a skewed ceramide profile and an overall more hexagonal, and therefore less compact, lipid organisation.<sup>44,52-54</sup> This reaffirms the dependency of the skin barrier function on the stratum corneum lipid composition.

In inflammatory diseases, the cutaneous barrier function is impacted. Skin barrier impairment has been observed in atopic dermatitis, seborrheic dermatitis, dandruff, ichthyosis and psoriasis patients.<sup>55-59</sup> For atopic dermatitis and psoriasis, this has been linked directly to changes in ceramide composition.<sup>60-62</sup> However, studies focusing solely on the lipid composition in ichthyosis, palmoplantar keratoderma and acne that did not directly link compositional changes to the impairment of barrier function have shown the ceramide composition is altered as well.<sup>63-67</sup> In-depth profiling of the ceramide profile in atopic dermatitis have shown that lesional skin was marked by a decrease in total fatty acids and ceramides, and compositional changes therein amounting to a lower average fatty acid and ceramide total chain length, increased unsaturation, increased CER[S] abundances and decreased CER[P] and CER[EO] abundances.<sup>60,68-71</sup> As with both synthetic lipid models and *in vitro* human skin equivalents, the organization in lesional skin was less densely organized.<sup>72,73</sup> Together, these observations have provided a rationale for skin barrier impairment resulting from aberrant lipid synthesis in the pathophysiology of atopic dermatitis, psoriasis and possibly other diseases.

### THE COMPLEXITY OF INFLAMMATORY SKIN DISEASES

Although both the immune system by name and the skin barrier by function are main pillars of the pathophysiology of inflammatory skin diseases, these conditions cannot be solely explained by these two concepts. Rather, it seems that the interplay between different modalities is crucial for their development. Intrinsically, there seems to be a genetic predisposition for these diseases which can be exemplified by a high prevalence of mutations in the gene for filaggrin in atopic dermatitis and an increased risk for psoriasis in children from psoriasis patients.<sup>74-76</sup> However, other individual factors seem to aggravate psoriasis, with stressors such as smoking, excessive drinking, being overweight and stress triggering disease. External factors such as air pollution have also been implicated in the development of inflammatory

skin diseases and its severity can be influenced by seasonal weather.<sup>77-80</sup> Furthermore, dysbiosis of the microbiome has been attributed a major role in atopic dermatitis and seborrheic dermatitis where *Staphylococcus aureus* and *Malassezia* species are regarded as possible drivers of disease, respectively.<sup>81,82</sup> Strikingly, many of these prementioned factors such as the exposome and presence of *Malassezia*, are not solely restricted to patients making it harder to establish causality and highlighting the likely interdependency of multiple factors in disease pathophysiology.<sup>83</sup>

### METHODOLOGY TO ENABLE A HOLISTIC UNDERSTANDING OF DISEASE

A multi-faceted disease might be best characterized by a multimodal approach. Many studies have focused on a single aspect of disease such as the immune system, barrier function or microbiome. However, by focusing on only a single aspect from a network of different mechanism the point of focus might shift away from aspects that are not actively being investigated and guide the field in a different direction. Ideally, one is able to understand all aspects of disease and integrate them into a holistic view.<sup>10</sup>

A wide array of tools has become available to investigate important hallmarks of disease. Obviously, dermatology can benefit immensely from the accessibility and visibility of lesions; making imaging techniques a highly relevant output parameter. Although (standardized) 2D-photography is readily used to produce images with high resemblance to its clinical phenotype the possibilities range beyond this with, examples given, multispectral imaging that obtains images uses multiple wavelengths to better reflect specific properties such as erythema and pigmentation, Laser Speckle Contrast Imaging that can actively measure the superficial perfusion of the skin and even Optical Coherence Tomography which provides the user with an optical biopsy enabling the assessment of the subcutaneous morphology in a non-invasive manner.<sup>84-87</sup> Skin barrier function can be effectively monitored by TEWL, and molecularly substantiated by profiling of the stratum corneum lipid composition.<sup>88</sup> Subsequently, techniques such as metabolomics, transcriptomics, proteomics and profiling of circulating and tissue-resident immune cells may be performed on blood and tissue samples to identify which processes might underly the presence of lesions and barrier dysfunction.<sup>89</sup> Concurrently, genetics and the external exposome, which might be retrieved from databases or a simple swab of the skin in regard to the microbiome, can

all be integrated and provide a holistic understanding of disease. This might offer novel insights that could lead to the discovery of new targets and advance the field of personal medicine in which patients may be stratified into different endotypes, and consequently treatment algorithms, depending on which modality contributes most to disease.<sup>13,90</sup>

## **ADOPTION OF MULTIMODAL ENDPOINTS IN CLINICAL STUDIES**

Besides providing a basis for pathogenesis, these multimodal endpoints can be adopted as biomarkers in clinical trials in order to better understand the effect of novel treatment. Briefly, biomarkers can be defined as characteristics of a biological process through which the state of an individual might be derived.<sup>91</sup> This can range from physiological properties such as heart rate to more subjective measures such as sleep quality. In a trial setting, these might be applied to follow the time course of treatment and thereby quantify treatment responses.

In both clinical practice and drug development in dermatology, the gold standard remains physician-performed clinical scoring. This resulted in widely adopted and standardized physician-performed scoring tools such as the 5- or 6-point physician global assessment (PGA) that can be applied to most conditions and more extensive scoring systems tailored to specific diseases such as the area and severity indexes for Psoriasis, Eczema or Seborrheic Dermatitis (PASI, EASI, SDASI, respectively) and SCORing Atopic Dermatitis (SCORAD), of which the latter also includes a patient-reported component for itch and sleep loss.<sup>15,92,93</sup> However, clinical scoring can be subject to intra- and inter-rater variability, subjectivity and insensitivity.<sup>94,95</sup> Although clinical scoring has proven itself as suitable measures to monitor disease severity in clinical practice and large patient cohorts, these shortcomings might impact their applicability to smaller early-phase clinical trials and warrant a more objective data-rich approach. Biomarkers might present suitable alternatives but should meet certain criteria to deem them fit-for-purpose:<sup>96,97</sup>

- 1 They should respond to (effective) interventions,
- 2 they should be able to consistently indicate a response regardless of their mode-of-action,
- 3 there should be a dose-response relationship,
- 4 there should be a plausible relation to the mechanism of disease.

After the selection of a candidate biomarker, its technical validity should be explored to assess its accuracy, precision and ability to differentiate patients from controls, or lesional skin from non-lesional skin. Thereafter, the biomarker can be validated for clinical use and correlated to existing and widely adopted clinical endpoints.<sup>98,99</sup> Of note, failure to correlate perfectly with traditional endpoints does not necessarily disqualify a biomarker for use as they might reflect different aspects of disease.<sup>99</sup> Instead, their integration into a more comprehensive readout might enhance the understanding of the treatment response to a higher extent. By doing so, a higher degree of confidence in the effect of an investigative treatment can be obtained that could boost its early-stage clinical development.

## **Outline of this thesis**

This thesis aims to establish the multimodal profiling of chronic inflammatory skin diseases for subsequent implementation in early-stage clinical research using seborrheic dermatitis and plaque psoriasis as two illustrative model diseases. This thesis' translational and clinical impact is exemplified through 3 sections. Firstly, a non-invasive deep-phenotyping approach is performed in seborrheic dermatitis and subsequently applied to a clinical trial. Secondly, a model trial in psoriasis is performed as a platform to explore and validate various biomarkers. Finally, section three describes and exemplifies the added value of stratum corneum ceramide profiling as objective biomarkers in clinical research.

### **SECTION 1 – MULTIMODAL CHARACTERIZATION OF THE SKIN OF SEBORRHEIC DERMATITIS PATIENTS.**

In here, a non-invasive deep-phenotyping study in seborrheic dermatitis is described and subsequently applied to a placebo and comparator controlled double-blind clinical trial.

**Chapter 2** describes how the lesional skin of patients with seborrheic dermatitis can be differentiated from their non-lesional skin using a multimodal approach. Comprehensive imaging, microbial profiling and skin barrier assessments are performed to show how these modalities contribute to the disease.

In **chapter 3**, the non-invasive and multimodal approach laid out in the previous chapter is applied to a trial in seborrheic dermatitis. Here, the

microbiome is targeted with the novel antimicrobial peptide omiganan and its efficacy and pharmacodynamic effects evaluated in a randomized, placebo- and comparator-controlled trial.

## **SECTION 2 – ENABLING THE POTENTIAL OF MILD PSORIASIS PATIENTS FOR CLINICAL RESEARCH USING A MULTIMODAL IMAGING APPROACH**

In this section, a deep-phenotyping approach is applied to a model trial in mild and moderate-to-severe plaque psoriasis. The use of novel multimodal methodology could be investigated after administration of guselkumab. A highly effective anti-interleukin (IL)-23 monoclonal antibody approved for moderate-to-severe psoriasis, to assure evident treatment effects.

This section begins with **chapter 4**, where the clinical effect of guselkumab in mild patients is presented. Besides characterizing the initial response of mild patients, the long-term effects of a short regimen of guselkumab are evaluated using a patient-centered approach.

**Chapter 5** explores the treatment response of mild psoriasis patients in more detail in an effort to establish this group of patients with a limited burden of disease as alternatives for the decreasing number of moderate-to-severe patients that are available for clinical trials in Western European countries. A multimodal imaging approach is employed to increase the confidence in traditional endpoints and enable a more thorough comparison of the response in mild compared to moderate-to-severe patients.

## **SECTION 3 – THE STRATUM CORNEUM CERAMIDE PROFILE AS BIOMARKER AND THERAPEUTIC TARGET**

The last section focusses on stratum corneum ceramide profiling and highlights its potential for use as a biomarker in clinical trials. Additionally, it shows how these abnormalities might be alleviated by targeting specific enzymes.

**Chapter 6** entails a systematic literature review and meta-analysis of stratum corneum ceramide profiles in disease. It aims to demonstrate how specific alterations in the ceramide profile are present throughout various dermatological conditions and might be exploited as a biomarker.

**Chapter 7** subsequently applies ceramide profiling in the aforementioned psoriasis trial as a useful non-invasive biomarker. In order to do so, it first characterizes the psoriatic ceramide profile in detail and contrasts this to the

ceramide profile of healthy volunteers after which markers of interest can be exploited in treatment monitoring.

Lastly, **chapter 8** highlights how epidermal lipid biosynthesis can be modulated in human skin equivalents by targeting key enzymes using small molecules. In here, stearyl-CoA desaturase-1 is inhibited in order to normalize the increased amount of monounsaturated fatty acids and ceramides that are present in these models, and has also been shown to be elevated in inflammatory skin diseases.

## REFERENCES

- 1 Ujiie, H. *et al.* Unmet Medical Needs in Chronic, Non-communicable Inflammatory Skin Diseases. *Front Med (Lausanne)* **9**, 875492 (2022).
- 2 Eyerich, S., Eyerich, K., Traidl-Hoffmann, C. & Biedermann, T. Cutaneous Barriers and Skin Immunity: Differentiating a Connected Network. *Trends Immunol* **39**, 315-327 (2018).
- 3 Passeron, T., Krutmann, J., Andersen, M. L., Katta, R. & Zouboulis, C. C. Clinical and biological impact of the exposome on the skin. *Journal of the European Academy of Dermatology and Venereology* **34**, 4-25 (2020).
- 4 De Stefano, G. M. & Christiano, A. M. The Genetics of Human Skin Disease. *Cold Spring Harb Perspect Med* **4**, (2014).
- 5 Vos, T. *et al.* Years lived with disability (YLDs) for 1160 sequelae of 289 diseases and injuries 1990-2010: a systematic analysis for the Global Burden of Disease Study 2010. *The Lancet* **380**, 2163-2196 (2012).
- 6 Richard, M. A. *et al.* Prevalence of most common skin diseases in Europe: a population-based study. *J Eur Acad Dermatol Venereol* **36**, 1088-1096 (2022).
- 7 Karimkhani, C. *et al.* Global Skin Disease Morbidity and Mortality: An Update From the Global Burden of Disease Study 2013. *JAMA Dermatol* **153**, 406-412 (2017).
- 8 Eicher, L. *et al.* A systematic review of factors influencing treatment adherence in chronic inflammatory skin disease - strategies for optimizing treatment outcome. *Journal of the European Academy of Dermatology and Venereology* **33**, 2253-2263 (2019).
- 9 Wong, C. H., Stah, K. W. & Lo, A. W. Estimation of clinical trial success rates and related parameters. *BioStatistics* **20**, 273-286 (2019).
- 10 Rissmann, R., Moerland, M. & van Doorn, M. B. A. Blueprint for mechanistic, data-rich early phase clinical pharmacology studies in dermatology. *Br J Clin Pharmacol* **86**, 1011 (2020).
- 11 Hagstrom, E. L. *et al.* Comparing cutaneous research funded by the US National Institutes of Health (NIH) with the US skin disease burden. *J Am Acad Dermatol* **73**, 383-391.e1 (2015).
- 12 Ahmed, Z. Precision medicine with multi-omics strategies, deep phenotyping, and predictive analysis. *Prog Mol Biol Transl Sci* **190**, 101-125 (2022).
- 13 Czarnowicki, T., He, H., Krueger, J. G. & Guttman-Yassky, E. Atopic dermatitis endotypes and implications for targeted therapeutics. *Journal of Allergy and Clinical Immunology* **143**, 1-11 (2019).
- 14 Kim, W. B., Jerome, D. & Yeung, J. Diagnosis and management of psoriasis. *Canadian Family Physician* **63**, 278 (2017).
- 15 Chakraborty, A. & Chakraborty, A. Disease severity scores in dermatology: An update of the various indices. *Indian J Dermatol Venereol Leprol* **0**, 1-15 (2023).
- 16 Strober, B. *et al.* Recategorization of psoriasis severity: Delphi consensus from the International Psoriasis Council. *J Am Acad Dermatol* **82**, 117-122 (2020).
- 17 Chopra, R. *et al.* Severity strata for Eczema Area and Severity Index (EASI), modified EASI, Scoring Atopic Dermatitis (SCORAD), objective SCORAD, Atopic Dermatitis Severity Index and body surface area in adolescents and adults with atopic dermatitis. *British Journal of Dermatology* **177**, 1316-1321 (2017).
- 18 Elmets, C. A. *et al.* Joint AAD-NPF Guidelines of care for the management and treatment of psoriasis with topical therapy and alternative medicine modalities for psoriasis severity measures. *J Am Acad Dermatol* **84**, 432-470 (2021).
- 19 Hengge, U. R., Ruzicka, T., Schwartz, R. A. & Cork, M. J. Adverse effects of topical glucocorticosteroids. *J Am Acad Dermatol* **54**, 1-15 (2006).
- 20 Menter, A. *et al.* Joint American Academy of Dermatology-National Psoriasis Foundation guidelines of care for the management of psoriasis with systemic nonbiologic therapies. *J Am Acad Dermatol* **82**, 1445-1486 (2020).
- 21 Drucker, A. M. *et al.* Systemic Immunomodulatory Treatments for Atopic Dermatitis: Update of a Living Systematic Review and Network Meta-analysis. *JAMA Dermatol* **158**, 523-532 (2022).
- 22 Sahni, V. N., Balogh, E. A., Strowd, L. C. & Feldman, S. R. The evolving atopic dermatitis management landscape. *Expert Opin Pharmacother* **23**, 517-526 (2022).
- 23 Sbidian, E. *et al.* Systemic pharmacological treatments for chronic plaque psoriasis: a network meta-analysis. *Cochrane Database of Systematic Reviews* **2022**, (2022).
- 24 Masson Regnault, M., Shourick, J., Jendoubi, F., Tauber, M. & Paul, C. Time to Relapse After Discontinuing Systemic Treatment for Psoriasis: A Systematic Review. *Am J Clin Dermatol* **23**, 433 (2022).
- 25 Miyamoto, S., Imai, Y., Natsuaki, M., Yamanishi, K. & Kanazawa, N. Long-term Remission of Atopic Dermatitis after Discontinuation of Dupilumab. *Acta Derm Venereol* **102**, (2022).
- 26 Mastorino, L. *et al.* Patients with psoriasis resistant to multiple biological therapies: characteristics and definition of a difficult-to-treat population. *Br J Dermatol* **187**, 263 (2022).
- 27 Ameen, M., Meller, S., Pinter, A., Shear, N. H. & Soria, A. Perception and Experience of Biologic Therapy in Atopic Dermatitis: A Qualitative Focus Group Study of Physicians and Patients in Europe and Canada. *Dermatol Ther (Heidelb)* **11**, 2159 (2021).
- 28 Proksch, E., Brandner, J. M. & Jensen, J. M. The skin: An indispensable barrier. *Exp Dermatol* **17**, 1063-1072 (2008).
- 29 Candi, E., Schmidt, R. & Melino, G. The cornified envelope: A model of cell death in the skin. *Nat Rev Mol Cell Biol* **6**, 328-340 (2005).
- 30 Guttman-Yassky, E., Zhou, L. & Krueger, J. G. The skin as an immune organ: Tolerance versus effector responses and applications to food allergy and hypersensitivity reactions. *Journal of Allergy and Clinical Immunology* **144**, 362-374 (2019).
- 31 Gudjonsson, J. E., Kabashima, K. & Eyerich, K. Mechanisms of skin autoimmunity: Cellular and soluble immune components of the skin. *Journal of Allergy and Clinical Immunology* **146**, 8-16 (2020).
- 32 Eyerich, K., Novak, N., Eyerich, K. & Weidinger, S. Immunology of atopic eczema: overcoming the Th1/Th2 paradigm. *Allergy* **68**, 974-982 (2013).
- 33 Mowad, C. M. *et al.* Allergic contact dermatitis: Patient diagnosis and evaluation. *J Am Acad Dermatol* **74**, 1029-1040 (2016).
- 34 Antia, C., Baquerizo, K., Korman, A., Bernstein, J. A. & Alikhan, A. Urticaria: A comprehensive review: Epidemiology, diagnosis, and work-up. *J Am Acad Dermatol* **79**, 599-614 (2018).
- 35 Guttman-Yassky, E. & Krueger, J. G. Atopic dermatitis and psoriasis: two different immune diseases or one spectrum? *Curr Opin Immunol* **48**, 68-73 (2017).
- 36 van Muijen, M. E. *et al.* Direct Comparison of Real-world Effectiveness of Biologics for Psoriasis using Absolute and Relative Psoriasis Area and Severity Index Scores in a Prospective Multicentre Cohort. *Acta Derm Venereol* **102**, (2022).
- 37 Wu, J. & Guttman-Yassky, E. Efficacy of biologics in atopic dermatitis. *Expert Opin Biol Ther* **20**, 525-538 (2020).
- 38 Feingold, K. R. & Elias, P. M. Role of lipids in the formation and maintenance of the cutaneous permeability barrier. *Biochim Biophys Acta Mol Cell Biol Lipids* **1841**, 280-294 (2014).
- 39 Van Smeden, J., Janssens, M., Gooris, G. S. & Bouwstra, J. A. The important role of stratum corneum lipids for the cutaneous barrier function. *Biochim Biophys Acta Mol Cell Biol Lipids* **1841**, 295-313 (2014).
- 40 Kihara, A. Synthesis and degradation pathways, functions, and pathology of ceramides and epidermal acylceramides. *Progress in Lipid Research* vol. 63 50-69 Preprint at <https://doi.org/10.1016/j.plipres.2016.04.001> (2016).
- 41 Kawana, M., Miyamoto, M., Ohno, Y. & Kihara, A. Comparative profiling and comprehensive quantification of stratum corneum ceramides in humans and mice by LC/MS/MS. *J Lipid Res* **61**, 884 (2020).
- 42 Elias, P. M. *et al.* Formation and functions of the corneocyte lipid envelope (CLE). *Biochimica et Biophysica Acta - Molecular and Cell Biology of Lipids* vol. 1841 314-318 Preprint at <https://doi.org/10.1016/j.bbalip.2013.09.011> (2014).
- 43 Bouwstra, J. A. *et al.* The skin barrier: An extraordinary interface with an exceptional lipid organization. *Prog Lipid Res* **92**, 101252 (2023).
- 44 Thakoersing, V. S. *et al.* Unraveling Barrier Properties of Three Different In-House Human Skin Equivalents. *Tissue Eng Part C Methods* **18**, 1-11 (2012).
- 45 Machado, M., Salgado, T. M., Hadgraft, J. & Lane, M. E. The relationship between transepidermal water loss and skin permeability. *Int J Pharm* **384**, 73-77 (2010).
- 46 Nádában, A. *et al.* Effect of sphingosine and phytosphingosine ceramide ratio on lipid arrangement and barrier function in skin lipid models. *J Lipid Res* **64**, 100400 (2023).
- 47 Mojudar, E. H., Kariman, Z., van Kerckhove, L., Gooris, G. S. & Bouwstra, J. A. The role of ceramide chain length distribution on the barrier properties of the skin lipid membranes. *Biochimica et Biophysica Acta (BBA) - Biomembranes* **1838**, 2473-2483 (2014).
- 48 Mojudar, E. H., Helder, R. W. J., Gooris, G. S. & Bouwstra, J. A. Monounsaturated fatty acids reduce the barrier of stratum corneum lipid membranes by enhancing the formation of a hexagonal lateral packing. *Langmuir* **30**, 6534-6543 (2014).
- 49 Uche, L. E., Gooris, G. S., Bouwstra, J. A. & Beddoes, C. M. Increased Levels of Short-Chain Ceramides Modify the Lipid Organization and Reduce the Lipid Barrier of Skin Model Membranes. *Langmuir* **37**, 9478-9489 (2021).
- 50 Uche, L. E., Gooris, G. S., Bouwstra, J. A. & Beddoes, C. M. Barrier Capability of Skin Lipid Models: Effect of Ceramides and Free Fatty Acid Composition. *Langmuir* **35**, 15376-15388 (2019).
- 51 Skolová, B. *et al.* Ceramides in the skin lipid membranes: length matters. *Langmuir* **29**, 15624-15633 (2013).
- 52 Helder, R. W. J. *et al.* Improved organotypic skin model with reduced quantity of monounsaturated ceramides by inhibiting stearyl-CoA desaturase-1. *Biochimica et Biophysica Acta (BBA) - Molecular and Cell Biology of Lipids* **1866**, 158885 (2021).
- 53 Mieremet, A. *et al.* Multitargeted approach for the optimization of morphogenesis and barrier formation in human skin equivalents. *Int J Mol Sci* **22**, (2021).
- 54 Helder, R. W. J. *et al.* Improved organotypic skin model with reduced quantity of monounsaturated ceramides by inhibiting stearyl-CoA desaturase-1. *Biochimica et Biophysica Acta (BBA) - Molecular and Cell Biology of Lipids* **1866**, 158885 (2021).
- 55 Suchonwanit, P., Triyangkulsri, K., Ploydaeng, M. & Leerunyakul, K. Assessing Biophysical and Physiological Profiles of Scalp Seborrheic Dermatitis in the Thai Population. *Biomed Res Int* **2019**, (2019).
- 56 Tolleson, A. & Frithz, A. Transepidermal water loss and water content in the stratum corneum in infantile seborrheic dermatitis. *Acta Derm Venereol* **73**, 18-20 (1993).
- 57 Montero-Vilchez, T. *et al.* Skin Barrier Function in Psoriasis and Atopic Dermatitis: Transepidermal Water Loss and Temperature as Useful Tools to Assess Disease Severity. *Journal of Clinical Medicine* **2021**, Vol. 10, Page 359 **10**, 359 (2021).
- 58 Harding, C. R. *et al.* Dandruff: a condition characterized by decreased levels of intercellular lipids in scalp stratum corneum and impaired barrier function. *Arch Dermatol Res* **294**, 221-230 (2002).
- 59 Erickson, T. R. *et al.* Transepidermal water loss in the orphan forms of ichthyosis. *Pediatr Dermatol* **37**, 771-773 (2020).
- 60 Van Smeden, J. *et al.* Atopic eczema patients show a decreased ceramide chain length that associates with a decreased barrier function. *Journal of Investigative Dermatology* **132**, S76 (2012).
- 61 Janssens, M. *et al.* Non-lesional skin in atopic eczema patients shows a change in lipid organization that correlates with a decreased barrier function. *Journal of Investigative Dermatology* **132**, S77 (2012).
- 62 Motta, S. *et al.* Abnormality of water barrier function in psoriasis. Role of ceramide fractions. *Arch Dermatol* **130**, 452-456 (1994).
- 63 Van Smeden, J. *et al.* Intercellular skin barrier lipid composition and organization in netherton syndrome patients. *Journal of Investigative Dermatology* **134**, 1238-1245 (2014).
- 64 Pappas, A., Meyer, K., Tannahill, R. & Batchvarova, N. Skin lipids in acne-skin lesions and effect on the epidermal barrier. *J Am Acad Dermatol* **74**, AB9 (2016).
- 65 Arai, A. *et al.* Ceramide profiling of stratum corneum in Sjögren-Larsson syndrome. *J Dermatol Sci* **107**, 114-122 (2022).
- 66 Yamamoto, M. *et al.* Comprehensive stratum corneum ceramide profiling reveals reduced acylceramides in ichthyosis patient with CERS3 mutations. *J Dermatol* **48**, 447-456 (2021).
- 67 Küster, W., Melnik, B., Traupe, H. & Hamm, H. Lipid composition of outer stratum corneum in hereditary palmoplantar keratoderms. *Dermatology* **206**, 131-135 (2003).
- 68 Yokose, U. *et al.* The ceramide [NP1]/[NS] ratio in the stratum corneum is a potential marker for skin properties and epidermal differentiation. *BMC Dermatol* **20**, (2020).
- 69 Danso, M. *et al.* Altered expression of epidermal lipid bio-synthesis enzymes in atopic dermatitis skin is accompanied by changes in stratum corneum lipid composition. *J Dermatol Sci* **88**, 57-66 (2017).
- 70 Van Smeden, J., Janssens, M., Vreeken, R., Lavrijsen, A. & Bouwstra, J. Free fatty acids and lipid chain length correlate with the impaired skin barrier of atopic eczema patients. *Journal of Investigative Dermatology* **133**, S123 (2013).

- 71 Boer, D. E. C. *et al.* Skin of atopic dermatitis patients shows disturbed -glucocerebrosidase and acid sphingomyelinase activity that relates to changes in stratum corneum lipid composition. *Biochimica et Biophysica Acta (BBA) – Molecular and Cell Biology of Lipids* **1865**, 158673 (2020).
- 72 Janssens, M. *et al.* Atopic eczema: Deviation in ceramide composition correlates with an aberrant lipid organization. *Journal of Investigative Dermatology* **132**, S55 (2012).
- 73 Pilgram, G. S. *et al.* Aberrant lipid organization in stratum corneum of patients with atopic dermatitis and lamellar ichthyosis. *J Invest Dermatol* **117**, 710-717 (2001).
- 74 Drislane, C. & Irvine, A. D. The role of filaggrin in atopic dermatitis and allergic disease. *Annals of Allergy, Asthma & Immunology* **124**, 36-43 (2020).
- 75 Tsoi, L. C. *et al.* Identification of 15 new psoriasis susceptibility loci highlights the role of innate immunity. *Nature Genetics* **2012** 44:12 **44**, 1341-1348 (2012).
- 76 Huang, Y. H., Kuo, C. F., Huang, L. H. & Hsieh, M. Y. Familial Aggregation of Psoriasis and Co-Aggregation of Autoimmune Diseases in Affected Families. *J Clin Med* **8**, (2019).
- 77 Pascoe, V. L. & Kimball, A. B. Seasonal variation of acne and psoriasis: A 3-year study using the Physician Global Assessment severity scale Presented in poster form at the 73rd Annual Meeting of the Academy of Dermatology, San Francisco, CA, March 20-24, 2015. *J Am Acad Dermatol* **73**, 523-525 (2015).
- 78 Hui-Beckman, J. W., Goleva, E., Leung, D. Y. M. & Kim, B. E. The impact of temperature on the skin barrier and atopic dermatitis. *Annals of Allergy, Asthma & Immunology* **131**, 713-719 (2023).
- 79 Park, S. K., Kim, J. S. & Seo, H. M. Exposure to air pollution and incidence of atopic dermatitis in the general population: A national population-based retrospective cohort study. *J Am Acad Dermatol* **87**, 1321-1327 (2022).
- 80 Bellinato, F. *et al.* Association Between Short-term Exposure to Environmental Air Pollution and Psoriasis Flare. *JAMA Dermatol* **158**, 375-381 (2022).
- 81 Kobayashi, T. *et al.* Dysbiosis and Staphylococcus aureus colonization drives inflammation in atopic dermatitis. *Immunity* **42**, 756 (2015).
- 82 Wikramanayake, T. C., Borda, L. J., Miteva, M. & Paus, R. Seborrheic dermatitis—Looking beyond Malassezia. *Exp Dermatol* **28**, 991-1001 (2019).
- 83 Vonaesch, P., Anderson, M. & Sansonetti, P. J. Pathogens, microbiome and the host: emergence of the ecological Koch's postulates. *FEMS Microbiol Rev* **42**, 273-292 (2018).
- 84 Tao, M. *et al.* Objectively quantifying facial erythema in rosacea aided by the ImageJ analysis of VISIA red images. *Skin Research and Technology* **29**, e13241 (2023).
- 85 Huisman, B. W. *et al.* Dermatoscopy and Optical Coherence Tomography in Vulvar High-Grade Squamous Intraepithelial Lesions and Lichen Sclerosus: A Prospective Observational Trial. *J Low Genit Tract Dis* **27**, 255-261 (2023).
- 86 Rjnsbergen, M. *et al.* Stereophotogrammetric three-dimensional photography is an accurate and precise planimetric method for the clinical visualization and quantification of human papilloma virus-induced skin lesions. *J Eur Acad Dermatol Venerol* **33**, 1506-1512 (2019).
- 87 Ten Voorde, W. *et al.* A multimodal, comprehensive characterization of a cutaneous wound model in healthy volunteers. *Exp Dermatol* **00**, 1-14 (2023).
- 88 Janssens, M. *et al.* Increase in short-chain ceramides correlates with an altered lipid organization and

decreased barrier function in atopic eczema patients. *J Lipid Res* **53**, 2755 (2012).

- 89 Guo, Y., Luo, L., Zhu, J. & Li, C. Multi-Omics Research Strategies for Psoriasis and Atopic Dermatitis. *Int J Mol Sci* **24**, 8018 (2023).
- 90 Acosta, J. N., Falcone, G. J., Rajpurkar, P. & Topol, E. J. Multimodal biomedical AI. *Nature Medicine* **2022** 28:9 **28**, 1773-1784 (2022).
- 91 Atkinson, A. J. *et al.* Biomarkers and surrogate endpoints: preferred definitions and conceptual framework. *Clin Pharmacol Ther* **69**, 89-95 (2001).
- 92 Baysal, V., Yildirim, M., Ozcanli, C. & Ceyhan, A. M. Itraconazole in the treatment of seborrheic dermatitis: a new treatment modality. *Int J Dermatol* **43**, 63-66 (2004).
- 93 Hanifin, J. M. *et al.* The Eczema Area and Severity Index—A Practical Guide. *Dermatitis* **33**, 187 (2022).
- 94 Gourraud, P. A. *et al.* Why Statistics Matter: Limited Inter-Rater Agreement Prevents Using the Psoriasis Area and Severity Index as a Unique Determinant of Therapeutic Decision in Psoriasis. *Journal of Investigative Dermatology* **132**, 2171-2175 (2012).
- 95 Papp, K. A. *et al.* The Proposed PASI-HD Provides More Precise Assessment of Plaque Psoriasis Severity in Anatomical Regions with a Low Area Score. *Dermatol Ther (Heidelb)* **11**, 1079-1083 (2021).
- 96 Visser, S. J. De, Post, J. Van Der, Pieters, M. S. M., Cohen, A. F. & Gerven, J. M. A. Van. Biomarkers for the effects of antipsychotic drugs in healthy volunteers. *Br J Clin Pharmacol* **51**, 119-132 (2001).
- 97 Cummings, J., Ward, T. H. & Dive, C. Fit-for-purpose biomarker method validation in anticancer drug development. *Drug Discov Today* **15**, 816-825 (2010).
- 98 Cummings, J., Ward, T. H., Greystoke, A., Ranson, M. & Dive, C. Biomarker method validation in anticancer drug development. *Br J Pharmacol* **153**, 646 (2008).
- 99 Kruizinga, M. D. *et al.* Development of Novel, Value-Based, Digital Endpoints for Clinical Trials: A Structured Approach Toward Fit-for-Purpose Validation. *Pharmacol Rev* **72**, 899-909 (2020).

## SECTION 1

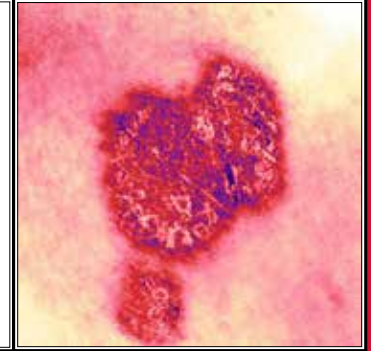
---

# Multimodal characterization of the skin of seborrheic dermatitis patients

## CHAPTER 2

### LESIONAL SKIN OF SEBORRHEIC DERMATITIS PATIENTS IS CHARACTERIZED BY SKIN BARRIER DYSFUNCTION AND CORRELATING ALTERATIONS IN THE STRATUM CORNEUM CERAMIDE COMPOSITION

Published in: *Experimental Dermatology*  
(*EXP DERMATOL.* 2024;33:e14952,  
DOI: <https://doi.org/10.1111/exd.14952>)



Jannik Rousel,<sup>1,2</sup> Andreea Nădăban,<sup>2</sup> Mahdi Saghari,<sup>1,3</sup> Lisa Pagan,<sup>1,3</sup> Ahnjili Zhuparris,<sup>1,3,4</sup> Bart Theelen,<sup>5</sup> Tom Gambrah,<sup>1</sup> Hein E.C. van der Wall,<sup>1</sup> Rob J. Vreeken,<sup>6</sup> Gary L. Feiss,<sup>7</sup> Tessa Niemeyer-van der Kolk,<sup>1,3</sup> Jacobus Burggraaf,<sup>1,2,3</sup> Martijn B.A. van Doorn,<sup>1,8</sup> Joke A. Bouwstra<sup>2</sup> and Robert Rissmann<sup>1,2,3</sup>

1. Centre for Human Drug Research, Leiden, NL / 2. Leiden Academic Centre for Drug Research, Leiden University, Leiden, NL / 3. Leiden University Medical Center, Leiden, NL / 4. Leiden Institute of Advanced Computer Science, Leiden University, Leiden, NL / 5. Westerdijk Fungal Biodiversity Institute, Utrecht, NL / 6. Maastricht Multimodal Molecular Imaging Institute, Maastricht University, Maastricht, NL / 7. Cutanea Life Sciences, Wayne, Pennsylvania, USA / 8. Department of Dermatology, Erasmus Medical Centre, Rotterdam, NL

## Abstract

**BACKGROUND:** Seborrheic dermatitis (SD) is a chronic inflammatory skin disease characterized by erythematous papulosquamous lesions in sebum rich areas such as the face and scalp. Its pathogenesis appears multifactorial with a disbalanced immune system, *Malassezia* driven microbial involvement and skin barrier perturbations. Microbial involvement has been well described in SD, but skin barrier involvement remains to be properly elucidated.

**OBJECTIVE:** To establish whether barrier impairment is a critical factor of inflammation in SD alongside microbial dysbiosis.

**METHODS:** A cross-sectional study was performed in 37 patients with mild-to-moderate facial SD. Their lesional and non-lesional skin was comprehensively and non-invasively assessed with standardized 2D-photography, optical coherence tomography, microbial profiling including *Malassezia* species identification, functional skin barrier assessments and ceramide profiling.

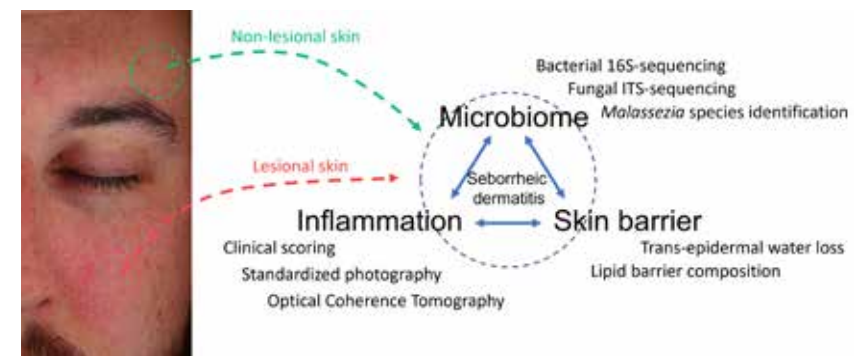
**RESULTS:** Inflammation was established through significant increases in erythema, epidermal thickness, vascularization and superficial roughness in lesional skin compared to non-lesional skin. Lesional skin showed a perturbed skin barrier with an underlying skewed ceramide subclass composition, impaired chain elongation and increased chain unsaturation. Changes in ceramide composition correlated with barrier impairment indicating interdependency of the functional barrier and ceramide composition. Lesional skin showed significantly increased *Staphylococcus* and decreased *Cutibacterium* abundances but similar *Malassezia* abundances and mycobial composition compared to non-lesional skin. Principal component analysis highlighted barrier properties as main discriminating features.

**CONCLUSIONS:** SD is associated with skin barrier dysfunction and changes in the ceramide composition. No significant differences in the abundance of *Malassezia* were observed. Restoring the cutaneous barrier might be a valid therapeutic approach in the treatment of facial SD.

## Introduction

Seborrheic dermatitis (SD) is an inflammatory, eczematous skin disease of the face and scalp with a multifactorial underlying pathophysiology. SD is characterized by the development of erythematous, scaly and itchy skin on seborrheic areas with high sebaceous gland activity such as the nasolabial folds, eyebrows and upper chest.<sup>1</sup> The exact pathophysiology of SD remains unclear due to its multifactorial and complex aetiology (figure 1). Three major interdependent driving factors of the aberrant immunological responses behind SD are I) individual susceptibility due to an imbalanced immune system leading to inflammation, II) cutaneous microbial dysbiosis with pronounced colonization by *Malassezia* species and III) a perturbed epidermal barrier.<sup>1,2</sup>

**Figure 1** Clinical presentation of a seborrheic dermatitis patient and overview of the study setup showing the assessments performed on lesional and non-lesional skin and the interdependency of inflammation, microbiome and barrier function. Note that the locations indicated are examples of lesional and non-lesional skin and can differ between subjects based on the availability of affected skin as listed in the supplemental data.



While these three hallmarks all contribute towards the development of SD, much emphasis has been on the microbiome and especially the involvement of *Malassezia*. *Malassezia* is a commensal yeast which is regarded as a key pathogen due to its concurrence with lesional skin and the clinical response of SD to antifungals.<sup>3</sup> It is hypothesised that the predilection of *Malassezia* for



sebum-rich skin sites is due to its inability to perform *de novo* fatty acid synthesis, necessitating the processing of exogenous lipids which disturbs the epidermal barrier integrity and enables inflammation.<sup>4,5</sup> While this provides rationale for why inflammation is limited to these areas, it has been shown that neither the amount of *Malassezia*<sup>5,6</sup> nor an increased level of sebum production<sup>1,2,6</sup> are strictly tied to the development of SD.

Due to the implication that external triggers such as *Malassezia* and its metabolites can penetrate the skin,<sup>7</sup> the cutaneous barrier function itself has been proposed to be involved in SD pathogenesis.<sup>6</sup> The epidermal barrier function is located in the stratum corneum which consists of layers of cornified cells embedded in a lipid matrix mainly composed of cholesterol, fatty acids and ceramides.<sup>8</sup> Changes in the composition and consequently the lipid organization of this matrix directly impacts skin permeability.<sup>9,10</sup> Barrier perturbations and simultaneous alterations of the lipid matrix composition, such as reduced chain length and changes in ceramide subclass composition, have been observed in other inflammatory skin diseases such as atopic dermatitis and psoriasis.<sup>11,12</sup> This raised the question whether barrier repair can be exploited as a treatment option.<sup>13</sup>

The apparent contribution of host immunity, the microbiome and cutaneous barrier to the development of SD warrants a multimodal assessment for phenotyping SD. In this study, we established cutaneous inflammation by clinical scoring complemented with imaging. We elucidated the bacterial and fungal composition as both are implicated in SD,<sup>14</sup> with additional species-level profiling of *Malassezia*. Lastly, the cutaneous barrier function was characterized in-depth by trans-epidermal water loss (TEWL) measurements complemented with ceramide profiling using lipidomic analysis. This might yield new insights into how these modalities are implicated in disease.

## Materials and methods

### STUDY DESIGN AND POPULATION

The study was conducted at the Centre for Human Drug Research (Leiden, the Netherlands) from November 2018 to January 2020 following the Declaration of Helsinki principles after approval by the medical ethics committee Stichting Beoordeling Ethiek Biomedisch Onderzoek (Assen, the Netherlands). This was a cross-sectional study which consisted of one screening and one visit. Patients gave written informed consent prior to participation in the study.

Inclusion criteria included being 18 years or older, SD scored with an Investigator's Global Assessment of 2 or 3 with sufficient surface area for all assessments, confirmation of SD by a dermatologist and willingness to refrain from any SD treatments during study participation. Exclusion criteria included the presence of any current or recurrent clinically significant (skin) condition other than SD, recent excessive sun exposure, adapting a different washing routine 1 week prior to screening and the use of SD topical treatments and dandruff shampoo 2 weeks, phototherapy 3 weeks and systemic treatments 4 weeks prior to enrolment.

In total, 37 patients exhibiting mild-to-moderate SD defined by an Investigator's Global Assessment (IGA) score of 2 to 3 after verification by a dermatologist were included and assessments performed during a single visit. All 37 included subjects underwent the visit as planned within 28 days of screening. No formal power calculations were performed to determine group size because of the exploratory nature of the study. Patients were instructed not to wash their face 12 hours preceding the study visit.

Due to the heterogeneous presentation of SD, assessments are performed on different sites of the face as listed in Supplemental Table S1-3. The different areas for measurements were chosen on a per-subject basis depending on the availability of sufficient lesional skin and the disqualification of areas due to invasive measurements. Non-lesional was defined as an area of skin without any clinical characteristics of SD and was similarly located on the face.

### CLINICAL CHARACTERISTICS

Disease severity was scored using the Seborrheic Dermatitis and Severity Index (SDASI) adapted from Baysal, *et al.* (2004),<sup>15</sup> 5-point IGA and percentage affected body surface area (%BSA). Patient reported outcomes included the 0-100 Numeric Rating Scale (NRS) itch, 5-Domain Itch Questionnaire<sup>16</sup> and Dermatology Life Quality Index (DLQI).<sup>17,18</sup>

The Seborrheic Dermatitis and Severity Index (SDASI) was adapted to include only the facial extent of SD as follows; Erythema, scaling and papules are scored 0-4 with; 0 = none, 1 = mild, 2 = moderate, 3 = severe and 4 = very severe symptoms. The area of involvement is estimated as the fraction of the face with lesional skin and is scored by: 1 = less than 10%, 2 = 11 - 30%, 3 = 31 - 50%, 4 = 51 - 70 and 5 = more than 70%. Erythema, scaling and papule scores are then summed and multiplied by the area score. The IGA is a general 5-point scale in which the severity of disease is scored with 0 = clear, 1 =

almost clear, 2 = mild, 3 = moderate and 4 = severe. Lastly, the %BSA represents the percentage of lesional skin and is estimated using the hand palm method where the surface of a patient's hand equals 1% of the total body surface area.

### STANDARDIZED PHOTOGRAPHY

Standardized two dimensional cross-polarized images of the face were taken using a VISIA-CR (Canfield Scientific, New Jersey, United States). Erythema Index calculations were performed based on a method by Yamamoto, *et al.* (2008).<sup>19</sup> In short, obtained Red Green Blue (RGB) images were split and the R and G channels log transformed using ImageJ (version 1.51h)<sup>20</sup>. After subtraction of the R channel with the G channel, brightness was increased by 3 and the mean grey value within a predefined region of interest of 50000 pixels was determined for a lesional and non-lesional area.

### OPTICAL COHERENCE TOMOGRAPHY

Lesional and non-lesional skin was imaged with a Vivosight Dx optical coherence tomography (OCT) system (Michelson Diagnostics, Kent, United Kingdom). The epidermal thickness, superficial roughness and average epidermal perfusion depth was determined from the resulting scans using the proprietary VivoTools 4.12 software. Individual perfusion-over-depth curves were reviewed and excluded if high superficial levels of perfusion were observed, indicating an invalid measurement in 4 lesional and 4 non-lesional measurements. Epidermal thickness could only be determined in 23 of 37 lesional and 34 of 37 non-lesional measurements because of pronounced epidermal disorganization resulting in troublesome localization of the dermal-epidermal junction.

### MICROBIOME COMPOSITION

Sterile 0.9% NaCl soaked skin swabs (Puritan Sterile Polyester Tipped Applicators, Puritan, Guilford, Maine, United States) were collected by rubbing over a lesional or non-lesional site for 10 seconds while rotating the swab and subsequently stored in DNA/RNA shield lysis buffer and beat beads (Zymo Research, Irvine, California, United States) at -80 °C. Swabs were transferred to Baseclear B.V. (Leiden, the Netherlands) for extraction and subsequent sequencing. DNA was extracted using a ZymoBIOMICS DNA Miniprep Kit (Zymo Research) according to manufacturer's instructions. Next-Generation Sequencing for the bacterial and fungal composition was performed

using amplification of 16S rRNA region V3-V4 and Internal transcribed spacer region 2 (ITS2), respectively. An Illumina NovaSeq 6000 or MiSeq system was used to generate single- or pair-end sequence reads. FASTQ read sequence files were generated using bcl2fastq version 2.18. Primary quality was assessed using the Illumina Chastity filtering and reads containing a PHIX control signal removed. Quality was finally assessed using the FASTQC quality control tool version 0.11.5. USEARCH version 9.2<sup>21</sup> was used to create pseudoreads and classification of these reads performed based on the alignment with SNAP version 1.0.23<sup>22</sup> against the RDP database for bacterial<sup>23</sup> and UNITE ITS gene database for fungal classification<sup>24</sup>. The resulting list of Operational Taxonomic Units per sample was filtered to genus level and the detected genera included in analysis if it exceeded 1% of the total composition within a sample. Data was presented in the Genome Explorer database (Baseclear B.V., Leiden, the Netherlands) and further processed in Python version 3.8.0 (Python Software Foundation, Wilmington, Delaware, United States) in which microbes contributing <1% of the total were excluded after which their relative abundance at the genus level was determined.

### MALASSEZIA CULTURING

9 cm diameter Agar plates with modified Dixon medium (Mediaproducts B.V., Groningen, the Netherlands) were pressed against a lesional and non-lesional site for 20 seconds. Plates were cultured at 33 °C for up to 21 days at the Microbiology department of the Alrijne Hospital (Leiden, the Netherlands). A sample from each colony forming unit was isolated after positive identification for bacterial or fungal growth through light microscopy. Mycological isolates were transported to the Westerdijk Fungal Biodiversity Institute (Utrecht, the Netherlands) for Malassezia species determination by matrix-assisted laser desorption ionization-time of flight mass spectrometry (MALDI-TOF MS) as described by Kolečka *et al.* (2014).<sup>25</sup>

### SKIN BARRIER INTEGRITY BY TRANS-EPIDERMAL WATER LOSS

Subjects were allowed to acclimatise to controlled environmental conditions (humidity <60%, temperature 22±2 °C) in rested state for at least 15 minutes prior to measurements. An AquaFlux AF200 (Biox Systems Ltd., London, United Kingdom) was used to measure the TEWL of lesional and non-lesional skin. Baseline calibration was performed and TEWL was measured for up to 200 seconds or until a steady state was reached.

## TAPE STRIPPING PROCEDURE

Stratum corneum was harvested by pressing polyphenylene sulfide tape (Nichiban, Tokyo, Japan) to the skin with a D500 D-squame Pressure Instrument (CuDerm Corporation, Dallas, Texas, United States) and exerting pressure 5 times. Tapes were transferred to a cutting board with the glue side up. 16 mm diameter holes were punched within the region that was pressed against the skin. The individual punched out tape samples were stored in 20 ml vials with 1.5 ml of chloroform:methanol (2:1) at -20 °C before extraction.

## SKIN BARRIER LIPIDOMICS

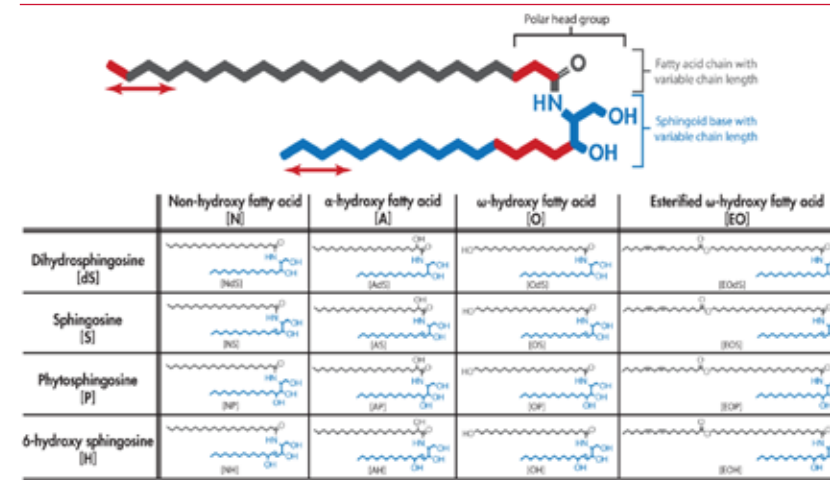
HPLC grade chloroform (Honeywell, Charlotte, North Carolina, United States), UPLC grade Methanol (Biosolve, Valkenswaard, the Netherlands), UPLC grade heptane (LiChorSolv, Merck, Darmstadt, Germany), UPLC grade isopropyl alcohol (Biosolve, Valkenswaard, the Netherlands), UPLC grade ethanol (Biosolve, Valkenswaard, the Netherlands), reagent grade potassium chloride (Sigma Aldrich, Saint-Louis, Missouri, United States) and ultrapure water from a Milli-Q Advantage A10 system (Merck, Darmstadt, Germany) were used. Synthetic ceramides and deuterated standards were purchased from Avanti Polar Lipids (Alabaster, Alabama, United States) or kindly provided by Evonik (Essen, Germany).

Tapes were extracted and the ceramide fraction analysed through a validated Liquid Chromatography-Mass Spectrometry (LC-MS) setup as described by Boiten *et al.* (2016).<sup>26</sup> Figure 2 lists the 12 most prevalent ceramide classes included in the analysis using the nomenclature by Motta *et al.* (1993).<sup>27</sup>

In short, individual tape samples were stored in 1.5 ml of chloroform:methanol (2:1) in a 20 ml glass vial and stored at -20 °C before analysis. Tapes were extracted by shaking the tape samples in an IKA S4000 rotary shaker at 120 rounds per minute at 40 °C for one hour. Solvent was isolated and shaking repeated three times with 1 ml of different solvent mixtures; chloroform:methanol:water (1:2:0.5), chloroform:methanol (1:1) and heptane: isopropylalcohol (1:1). Solvent was isolated each time and pooled with the previous collected organic solvent. 4 ml of 0.25M potassium chloride was added to the pooled solvent and phase separation achieved overnight. The organic layer was isolated and washed with the addition of 4 ml chloroform. The isolated organic layer was combined with the washing solvent and filtered through 0.45 µm PVDF syringe filters (Grace, Deerfield, Illinois, United

states). Samples were transferred to 1.5 ml HPLC vials and reconstituted in 750 µl chloroform:methanol (2:1). 225 µl of this stock was transferred to a separate HPLC vial, dried, and reconstituted in 60 µl heptane:chloroform:methanol (95:2.5:2.5) containing 10 µM CER[N(24DEU)S(18)] for analysis by UPLC-MS. Separation was achieved by a 5 µl injection using an Acquity UPLC H-class (Waters, Milford, Massachusetts, United States) and a normal phase PVA-silica column (5 µm particles, 100 × 2.1 mm i.d.) (YMC, Kyoto, Japan) over a gradient from 98% heptane and 2% heptane:isopropylalcohol:ethanol (2:1:1) to 50% heptane and 50% heptane: isopropylalcohol:ethanol (2:1:1) at a flow rate of 0.8 ml/min. Detection was performed using atmospheric pressure chemical ionization (APCI) on a XEVO TQ-S mass spectrometer (Waters, Milford, MA, USA) in positive ion mode scanning from 350 to 1200 m/z. Quality control samples from combined stratum corneum extracts and standard calibration curves containing 50, 20, 10, 5, 2, 1, 0.5, 0 µM of several ceramides (CER[NS, NDS, NP, AS, EOS AND EOP]) in triplicate were added to the run. Responses of 2 out of 64 samples were below the limit of detection and therefore excluded from analysis.

**Figure 2** General structure of a ceramide composed of a sphingoid base coupled to a fatty acid chain. The carbon chains attached to the polar head group can vary in length. Differences in the ceramide headgroup architecture is indicated using the naming convention conceived by Motta *et al.* (1993). This image was adapted from Janssens *et al.* (2012).<sup>28</sup>



Peaks at the ceramides monoisotopic mass were integrated using TargetLynx V4.1 (Waters, Milford, Massachusetts, United States) and Area Under the Curve (AUC) responses corrected for the internal standard in Excel (Microsoft 365, Redmond, Washington, United States). The monoisotopic AUC was further corrected by the degree of water loss as determined from quality control samples. AUC were further corrected by the ceramides theoretic  $^{13}\text{C}$  isotope distribution. Using the calibration curves, correction for increased responses at higher masses was performed. This corrected response per ceramide was converted to relative data using the total corrected AUC and calculations were made after grouping individual ceramides by class or chain lengths for further graphing.

### SEBUM MEASUREMENTS

Lesional and non-lesional skin was measured using a Sebumeter SM815 (Courage+Khazaka, Köln, Germany). The Sebumeter was calibrated before a patient was measured. Three measurements were performed next to each other on the same predefined lesional or non-lesional site. The average of this triplicate measurement was used for graphing.

### STATISTICAL ANALYSIS

Data visualisation and statistical testing was performed using PRISM 9 (Graphpad Software, San Diego, California, United States). 2-way ANOVA, or a mixed effects model in the case of missing data points, was performed using Bonferroni's multiple comparison test in the case of multiple variables and paired t-test in the case of two variables. P-values are denoted as \*:  $P < 0.05$ , -:  $P < 0.01$ , -\*:  $P < 0.001$ . Integrative data graphing by principal component analysis (PCA) and radar plot has been performed through Python version 3.8.0 (Python Software Foundation, Wilmington, Delaware, United States). PCA of the ceramides composition was performed using relative individual ceramide abundance as percentage of all detected saturated ceramides, with values below the limit of quantification set to 0 in order to prevent missing datapoints and allow for PCA. Multimodal integration through PCA was performed on all the data presented in the figures of this paper with mean imputation in the case of missing data, but without epidermal thickness data due to a high amount of data not missing at random in this set as higher epidermal disorganisation was more evident in lesional skin. Radar charts using min-max scaling were used to visualize differences between lesional

and non-lesional skin in an integrative and descriptive manner. Data used in generation of the ceramide PCA, integrative PCA and integrative radar plot is added as supplemental information.

## Results

In total, 37 patients were enrolled into the study. The patient population exhibited mild-to-moderate SD as shown by a SDASI score of  $7.0 \pm 4.3$  and IGA score of  $\leq 3$  for 97% of all patients (table 1). Patient reported disease burden was rated mild-to-moderate as evident from the DLQI ( $7.2 \pm 5.5/30$ ; "moderate effect on patient's life"), average itch rating scale ( $23.6 \pm 22.5/100$ ) and 5-Domain itch scale rating ( $11.6 \pm 3.2/25$ ).

**Table 1** Baseline demographics including clinical scoring and patient reported outcomes from the study population. The minimal and maximal values are indicated among their respective scores. BMI; Body Mass Index, SD; standard deviation.

Subjects (n)		37
Age (years)		$37.8 \pm 15.6$
BMI ( $\text{kg}/\text{m}^2$ )		$25.4 \pm 3.4$
Sex	Female	5 (13.5%)
	Male	32 (86.5%)
Race	Asian	1 (2.7%)
	Mixed (White, African)	1 (2.7%)
	Latino	1 (2.7%)
	White	34 (91.9%)
Fitzpatrick skin type	1	4 (10.8%)
	2	19 (51.4%)
	3	13 (35.1%)
	4	1 (2.7%)
	5	0 (0.0%)
	6	0 (0.0%)
Seborrheic Dermatitis Area and Severity index (0-45) (Mean $\pm$ SD)		$7.0 \pm 4.3$
Investigator's Global Assessment	1 (almost clear)	4 (10.8%)
	2 (mild)	19 (51.4%)
	3 (moderate)	13 (35.1%)
	4 (severe)	1 (2.7%)
Affected body surface area (%) (Mean $\pm$ SD)		$1.3 \pm 0.7$
Dermatology Life Quality Index (0-30) (Mean $\pm$ SD)		$7.2 \pm 5.5$
Average Itch Numeric Rating scale (0-100) (Mean $\pm$ SD)		$23.6 \pm 22.5$
5-Domain Itch Scale (5-25) (Mean $\pm$ SD)		$11.6 \pm 03.2$

## INFLAMMATION

Apart from clinical scoring, hallmarks of inflammation were assessed using standardized 2D-photography and OCT. Lesional skin had a significantly higher erythema index compared to non-lesional skin (67.62 AU vs. 49.19 AU,  $P \leq 0.001$ , figure 3A). Despite high epidermal disorganization hampering the localization of the dermal-epidermal junction in multiple measurements, the epidermis of lesional skin was significantly thicker compared to non-lesional skin (0.15 mm vs. 0.10 mm,  $P \leq 0.001$ , figure 3B). Superficial roughness of the skin was significantly increased in lesional skin (0.013 AU vs 0.009 AU,  $P \leq 0.001$ , figure 3C). Higher superficial vascularization was observed in lesional skin compared to non-lesional skin at a shallow skin depth of 0.1 to 0.25 mm ( $P \leq 0.05$ -0.001, figure 3D) with no significant differences at greater depths. This culminates to an increased average vascularization between 0.1 to 0.25 mm of 0.079 in lesional skin compared to 0.058 in non-lesional skin ( $P \leq 0.001$ , Supplemental Figure S1).

## MICROBIOME

After establishing the presence of inflammation, the facial microbial composition was investigated using 16S rRNA and ITS sequencing for the bacterial and fungal microbiome, respectively. Neither Shannon indexes showed a significant difference between lesional and non-lesional skin sites (1.55 vs 1.71,  $P > 0.24$  and 0.58 vs 0.66,  $P > 0.23$ , for bacteria and fungi respectively, figure 4A, 4C), indicating biodiversity on average did not differ between skin sites. However, *Staphylococcus* was significantly overrepresented and *Cutibacterium* significantly underrepresented in lesional skin compared to non-lesional skin (44.05% vs 19.50% and 23.04% vs 38.20%, respectively,  $P \leq 0.001$ , figure 4B). The mycobiome proved small with only 3 genera present over the detection thresholds used (figure 4D), of which over 80% comprised of *Malassezia* hits in both lesional and non-lesional skin without any significant differences (82.20% vs. 83.52%,  $P > 0.05$ ). Due to the limitations associated with reliable identification of *Malassezia* at the species-level using ITS-sequencing, axenic culture plates were taken and subsequent MALDI-TOF MS was performed as a more specific qualitative alternative. Using *Malassezia* specific protocols successful isolation and identification of 16 from 37 lesional and 18 from 37 non-lesional samples was possible. No clear differences were observed between skin sites with *M. sympodialis* being the most prevalent at both sites

(21.6% and 18.9% on lesional and non-lesional skin, respectively), followed by *M. slooffiae* (13.5%) on lesional and *M. globosa* (13.5%) on non-lesional skin (figure 4E).

## SKIN BARRIER

Finally, the skin barrier was studied as it represents the interface between external pathogens and the established epidermal inflammation. Firstly, the abundance of sebum was determined. However, sebum levels were not significantly different between lesional and non-lesional skin ( $90.70 \pm 54.93$  vs  $82.78 \pm 53.29$ ,  $p = 0.521$ , figure 5).

**Figure 3** Erythema index as determined by standardized photography (A) and the epidermal thickness (B), superficial roughness (C) and the degree of vascularization at different depths in the epidermis (D) as determined by optical coherence tomography of lesional and non-lesional skin. Epidermal thickness could only be determined in 23 of 37 lesional and 34 of 37 non-lesional measurements. AU; Arbitrary Units, NS; not significant.

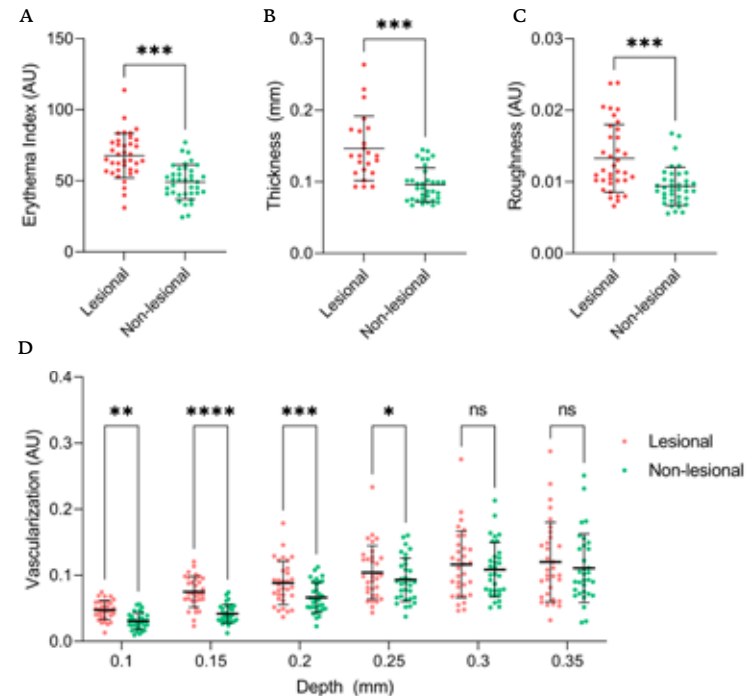


**Figure 4** Bacterial Shannon diversity index (A) and composition of the bacterial microbiome (B) by 16S rRNA sequencing along with the fungal Shannon diversity index (C) and composition of the fungal microbiome (D) by ITS sequencing. The presented genera are filtered for minimal prevalence of 1% over all samples and presented relative to the total amount of microbes detected per analysis. Presence of different *Malassezia* species per site after isolation with contact plates and subsequent MALDI-TOF MS analysis (E). None of the samples yielded two or more different isolates.

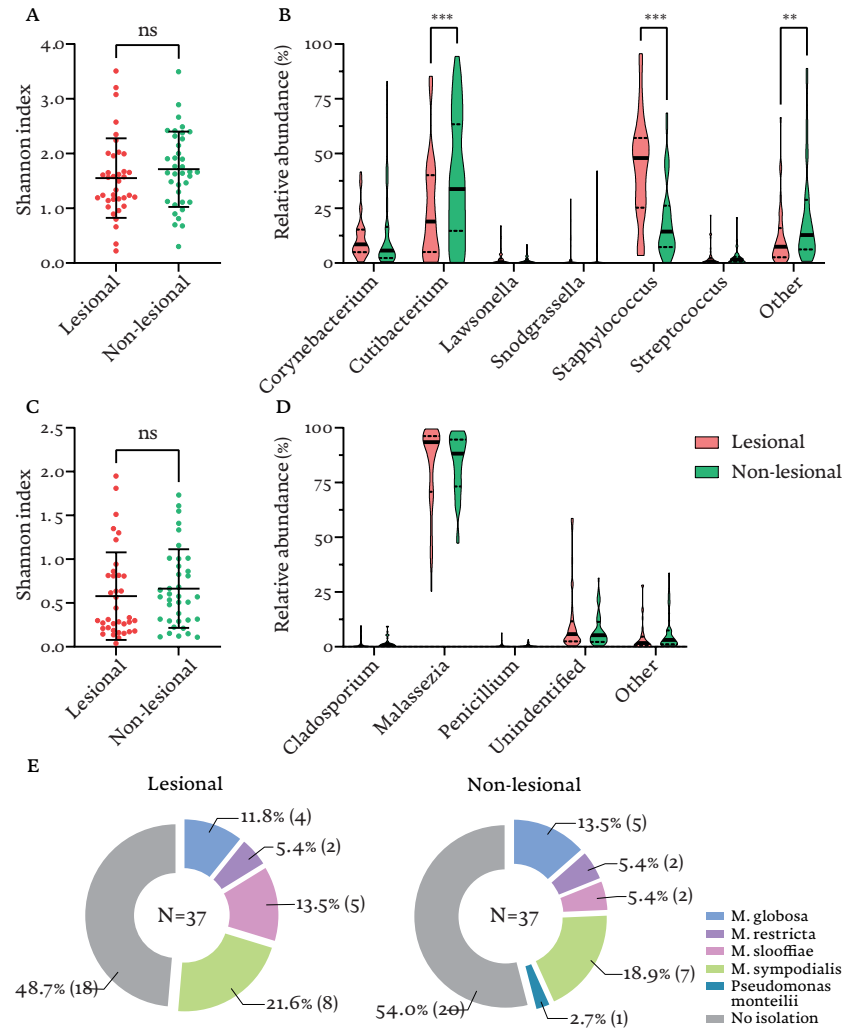
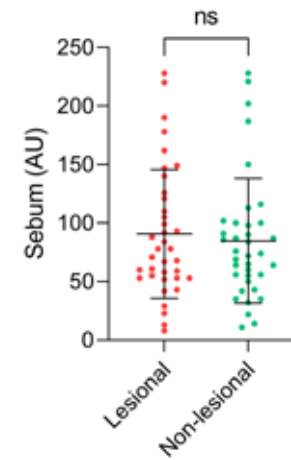


**Figure 5** Sebum measurements do not indicate significantly higher sebum levels on lesional compared to non-lesional skin. Datapoints represent the average value of a triplicate measurement. AU; arbitrary units.



TEWL was used as an endpoint for skin barrier integrity and was significantly higher in lesional skin compared to non-lesional skin indicating an impaired barrier function ( $35.89 \text{ g/m}^2/\text{hr}$  vs  $21.27 \text{ g/m}^2/\text{hr}$ ,  $p > 0.001$ , figure 6A). The relative abundance was determined of all twelve major ceramide classes. The lesional ceramide profile showed a significant increase in CER[NS] and CER[AS] (17.25% vs 11.86% and 16.99% vs 10.61%, respectively,  $P \leq 0.001$ ) and significantly decreased abundance of CER[NDS], CER[EOS] (7.15% vs 8.06% and 2.52% vs 3.51%, respectively,  $P \leq 0.01$ ) and CER[NP], CER[NH], CER[AP] (10.58% vs 14.29%, 10.87% vs 12.23%, 13.22% vs 16.03%, respectively,  $P \leq 0.001$ , figure 6B) compared to non-lesional skin. The abundance of other classes was not significantly different. The skewing of ceramide subclass synthesis can be easily interpreted by comparing the abundance of CER[NS] and CER[NP]. Indeed, alterations in lipid processing were evident from a significant increase of the CER[NS]:CER[NP] ratio in lesional compared to non-lesional skin (1.68 vs 0.87,  $P \leq 0.001$ , figure 6C). Additionally, the presence of CER[NSC34], a CER[NS] species with a total chain length of 34 carbons, was significantly elevated in lesional compared to non-lesional skin (8.19% vs 5.10%,  $P \leq 0.001$ , figure 6D). Using the monounsaturations in CER[NS] as an indicator for the overall monounsaturations, ceramides at lesional skin sites were further impacted by a higher degree of unsaturation compared to non-lesional skin (7.32% vs 3.71%,  $P \leq 0.001$ ,

figure 6E). Lastly, lipid elongation was impaired in lesional skin as evident from a decreased average total carbon chain length of the ceramides compared to non-lesional skin (42.64 carbons vs 43.85 carbons,  $P < 0.001$ , figure 6F).

Visualization of the roughly 300 individual ceramide responses using dimension reduction analysis by PCA showed two distinguishable populations when stratifying for skin site (figure 6G). This indicates the ceramide profile of lesional skin is alike between subjects, but differs from non-lesional skin. Plotting the TEWL values against ceramide parameters revealed a positive correlation for ceramide CER[NS]:CER[NP] ratio ( $r = 0.6474$ ), amount of CER[NSC34] ( $r = 0.5170$ ) and degree of unsaturation ( $r = 0.5920$ ) and a negative correlation against the ceramide chain length ( $r = -0.6668$ ) (figure 6H-K).

## INTEGRATION OF RESULTS

Integration of quantitative clinical characteristics (figure 3A, C, D), microbial properties (figure 4A-D) and barrier parameters (figure 6A-F) was performed using the entire dataset. The resulting PCA shows two distinguishable sets of data points with minimal overlap when stratifying for site (figure 7A). The abundance of CER[NS], the carbon chain length and the CER[NS]:CER[NP] ratio contribute most to the overall differential analysis (Supplemental Table S4). Min-max normalized visualisation of the most significant findings in a radar chart underline that the biggest differences are observed in the barrier compartment followed by inflammation (figure 5B). Small differences between lesional and non-lesional skin were observed in the microbial parameters, with only the abundance of *Staphylococcus* being markedly different.

## Discussion

SD is a multifactorial disease in which the interplay between the cutaneous microbiome, especially the presence of *Malassezia*, impaired skin barrier function and abnormal immunological responses seem integral to its pathogenesis.<sup>1</sup> In this study we comprehensively and non-invasively characterized the clinical representation of mild-to-moderate SD. We demonstrated a profound involvement of cutaneous barrier dysfunction with only small alterations in the microbiome, including the abundance of *Malassezia*, based on differences between lesional and non-lesional skin. This trial was performed in a sizeable number of 37 patients with similar disease burden after appropriate wash-outs and screening.

**Figure 6** Barrier parameters of lesional compared to non-lesional skin demonstrate impaired barrier function in lesional skin. Functional barrier integrity is measured by trans-epidermal water loss (A). The ceramide profile is depicted after grouping individual ceramides per subclass (B), with the ratio between the abundance of CER[NS] and CER[NP] highlighted (C). The abundance of short ceramide species CER[NSC34] (D) and degree of unsaturation (E) within CER[NS] is shown. The average carbon chain length (CCL) of the combined sphingosine base and fatty acid tail within the non-CER[EO] moiety is depicted (F). PCA analysis using all individual detected saturated ceramides yields two distinct population (G). Axes list the percentage of variance explained by the first two principal components, with the proximity of datapoints indicating similarity between samples. Correlations between TEWL and CER[NS]:CER[NP] (H), percentage CER[NSC34] (I), percentage of unsaturation (J) and CCL (K) are shown with a line representing the optimal fit from linear regression analysis and 95% confident interval and Pearson's correlation coefficient. TEWL; Trans-Epidermal Water Loss, MUCER; monounsaturated ceramide, CCL; carbon chain length, HR: hour.

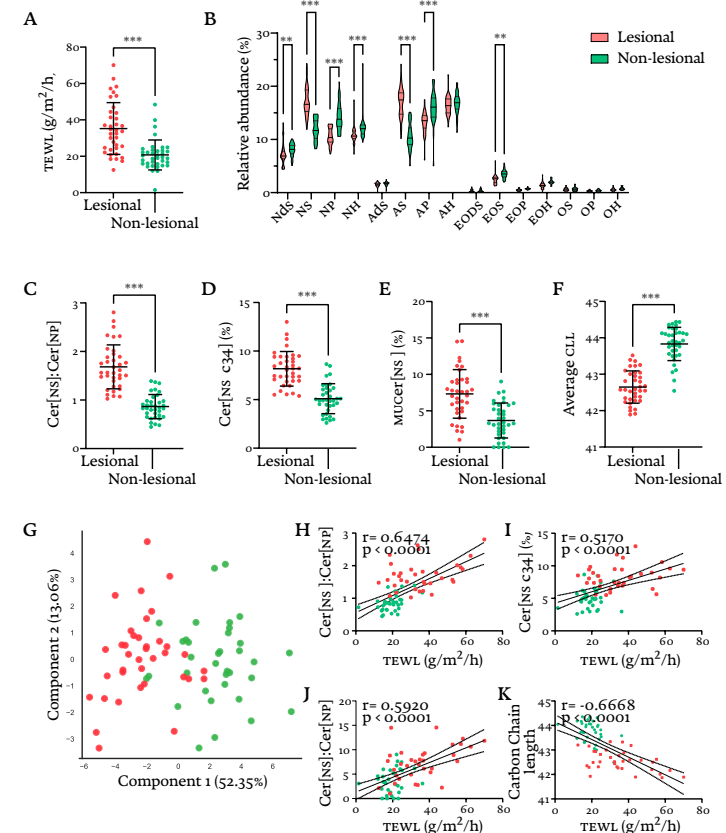
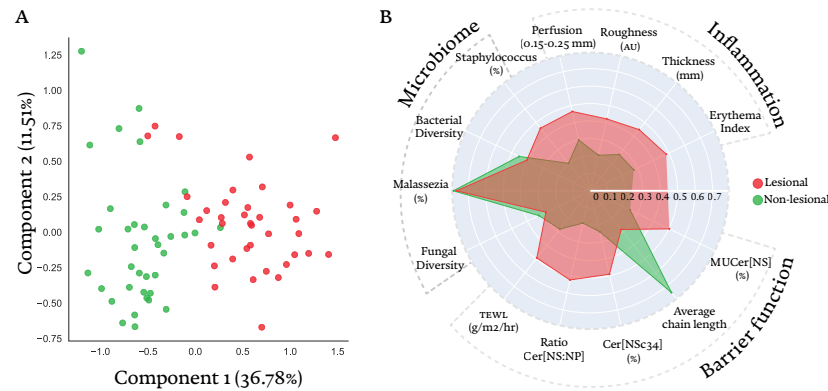


**Figure 7** Principal component analysis (PCA) of lesional and non-lesional skin using all individual datapoints (A). Axes list the percentage of variance explained by the first two principal components. Integrative visualization of major contributors within the three different axes by radar chart (B). The distance of a datapoint from the center represent the average value per parameter per site compared to the average value per parameter of both sites. AU; arbitrary units, TEWL; Trans-Epidermal Water Loss, MUCER; monounsaturated ceramide, CCL; carbon chain length, HR: hour



### INFLAMMATION OBJECTIVELY QUANTIFIED BY OPTICAL COHERENCE TOMOGRAPHY AND STANDARDIZED IMAGING

Visual assessment of SD, which includes the evaluation of erythema, is frequently used in daily clinical practice for disease monitoring. However, visual examination of the skin can be hampered by limited sensitivity, observer bias and overall intra- and inter-rater variability.<sup>29,30</sup> Therefore, we selected an objective approach to quantify cutaneous inflammation. Digitalized erythema assessments have been reported but not applied to SD.<sup>31-34</sup> Here, standardized cross-polarized light photography is used to capture consistent images and enhanced erythema,<sup>35</sup> resulting in a clear differentiation between lesional and non-lesional skin. Optical biopsies by OCT enabled the determination of additional (sub)cutaneous parameters. Inflammatory characteristics such as increased perfusion<sup>36</sup> and epidermal thickness, which corresponds to acanthosis,<sup>37,38</sup> were observed in lesional skin. Furthermore, a rougher lesional skin surface corresponds to the scaly phenotype of the disease.<sup>1</sup> Increased blood flow and epidermal thickness have been observed by

OCT in the involved skin of psoriasis and atopic dermatitis patients compared to uninvolved skin and healthy controls.<sup>39,40</sup> Stand-alone, but also combined, standardized photography and OCT qualify as valuable non-invasive tools which enable sensitive and selective endpoints for disease monitoring and detection of treatment responses in clinical trials.<sup>41</sup>

### MALASSEZIA AND STAPHYLOCOCCUS DOMINATE THE LESIONAL MICROBIOME

Bacterial analysis of the skin surface showed an increased abundance of *Staphylococcus* and decreased abundance of *Cutibacterium* on lesional skin which concurs with previous SD profiling studies.<sup>14,42</sup> *Staphylococcus*, and especially *S. aureus*, is considered to be a pro-inflammatory mediator in atopic dermatitis.<sup>43</sup> While limited phylogenetic resolution prevents the identification of *S. aureus* in this study, the observed increase of *Staphylococcus* combined with reports that *S. aureus* is more abundant in SD patients compared to healthy controls might indicate bacterial involvement in SD pathogenesis.<sup>44</sup> Despite reports of bacterial involvement in SD, microbial involvement remains primarily focussed on *Malassezia* as a key pathogen. However, no differences were observed between the abundance of *Malassezia* on lesional and non-lesional skin. This is in accordance with findings showing the presence of *Malassezia* is neither limited to lesional skin nor SD patients.<sup>3,6,14</sup> Additionally, facial skin of healthy volunteers also showed a seemingly small and *Malassezia* dominated mycobiome.<sup>45,46</sup> Although it is hypothesised that specific *Malassezia* species might be responsible for instigating inflammation as virulence factors differ between *Malassezia* species,<sup>47-49</sup> no significant differences on species level were observed in this study. Culturing led to successful isolation of *Malassezia* species in approximately half of the subjects, illustrating the known challenges of isolating *Malassezia* from clinical samples.<sup>50</sup> Except for *M. slooffiae*, all species are relatively frequently isolated from healthy and SD skin.<sup>51</sup> Remarkably, *M. slooffiae* has been reported to have little virulence when directly compared to *M. globosa* and *M. sympodialis*.<sup>48</sup> However, intra-species variation in virulence has been reported indicating that microbial activity rather than abundance is an important factor for the association of specific species to lesional skin.<sup>52,53</sup> Based on these results, it seems too straightforward to attribute SD pathogenesis to the presence of *Malassezia* alone.



## SUBSTANTIAL FUNCTIONAL AND COMPOSITIONAL BARRIER ALTERATIONS

Until now, the limited studies that have demonstrated functional barrier impairment in SD have neglected the lipid compartment as barrier component.<sup>54,55</sup> In this study, we show a substantially impacted barrier in lesional skin on functional grounds by TEWL and demonstrate concomitant changes in the ceramide profile. These compositional changes correlated with the degree of barrier impairment as judged by TEWL. In line with our study in SD, changes in the CER[NS]:CER[NP] ratio,<sup>56</sup> degree of unsaturation,<sup>57</sup> ceramide chain length<sup>12,58</sup> and presence of extremely short chain CER[NSC34]<sup>12,57,59,60</sup> in lesional skin have been observed in atopic dermatitis where barrier involvement is firmly established. These changes to the lipid profile appear to be induced by inflammation as lipid alterations can be evoked by atopic dermatitis and psoriasis associated pro-inflammatory cytokines *in vitro*<sup>61-63</sup> and normalize in response to anti-inflammatory treatment in atopic dermatitis patients.<sup>64</sup> Whether these alterations are therefore primarily linked to inflammation and only coincide with barrier dysfunction has been investigated in mechanistic studies using lipid model systems. Lacking an inflammatory component, these models have shown that increased CER[NS],<sup>65,66</sup> increased unsaturation<sup>67</sup> and decreased lipid chain length<sup>68</sup> directly increase permeability. Additionally, studies in healthy volunteers have shown CER[NS]:CER[NP] ratios in the face comparable to non-lesional skin without a location-dependent effect on CER[NSC34] abundances.<sup>69,70</sup> It is of note that total ceramide levels can change with age and seasons as demonstrated in healthy skin and acne, but without much effect on the relative ceramide subclass composition as reported on in the current study.<sup>69,71,72</sup> Additionally, the impact of these factors might be limited as patients serve as their own control. The predilection of SD lesions with areas known for increased water loss such as the mouth, eyelids and nasolabial folds might be confounding for the increased TEWL.<sup>55,73</sup> Indeed, healthy volunteers have shown TEWL values at the nasolabial fold that approach the lesional values observed in this study with comparable TEWL values at the cheek or forehead, sites where non-lesional measurements were often conducted.<sup>74,75</sup> Therefore, increased TEWL values in lesional skin may not reflect barrier impairment but rather indicate differences in normal physiological functioning between skin sites. However, the concurrent

correlations between the TEWL values and ceramide composition reaffirm the interdependence of SD functional barrier impairment and ceramide-compositional alterations.

## INTEGRATIVE DATA ANALYSIS EMPHASIZES IMPORTANCE OF BARRIER DYSFUNCTION

An integrative approach was taken to visualize the data after investigating the three hallmarks of SD separately. Using PCA, we elucidated which parameters of our dataset predominantly contribute to the SD phenotype. The abundance of CER[NS] and ceramide chain length showed to be the most important discriminating features. Indeed, the radar plot directs emphasis towards barrier function with little differences in the micro- and mycobiome. While the contribution of *Malassezia* seems to be negligible when only considering relative abundances, it should be re-emphasized that SD appears to be neither caused solely by barrier dysfunction nor microbial involvement but rather by the interplay between factors. This finding correlates with the shifting belief in literature that *Malassezia* might not be solely responsible for causing SD.<sup>5,6</sup> This highlights the added value of a multimodal and integrative approach to disease profiling which enables in-depth characterisation with the possibility to unravel part of pathogenesis.<sup>41</sup>

## Conclusion

In conclusion, this study demonstrates the importance of the barrier-inflammation axis in mild-to-moderate SD which seems to be more prominently involved compared to the microbiome. While not incorporating an internal healthy control group, our results are compared thoroughly with prior research in healthy volunteers through literature. Moreover, the results agree with and support existing literature regarding inflammation and microbial involvement in SD while complementing the current understanding of barrier dysfunction in SD. Barrier impairment parallels that of atopic dermatitis where emollients are used effectively.<sup>76</sup> Treating SD by improving the skin barrier function has been proposed as a potential adjuvant therapy,<sup>77</sup> but the management of SD remains focussed on anti-inflammatory and anti-fungal treatments.<sup>78</sup> Taken together, the incorporation of emollients, humectants or other barrier repair agents should not be neglected in the management of SD and might support current treatment modalities.

## REFERENCES

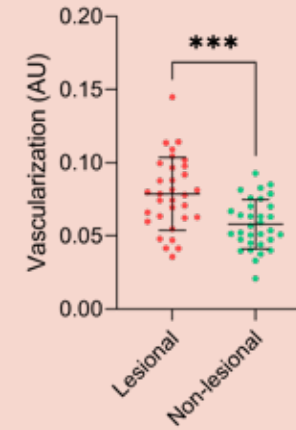
- Borda, L. J. & Wikramanayake, T. C. Seborrheic Dermatitis and Dandruff: A Comprehensive Review. *J Clin Invest Dermatol* 3, (2015).
- Goldenberg, G. Optimizing Treatment Approaches in Seborrheic Dermatitis. *J Clin Aesthet Dermatol* 6, 44 (2013).
- del Rosso, J. Q. & Kim, G. K. Seborrheic Dermatitis and Malassezia species: How Are They Related? *J Clin Aesthet Dermatol* 2, 14 (2009).
- Juntachai, W., Oura, T., Murayama, S. Y. & Kajiwara, S. The lipolytic enzymes activities of Malassezia species. *Med Mycol* 47, 477-484 (2009).
- Adalsteinsson, J. A., Kaushik, S., Muzumdar, S., Guttman, E. & Ungar, J. An update on the microbiology, immunology and genetics of seborrheic dermatitis. *Exp Dermatol* 29, 481-489 (2020).
- Wikramanayake, T. C., Borda, L. J., Miteva, M. & Paus, R. Seborrheic dermatitis—Looking beyond Malassezia. *Exp Dermatol* 28, 991-1001 (2019).
- Goh, J. P. Z. et al. The human pathobiont Malassezia furfur secretes protease Mfsap1 regulates cell dispersal and exacerbates skin inflammation. *Proceedings of the National Academy of Sciences* 119, e2212533119 (2022).
- Proksch, E., Brandner, J. M. & Jensen, J. M. The skin: an indispensable barrier. *Exp Dermatol* 17, 1063-1072 (2008).
- Uche, L. E., Gooris, G. S., Bouwstra, J. A. & Beddoes, C. M. High concentration of the ester-linked -hydroxy ceramide increases the permeability in skin lipid model membranes. *Biochimica et Biophysica Acta (BBA) - Biomembranes* 1863, 183487 (2021).
- Beddoes, C. M. et al. The importance of ceramide headgroup for lipid localisation in skin lipid models. *Biochimica et Biophysica Acta (BBA) - Biomembranes* 1864, 183886 (2022).
- Ishikawa, J. et al. Changes in the Ceramide Profile of Atopic Dermatitis Patients. *Journal of Investigative Dermatology* 130, 2511-2514 (2010).
- Janssens, M. et al. Increase in short-chain ceramides correlates with an altered lipid organization and decreased barrier function in atopic eczema patients. *J Lipid Res* 53, 2755-2766 (2012).
- Elias, P. M. Optimizing emollient therapy for skin barrier repair in atopic dermatitis. *Annals of Allergy, Asthma & Immunology* 128, 505-511 (2022).
- Tao, R., Li, R. & Wang, R. Skin microbiome alterations in seborrheic dermatitis and dandruff: A systematic review. *Exp Dermatol* 30, 1546-1553 (2021).
- Baysal, V., Yildirim, M., Ozcanli, C. & Ceyhan, A. M. Itraconazole in the treatment of seborrheic dermatitis: a new treatment modality. *Int J Dermatol* 43, 63-66 (2004).
- Elman, S., Hynan, L. S., Gabriel, V. & Mayo, M. J. The 5-D itch scale: a new measure of pruritus. *Br J Dermatol* 162, 587-593 (2010).
- Finlay, A. Y. & Khan, G. K. Dermatology Life Quality Index (DLQI)—a simple practical measure for routine clinical use. *Clin Exp Dermatol* 19, 210-216 (1994).
- Basra, M. K. A., Fenech, R., Gatt, R. M., Salek, M. S. & Finlay, A. Y. The Dermatology Life Quality Index 1994-2007: a comprehensive review of validation data and clinical results. *British Journal of Dermatology* 159, 997-1035 (2008).
- Yamamoto, T., Takiwaki, H., Arase, S. & Ohshima, H. Derivation and clinical application of special imaging by means of digital cameras and ImageJ freeware for quantification of erythema and pigmentation. *Skin Res Technol* 14, 26-34 (2008).
- Rasband, W. S. ImageJ. Preprint at <https://imagej.nih.gov/ij/>.
- Edgar, R. C. Search and clustering orders of magnitude faster than BLAST. *Bioinformatics* 26, 2460-2461 (2010).
- Zaharia, M. et al. Faster and More Accurate Sequence Alignment with SNAP. (2011) DOI:10.48550/arxiv.1111.5572.
- Cole, J. R. et al. Ribosomal Database Project: data and tools for high throughput rRNA analysis. *Nucleic Acids Res* 42, (2014).
- Abarenkov, K. et al. The UNITE database for molecular identification of fungi - recent updates and future perspectives. *New Phytologist* 186, 281-285 (2010).
- Kolecka, A. et al. Efficient identification of Malassezia yeasts by matrix-assisted laser desorption/ionization-time of flight mass spectrometry (MALDI-ToF MS). *British Journal of Dermatology* 170, 332-341 (2014).
- Boiten, W., Absalah, S., Vreeken, R., Bouwstra, J. & van Smeden, J. Quantitative analysis of ceramides using a novel lipidomics approach with three dimensional response modelling. *Biochimica et Biophysica Acta (BBA) - Molecular and Cell Biology of Lipids* 1861, 1652-1661 (2016).
- Motta, S. et al. Ceramide composition of the psoriatic scale. *Biochim Biophys Acta* 1182, 147-151 (1993).
- Janssens, M. et al. Non-lesional skin in atopic eczema patients shows a change in lipid organization that correlates with a decreased barrier function. *Journal of Investigative Dermatology* 132, S77 (2012).
- Poon, T. S. C. et al. Objective Measurement of Minimal Erythema and Melanogenic Doses Using Natural and Solar-simulated Light. *Photochem Photobiol* 78, 331-336 (2003).
- Ten Voorde, W. et al. A multimodal, comprehensive characterization of a cutaneous wound model in healthy volunteers. *Exp Dermatol* 00, 1-14 (2023).
- Logger, J. G. M., de Jong, E. M. G. J., Driessen, R. J. B. & van Erp, P. E. J. Evaluation of a simple image-based tool to quantify facial erythema in rosacea during treatment. *Skin Res Technol* 26, 804-812 (2020).
- Ohshima, H. et al. Quantitative evaluation of patch test reactions: a comparison between visual grading and erythema index image analysis. *Skin Research and Technology* 17, 220-225 (2011).
- Tao, M. et al. Objectively quantifying facial erythema in rosacea aided by the ImageJ analysis of VISIA red images. *Skin Research and Technology* 29, e13241 (2023).
- Frew, J. et al. The erythema Q-score, an imaging biomarker for redness in skin inflammation. *Exp Dermatol* 30, 377 (2021).
- Oh, Y., Markova, A., Noor, S. J. & Rotemberg, V. Standardized clinical photography considerations in patients across skin tones. *British Journal of Dermatology* 186, 352-354 (2022).
- Rajabi-Estarabadi, A., Tsang, D. C., Nouri, K. & Tosti, A. Evaluation of positive patch test reactions using optical coherence tomography: A pilot study. *Skin Research and Technology* 25, 625-630 (2019).
- Odorici, G., Losi, A., Ciardo, S., Pellacani, G. & Conti, A. Non-invasive evaluation of Secukinumab efficacy in severe plaque psoriasis with confocal microscopy and optical coherence tomography: A case report. *Skin Research and Technology* 24, 160-162 (2018).
- Yélamos, O. et al. Non-invasive clinical and microscopic evaluation of the response to treatment with clobetasol cream vs. calcipotriol/betamethasone dipropionate foam in mild to moderate plaque psoriasis: an investigator-initiated, phase IV, unicentric, open, randomized clinical trial. *Journal of the European Academy of Dermatology and Venereology* 35, 143 (2021).
- Byers, R. A. et al. Sub-clinical assessment of atopic dermatitis severity using angiographic optical coherence tomography. *Biomed Opt Express* 9, 2001 (2018).
- Ha-Wissel, L. et al. Case report: Optical coherence tomography for monitoring biologic therapy in psoriasis and atopic dermatitis. *Front Med (Lausanne)* 9, 2932 (2022).
- Rissmann, R., Moerland, M. & van Doorn, M. B. A. Blueprint for mechanistic, data-rich early phase clinical pharmacology studies in dermatology. *Br J Clin Pharmacol* 86, 1011 (2020).
- Sanders, M. G. H., Nijsten, T., Verlouw, J., Kraaij, R. & Pardo, L. M. Composition of cutaneous bacterial microbiome in seborrheic dermatitis patients: A cross-sectional study. *PLoS One* 16, e0251136 (2021).
- Geoghegan, J. A., Irvine, A. D. & Foster, T. J. Staphylococcus aureus and Atopic Dermatitis: A Complex and Evolving Relationship. *Trends Microbiol* 26, 484-497 (2018).
- Tamer, F., Yuksel, M., Sarifakioglu, E. & Karabag, Y. Staphylococcus aureus is the most common bacterial agent of the skin flora of patients with seborrheic dermatitis. *Dermatol Pract Concept* 8, 80-84 (2018).
- Findley, K. et al. Topographic diversity of fungal and bacterial communities in human skin. *Nature* 2013 498:7454 498, 367-370 (2013).
- Tao, R. et al. Comparative analysis of the facial microbiome between rosacea and seborrheic dermatitis. *Indian J Dermatol Venereol Leprol* 0, 1-3 (2023).
- Grice, E. A. & Dawson, T. L. Host-microbe interactions: Malassezia and human skin. *Curr Opin Microbiol* 40, 81-87 (2017).
- Angiolella, L. et al. Biofilm formation, adherence, and hydrophobicity of M. sympodialis, M. globosa, and M. slooffiae from clinical isolates and normal skin virulence factors of M. sympodialis, M. globosa and M. slooffiae. *Med Mycol* 58, 1162-1168 (2020).
- Theelen, B. et al. Malassezia ecology, pathophysiology, and treatment. *Med Mycol* 56, S10-S25 (2018).
- Abdillah, A. & Ranque, S. MalaSelect: A Selective Culture Medium for Malassezia Species. *Journal of Fungi* 7, (2021).
- Prohic, A., Jovovic Sadikovic, T., Krupalija-Fazlic, M. & Kusunovic-Vlahovljak, S. Malassezia species in healthy skin and in dermatological conditions. *Int J Dermatol* 55, 494-504 (2016).
- Angiolella, L. et al. Biofilm, adherence, and hydrophobicity as virulence factors in Malassezia furfur. *Med Mycol* 56, 110-116 (2018).
- Chebil, W. et al. Virulence factors of Malassezia strains isolated from pityriasis versicolor patients and healthy individuals. *Med Mycol* 60, 60 (2022).
- Tolleson, A. & Frithz, A. Transepidermal water loss and water content in the stratum corneum in infantile seborrheic dermatitis. *Acta Derm Venereol* 73, 18-20 (1993).
- Suchonwanit, P., Triyankulsri, K., Ploydaeng, M. & Leerunyakul, K. Assessing Biophysical and Physiological Profiles of Scalp Seborrheic Dermatitis in the Thai Population. *Biomed Res Int* 2019, (2019).
- Yokose, U. et al. The ceramide [NP]/[NS] ratio in the stratum corneum is a potential marker for skin properties and epidermal differentiation. *BMC Dermatol* 20, (2020).
- Danso, M. et al. Altered expression of epidermal lipid bio-synthesis enzymes in atopic dermatitis skin is accompanied by changes in stratum corneum lipid composition. *J Dermatol Sci* 88, 57-66 (2017).
- Berdyshev, E. et al. Dupilumab significantly improves skin barrier function in patients with moderate-to-severe atopic dermatitis. *Allergy* 77, 3388-3397 (2022).
- Ito, S. et al. Ceramide synthase 4 is highly expressed in involved skin of patients with atopic dermatitis. *J Eur Acad Dermatol Venereol* 31, 135-141 (2017).
- Kim, B. K. et al. Decrease of ceramides with long-chain fatty acids in psoriasis: Possible inhibitory effect of interferon gamma on chain elongation. *Exp Dermatol* 31, 122-132 (2022).
- Danso, M. O. et al. TNF- and Th2 cytokines induce atopic dermatitis-like features on epidermal differentiation proteins and stratum corneum lipids in human skin equivalents. *J Invest Dermatol* 134, 1941-1950 (2014).
- Tawada, C. et al. Interferon- Decreases Ceramides with Long-Chain Fatty Acids: Possible Involvement in Atopic Dermatitis and Psoriasis. *Journal of Investigative Dermatology* 134, 712-718 (2014).
- Berdyshev, E. et al. Lipid abnormalities in atopic skin are driven by type 2 cytokines. *JCI Insight* 3, (2018).
- Berdyshev, E. et al. Dupilumab significantly improves skin barrier function in patients with moderate-to-severe atopic dermatitis. *Allergy* 77, 3388-3397 (2022).
- Uche, L. E., Gooris, G. S., Bouwstra, J. A. & Beddoes, C. M. Barrier Capability of Skin Lipid Models: Effect of Ceramides and Free Fatty Acid Composition. *Langmuir* 35, 15376-15388 (2019).
- Nádabán, A. et al. The effect of sphingosine and phytosphingosine ceramide ratio on lipid arrangement and barrier functionality in skin lipid models. *J Lipid Res* (2023).
- Mojumdar, E. H., Helder, R. W. J., Gooris, G. S. & Bouwstra, J. A. Monounsaturated fatty acids reduce the barrier of stratum corneum lipid membranes by enhancing the formation of a hexagonal lateral packing. *Langmuir* 30, 6534-6543 (2014).
- Uche, L. E., Gooris, G. S., Bouwstra, J. A. & Beddoes, C. M. Increased Levels of Short-Chain Ceramides Modify the Lipid Organization and Reduce the Lipid Barrier of Skin Model Membranes. *Langmuir* 37, 9478-9489 (2021).
- Ishikawa, J. et al. Variations in the ceramide profile in different seasons and regions of the body contribute to stratum corneum functions. *Arch Dermatol Res* 305, 151-162 (2013).
- Mori, S. et al. Characterization of skin function associated with obesity and specific correlation to local/systemic parameters in American women. *Lipids Health Dis* 16, (2017).
- Rogers, J., Harding, C., Mayo, A., Banks, J. & Rawlings, A. V. Stratum corneum lipids: the effect of ageing and the seasons. *Arch Dermatol Res* 288, 765-770 (1996).
- Pappas, A., Kendall, A. C., Brownbridge, L. C., Batchvarova, N. & Nicolaou, A. Seasonal changes in epidermal ceramides are linked to impaired barrier function in acne patients. *Exp Dermatol* 27, 833-836 (2018).
- Voegeli, R., Gierschendorf, J., Summers, B. & Rawlings, A. V. Facial skin mapping: from single point bio-instrumental evaluation to continuous visualization of skin hydration, barrier function, skin surface pH, and sebum in different ethnic skin types. *Int J Cosmet Sci* 41, 411-424 (2019).
- Kobayashi, H. & Tagami, H. Distinct locational differences observable in biophysical functions of the

facial skin: with special emphasis on the poor functional properties of the stratum corneum of the perioral region. *Int J Cosmet Sci* 26, 91-101 (2004).

- 75 Voegeli, R., Rawlings, A. V., Seroul, P. & Summers, B. A novel continuous colour mapping approach for visualization of facial skin hydration and transepidermal water loss for four ethnic groups. *Int J Cosmet Sci* 37, 595-605 (2015).
- 76 van Zuuren, E. J., Fedorowicz, Z., Christensen, R., Lavrijsen, A. & Arents, B. W. M. Emollients and moisturisers for eczema. *Cochrane Database Syst Rev* 2017, (2017).
- 77 Mangion, S. E., Mackenzie, L., Roberts, M. S. & Holmes, A. M. Seborrheic dermatitis: topical therapeutics and formulation design. *European Journal of Pharmaceutics and Biopharmaceutics* 185, 148-164 (2023).
- 78 Desai, S., McCormick, E. & Friedman, A. An Up-to-Date Approach to the Management of Seborrheic Dermatitis. *J Drugs Dermatol* 21, 1373-1374 (2022).

## SUPPLEMENTAL MATERIAL

**Supplemental Figure s1** Average vascularization between 0.15 mm up to and including 0.25 mm of lesional and non-lesional skin as determined by optical coherence tomography.



**Supplemental Table s1** Overview of the location that imaging and Trans-epidermal Water Loss (TEWL) assessments were performed. Imaging includes both the Erythema Index as determined through standardized 2D-photography with VISIA and Optical Coherence Tomography (OCT). The table is continued in Supplemental Table 2.

Subject	Lesional Erythema and OCT	Non-lesional Erythema and OCT	Lesional TEWL	Non-lesional TEWL
1	Nosebridge	Left forehead	Nosebridge	Right forehead
2	Right nosefold	Right forehead	Right nosefold	Right forehead
3	Right nosefold	Right cheek	Right nosefold	Right cheek
4	Left nosefold	Right forehead	Left nosefold	Right forehead
5	Right nosefold	Right cheek	Left nosefold	Right cheek
6	Right nosefold	Left forehead	Right nosefold	Left forehead
7	Left forehead	Right cheek	Left forehead	Right cheek
8	Right nosefold	Right forehead	Right nosefold	Right forehead
9	Right nosefold	Right forehead	Right nosefold	Right forehead
10	Right nosefold	Right lower eyelid	Right nosefold	Right lower eyelid
11	Chin	Right forehead	Right nosefold	Right forehead
12	Right nosefold	Right forehead	Right nosefold	Right forehead
13	Right nosefold	Right forehead	Right nosefold	Right forehead
14	Right upper lip	Right forehead	Right upper lip	Right forehead
15	Right eyebrow, upper	Right cheek	Right eyebrow, upper	Right cheek
16	Nosebridge	Right cheek	Nosebridge	Right cheek
17	Right nosefold	Left forehead	Right nosefold	Left forehead
18	Left nosefold	Right forehead	Left nosefold	Right forehead
19	Right nosefold	Right forehead	Right nosefold	Right forehead
20	Right nosefold	Right cheek	Right nosefold	Right cheek
21	Left upper lip	Left forehead	Left upper lip	Left forehead
22	Right nosefold	Right forehead	Right nosefold	Right forehead
23	Right nosefold	Left forehead	Right nosefold	Left forehead
24	Right nosefold	Right forehead	Right nosefold	Right forehead
25	Right nosefold	Right forehead	Right nosefold	Right forehead
26	Right nosefold	Left forehead	Right nosefold	Left forehead
27	Right forehead	Left Cheek	Right forehead	Left Cheek
28	Left nosefold	Right cheek	Left nosefold	Right cheek
29	Right nosefold	Right forehead	Right nosefold	Right forehead
30	Nosebridge	Right cheek	Nosebridge	Right cheek
31	Left forehead	Left Cheek	Left forehead	Left Cheek
32	Left nosefold	Left Cheek	Left nosefold	Left Cheek
33	Right nosefold	Right cheek	Right nosefold	Right cheek
34	Left nosefold	Left Cheek	Left nosefold	Left Cheek
35	Left nosefold	Left forehead	Left nosefold	Left forehead
36	Left nosefold	Right forehead	Left nosefold	Right forehead
37	Right nosefold	Right forehead	Right nosefold	Right forehead

**Supplemental Table s2** Overview of the location that microbial assessments were performed. This is a continuation of Supplemental Table 1.

Subject	Lesional Swab location	Non-lesional Swab location	Lesional agar plates	Non-lesional agar plates
1	Nosebridge	Right forehead	Nosebridge	Left Cheek
2	Right nosefold	Right cheek	Nosebridge	Right forehead
3	Right nosefold	Right cheek	Left nosefold	Left Cheek
4	Left nosefold	Nosebridge	Left nosefold	Right forehead
5	Right nosefold	Left lower lip	Central forehead	Left lower eyelid
6	Right cheekbone	Left Cheekbone	Left nosefold	Right forehead
7	Right nosefold	Right cheek	Left forehead	Right cheek
8	Right nosefold	Right cheek	Nosebridge	Right forehead
9	Left nosefold	Left forehead	Left nosefold	Right forehead
10	Right upper lip	Right cheek	Left nosefold	Left Cheek
11	Left nosefold	Right forehead	Left Cheek	Left forehead
12	Right lower lip	Right forehead	Left lower lip	Left forehead
13	Right nosefold	Right forehead	Left nosefold	Left forehead
14	Left upper lip	Left forehead	Left eyebrow, upper	Right forehead
15	Left nosefold	Right cheek	Nosebridge	Left Cheek
16	Left Cheek	Right cheek	Nosebridge	Chin
17	Nosebridge	Left Cheek	Left nosefold	Right forehead
18	Right nosefold	Left Cheekbone	Left nosefold	Right forehead
19	Left nosefold	Right forehead	Right cheek	Left forehead
20	Left nosefold	Left forehead	Nosebridge	Left Cheek
21	Nosebridge	Left Cheek	Right upper lip	Right forehead
22	Left nosefold	Left forehead	Right lower lip	Left Cheek
23	Nosebridge	Left Cheek	Left nosefold	Right forehead
24	Left nosefold	Left forehead	Right cheek	Left Cheek
25	Left nosefold	Left forehead	Left nosefold	Left Cheek
26	Right nosefold	Left forehead	Nosebridge	Right cheekbone
27	Left Cheekbone	Left Cheek	Nosebridge	Left Cheek
28	Left nosefold	Right cheek	Nosebridge	Right cheekbone
29	Right nosefold	Left forehead	Right lower lip	Left forehead
30	Left nosefold	Left Cheek	Nosebridge	Left Cheek
31	Right forehead	Left Cheek	Left forehead	Right cheek
32	Nosebridge	Right cheek	Left nosefold	Left Cheek
33	Left nosefold	Left Cheek	Nosebridge	Right cheek
34	Nosebridge	Right cheekbone	Right nosefold	Left Cheek
35	Nosebridge	Right forehead	Right nosefold	Right cheek
36	Left upper lip	Right forehead	Left nosefold	Left Cheek
37	Chin	Right forehead	Left nosefold	Right forehead

**Supplemental Table s3** Overview of the location that lipidomics assessments were performed. This is a continuation of Supplemental Table 1 and 2.

Subject	Lesional tape stripping	Non-lesional tape stripping	Lesional sebum measurement	Non-lesional sebum measurement
1	Right nosefold	Right cheek	Nosebridge	Right forehead
2	Right nosefold	Left forehead	Left nosefold	Right forehead
3	Right nosefold	Left forehead	Right nosefold	Right cheekbone
4	Right nosefold	Left forehead	Left nosefold	Right forehead
5	Left nosefold	Right cheek	Left nosefold	Right cheekbone
6	Right nosefold	Left forehead	Right nosefold	Left forehead
7	Left forehead	Right forehead	Left forehead	Right cheekbone
8	Right nosefold	Left forehead	Right nosefold	Right forehead
9	Right nosefold	Right cheek	Right nosefold	Right forehead
10	Left upper lip	Left forehead	Right nosefold	Left forehead
11	Right nosefold	Right cheek	Right nosefold	Right forehead
12	Left eyebrow, upper	Right cheekbone	Right nosefold	Right forehead
13	Nosebridge	Left forehead	Right nosefold	Right forehead
14	Right upper lip	Right cheekbone	Right lip, upper	Right eyebrow, upper
15	Left eyebrow, upper	Left Cheek	Right eyebrow, upper	Right cheekbone
16	Right forehead	Left Cheek	Nosebridge	Right cheekbone
17	Right nosefold	Left forehead	Right nosefold	Left forehead
18	Nosebridge	Left forehead	Left forehead	Right forehead
19	Left nosefold	Left Cheekbone	Right cheekbone	Right forehead
20	Right nosefold	Right cheek	Right nosefold	Right cheek
21	Left upper lip	Left forehead	Left forehead	Left forehead
22	Left lower lip	Right cheekbone	Right nosefold	Right forehead
23	Left nosefold	Right forehead	Right nosefold	Left forehead
24	Left nosefold	Left forehead	Right nosefold	Left nosefold
25	Nosebridge	Left forehead	Right nosefold	Right forehead
26	Right nosefold	Right forehead	Right nosefold	Left forehead
27	Right cheekbone	Right cheek	Left cheek	Right forehead
28	Right nosefold	Right cheek	Left forehead	Right cheekbone
29	Left lower lip	Left Cheek	Right nosefold	Right forehead
30	Right nosefold	Right cheek	Nosebridge	Right cheek
31	Right forehead	Left Cheek	Left forehead	Left cheekbone
32	Right nosefold	Right forehead	Left nosefold	Left cheek
33	Right nosefold	Right cheekbone	Right nosefold	Left cheek
34	Left nosefold	Right cheek	Left forehead	Left cheek
35	Left nosefold	Left forehead	Left forehead	Left forehead
36	Right nosefold	Right cheek	Left nosefold	Right forehead
37	Right nosefold	Right cheekbone	Right nosefold	Right forehead

**Supplemental Table s4** The loadings per parameter used in the generation of the Principal Component Analysis in figure 7A.

Principal component 1 (36.78%)		Principal component 2 (11.51%)	
Parameter	Loading	Parameter	Loading
1 CER[NS]	0.304353	1 CER[OS]	0.377582
2 Ratio CER[NS:NP]	0.291921	2 CER[OP]	0.337539
3 CER[AS]	0.291615	3 CER[OH]	0.329363
4 CER[NSC34]	0.251295	4 CER[EODS]	0.242378
5 <i>Staphylococcus</i> (%)	0.207942	5 Fungal Diversity	0.214079
6 Trans-epidermal water loss	0.186069	6 Bloodflow at 0.2 mm	0.170678
7 Roughness	0.183875	7 Erythema	0.170665
8 MUCER[NS]	0.182895	8 Ratio CER[NS:NP]	0.168114
9 Erythema	0.143098	9 Bloodflow at 0.25 mm	0.16635
10 <i>Malassezia</i> (%)	0.028224	10 CER[EOH]	0.162232
11 Bloodflow at 0.15 mm	0.004897	11 CER[EOS]	0.161557
12 Bloodflow at 0.35 mm	0.003023	12 Bloodflow at 0.15 mm	0.158108
13 Bloodflow at 0.3 mm	-0.00488	13 Bloodflow at 0.3 mm	0.156788
14 Bloodflow at 0.2 mm	-0.0056	14 Bloodflow at 0.35 mm	0.145911
15 CER[ADS]	-0.00785	15 Bloodflow at 0.1 mm	0.130806
16 Bloodflow at 0.25 mm	-0.01004	16 CER[AH]	0.128493
17 Bloodflow at 0.1 mm	-0.01428	17 Trans-epidermal water loss	0.116807
18 CER[AH]	-0.02809	18 CER[AS]	0.116675
19 Bacterial Diversity	-0.02977	19 MUCER[NS]	0.109013
20 Fungal Diversity	-0.06081	20 CER[NS]	0.088148
21 CER[INDS]	-0.07766	21 CER[EOP]	0.039438
22 CER[NH]	-0.08445	22 CER[NH]	0.019096
23 CER[OS]	-0.11084	23 Roughness	-0.00196
24 CER[EODS]	-0.11781	24 CER[ADS]	-0.02022
25 CER[AP]	-0.12997	25 CER[NSC34]	-0.05328
26 CER[OP]	-0.14308	26 <i>Staphylococcus</i> (%)	-0.07786
27 CER[OH]	-0.18532	27 Bacterial Diversity	-0.09176
28 CER[EOS]	-0.22501	28 Carbon chain length	-0.13019
29 CER[NP]	-0.22817	29 CER[AP]	-0.15411
30 CER[EOH]	-0.24775	30 <i>Malassezia</i> (%)	-0.18649
31 CER[EOP]	-0.26718	31 CER[INDS]	-0.24213
32 Carbon chain length	-0.39401	32 CER[NP]	-0.24222

### CHAPTER 3

**TREATMENT WITH THE TOPICAL ANTIMICROBIAL PEPTIDE OMIGANAN IN MILD-TO-MODERATE FACIAL SEBORRHEIC DERMATITIS VERSUS KETOCONAZOLE AND PLACEBO: RESULTS OF A RANDOMIZED CONTROLLED PROOF-OF-CONCEPT TRIAL**

Published in: The International Journal of Molecular Sciences (INT. J. MOL. SCI. 2023, 24(18), 14315, DOI: 10.3390/ijms241814315)



Jannik Rousel,<sup>1,2</sup> Mahdi Saghari,<sup>1,3</sup> Lisa Pagan,<sup>1,3</sup> Andreea Nădăban,<sup>2</sup> Tom Gambragh,<sup>1</sup> Bart Theelen,<sup>4</sup> Marieke L. de Kam,<sup>1</sup> Jorine Haakman,<sup>1</sup> Hein E.C. van der Wall,<sup>1</sup> Gary L. Feiss,<sup>5</sup> Tessa Niemeyer-van der Kolk,<sup>1</sup> Jacobus Burggraaf,<sup>1,2,3</sup> Joke A. Bouwstra,<sup>2</sup> Robert Rissmann<sup>1,2,3</sup> and Martijn B.A. van Doorn<sup>1,6</sup>  
1. Centre for Human Drug Research, Leiden, NL / 2. Leiden Academic Centre for Drug Research, Leiden University, Leiden, NL / 3. Leiden University Medical Center, Leiden University, Leiden, NL / 4. Westerdijk Fungal Biodiversity Institute, Utrecht, NL / 5. Cutanea Life Sciences, Wayne, Pennsylvania, USA / 6. Department of Dermatology, Erasmus Medical Centre, Rotterdam, NL

## Abstract

**BACKGROUND:** Facial Seborrheic dermatitis (SD) is an inflammatory skin disease characterized by erythematous and scaly lesions on skin with high sebaceous gland activity. The yeast *Malassezia* is regarded as a key pathogenic driver in this disease, but increased *Staphylococcus* abundances and barrier dysfunction are implicated as well. Here, we evaluated the antimicrobial peptide omiganan as treatment for SD since it has shown both antifungal and antibacterial activity.

**METHODS:** A randomized, patient and evaluator-blinded trial was performed comparing the four-week twice daily topical administration of omiganan 1.75%, comparator ketoconazole 2.00% and placebo in patients with mild-to-moderate facial SD. Safety was monitored and efficacy determined by clinical scoring complemented with imaging. Microbial profiling was performed and barrier integrity assessed by trans-epidermal water loss and ceramide lipidomics.

**RESULTS:** Omiganan was safe and well tolerated but did not result in a significant clinical improvement of SD, nor affected other biomarkers, compared to placebo. Ketoconazole significantly reduced disease severity compared to placebo with reduced *Malassezia* abundances, increased microbial diversity and restored skin barrier function and decreased short chain ceramide species CER[NSC34]. No significant decreases in *Staphylococcus* abundances were observed compared to placebo.

**CONCLUSION:** Omiganan is well tolerated but not efficacious in the treatment of facial SD. Previously established antimicrobial and antifungal properties of omiganan could not be demonstrated. Our multimodal characterization of the response to ketoconazole has reaffirmed previous insights into its mechanism of action.

## Introduction

Seborrheic dermatitis (SD) is a chronic inflammatory skin disease characterized by erythematous, scaling and indurated papules and plaques in the face, scalp and upper chest which affects up to 3% of the general population. While aberrant immunological responses are integral to its pathophysiology, these appear to be induced or exacerbated by multiple co-factors such as an impaired barrier function, environmental factors and microbial disturbances.<sup>1</sup>

Microbial involvement is characterized by the commensal yeast *Malassezia* that acts as a key pathogenic driver in SD.<sup>2</sup> *Malassezia* thrives on the sebum-rich areas of the face and scalp where its lipase activity disturbs the skin barrier, facilitating the penetration of exogenous compounds including *Malassezia*'s own pro-inflammatory metabolites.<sup>3,4</sup> Besides clear mycobial involvement, SD is associated with microbial dysbiosis exemplified by increased abundances of *Staphylococcus*.<sup>5</sup> The potential contribution of *Staphylococcus* to the pathophysiology of SD is less clear but may be highly relevant in view of the prominent role of *S. aureus* in atopic dermatitis where it is considered a potential target for treatment.<sup>6,7</sup>

While it is hypothesized that the presence of *Malassezia* only facilitates inflammation instead of being a causative factor in SD development, antifungal treatment with imidazole derivatives such as ketoconazole are an established first-line topical treatment for mild SD.<sup>8</sup> As standalone antifungal therapy might not be sufficiently effective, combination treatment with topical corticosteroids is often required. However, corticosteroid use is constrained by several well-known side effects upon long-term exposure.<sup>9</sup> The absence of efficacious and safe treatment modalities highlights the need for novel therapies as SD continues to impact the quality of life, especially when located in the face.<sup>10</sup>

Based on the high degree of microbial involvement, targeting both the fungal and bacterial microbiome through antimicrobial peptides (AMPS) is hypothesised to be a promising therapeutic option. AMPS are part of the skin's innate immune response and are upregulated upon injury or cutaneous inflammation, providing and immediate host response against pathogens on the skin.<sup>11</sup>

Omiganan is an AMP that is analogous to indolicidin, a bovine member of the cathelicidin family. Its naturally occurring human counterpart LL-37

and derivatives have shown to be effective against selected *Malassezia* and *Staphylococcus* strains.<sup>12-15</sup> Omiganan itself has shown antibacterial and antifungal activity throughout a range of preclinical and clinical studies<sup>16-22</sup> with a favourable safety profile and microbial target engagement in doses from 1% to 2.5%.<sup>20-24</sup>

Ultimately, the broader spectrum activity of AMPS such as omiganan could make these compounds a valuable therapeutic option for patients with SD that might render combination with corticosteroids unnecessary. In this study, we investigated the clinical efficacy, safety, tolerability, microbiological and pharmacodynamic effects of omiganan 1.75% versus ketoconazole and placebo in patients with mild-to-moderate facial SD.

## Materials and methods

### MATERIALS

Chloroform (Honeywell, Charlotte, North Carolina, United States), methanol (Biosolve, Valkenswaard, the Netherlands), heptane (LiChorSolv, Merck, Darmstadt, Germany), UPLC grade isopropyl alcohol (Biosolve, Valkenswaard, the Netherlands) and ethanol (Biosolve, Valkenswaard, the Netherlands) were of HPLC grade or higher. Reagent grade potassium chloride (Sigma Aldrich, Saint-Louis, Missouri, USA) and ultrapure water from a Milli-Q Advantage A10 system (Merck, Darmstadt, Germany) were used. Synthetic ceramides and deuterated standards were purchased from Avanti Polar Lipids (Alabaster, Alabama, United States) or provided by Evonik (Essen, Germany).

### STUDY DESIGN, RANDOMIZATION AND TREATMENTS

The trial was registered under ClinicalTrials.gov Identifier NCT03688971 and EudraCT number 2017-003106-41. The study was performed from November 2019 to January 2022 at the Centre for Human Drug Research (Leiden, the Netherlands) following the Declaration of Helsinki principles and after ethical approval from the Stichting Beoordeling Ethiek Biomedisch Onderzoek (Assen, the Netherlands). Patients gave written informed consent prior to participation in the study. This was an evaluator and subject blinded parallel design evaluating the synthetic indolicidin-analog omiganan pentahydrochloride, a 12-amino-acid cationic peptide of H-Ile-Leu-Arg-Trp-Pro-Trp-Trp-Pro-Trp-Arg-Arg-Lys-NH<sub>2</sub>·5HCl formulated in a glycerol-based gel (see protocol). Eligible patients were randomized to twice daily topical

administration of 1.75% omiganan gel, vehicle gel or 2.00% ketoconazole cream on all facial lesional sites for 28 days. The first administration was performed under supervision of a dedicated and study-independent physician who also weighed the drug to monitor compliance and exposure. All subjects and other study staff remained blinded. An independent statistician generated the randomization in blocks of 3. Patient visits were scheduled at baseline, 7, 14, 21, 28 (end of treatment, EOT), 35 and 42 (end of study, EOS) days. Washing the face or applying medication was prohibited from 12 hours preceding a visit. Different skin sites were selected and monitored to accommodate all assessments. For each assessment, the same site was monitored on all visits. The full study protocol and assessment schedule is provided with the supplemental information.

### PATIENTS

Included patients exhibited mild-to-moderate facial SD as defined by an Investigator's Global Assessment (IGA) score of ≤2 at screening without any other clinically significant conditions, recent tanning and recent exposure to other SD treatments. Recent exposure was defined as two weeks for topical treatments and anti-dandruff shampoo, three weeks for phototherapy and four weeks for systemic treatment. Diagnosis of SD was confirmed by a dermatologist.

### PHYSICIAN AND PATIENT-REPORTED SCORING

SD severity was scored by the Seborrheic Dermatitis and Severity Index (SDASI),<sup>25</sup> limited to only the facial extent, 5-point IGA (0; clear, 1; almost clear, 2; mild, 3; moderate, 4; severe) and percentage of affected body surface area (%BSA). Patients completed the Dermatology Life Quality Index (DLQI),<sup>26</sup> and 5-Domain (5D) Itch score<sup>27</sup> in-clinic. Patients self-reported the daily 0 - 100 Numeric Rating Scale (NRS) Itch.

### CUTANEOUS IMAGING

Cross-polarized facial photography was performed using a VISIA-CR (Canfield Scientific, New Jersey, United States). The erythema index was determined through ImageJ (version 1.51h)<sup>28</sup> based on Yamamoto, *et al.* (2008).<sup>29</sup> An original Red Green Blue (RGB) image was split and the Red and Green channels log transformed. Subsequently, the green image was subtracted from the red channel and the resulting image multiplied by 3. The erythema index was



determined from a subject specific region of interest that spanned 380000 pixels. Epidermal thickness, superficial roughness and average degree of vascularisation between 0.1 and 0.25 mm was determined by Optical Coherence Tomography using a Vivosight Dx OCT and proprietary VivoTools 4.12 software (Michelson Diagnostics, Kent, United Kingdom).

### TRANS-EPIDERMAL WATER LOSS MEASUREMENTS

Trans-epidermal Water Loss (TEWL) was determined using an AquaFlux AF200 (Biox Systems Ltd., London, United Kingdom) after subjects acclimatized to the controlled environmental conditions (humidity <60%, temperature 22±2 °C) for at least 15 minutes. TEWL was normalized with an additional measurement of non-lesional skin elsewhere on the face to account for between-day variation as described before.<sup>30</sup>

### SEBUM MEASUREMENTS

Sebum levels were measured in triplicate on adjacent skin using a Sebumeter SM815 (Courage & Khazaka, Cologne, Germany). The average of three measurements was calculated.

### LIPIDOMICS ANALYSIS USING LIQUID CHROMATOGRAPHY-MASS SPECTROMETRY AFTER TAPE-STRIPPING

For lipidomics, Stratum corneum was sampled with 5 subsequent polyphenylene sulfide tape strips (Nichiban, Tokyo, Japan) of which the first one was discarded. Pressure was applied to each tape with a D500 D-squame Pressure Instrument (CuDerm Corporation, Dallas, Texas, United States). A 16 mm diameter hole was punched out from the section that was pressed onto the skin and the tape stored in chloroform:methanol (2:1). For extraction, tapes were shaken at 40 °C for one hour each in chloroform:methanol (2:1), chloroform:methanol:water (1:2:0.5), chloroform:methanol (1:1) and heptane:isopropylalcohol (1:1). The solvent was collected and a liquid-liquid extraction performed with the addition of 0.25M potassium chloride. The organic layer was washed with chloroform, filtered with 0.45 µm PVDF syringe filters (Grace, Deerfield, Illinois, United States) and concentrated.

Analysis was performed as described by Boiten *et al.* (2016).<sup>31</sup> Samples were dried and reconstituted in heptane:chloroform: methanol (95:2.5:2.5) containing 10 µM CER[N(24DEU)S(18)] at a concentration of 20 tapes/ml. Separation was achieved on an Acquity UPLC H-class (Waters, Milford, MA, USA)

with a normal phase PVA-silica column (5 µm particles, 100 × 2.1 mm i.d.) (YMC, Kyoto, Japan) with a binary gradient between heptane and heptane:isopropylalcohol:ethanol (2:1:1) from 98:2 to 50:50 at a flow rate of 0.8 ml/min. An XEVO TQ-S mass spectrometer (Waters, Milford, Massachusetts, United States) with APCI in positive ion mode scanning from 350 to 1200 m/z was used. Quality control samples from combined stratum corneum extracts and standard calibration curves containing 50, 20, 10, 5, 2, 1, 0.5, 0 µM of several ceramides (CER[NS, NDS, NP, AS, EOS AND EOP]) in triplicate were added to the run.

All detectable ceramides from the following ceramide classes were integrated based on their monoisotopic mass using TargetLynx V4.1 (Waters, Milford, Massachusetts, United States); CER[NDS], CER[NS], CER[NP], CER[NH], CER[ADS], CER[AS], CER[AP], CER[AH], CER[ODS], CER[OS], CER[OP], CER[OH], CER[EODS], CER[EOS], CER[EOP], CER[EOH]. Area Under the Curve (AUC) of the monoisotopic masses were corrected for the internal standard in Excel (Microsoft 365, Redmond, Washington, United States). The monoisotopic AUC was further corrected by the degree of water loss, theoretic <sup>13</sup>C isotope distribution and differences in ionization at higher molecular masses. The response per ceramide was converted to relative data using the total corrected AUC and calculations were made after grouping individual ceramides by their aforementioned class further graphing. The CER[NS]:CER[NP] ratio is the ratio between the relative total abundance of the subclasses. Average ceramide chain length is derived from the non-acyl ceramides moiety: CER[NDS], CER[NS], CER[NP], CER[NH], CER[ADS], CER[AS], CER[AP], CER[AH]. The abundance of CER[NSC34] and the amount of unsaturated CER[NS] is determined relative to all CER[NS] detected. Ceramide nomenclature from Motta *et al.* (1993) is used (see chapter 2, figure 2).<sup>32</sup>

### MICROBIAL PROFILING

Skin was swabbed for 10 seconds while constantly rotating using a sterile polyester tipped applicator (Puritan, Guilford, Maine, United States) soaked in 0.9% NaCl. Swabs were stored in DNA/RNA shield lysis buffer and beat beads (Zymo Research, Irvine, California, United States) at -80 °C until analysis. Extraction, sequencing and data generation was performed at Baseclear B.V. (Leiden, the Netherlands). Extraction was performed using a Zymo-BIOMICS DNA Miniprep Kit (Zymo Research) according to manufacturer's instructions. The sample was split and 16S RNA region v3-v4 or Internal

transcribed spacer region 2 (ITS2) sequencing was performed on a NovaSeq 6000 or MiSeq (Illumina, San Diego, California, United States of America) after appropriate sample quality control, for bacterial and fungal profiling respectively. The Reads were classified using the RDP database for bacterial<sup>33</sup> and UNITE ITS gene database for fungal<sup>34</sup> classification and extracted from the Genome Explorer portal (Baseclear B.V., Leiden, the Netherlands) before genera contributing <1% of the total hits were excluded using Python scripts (version 3.8.0, Python Software Foundation, Wilmington, Delaware, United States) and the relative abundance of the remaining microbes was determined. The relative abundance of genera comprising >1% of the total hits were included in the microbial profile (Supplemental Figure s5).

### MALASSEZIA SPECIES IDENTIFICATION BY MATRIX-ASSISTED LASER DESORPTION IONIZATION-TIME OF FLIGHT MASS SPECTROMETRY

Agar plates of 5.5 cm in diameter with modified Dixon agar medium (tritium microbiology B.V., Eindhoven, the Netherlands) were pressed against the skin for 20 minutes. Plates were transferred to the Alrijne Hospital (Leiden, the Netherlands) and cultured for up to 21 days at 33 °C. If mycological growth was observed, an isolate was taken and frozen in microbank 2D tubes (pro-lab diagnostics, Richmond Hill, Ontario, Canada). Isolates were transported to the Westerdijk Fungal Biodiversity Institute (Utrecht, the Netherlands), defrosted and further cultured on modified Leeming and Notman medium before analysis using matrix-assisted laser desorption ionization-time of flight mass spectrometry as described by Kolecka *et al.* (2014).<sup>35</sup>

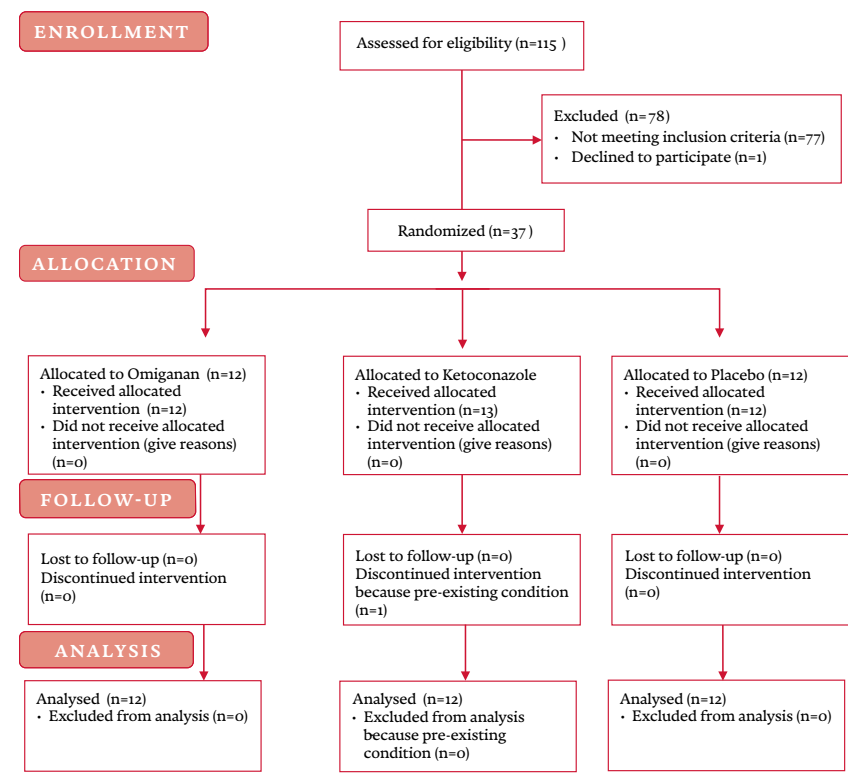
### STATISTICAL ANALYSIS

Calculations were performed using SAS version 9.4 (SAS Institute, Cary, North Carolina, United States). Group size was based on a previous trial with omiganan with significant clinical effects rather than a formal power calculation.<sup>30</sup> A mixed model of repeated measures with treatment, time and treatment-by-time as fixed factors and time as repeated factor within patient and an unstructured variance-covariance matrix was used. Contrasts between the omiganan and ketoconazole versus the placebo group were reported for EOT with p-value as \*:  $P \leq 0.05$ , -:  $P \leq 0.01$ , -\*:  $P \leq 0.001$ . Graphs show the change from baseline Least Square Means estimates and 95% confidence interval (CI).

## Results

a total of 115 patients were screened of which 37 were enrolled into the study and 36 patients successfully completed the study (figure 1). One patient randomized to ketoconazole was replaced due to a history of atopic dermatitis that remained undeclared at screening until flare-up during the study which was in violation of the study protocol.

**Figure 1** The consort 2010 flow diagram showing the number of patients that have been screened, were randomized and have successfully completed the trial and were subsequently included in the analysis.



Baseline characteristics and exposure were comparable between treatment groups (table 1). A total of 12 treatment emergent adverse events were reported by 11 subjects. Application site reactions in the omiganan and placebo group occurred in two subjects. Other adverse events were not considered related to the study drug.

**Table 1** Demographics of the study population and adverse events.

	Omiganan 1.75% (n=12)	Ketoconazole 2% (n =13)	Placebo (n=12)
<b>Demographics</b>			
Sex, n (%)			
Female	1 (8.3%)	2 (15.4%)	2 (16.7%)
Male	11 (91.7%)	11 (84.6%)	10 (83.3%)
Age, mean (SD)	32.2 (11.0)	39.7 (20.7)	41.3 (12.5)
Race, n (%)			
Asian	0 (0%)	1 (7.7%)	0 (0%)
Mixed	0 (0%)	1 (7.7%)	0 (0%)
Other	1 (8.3%)	0 (0%)	0 (0%)
White	11 (91.7%)	11 (84.6%)	12 (100%)
<b>Exposure</b>			
Total dose (g), mean (SD)	18.83 (10.83)	18.38 (13.64)	21.35 (8.50)
Dose per day (mg), mean (SD)	716.48 (413.46)	726.78 (461.27)	896.37 (349.10)
Dose per application (mg), mean (SD)	402.77 (237.05)	402.82 (248.930)	479.32 (187.16)
<b>Treatment emergent adverse events</b>			
Total Events	4	4	4
<b>General Disorders And Administration Site Conditions</b>			
Application Site Discomfort	1		
Influenza Like Illness	1	1	
<b>Infections And Infestations</b>			
Rhinolaryngitis			1
<b>Injury, Poisoning And Procedural Complications</b>			
Application Site Pruritus			1
Arthropod Bite	1		
Ligament Sprain		1	
<b>Nervous System Disorders</b>			
Headache			2
<b>Respiratory, Thoracic And Mediastinal Disorders</b>			
Cough		1	
Rhinorrhoea	1		

## OMIGANAN DOES NOT SHOW CLINICAL IMPROVEMENT COMPARED TO PLACEBO

Disease severity did not significantly decrease in the omiganan group compared to placebo as scored by SDASI (-1.5, CI -3.6 to 0.5,  $p = 0.1429$ ), IGA (-0.3, CI -0.7 to 0.1,  $p = 0.0971$ ) and %BSA (-0.11, CI -0.47 to 0.24,  $p = 0.5220$ ) at EOT (figures. 2A-C). In contrast, disease severity significantly decreased after treatment with ketoconazole (SDASI; -2.4, 95% CI -4.4 to -0.3,  $p = 0.0247$ , IGA; -0.5, 95% CI -0.9 to -0.2,  $p = 0.0054$ , %BSA; -0.51, 95% CI -0.86 to -0.16,  $p = 0.0052$ ). Patients completed questionnaires during their visit and twice daily NRS itch at home. Quality of life determined by DLQI ameliorated in both the omiganan (-2.6, 95% CI -6.4 to -1.1,  $p = 0.1671$ ) and ketoconazole (-2.1, 95% CI -5.8 to -1.7,  $p = 0.2811$ ) treatment group compared to placebo at EOT but did not reach statistical significance (figure 2D). The severity of itch in all three groups was similar (figures. 2E-F) as the 5D-itch questionnaire, completed during the study visit, and twice daily NRS itch, completed by patients at home, showed a similar time-course upon starting either treatment.

## NEITHER OMIGANAN NOR KETOCONAZOLE SHOW EFFECTS ON CLINICAL IMAGING COMPARED TO PLACEBO

Erythema was comparable to placebo in the omiganan group (-0.1682, 95% CI -2.9839 to 2.6475,  $p = 0.9044$ ) and non-significantly reduced in the ketoconazole group (-2.0531, 95% CI -4.7713 to 0.6652,  $p = 0.1346$ ) at EOT (figure 3A). No statistically significant differences were observed for epidermal thickness, roughness or vascularization determined by OCT over the course of the treatment period (figure 3B-C). Compared to placebo, skin roughness was slightly reduced by -5.3% for omiganan (95% CI -19.8% to 11.8%,  $p = 0.5090$ ) and -10.4% for ketoconazole (95% CI -23.7% to 5.3%,  $p = 0.1778$ ). Changes in blood flow were similar for both omiganan (-6.6%, 95% CI -37.0% to 38.6%,  $p = 0.7279$ ) and ketoconazole (0.2%, 95% CI -33.0% to 50.0%,  $p = 0.9901$ ) at EOT. Epidermal thickness was reduced but not significantly lower compared to placebo at EOT (omiganan; -5.3%, 95% CI -19.8% to 11.8%,  $p = 0.5090$ , ketoconazole; -10.4%, 95% CI -23.7% to 5.3%,  $p = 0.1778$ ). For ketoconazole only, this reduction culminated into a significant 14.9% (95% CI -25.2% to -3.1%,  $p = 0.0185$ ) reduction in epidermal thickness two weeks after the final administration.

**Figure 2** Clinical scoring by Seborrheic Dermatitis Area and Severity Index (A), Investigator’s Global Assessment (B) and percentage body surface area affected (C). Patient-reported outcomes by the Dermatology Life Quality Index (D) and 5D-itch questionnaire (E) are supplemented with twice daily reporting of the numeric rating scale (NRS) for the severity of itch (F). For clarity, only evening NRS itch has been graphed. Note that NRS itch was log-transformed to allow for statistical analysis and therefore is shown as percent change. P-values denote significance at End of Treatment (EOT). End of study (EOS) denotes the final follow-up visit.

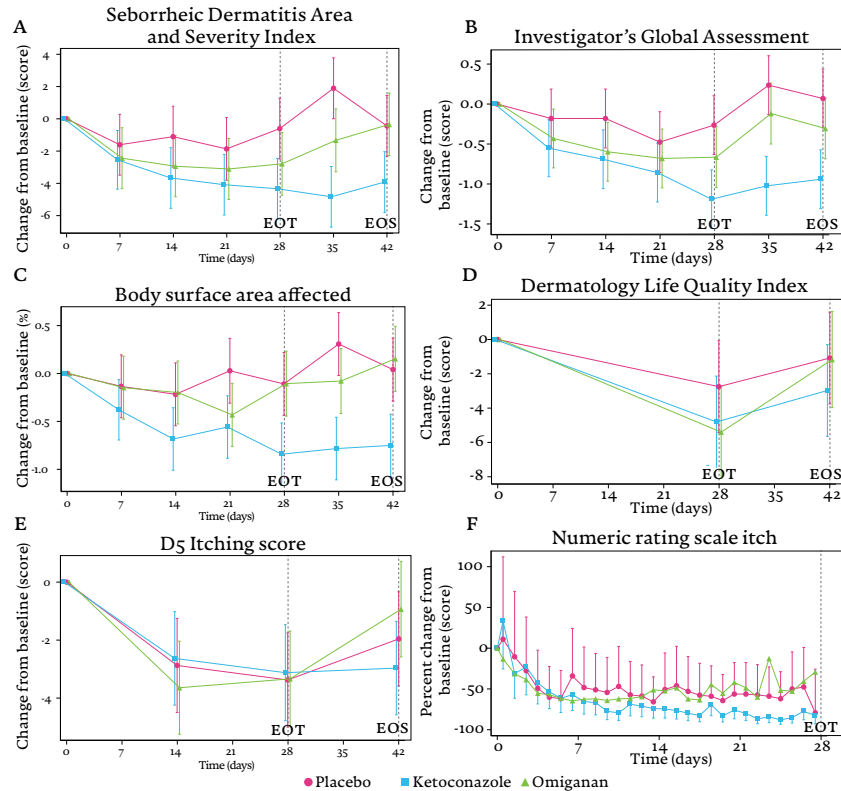
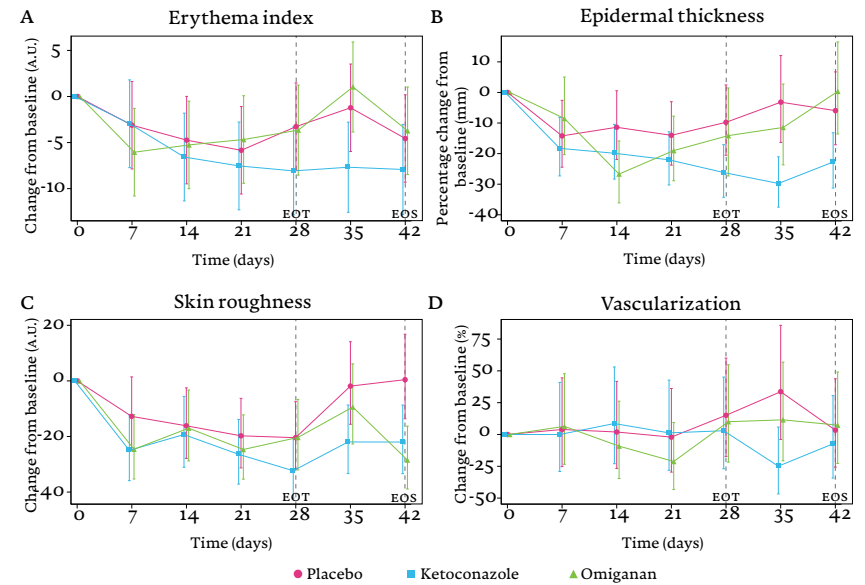


**Figure 3** Degree of erythema as determined by erythema index through standardized photography (A). Optical coherence tomography was used to measure the epidermal thickness (B), superficial skin roughness (C) and degree of vascularization (D). Epidermal thickness could not be determined in all scans due to high epidermal disorganization, see supplemental information. P-values denote significance at End of Treatment (EOT). End of study (EOS) denotes the final follow-up visit.



### SKIN BARRIER FUNCTION IMPROVES UPON TREATMENT WITH KETOCONAZOLE

TEWL was not significantly reduced compared to placebo at EOT for omiganan (-5.935, 95% CI -12.265 to 0.395,  $p = 0.0654$ ), but was significantly lower for ketoconazole (-8.932, 95% CI -15.367 to -2.497,  $p = 0.0076$ ) (figure 4). Molecular features correlating to barrier integrity showed improvements. Skewing of the ceramide subclass synthesis can be visualized with the CER[NS]:CER[NP] ratio (figure 4B). This ratio is reduced compared to placebo by both omiganan (-0.1155, 95% CI -0.5114 to 0.2805,  $p = 0.5563$ ) and ketoconazole (0.1549, 95% CI -0.5529 to 0.2430,  $p = 0.4332$ ) but does not reach significance. Similarly, the degree of unsaturation within CER[NS] reduced (omiganan: -0.2522, 95% CI -3.1697 to 2.6653,  $p = 0.8612$ , ketoconazole: -0.7301, 95% CI -3.5100 to 2.0498,

$p = 0.5960$ ) and the ceramide elongation increases (omiganan: 0.340, 95% CI -0.073 to 0.752,  $p = 0.1034$ , ketoconazole: 0.332, 95% CI -0.061 to 0.726,  $p = 0.0951$ ) for both treatments compared to placebo without reaching statistical significance. However, the abundance of CER[NSC34] is significantly lower compared to placebo in the ketoconazole group (-2.2344%, 95% CI -3.9182 to -0.5505,  $p = 0.0110$ ), but not in the omiganan group (-1.0454%, 95% CI -2.7724 to 0.6816,  $p = 0.2263$ ) (figure 4D). Sebum measurements did not show any differences and were troubled by high standard deviations (Supplemental Figure s1).

### KETOCONAZOLE BUT NOT OMIGANAN REDUCES MALASSEZIA ABUNDANCES

Treatment with omiganan did not result in significant mycobial changes with a -3.662% decrease in *Malassezia* (95% CI -16.366 to 9.042,  $p = 0.5630$ ) and a 0.1086 increase in the Shannon diversity index (95% CI -0.2097 to -0.4270,  $p = 0.4942$ ) compared to placebo (figures 5A-B). The impact of ketoconazole on the mycobioime was considerable with significant changes compared to placebo in both the abundance of *Malassezia* (-59.018%, 95% CI -71.952 to -46.084,  $p < 0.0001$ ) and fungal Shannon diversity index (1.39415, 95% CI 1.0959 to 1.6924,  $p < 0.0001$ ). While a decrease in the abundance of *Staphylococcus* is observed, this decrease is evident in all three groups and does not result in a significant treatment effect compared to placebo for omiganan (2.53%, 95% CI -9.73 to 14.79,  $p = 0.6783$ ) or ketoconazole (-7.46%, 95% CI -20.09 to 5.17,  $p = 0.2390$ ) (figure 5C). Concurrently, the bacterial biodiversity index did not significantly increase compared to placebo in the omiganan treatment group (0.0922, 95% CI -0.1583 to 0.3427,  $p = 0.4621$ ) (figure 5D). However, an increased microbial biodiversity is observed in the ketoconazole group (0.3412, 95% CI 0.0859 to 0.5964,  $p = 0.0100$ ). Overall, a strong correlation between biodiversity index and abundance of *Malassezia*, but not *Staphylococcus*, is observed (figure 6). Full microbial profiles and an overview of *Malassezia* species detected using contact plates are presented in Supplemental Figure s2 and Supplemental Table 1, respectively.

**Figure 4** Assessment of the cutaneous barrier function over time by trans-epidermal water loss measurements (A). Corresponding molecular ceramide biomarkers for barrier integrity were derived from the total stratum corneum ceramide profile and show the change in the ratio of the relative abundance of CER[NS] and CER[NP] (B), the carbon chain length of ceramides (C), the abundance of CER[NSC34] of total CER[NS] (D) and the fraction unsaturated ceramides of total CER[NS] (E). P-values denote significance at End of Treatment (EOT). End of study (EOS) denotes the final follow-up visit.

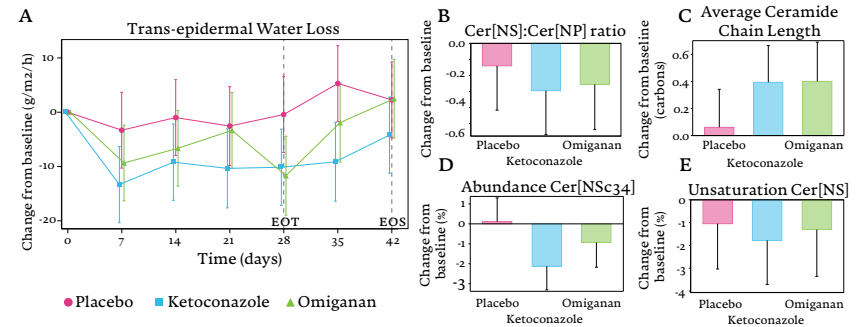


**Figure 5** The change in relative abundance of *Malassezia* (A) and *Staphylococcus* (C) and the corresponding microbial Shannon diversity indexes for the fungal (B) and bacterial (D) microbiome. Abundances and diversity indexes are condensed from the full microbial profiles as shown in the supplementary information. P-values denote significance at End of Treatment (EOT). End of study (EOS) denotes the final follow-up visit.

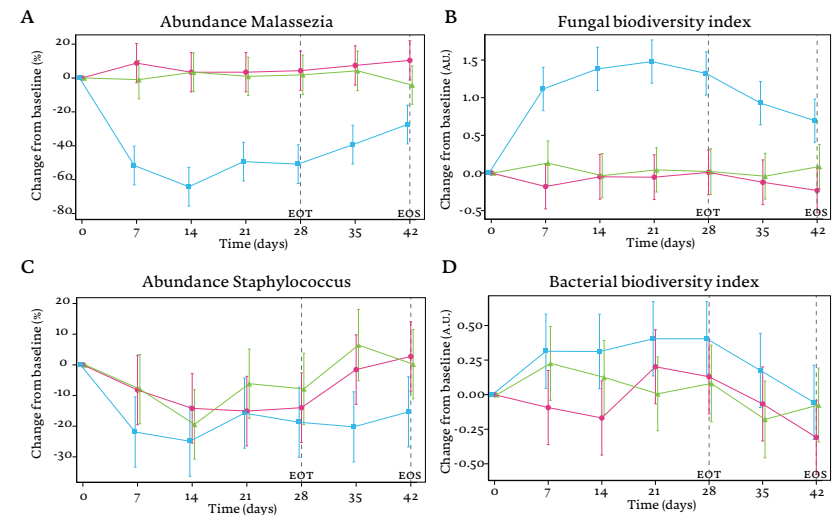
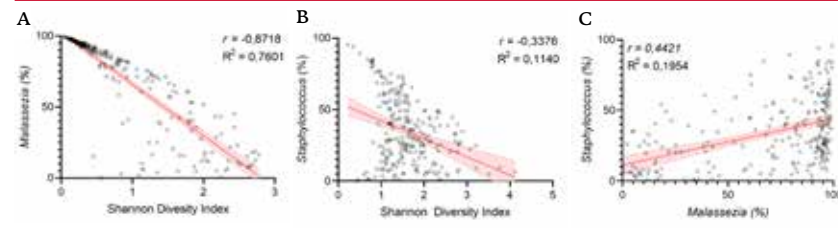


**Figure 6** Correlation between the fungal Shannon diversity index and *Malassezia* abundance (A), between the bacterial Shannon diversity index and *Staphylococcus* abundance (B) and between the abundances of *Malassezia* and *Staphylococcus* (C). Datapoints from all samples throughout the study have been plotted. A straight line with least square fit and 95% confidence area is plotted through the data. Pearson correlation coefficient ( $r$ ) and goodness of fit ( $R^2$ ) of the trendline is reported.



## Discussion

The use of topical AMPS holds promise for the treatment of SD since both anti-fungal and -bacterial involvement has been previously established in this disease. In this randomized, comparator- and placebo-controlled clinical trial, the efficacy of 1.75% omiganan gel was compared to its vehicle and standard-of-care 2% ketoconazole cream in a cohort of 36 patients with facial SD. Twice daily administration of omiganan did not result in significant decreased clinical scores compared to placebo. In contrast, a significant decrease in disease activity compared to placebo was observed in the ketoconazole treated group, which was paralleled by an improved barrier function and a reduced abundance of *Malassezia*.

Firstly, multiple physician-reported scores were performed to establish a treatment effect which yielded conclusive evidence of disease improvement in the ketoconazole treated group versus placebo. Clinical photography and OCT were performed to objectively reinforce these outcomes, but no differences were observed even though these methods could detect the reduction of cutaneous inflammation over time in previous studies.<sup>36,37</sup> The inclusion of mild patients with low baseline severity and a relatively small treatment effect size could have obscured these differences. Additionally, these localized digital assessments do not take a decreasing BSA into account in contrast to the SDASI. Patient-reported outcomes show improvement in all three treatment groups, highlighting the degree of placebo responses associated with metrics such as itch.<sup>38</sup> While the localized nature of SD impacts the responsiveness of

the SD-itch,<sup>27</sup> all scores still remain in agreement as previously reported.<sup>39,40</sup>

The absence of significant clinical effects in the omiganan-treated group was unexpected considering the clear microbiome-modulating effects found *in vitro* and *in vivo*.<sup>16-23,30</sup> Further investigation of the microbial composition showed that twice daily dosing with 1.75% omiganan did not significantly affect the abundance of *Staphylococcus* in our cohort of SD patients. Previous studies in atopic dermatitis patients demonstrated a clear staphylocidal effect and decreased microbial dysbiosis compared to placebo with doses as low as 1% once or twice daily.<sup>23,30</sup> Involvement of *Staphylococcus*, and especially *S. aureus*, in the pathophysiology of atopic dermatitis has gained attention,<sup>6,7</sup> and microbial profiling studies in SD have shown increased *Staphylococcus* abundances accordingly.<sup>5,41-43</sup> However, this might not necessarily constitute dysbiosis as these studies have shown similar<sup>42,43</sup> or higher<sup>41</sup> biodiversity indexes compared to healthy controls. Moreover, this study is limited by insufficient phylogenetic resolution which does not enable differentiation between *S. aureus* and *S. epidermidis* that are regarded as pathobiont and commensal species, respectively.<sup>44</sup> Ultimately, we demonstrate a decreased *Staphylococcus* abundance compared to baseline that did not correlate with clinical improvement as all three treatment groups, including placebo, showed a reduction in *Staphylococcus*. Combined with the fact that omiganan has successfully alleviated dysbiosis at lower dosages, we therefore postulate that microbial dysbiosis in SD may play a less important role based on the absence of a significant treatment-related effect.

While bacterial involvement might not be integral to SD pathophysiology, the involvement of *Malassezia* has been well established.<sup>1</sup> However, anti-fungal properties previously attributed to omiganan were not observed in this study.<sup>17-19</sup> Discord between the *in vitro* susceptibility of *Malassezia* and the clinical outcome of antimicrobial treatment has been described before and might in part be caused by the high between and within-species variation present among different *Malassezia* strains.<sup>45</sup> One could hypothesise that the lipid-rich environment at seborrheic skin sites may have presented a mismatch for the aqueous glycerol-based formulation of omiganan, possibly hampering direct interaction with *Malassezia*. Abundant interaction might be important as omiganan is thought to exert its antimicrobial function by association with the cell wall through cationic interactions, thereby destabilizing it and causing cell death.<sup>46</sup> However, the precise mechanism of omiganan and derivatives might extend beyond cell wall interactions.<sup>47,48</sup>

Additionally, *in vitro* assays do not incorporate a host compartment which could further distort translation to patients as omiganan has previously shown to enhance innate immune responses.<sup>49</sup> However, clinical scores used to establish disease severity did not indicate an increased degree of inflammation upon omiganan treatment in this study nor in previous studies in atopic dermatitis.<sup>23,24</sup>

In contrast to omiganan, ketoconazole demonstrated potent fungicidal effects. It remains debated whether ketoconazole's therapeutic effect can be contributed solely to its ability to impair mycobial cell-wall synthesis.<sup>50</sup> Ketoconazole has shown to concomitantly reduce disease burden and *Malassezia* abundances in SD,<sup>51,52</sup> but has also been efficacious without affecting *Malassezia* levels sparking debate on whether secondary interactions on microbial gene expression or host inflammatory responses are responsible.<sup>53</sup> In this study, we show that treatment with ketoconazole reduced disease severity and increased mycobial diversity which was strongly associated with a reduced abundance of *Malassezia*.

Interestingly, analysis of skin permeability and underlying molecular ceramide markers of barrier integrity yielded significant differences for ketoconazole compared to placebo. Barrier impairment is a hallmark of atopic dermatitis and barrier recovery is associated with clinical improvement.<sup>54,55</sup> Similarly, barrier dysfunction is implicated in SD.<sup>56-58</sup> While ketoconazole significantly recovered barrier function compared to placebo, effects on the relative ceramide composition were small. Ceramides constitute part of the lipid matrix in the stratum corneum and are linked to skin barrier performance.<sup>59</sup> In this study we observe a significant decrease in the abundance of CER[NSC34] in the ketoconazole group. This, and the non-significant observed increase in CER[NS]:CER[NP] ratio, increased ceramide chain length and reduced fraction of unsaturated CER[NS] compared with baseline can be associated with barrier recovery in atopic dermatitis and psoriasis.<sup>55,60-64</sup> Indeed, incorporation of more CER[NS],<sup>65,66</sup> unsaturated lipids<sup>67</sup> and shorter ceramides<sup>68</sup> resulted in increased permeability of skin lipid models. While the individual parameters do not show significant changes, their joint contribution might amount to a significant synergistic effect on cutaneous barrier function. The combination of barrier recovery and amelioration of barrier markers in response to treatment underlines the involvement of barrier dysfunction in SD.<sup>56</sup>

## Conclusion

In conclusion, this randomized controlled study shows that topical administration of the AMP omiganan is safe and well tolerated but does not lead to clinical improvement in patients with facial SD. Microbial abundances and skin barrier parameters were not significantly altered compared to placebo, either. In contrast, clinical scores significantly decreased in the ketoconazole group along with a potent fungicidal effect and an improved skin barrier function. This study underlines the efficacy of ketoconazole for the treatment of SD. Additionally, our comprehensive overview of the treatment response for ketoconazole as comparative treatment supports the conception that *Malassezia* plays a central role in SD pathophysiology. Moreover, it demonstrates the dynamics of the skin barrier function in response to treatment which supports previous studies that have implicated barrier dysfunction as a key factor in the pathophysiology of SD.

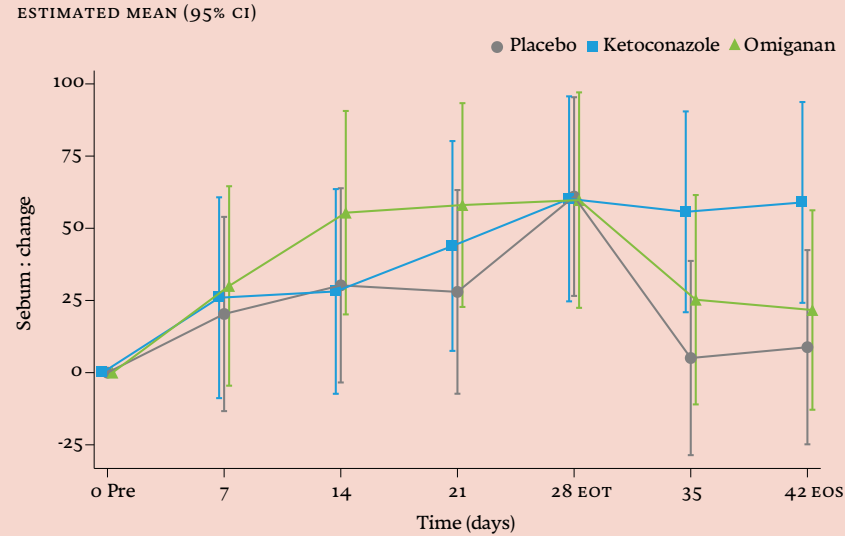
## REFERENCES

- Borda, L. J. & Wikramanayake, T. C. Seborrheic Dermatitis and Dandruff: A Comprehensive Review. *J Clin Invest Dermatol* 3, (2015).
- Wikramanayake, T. C., Borda, L. J., Miteva, M. & Paus, R. Seborrheic dermatitis—Looking beyond Malassezia. *Exp Dermatol* 28, 991-1001 (2019).
- Grice, E. A. & Dawson, T. L. Host-microbe interactions: Malassezia and human skin. *Curr Opin Microbiol* 40, 81-87 (2017).
- Sparber, F. et al. The Skin Commensal Yeast *Malassezia* Triggers a Type 17 Response that Coordinates Anti-fungal Immunity and Exacerbates Skin Inflammation. *Cell Host Microbe* 25, 389-403.e6 (2019).
- Tamer, F., Yuksel, M., Sarifakioglu, E. & Karabag, Y. *Staphylococcus aureus* is the most common bacterial agent of the skin flora of patients with seborrheic dermatitis. *Dermatol Pract Concept* 8, 80-84 (2018).
- Geoghegan, J. A., Irvine, A. D. & Foster, T. J. *Staphylococcus aureus* and Atopic Dermatitis: A Complex and Evolving Relationship. *Trends Microbiol* 26, 484-497 (2018).
- Ogonowska, P., Gilaberte, Y., Barańska-Rybak, W. & Nakonieczna, J. Colonization With *Staphylococcus aureus* in Atopic Dermatitis Patients: Attempts to Reveal the Unknown. *Front Microbiol* 11, 3468 (2021).
- del Rosso, J. Q. & Kim, G. K. Seborrheic Dermatitis and *Malassezia* species: How Are They Related? *J Clin Aesthet Dermatol* 2, 14 (2009).
- Goldust, M. et al. Diagnosis and Treatment of Seborrheic Dermatitis. *Am Fam Physician* 91, 185-190 (2015).
- Szepietowski, J. C. & Reich, A. Quality of life in patients with seborrheic dermatitis. <http://dx.doi.org/10.1586/17469872.3.1.43> (2014) DOI:10.1586/17469872.3.1.43
- Zhang, L. J. & Gallo, R. L. Antimicrobial peptides. *Current Biology* 26, R14-R19 (2016).
- López-García, B., Lee, P. H. A. & Gallo, R. L. Expression and potential function of cathelicidin antimicrobial peptides in dermatophytosis and tinea versicolor. *J Antimicrob Chemother* 57, 877-882 (2006).
- Haisma, E. M. et al. LL-37-derived peptides eradicate multidrug-resistant *Staphylococcus aureus* from thermally wounded human skin equivalents. *Antimicrob Agents Chemother* 58, 4411-4419 (2014).
- Geitani, R., Ayoub Moubareck, C., Touqui, L. & Karam Sarkis, D. Cationic antimicrobial peptides: Alternatives and/or adjuvants to antibiotics active against methicillin-resistant *Staphylococcus aureus* and multidrug-resistant *Pseudomonas aeruginosa*. *BMC Microbiol* 19, 1-12 (2019).
- Kang, J., Dietz, M. J. & Li, B. Antimicrobial peptide LL-37 is bactericidal against *Staphylococcus aureus* biofilms. *PLoS One* 14, (2019).
- Fritsche, T. R., Rhomberg, P. R., Sader, H. S. & Jones, R. N. Antimicrobial activity of omiganan pentahydrochloride tested against contemporary bacterial pathogens commonly responsible for catheter-associated infections. *J Antimicrob Chemother* 61, 1092-1098 (2008).
- Fritsche, T. R., Rhomberg, P. R., Sader, H. S. & Jones, R. N. Antimicrobial Activity of Omiganan Pentahydrochloride against Contemporary Fungal Pathogens Responsible for Catheter-Associated Infections. *Antimicrob Agents Chemother* 52, 1187 (2008).
- Żyrek, D. et al. The antimicrobial activity of omiganan alone and in combination against candida isolated from vulvovaginal candidiasis and bloodstream infections. *Antibiotics* 10, (2021).
- Sader, H. S., Fedler, K. A., Rennie, R. P., Stevens, S. & Jones, R. N. Omiganan pentahydrochloride (MBI 226), a topical 12-amino-acid cationic peptide: spectrum of antimicrobial activity and measurements of bactericidal activity. *Antimicrob Agents Chemother* 48, 3112-3118 (2004).
- Study of Antimicrobial Activity of Omiganan 1% Gel vs. Chlorhexidine 2% for Topical Skin Antisepsis in Healthy Adult Subjects - Study Results - ClinicalTrials.gov. <https://clinicaltrials.gov/ct2/show/results/NCT00608959>.
- Study of Omiganan 1% Gel in Preventing Catheter Infections/Colonization in Patients With Central Venous Catheters - Study Results - ClinicalTrials.gov. <https://clinicaltrials.gov/ct2/show/results/NCT00231153>.
- Rijsbergen, M. et al. Results of phase 2 trials exploring the safety and efficacy of omiganan in patients with human papillomavirus-induced genital lesions. *Br J Clin Pharmacol* 86, 2133-2143 (2020).
- Niemeyer-van der Kolk, T. et al. Topical antimicrobial peptide omiganan recovers cutaneous dysbiosis but does not improve clinical symptoms in patients with mild to moderate atopic dermatitis in a phase 2 randomized controlled trial. *J Am Acad Dermatol* 86, 854-862 (2022).
- Niemeyer-van der Kolk, T. et al. Pharmacodynamic Effects of Topical Omiganan in Patients With Mild to Moderate Atopic Dermatitis in a Randomized, Placebo-Controlled, Phase II Trial. *Clin Transl Sci* 13, 994-1003 (2020).
- Baysal, V., Yildirim, M., Ozcanli, C. & Ceyhan, A. M. Itraconazole in the treatment of seborrheic dermatitis: a new treatment modality. *Int J Dermatol* 43, 63-66 (2004).
- Finlay, A. Y. & Khan, G. K. Dermatology Life Quality Index (DLQI)—a simple practical measure for routine clinical use. *Clin Exp Dermatol* 19, 210-216 (1994).
- Elman, S., Hynan, L. S., Gabriel, V. & Mayo, M. J. The 5-D itch scale: a new measure of pruritus. *Br J Dermatol* 162, 587-593 (2010).
- Rasband, W. S. ImageJ. Preprint at <https://imagej.nih.gov/ij/>.
- Yamamoto, T., Takiwaki, H., Arase, S. & Ohshima, H. Derivation and clinical application of special imaging by means of digital cameras and Image J freeware for quantification of erythema and pigmentation. *Skin Res Technol* 14, 26-34 (2008).
- Niemeyer-van der Kolk, T. et al. Pharmacodynamic Effects of Topical Omiganan in Patients With Mild to Moderate Atopic Dermatitis in a Randomized, Placebo-Controlled, Phase II Trial. *Clin Transl Sci* 13, 994 (2020).
- Boiten, W., Absalah, S., Vreeken, R., Bouwstra, J. & van Smeden, J. Quantitative analysis of ceramides using a novel lipidomics approach with three dimensional response modelling. *Biochimica et Biophysica Acta (BBA) - Molecular and Cell Biology of Lipids* 1861, 1652-1661 (2016).
- Motta, S. et al. Ceramide composition of the psoriatic scale. *Biochim Biophys Acta* 1182, 147-151 (1993).
- Cole, J. R. et al. Ribosomal Database Project: data and tools for high throughput rRNA analysis. *Nucleic Acids Res* 42, (2014).
- Abarenkov, K. et al. The UNITE database for molecular identification of fungi - recent updates and future perspectives. *New Phytologist* 186, 281-285 (2010).
- Kolecka, A. et al. Efficient identification of *Malassezia* yeasts by matrix-assisted laser desorption/ionization-time of flight mass spectrometry (MALDI-TOF MS). *British Journal of Dermatology* 170, 332-341 (2014).
- Logger, J. G. M., de Jong, E. M. G. J., Driessen, R. J. B. & van Erp, P. E. J. Evaluation of a simple image-based tool to quantify facial erythema in rosacea during treatment. *Skin Res Technol* 26, 804-812 (2020).
- ten Voorde, W. et al. A Multimodal, Comprehensive Characterization of a Cutaneous Wound Model in Healthy Volunteers. *Exp Dermatol* (2023) DOI:10.1111/exd.14808.
- Van Laarhoven, A. I. M. et al. Placebo Effects on Itch: A Meta-Analysis of Clinical Trials of Patients with Dermatological Conditions. *Journal of Investigative Dermatology* 135, 1234-1243 (2015).
- Lai, J. W. et al. Transformation of 5-D itch scale and numerical rating scale in chronic hemodialysis patients. *BMC Nephrol* 18, 1-5 (2017).
- Kimel, M., Zeidler, C., Kwon, P., Revicki, D. & Ständer, S. Validation of Psychometric Properties of the Itch Numeric Rating Scale for Pruritus Associated With Prurigo Nodularis: A Secondary Analysis of a Randomized Clinical Trial. *JAMA Dermatol* 156, 1 (2020).
- Sanders, M. G. H., Nijsten, T., Verlouw, J., Kraaij, R. & Pardo, L. M. Composition of cutaneous bacterial microbiome in seborrheic dermatitis patients: A cross-sectional study. *PLoS One* 16, e0251136 (2021).
- Dityen, K. et al. Analysis of cutaneous bacterial microbiota of Thai patients with seborrheic dermatitis. *Exp Dermatol* 31, 1949-1955 (2022).
- Lin, Q. et al. *Malassezia* and *Staphylococcus* dominate scalp microbiome for seborrheic dermatitis. *Bioprocess Biosyst Eng* 44, 965-975 (2021).
- Brown, M. M. & Horswill, A. R. *Staphylococcus epidermidis*—Skin friend or foe? *PLoS Pathog* 16, (2020).
- Theelen, B. et al. *Malassezia* ecology, pathophysiology, and treatment. *Med Mycol* 56, S10-S25 (2018).
- Batista Araujo, J., Sastre de Souza, G. & Lorenzon, E. N. Indolicidin revisited: biological activity, potential applications and perspectives of an antimicrobial peptide not yet fully explored. *World J Microbiol Biotechnol* 38, 1-11 (2022).
- Melo, M. N. & Castanho, M. A. R. B. Omiganan interaction with bacterial membranes and cell wall models. Assigning a biological role to saturation. *Biochimica et Biophysica Acta (BBA) - Biomembranes* 1768, 1277-1290 (2007).
- Cardoso, M. H. et al. Non-Lytic Antibacterial Peptides That Translocate Through Bacterial Membranes to Act on Intracellular Targets. *Int J Mol Sci* 20, (2019).
- Grievink, H. W. et al. Antimicrobial Peptide Omiganan Enhances Interferon Responses to Endosomal Toll-Like Receptor Ligands in Human Peripheral Blood Mononuclear Cells. *Clin Transl Sci* 13, 891 (2020).
- Goularte-Silva, V. & Paulino, L. C. Ketoconazole beyond antifungal activity: Bioinformatic-based hypothesis on lipid metabolism in dandruff and seborrheic dermatitis. *Exp Dermatol* 31, 821-822 (2022).
- Tao, R. et al. Ketoconazole 2% cream alters the skin fungal microbiome in seborrheic dermatitis: a cohort study. *Clin Exp Dermatol* 47, 1088-1096 (2022).
- Katsambas, A. et al. A double-blind trial of treatment of seborrheic dermatitis with 2% ketoconazole cream compared with 1% hydrocortisone cream. *British Journal of Dermatology* 121, 353-357 (1989).
- Zani, M. B., Soares, R. C., Arruda, A. C. B. B., de Arruda, L. H. F. & Paulino, L. C. Ketoconazole does not decrease fungal amount in patients with seborrheic dermatitis. *British Journal of Dermatology* 175, 417-421 (2016).
- Tsakok, T., Woolf, R., Smith, C. H., Weidinger, S. & Flohr, C. Atopic dermatitis: the skin barrier and beyond. *British Journal of Dermatology* 180, 464-474 (2019).
- Berdyshev, E. et al. Dupilumab significantly improves skin barrier function in patients with moderate-to-severe atopic dermatitis. *Allergy* 77, 3388-3397 (2022).
- Jannik Rousel et al. Lesional Skin of Seborrheic Dermatitis Patients Is Characterized by Skin Barrier Dysfunction and Correlating Alterations in the Stratum Corneum Ceramide Composition. *Experimental Dermatology* (Submitted).
- Tolleson, A. & Frithz, A. Transepidermal water loss and water content in the stratum corneum in infantile seborrheic dermatitis. *Acta Derm Venereol* 73, 18-20 (1993).
- Suchonwanit, P., Triyankulsri, K., Ploydaeng, M. & Leerunyakul, K. Assessing Biophysical and Physiological Profiles of Scalp Seborrheic Dermatitis in the Thai Population. *Biomed Res Int* 2019, (2019).
- Proksch, E., Brandner, J. M. & Jensen, J. M. The skin: an indispensable barrier. *Exp Dermatol* 17, 1063-1072 (2008).
- Yokose, U. et al. The ceramide [NPI]/[NS] ratio in the stratum corneum is a potential marker for skin properties and epidermal differentiation. *BMC Dermatol* 20, (2020).
- Danso, M. et al. Altered expression of epidermal lipid bio-synthesis enzymes in atopic dermatitis skin is accompanied by changes in stratum corneum lipid composition. *J Dermatol Sci* 88, 57-66 (2017).
- Ito, S. et al. Ceramide synthase 4 is highly expressed in involved skin of patients with atopic dermatitis. *J Eur Acad Dermatol Venereol* 31, 135-141 (2017).
- Kim, B. K. et al. Decrease of ceramides with long-chain fatty acids in psoriasis: Possible inhibitory effect of interferon gamma on chain elongation. *Exp Dermatol* 31, 122-132 (2022).
- Uchino, T. et al. Comparative analysis of intercellular lipid organization and composition between psoriatic and healthy stratum corneum. *Chem Phys Lipids* 254, (2023).
- Uche, L. E., Gooris, G. S., Bouwstra, J. A. & Beddoes, C. M. Barrier Capability of Skin Lipid Models: Effect of Ceramides and Free Fatty Acid Composition. *Langmuir* 35, 15376-15388 (2019).
- Nádán, A. et al. Effect of sphingosine and phytosphingosine ceramide ratio on lipid arrangement and barrier function in skin lipid models. *J Lipid Res* 64, 100400 (2023).
- Mojumdar, E. H., Helder, R. W. J., Gooris, G. S. & Bouwstra, J. A. Monounsaturated fatty acids reduce the barrier of stratum corneum lipid membranes by enhancing the formation of a hexagonal lateral packing. *Langmuir* 30, 6534-6543 (2014).
- Uche, L. E., Gooris, G. S., Bouwstra, J. A. & Beddoes, C. M. High concentration of the ester-linked -hydroxy ceramide increases the permeability in skin lipid model membranes. *Biochimica et Biophysica Acta (BBA) - Biomembranes* 1863, 183487 (2021).

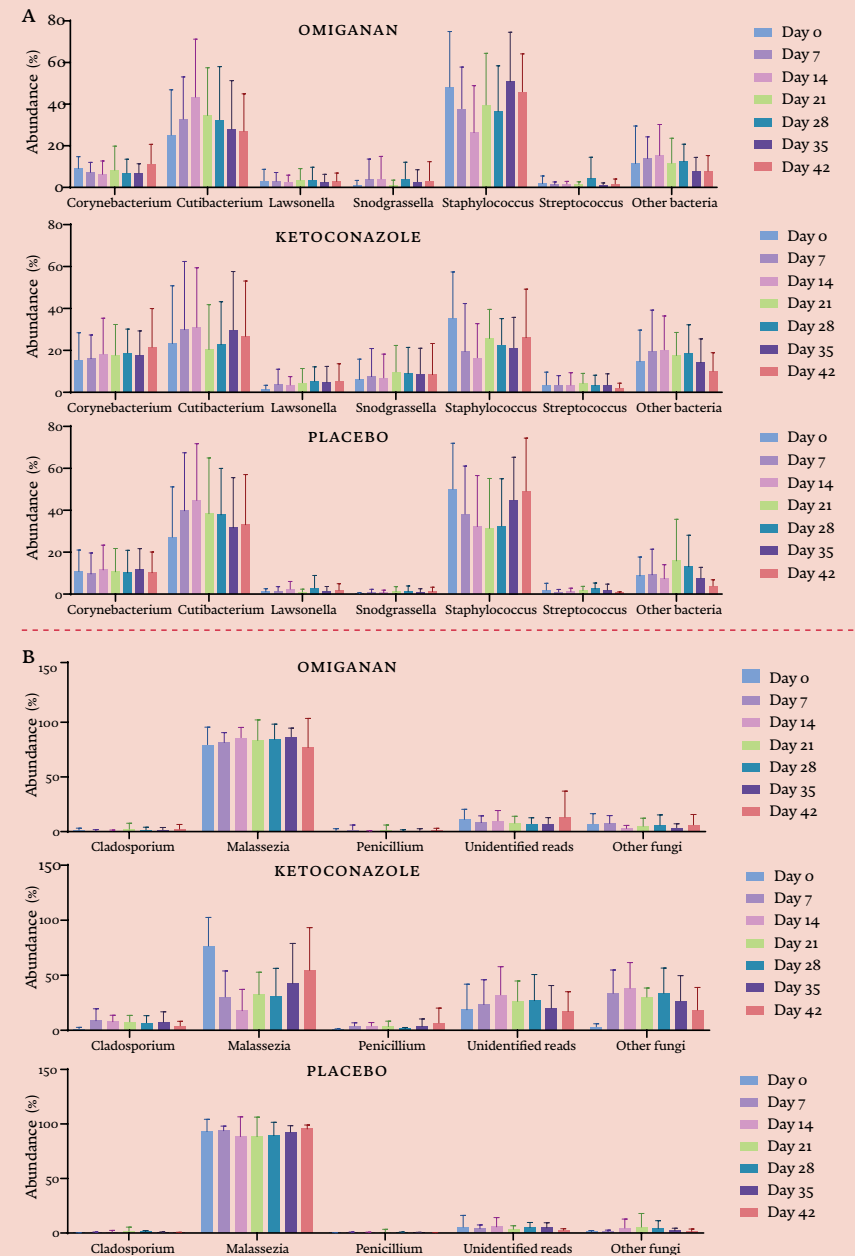


**SUPPLEMENTAL MATERIAL**

**Supplemental Figure s1** Change in the superficial sebum levels over time. Data shown represents the mean and 95% Confidence interval (CI). No significant change is observed compared to placebo for omiganan (2.53, 95% CI -9.73 to 14.79,  $p = 0.678$ ) and ketoconazole (-7.46, 95% CI -20.09 to 5.17,  $p = 0.239$ ).



**Supplemental Figure s2** The bacterial (A) and fungal (B) profile over time per treatment group. Error bars represent standard deviations. Bacteria that do not comprise 1% of the total abundance found between samples are grouped under “other”.



**Supplemental Table s1** Counts of *Malassezia* species identified by matrix-assisted laser desorption ionization-time of flight mass spectrometry per treatment. No agar plate yielded more than 1 different species of *Malassezia*. The total represents the total amount of detected species identified from the total of 12 agar plates.

	Day 0	Day 7	Day 14	Day 21	Day 28	Day 35	Day 42
<b>OMIGANAN</b>							
<i>M. slooffiae</i>	1	0	0	0	1	1	0
<i>M. sympodialis</i>	2	2	4	1	2	2	1
<i>M. globosa</i>	1	2	0	3	0	1	3
<i>M. restricta</i>	1	0	0	0	1	0	0
<i>M. obtusa</i>	0	0	0	0	1	0	0
<b>Total</b>	5/12	4/12	4/12	4/12	5/12	4/12	4/12
<b>KETOCONAZOLE</b>							
<i>M. slooffiae</i>	3	0	0	0	0	0	0
<i>M. sympodialis</i>	2	0	0	0	0	1	0
<i>M. globosa</i>	1	0	0	0	0	0	0
<i>M. restricta</i>	0	0	0	0	0	0	0
<i>M. obtusa</i>	0	0	0	0	0	0	0
<b>Total</b>	6/12	0/12	0/12	0/12	0/12	1/12	0/12
<b>PLACEBO</b>							
<i>M. slooffiae</i>	1	1	0	0	1	0	1
<i>M. sympodialis</i>	3	1	2	0	3	1	1
<i>M. globosa</i>	2	0	0	3	0	0	0
<i>M. restricta</i>	1	1	0	0	1	0	0
<i>M. obtusa</i>	0	0	0	0	0	0	0
<b>Total</b>	7/12	3/12	2/12	3/12	5/12	1/12	2/12

## SECTION 2

---

Enabling the potential of  
mild psoriasis patients  
for clinical research using  
a multimodal imaging  
approach

## CHAPTER 4

### GUSELKUMAB INDUCTION THERAPY DEMONSTRATES LONG-LASTING EFFICACY IN PATIENTS WITH MILD PSORIASIS: RESULTS FROM A RANDOMIZED, PLACEBO- CONTROLLED EXPLORATORY CLINICAL TRIAL

Adapted from: The Journal of the American  
Academy of Dermatology (90 (2) (2023), pp. 395-397,  
DOI: <https://doi.org/10.1016/j.jaad.2023.09.071>)



Jannik Rousel,<sup>1,2,\*</sup> Menthe E. Bergmans,<sup>1,3,\*</sup> Laura W.J. van der Meulen,<sup>1,5</sup> Lisa Pagan,<sup>1,3</sup> Digna T. de Bruin,<sup>1,3</sup> Marieke L. de Kam,<sup>1</sup> Naomi B. Klarenbeek,<sup>1</sup> Joke A. Bouwstra,<sup>2</sup> Marieke M.B. Seyger,<sup>4</sup> Juul M.P.A. van den Reek,<sup>4</sup> Tessa Niemeyer-van der Kolk,<sup>1</sup> Robert Rissmann,<sup>1,2,3</sup> and Martijn B.A. van Doorn, MD, PhD,<sup>1,5</sup> from the Next-Generation ImmunoDermatology (NGID) Consortium. \*These authors contributed equally.

1. Centre for Human Drug Research, Leiden, NL / 2. Leiden Academic Centre for Drug Research, Leiden University, Leiden, NL / 3. Leiden University Medical Centre, Leiden, NL / 4. Department of Dermatology, Radboud University Medical Center, Nijmegen, NL / 5. Department of Dermatology, Erasmus Medical Center, Rotterdam, NL.

## Abstract

**INTRODUCTION:** Biologics are effectively used to treat moderate-to-severe psoriasis but remain unavailable for mild psoriasis patients. Here, we report on the efficacy of ANTI-IL-23 therapy in mild psoriasis which might provide efficacious and long-term disease remission.

**METHODS:** We conducted a randomized double-blind, placebo-controlled single centre study in twenty mild psoriasis patients defined by a Psoriasis Area and Severity Index (PASI) score of  $\leq 5$  at screening. All patients were naïve to systemic and biologic therapies. Fifteen patients received guselkumab induction therapy and five patients received placebo. Subcutaneous injections with 100 mg guselkumab or placebo were administered at baseline, week 4 and week 12. PASI scores were evaluated up to week 24 at in-clinic visits. Thereafter, remote follow-up was performed to obtain patient self-assessments of remission.

**RESULTS:** Guselkumab treatment significantly reduced PASI scores compared to placebo as early as week 4. At week 24, mean absolute PASI scores in the guselkumab group decreased with  $91 \pm 8.8\%$  to  $0.52 \pm 0.51$ . PASI 100, -90, and -75 responses were achieved by 6 (40%), 8 (53%) and 15 (100%) guselkumab-treated patients, respectively. Adverse events were few and mild. All patients reported worsening of symptoms at on average  $32 \pm 9.7$  weeks after last dose.

**CONCLUSION:** We demonstrated that mild patients benefit immensely from a short regimen of guselkumab for a prolonged period of time. Our results indicate that a short blockade of IL-23 in mild psoriasis patients does not induce disease modification, but effects in patients using other approaches such as early intervention remain to be explored.

## Introduction

Biologics are rapidly becoming the standard of care for managing moderate-to-severe psoriasis but remain unavailable for mild psoriasis patients.<sup>1</sup> After exhausting topical treatment options, these patients are commonly left without effective treatment modalities due to the unfavorable benefit-to-risk profile associated with systemic treatments and financial constraints regarding the use of biologics.<sup>2</sup>

A ‘hit hard and early’ approach for moderate-to-severe psoriasis patients has been proposed that holds prospects of long-term disease modification. By addressing psoriatic inflammation at an early stage, it is postulated that the development of associated skin-resident T-CELLS can be halted and might even be able to modulate the course of disease.<sup>3</sup> Extending this approach to mild psoriasis may constitute a novel therapeutic strategy.

Here, we conducted a randomized double-blind, placebo-controlled study in twenty psoriasis patients that were defined as mild by a Psoriasis Area and Severity Index (PASI) score of  $\leq 5$  and the absence of psoriasis around special areas.<sup>4</sup> Patients were randomized to an induction regimen of guselkumab, an ANTI-IL-23P19 monoclonal antibody approved for the treatment of moderate-to-severe plaque psoriasis for which it has shown a high degree of efficacy, both in phase 3 trials and in clinical practice.<sup>5-7</sup> The efficacy of guselkumab therapy was assessed in-clinic over 24 weeks after which time to relapse was remotely monitored.

Altogether, this study contributes to the sparse knowledge available on biologic therapy in mild psoriasis patients and could help emphasize the long-lasting effect of a short treatment of guselkumab, with possible implications for clinical practice.

## Patients and methods

### CLINICAL TRIAL PROTOCOL

This study was an exploratory, single-centre, double-blinded and placebo controlled randomized clinical trial conducted at the Centre for Human Drug Research (CHDR) in Leiden, the Netherlands. The trial was conducted from September 2020 to January 2023 when 20 mild patients successfully completed their study participation. Remote follow-up was completed in March 2023. The trial protocol, informed consent form and associated documents

were reviewed and approved by the Medische Ethische ToetsingsCommissie Brabant (approval number P1926) prior to study start. The trial was conducted in accordance with the Declaration of Helsinki and Good Clinical Practice guidelines. All subjects provided informed consent prior to any study-related activities. The trial is registered under NCT04394936 “An Explorative Psoriasis Biomarker Study” at the ClinicalTrials.gov website.

### SCREENING AND ELIGIBILITY

Up to 4 weeks prior to study start, patients will undergo a medical screening to determine eligibility for the study. Screening was performed in a fasting state ( $\geq 4$  hours) and consisted of signing the informed consent form, a medical history check, a physical examination, a 12-lead ECG, recording of vital signs, determination of the subject’s demography, height and weight, blood sampling (haematology, biochemistry, virology, urinalysis and a pregnancy test for female subjects). A QuantiFERon test was performed to exclude the presence of a (latent) tuberculosis infection as per guselkumab Summary of Product Characteristics guidelines. In addition, skin types were assessed according to the Fitzpatrick classification; I) highly sensitive; always burn, never tan, II) highly sensitive; usually burn, tan less than average, III) Sensitive; sometimes mild burn, tan about average, IV) moderate sensitivity; rarely burn, tan more than average, V) low sensitivity; rarely burn, tans profusely, dark skin colour and VI) not sensitive: never burn, always tans, darkest skin colour. Furthermore, a thorough dermatological examination took place including clinical assessment of the severity of psoriasis by PASI scoring. The patient’s history with psoriasis and their past medication was recorded. A listing of in- and exclusion criteria is presented in the supplement.

### STUDY DESIGN

An estimated total of 20 patients with mild psoriasis, defined as having a PASI of  $\leq 5$ , were to be included in the study. Patients were randomized 3:1 to 100 mg guselkumab or placebo in blocks of four. To ensure randomization between males and females, males were assigned subject number 1 and up while females were assigned subject number 20 and down. Subjects visited the CHDR at day 0, day 14 ( $\pm 2$  days), day 28 ( $\pm 2$  days), day 56 ( $\pm 4$  days), day 84 ( $\pm 4$  days), day 112 ( $\pm 4$  days) and day 168 ( $\pm 4$  days). Subcutaneous drug administration was performed at the day 0, day 28 and day 84 visit. Because guselkumab visually differed from the placebo, administration was

performed by physicians who were not involved in study conduct to maintain blinding. Additionally, subjects were informed of this and instructed to look away during the administration of the study drug. After the last visit at day 168, patients were followed-up telephonically every three months until relapse was reported. Patients were asked 1) if they remained free of psoriasis since the last study visit, 2) when psoriasis had recurred or worsened since the day 168 visit, 3) if any psoriasis treatments were used between relapse or worsening and the day 168 visit, 4) where the psoriasis occurred or worsened, 5) how much body surface area was affected by psoriasis using the hand palm method, 6) if and how they are currently treating the psoriasis and 7) if their current treatment method is effective.

### CLINICAL OUTCOME MEASURES

Drug efficacy was determined by the change in PASI scoring assessed at all study visits. Due to the exploratory nature of the study, no absolute primary endpoint in terms of, e.g., the percentage of subjects obtaining PASI75 was set. Relapse was defined as a negative answer to the question “are you free of psoriasis since the last study visit” and a confirmative answer to “if not, when did psoriasis recur or worsen compared to the day 168 visit”.

### STATISTICAL ANALYSIS

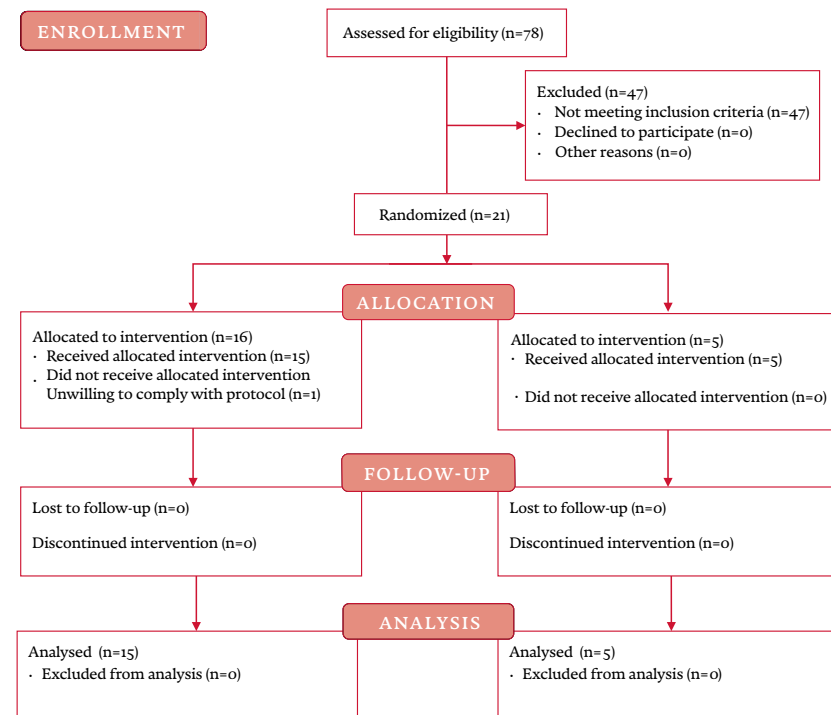
Graphing and calculation of the Pearson correlation coefficient ( $r$ ) was performed using PRISM 9 (Graphpad Software, San Diego, California, United States). Statistical analysis is performed in SAS 9.4 (SAS Institute Inc., Cary, North Carolina, United States). Power calculations were performed based on the ‘percentage of patients obtaining a 90% reduction in PASI score at week 16 using the data available based in literature of phase III guselkumab clinical trials.’<sup>5,6</sup> Based on this, a minimum sample size of 10 persons was needed to obtain at least 80% power when comparing the guselkumab and placebo group, with a two-sided alpha of 0.05. A repeated measures mixed effects model is performed with treatment, time and the interaction as fixed factors, and time as a repeated factor and the baseline measurement as covariate. The log-normal distributed data is log transformed before analysis, whereby the zeroes are treated as missing within the model. Analysis results are back transformed and estimated differences presented as % change. Treatment effects are reported with the estimated difference and the 95% confidence interval, the least square mean (LSM) estimates and the p-value. Estimates are

reported for each visit day and corresponding P-values are used for graphical representation. P-values denote significant differences between the guselkumab and placebo group and are reported as \*:  $P \leq 0.05$ , -:  $P \leq 0.01$ , -\*:  $P \leq 0.001$ .

## Results

A total of 78 patients were screened for eligibility of which 47 were excluded based on the in- and exclusion criteria (figure 1). Of the 21 included patients, 16 were randomized to guselkumab 100 mg and 5 were randomized to placebo. Except for 1 patient who dropped out prior to first dose citing unwillingness to comply with the protocol, all 20 subjects completed the in-clinic visits and all subjects completed the remote follow-up as per protocol.

**Figure 1** Consort flow chart for Randomized Controlled Trials. The flow diagram includes the number of patients screened, included per treatment arm and analysed per treatment arm.



All patients were naïve to systemic therapies including biologics. Disease duration ranged between 4 and 39 years. The demographics of the treatment population are shown in table 1.

**Table 1** Demographics of the study population.

		Guselkumab	Placebo	Total
Total number of patients		15	5	20
Age at first dose	≤ 18 years	0 (0%)	0 (0%)	0 (0%)
	18-65 years	14 (93%)	5 (100%)	19 (95%)
	≥ 65 years	1 (7%)	0 (0%)	1 (5%)
Sex	Female	3 (20%)	1 (20%)	4 (20%)
	Male	12 (80%)	4 (80%)	16 (80%)
Race	White	13 (87%)	4 (80%)	17 (85%)
	Asian	0 (0%)	1 (20%)	1 (5%)
	More than one	2 (13%)	0 (0%)	2 (10%)
Fitzpatrick	I	1 (7%)	0 (0%)	1 (5%)
	II	5 (33%)	2 (40%)	7 (35%)
	III	9 (60%)	2 (40%)	11 (55%)
	IV	0 (0%)	0 (0%)	0 (0%)
	V	0 (0%)	0 (0%)	0 (0%)
	VI	0 (0%)	1 (20%)	1 (5%)
Disease onset	≤ 4 years	0 (0%)	0 (0%)	0 (0%)
	4-10 years	4 (27%)	2 (40%)	6 (30%)
	10-20 years	6 (40%)	1 (20%)	7 (35%)
	≥ 20 years	5 (33%)	2 (40%)	7 (35%)

Before treatment the average PASI score was  $5.61 \pm 1.97$  and  $4.50 \pm 2.28$  for patients in the guselkumab and placebo group, respectively. Guselkumab treatment significantly reduced PASI scores compared to placebo from week 4 onwards (figure 2). At the last visit at week 24, this decrease culminated in an absolute PASI-score of  $0.52 \pm 0.51$  which corresponds to an average PASI reduction of  $91 \pm 8.8\%$ . For placebo, PASI remained comparable to baseline with  $4.42 \pm 2.51$  at week 24 compared to  $4.62 \pm 4.39$  at baseline. The response of patients is often expressed in the number of patients obtaining a 100%, 90%

or 75% reduction in PASI-score compared to the PASI-score at baseline. In the guselkumab-treated patients PASI-100, -90, and -75 responses were achieved by 6 (40%), 8 (53%) and 15 (100%) patients, respectively (figure 3).

**Figure 2** Treatment responses of guselkumab during the in-clinic period assessed using the Psoriasis Area and Severity Index (PASI) score. Data is expressed as mean absolute PASI and 95% confidence interval over time for patients randomized to guselkumab (n=15) or placebo (n=5). Patients were administered guselkumab 100 mg or placebo at day 0 (dose #1), week 4 (dose #2) and week 12 (dose #3). P-values denote significant differences between the guselkumab and placebo group from the results of a mixed-effects model and are reported as \*:  $P \leq 0.05$ , -:  $P \leq 0.01$ , -\*:  $P \leq 0.001$ .

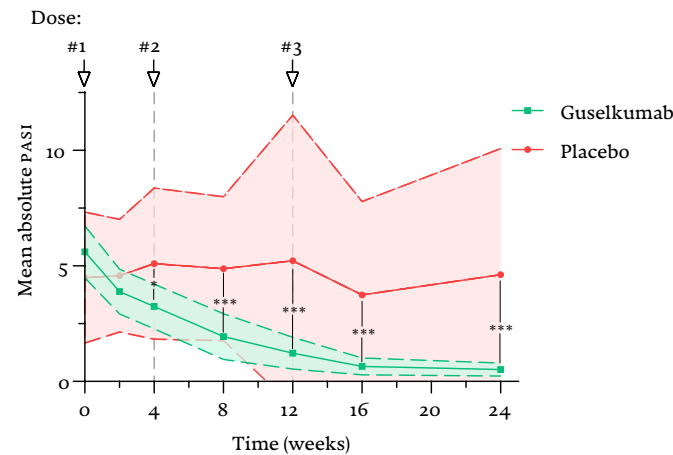
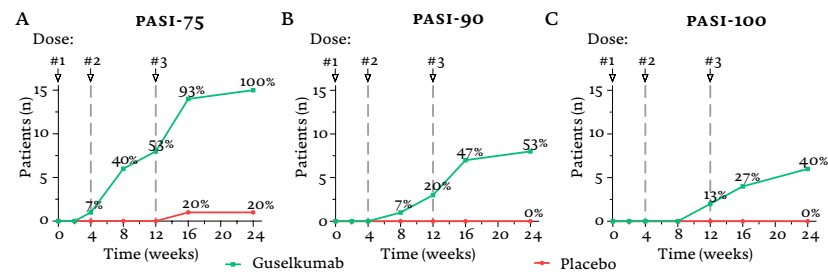


**Figure 3** The number of patients obtaining a Psoriasis Area And Severity Index (PASI)-75 (A), PASI90 (B) or PASI100 (C) response are shown over time. Responses indicate a 75%, 90% or 100% reduction in PASI score compared to baseline, respectively. The percentages indicate the percentage of patients per treatment group achieving the specified response.



During the in-clinic period, no serious adverse events were registered with the other observed adverse events being few in number, mild and transient (table 2). The most frequently reported treatment-emergent adverse event in the guselkumab group during the in-clinic treatment period was headache, reported by 4 patients (27%), followed by a SARS-COV-2 infection, reported by 3 patients (20%). These treatment-emergent adverse events were also reported in the placebo group with headache being reported by one patient (20%) and a SARS-COV-2 infection reported by 4 patients (80%).

**Table 2** Listing of all adverse events that occurred during the treatment period from week 0 up to week 24. Adverse events are grouped per high-level term. The number of adverse events and the number of subjects reporting that adverse events are reported per group.

		Guselkumab	Placebo	Total
TOTAL ADVERSE EVENTS		22 (11/15)	16 (5/5)	38 (16/20)
Eye disorders	Glaucoma	1 (1/15)	0 (0/5)	1 (1/20)
Gastrointestinal disorders	Diarrhea	1 (1/15)	3 (2/5)	4 (3/20)
	Abdominal pain	1 (1/15)	0 (0/5)	1 (1/20)
General disorders and administration site conditions	Fatigue	2 (2/15)	0 (0/5)	2 (2/20)
	Fever	1 (1/15)	0 (0/5)	1 (1/20)
	Injection site erythema	1 (1/15)	0 (0/5)	1 (1/20)
Infections and infestations	SARS-COV-2 infection	3 (3/15)	4 (4/5)	7 (7/20)
	Influenza	0 (0/15)	2 (2/5)	2 (2/20)
	Upper respiratory tract infections	2 (2/15)	1 (1/5)	3 (3/20)
	Vaginal yeast infection	0 (0/15)	1 (1/5)	1 (1/20)
	Impetigo	1 (1/15)	0 (0/5)	1 (1/20)
Injury poisoning and procedural complications	Traumatic hematoma	0 (0/15)	1 (1/5)	1 (1/20)
	Post vaccination syndrome	1 (1/15)	0 (0/5)	1 (1/20)
	Scarring	1 (1/15)	0 (0/5)	1 (1/20)
Nervous systems disorders	Headache	4 (4/15)	1 (1/5)	5 (5/20)
Skin and subcutaneous tissue disorders	Alopecia	1 (1/15)	1 (1/5)	2 (2/20)
	Allergic dermatitis	1 (1/15)	0 (0/5)	1 (1/20)
	Pruritus	1 (1/15)	1 (1/5)	2 (2/20)
Surgical and medical procedures	Dental operation	0 (0/15)	1 (1/5)	1 (1/20)



In order to determine whether the responses obtained during the in-clinic period were permanent, all patients randomized to guselkumab were followed-up after their last visit. Follow-up was performed by phone and patients were asked to report if their psoriasis had worsened compared to their last visit at week 24. All patients reported relapse (figure 4). Treatment effects at week 24 seemed were maintained for an additional  $20 \pm 9.7$  weeks, or with an average of  $32 \pm 9.7$  weeks after last dose. The earliest relapse was reported at 20 weeks after last dose by two subjects. Contrarily, one patient reported relapse to have occurred only 52 weeks after last dose.

Although sample size does not permit formal statistical testing, the PASI responses in the guselkumab group at week 24 appear positively correlated with time to relapse (figure 5). On the other hand, disease duration seemed neither to correlate with the efficacy of treatment at week 24 nor to the time to relapse. In this small cohort of patients, no clear association between joint involvement and response or time to relapse was observed.

## Discussion

This study shows that guselkumab induction therapy efficaciously decreases disease severity in mild psoriasis patients compared to placebo without significant adverse events. Milder forms of psoriasis are associated with slight differences in the transcriptomic profile compared to moderate-to-severe patients.<sup>8,9</sup> However, responses obtained in the current study remain comparable to those of phase 3 trials in moderate-to-severe psoriasis.<sup>6</sup> This reaffirms that mild patients can be effectively and safely treated with biologics, as previously demonstrated with the IL-17 inhibitor secukinumab in mild-to-moderate psoriasis patients.<sup>10</sup>

This study was performed during the COVID-19 pandemic. Several patients randomized to guselkumab experienced a SARS-COV-2 infection although all but one had been vaccinated prior to the time of infection. However, infection did not result in severe complications and were also prevalent in the placebo group. In line with previous reports, guselkumab therapy had not shown to increase the risk of infection or result in a more severe outcome of disease.<sup>11,12</sup>

Although highly efficacious, all patients randomized to guselkumab demonstrated relapse after cessation therapy. The associated median of 32 weeks in this study, exceeds the duration of 23 weeks reported for moderate-to-severe patients based on loss of PASI90 response.<sup>6</sup> Although loss of PASI

improvement from baseline or achieving higher Physician Global Assessment responses constitute more conventional measures to assess relapse,<sup>13</sup> clinical scoring in mild patients is associated with low sensitivity which complicate its effective use in this population.<sup>14</sup> Instead, patient-assessed remission was implemented to monitor whether remission was permanent. This patient-centric alternative was minimally burdensome for patients and facilitated complete follow-up of all enrolled subjects.

**Figure 4** Time until patient-reported relapse in weeks after withdrawal from guselkumab therapy. Patients are stratified in their corresponding response group based on their Psoriasis Area And Severity Index (PASI) score at the end of the treatment period at week 24.

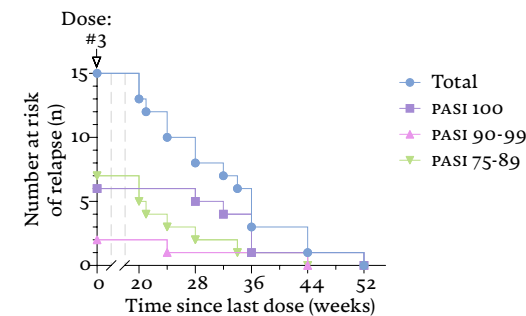
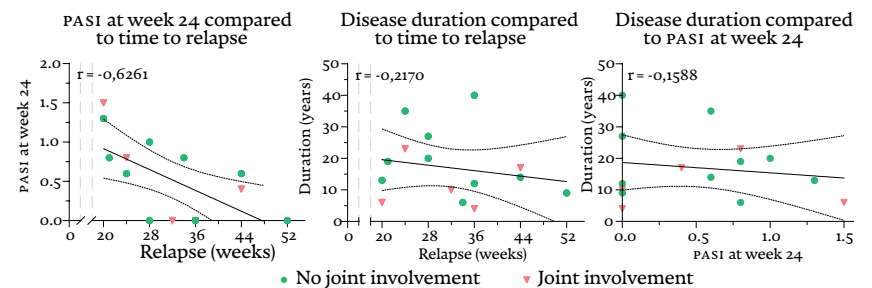


**Figure 5** Correlations between the final Psoriasis Area and Severity Index (PASI) obtained at the last study visit at week 24 and time to relapse, correlation between the disease onset and time to relapse, and correlation between the disease onset and final PASI obtained. Subjects that reported joint complaints at screening are indicated with a triangle. A line representing the best fitting linear regression through all data-points (regardless of joint involvement) and corresponding 95% confidence intervals are presented along with the Pearson correlation coefficient ( $r$ ).



The exploratory and small size of the guselkumab cohort in this study provides insufficient grounds to correlate between disease characteristics, treatment response and time to relapse. However, PASI responses at week 24 appear positively correlated with time to relapse which is in line with results from moderate-to-severe patients.<sup>15</sup> No correlations were observed between disease duration and time to relapse nor response at end of study. Although negative correlations between disease duration and time to relapse have been observed before,<sup>16,17</sup> the minimum disease duration of this cohort with 4 years might have already been too high.

## Conclusion

To conclude, we demonstrate that mild patients can benefit immensely from a short regimen of guselkumab for a prolonged period of time. Our results indicate that blocking IL-23 in mild psoriasis does not induce disease modification, but effects in patients with shorter disease duration or after extended treatment remain to be explored.

## REFERENCES

- Puig, L. PASI90 response: the new standard in therapeutic efficacy for psoriasis. *J Eur Acad Dermatol Venereol* **29**, 645-648 (2015).
- Menter, A. *et al.* Joint American Academy of Dermatology-National Psoriasis Foundation guidelines of care for the management of psoriasis with systemic nonbiologic therapies. *J Am Acad Dermatol* **82**, 1445-1486 (2020).
- Eyerich, K. *et al.* Protocol: IL-23 blockade with guselkumab potentially modifies psoriasis pathogenesis: rationale and study protocol of a phase 3b, randomised, double-blind, multicentre study in participants with moderate-to-severe plaque-type psoriasis (Guide). *BMJ Open* **11**, 49822 (2021).
- Strober, B. *et al.* Recategorization of psoriasis severity: Delphi consensus from the International Psoriasis Council. *J Am Acad Dermatol* **82**, 117-122 (2020).
- Blauvelt, A. *et al.* Efficacy and safety of guselkumab, an anti-interleukin-23 monoclonal antibody, compared with adalimumab for the continuous treatment of patients with moderate to severe psoriasis: Results from the phase III, double-blinded, placebo- and active comparator-controlled Voyage 1 trial. *J Am Acad Dermatol* **76**, 405-417 (2017).
- Reich, K. *et al.* Efficacy and safety of guselkumab, an anti-interleukin-23 monoclonal antibody, compared with adalimumab for the treatment of patients with moderate to severe psoriasis with randomized withdrawal and retreatment: Results from the phase III, double-blind, placebo- and active comparator-controlled Voyage 2 trial. *J Am Acad Dermatol* **76**, 418-431 (2017).
- Puig, L., Daudén, E., Cuervas-Mons, M., Novella, C. & Guisado, C. Persistence and effectiveness of guselkumab treatment in patients with moderate-to-severe plaque psoriasis in a non-interventional real-world setting: The Spring study. *Journal of the European Academy of Dermatology and Venereology* **00**, 1-11 (2023).
- Nikamo, P., Lysell, J. & Ståhle, M. Association with Genetic Variants in the IL-23 and NF-B Pathways Discriminates between Mild and Severe Psoriasis Skin Disease. *Journal of Investigative Dermatology* **135**, 1969-1976 (2015).
- Kim, J. *et al.* Molecular Phenotyping Small (Asian) versus Large (Western) Plaque Psoriasis Shows Common Activation of IL-17 Pathway Genes, but Different Regulatory Gene Sets. *J Invest Dermatol* **136**, 161 (2016).
- Kim, J. *et al.* Secukinumab improves mild-to-moderate psoriasis: A randomized, placebo-controlled exploratory clinical trial. *J Am Acad Dermatol* **88**, 428-430 (2023).
- Gisoni, P. *et al.* Incidence rates of hospitalization and death from COVID-19 in patients with psoriasis receiving biological treatment: A Northern Italy experience. *J Allergy Clin Immunol* **147**, 558 (2021).
- Piaserico, S., Gisoni, P., Cazzaniga, S. & Naldi, L. Lack of Evidence for an Increased Risk of Severe COVID-19 in Psoriasis Patients on Biologics: A Cohort Study from Northeast Italy. *Am J Clin Dermatol* **21**, 749 (2020).
- Tian, D. & Lai, Y. The Relapse of Psoriasis: Mechanisms and Mysteries. *JID Innov* **2**, 100116 (2022).
- Papp, K. A. *et al.* The Proposed PASI-HD Provides More Precise Assessment of Plaque Psoriasis Severity in Anatomical Regions with a Low Area Score. *Dermatol Ther (Heidelb)* **11**, 1079-1083 (2021).
- Chiu, H. Y. *et al.* Predictors of time to relapse following ustekinumab withdrawal in patients with psoriasis who had responded to therapy: An 8-year multicenter study. *J Am Acad Dermatol* **88**, 71-78 (2023).
- Liu, X. *et al.* Identification of clinical and biomarker parameters associated with long-term maintenance of PASI 90 response following guselkumab treatment withdrawal in psoriasis. *Journal of the European Academy of Dermatology and Venereology* **33**, 3-19 (2019).
- Schäkel, K. *et al.* Early disease intervention with guselkumab in psoriasis leads to a higher rate of stable complete skin clearance ('clinical super response'): Week 28 results from the ongoing phase IIIb randomized, double-blind, parallel-group, Guide study. *J Eur Acad Dermatol Venereol* **37**, 2016-2027 (2023).

## SUPPLEMENTAL MATERIAL

### IN- AND EXCLUSION CRITERIA

#### INCLUSION CRITERIA

*Eligible psoriasis patients must meet all of the following inclusion criteria at screening:*

- 1 Male or non-pregnant female subjects, 18 to 75 years of age (inclusive),
- 2 Diagnosed with plaque psoriasis at least 6 months prior to study participation,
- 3 Willing to discontinue any psoriasis therapy other than emollients,
- 4 Having mild (PASI  $\geq 1$  and  $\leq 5$ ) plaque psoriasis,
- 5  $\geq 2$  plaques suitable for repeated assessments with at least one of these lesions on the extremities with a minimal target lesion score between 6 and 9 (target lesion scoring constituted the summed erythema, induration and scaling score of the PASI score for an individual plaque),
- 6 Willing to give written informed consent and willing and able to comply with the study protocol.

#### EXCLUSION CRITERIA

*Eligible psoriasis patients must meet none of the following exclusion criteria at screening:*

- 1 Having primarily erythrodermic, pustular or guttate psoriasis,
- 2 Having medication-induced psoriasis,
- 3 Having previously failed on ANTI-IL23 therapy,
- 4 Having received treatments for psoriasis within the following intervals prior to the start of the study:  $< 2$  weeks for topical

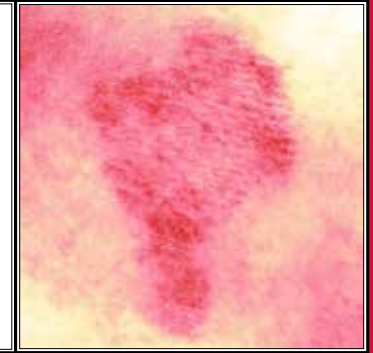
treatment,  $< 4$  weeks for phototherapy,  $< 4$  weeks for non-biologic systemic treatment,  $< 4$  weeks for etanercept,  $< 8$  weeks for adalimumab and  $< 3$  months for ANTI-IL17, ANTI-IL12(/23) and ANTI-IL23 treatments,

- 5 History or symptoms of any significant uncontrolled disease that may interfere with the study objectives in the opinion of the Investigator (excluding psoriasis and conditions that are related to psoriasis),
- 6 History of immunological abnormality that may interfere with study objectives in the opinion of the Investigator,
- 7 Known infection requiring antibiotic therapy within the last 3 months prior to the study including latent tuberculosis,
- 8 Systemic immunosuppressive or immunomodulatory treatment within 30 days prior to the study,
- 9 Body mass index (BMI)  $\leq 18.0$  or  $\geq 40.0$  kg/m<sup>2</sup>,
- 10 Participation in an investigational drug study within 3 months prior to screening or more than 4 times a year,
- 11 Loss or donation of blood over 500 mL within three months prior to screening,
- 12 The use of any medication or vitamin, mineral, herbal or dietary supplement within less than 5 half-lives prior to study participation if the Investigator judges that it may interfere with the study objectives,
- 13 History of alcohol consumption exceeding 5 standard drinks per day on average within 3 months of screening,
- 14 Any other condition that could interfere with the conduct of the study or the study objectives in the opinion of the Investigator.

## CHAPTER 5

MILD PSORIASIS PATIENTS ARE  
SUITABLE ALTERNATIVES FOR  
MODERATE-TO-SEVERE PSORIASIS  
PATIENTS IN EARLY-PHASE CLINICAL  
TRIALS: RESULTS OF A RANDOMIZED  
CONTROLLED TRIAL WITH  
GUSELKUMAB

Submitted



Jannik Rousel,<sup>1,2</sup> Menthe E. Bergmans,<sup>1</sup> Lisa J. Bruijninx,<sup>1</sup> Sissi Lin,<sup>1</sup> Tessa Niemeyer-van der Kolk,<sup>1</sup> Roman Bohoslavsky,<sup>1</sup> Yalçin Yavuz,<sup>1</sup> Naomi B. Klarenbeek,<sup>1</sup> Joke A. Bouwstra,<sup>2</sup> Robert Rissmann,<sup>1,2,3</sup> and Martijn B.A. van Doorn<sup>1,4</sup> from the Next-Generation ImmunoDermatology (NGID) Consortium

1. Centre for Human Drug Research, Leiden, NL / 2. Leiden Academic Centre for Drug Research, Leiden University, Leiden, NL / 3. Leiden University Medical Centre, Leiden, NL / 4. Erasmus Medical Centre, Rotterdam, NL

## Abstract

**BACKGROUND:** Early clinical development of novel psoriasis therapies is hampered by a decreasing number of patients eligible for participation in clinical trials since safe and efficacious therapeutics have become readily available. This will hamper drug research as patient participation remains key in developing new therapies. As mild psoriasis patients are generally not considered for systemic treatment as their disease burden is low, they might present a suitable alternative trial population presuming similar treatment responses can be demonstrated.

**METHODS:** A randomized double-blind controlled trial was performed in 20 mild psoriasis patients (Psoriasis Area and Severity Index (PASI)  $\leq 5$ ), randomized 3:1 to guselkumab 100 mg or placebo, and 5 moderate-to-severe psoriasis patients (PASI  $\geq 10$ ) on guselkumab 100mg. Treatment responses were monitored for 24 weeks by clinician-reported outcomes and target lesion scoring substantiated with a multimodal imaging approach comprising multispectral imaging, optical coherence tomography and laser speckle contrast imaging.

**RESULTS:** Clinician-reported outcomes demonstrated significant treatment effects compared to placebo for mild patients. Focusing on a single target lesion, target severity scores significantly decreased during treatment with guselkumab. Additional objective modalities demonstrated concomitant significant decreases in erythema, maximal height within the lesion and cutaneous perfusion compared to placebo. Imaging did not detect differences between mild and moderate-to-severe patients, and moderate-to-severe patients showed a similar response as mild patients when compared to baseline.

**CONCLUSION:** Clinical scoring and multimodal target lesion monitoring enable the detection of a clear treatment effect in mild psoriasis patients. Although this trial was not powered to demonstrate equivalence between the severity groups, our results indicate that the treatment responses follow the same trend in mild and moderate-to-severe patients with a high degree of similarity. This indicates clinical trials can also be reliably performed with mild psoriasis patients instead of only moderate-to-severe patients.

## Introduction

Plaque psoriasis is a common chronic skin disease that affects 2-3% of the world's population.<sup>1,2</sup> The quality of life of moderate-to-severe psoriasis patients has increased tremendously in recent years due to the emergence of biologic therapies that are safer and more efficacious compared to conventional systemic therapies such as methotrexate and cyclosporine.<sup>3</sup> As a result, the number of moderate-to-severe psoriasis patients in western countries that are eligible for clinical trials and are willing to abstain from therapy awaiting enrolment has markedly decreased. This impacts the development of innovative and potentially curative treatments as participation of psoriasis patients is still needed in their clinical development.

Being the intended treatment group for biologics, clinical trials have been primarily conducted in this shrinking moderate-to-severe psoriasis population. However, up to 80% of psoriasis patients is estimated to have a milder form of psoriasis with limited skin involvement.<sup>4,5</sup> In this population, treatment with conventional systemic treatments or biologics is deemed unwarranted due to unfavourable risk-benefit and cost-benefit ratios.<sup>6,7</sup> Instead, their treatment options remain limited to the use of topical corticosteroids that are associated with poor efficacy and rapid relapse upon cessation of treatment.<sup>8</sup> This group of patients with negligible systemic exposure, active symptoms and limited burden could be valuable candidates for clinical trials.

However, it is critical that results obtained in this mild population translate well to moderate-to-severe patients and reflect trial outcomes similarly. While differences in the transcriptomic profile of plaques between these groups have been observed, they appear rather limited and do not result in major differences in treatment responses.<sup>9,10</sup> Rather, the challenge may lie in reliable detection of treatment responses as the widely adopted Psoriasis Area and Severity Index (PASI) has low sensitivity when disease severity is low.<sup>11-13</sup> This might be resolved by adapting an objective and data-rich multimodal approach that extends past physician reported outcomes.<sup>14</sup> Imaging has been extensively applied in dermatology to monitor treatment responses and its digitalized nature precludes inter- and intra-observer variability associated with physician-reported outcomes which might yield higher sensitivity regardless of severity.<sup>15,16</sup> However, their applicability in psoriasis should first be addressed before these methods can be used.

The objective of this study was to demonstrate that the clinical response of mild patients can reliably be detected in a trial setting. We have conducted a placebo-controlled double-blind clinical trial with the anti-interleukine-23 monoclonal antibody guselkumab in which we characterized the treatment-response of mild patients with at least one moderate target plaque and include several moderate-to-severe patients as reference. Classic PASI-based endpoints were complemented with a multimodal imaging-toolbox to bolster confidence for the small group sizes employed in Phase I/II trials. This trial can establish mild psoriasis patients as relevant model for moderate-to-severe patients with methodology that can be readily adopted in upcoming early-stage clinical trials. Moreover, highlighting similar responses in mild psoriasis patients further highlights the applicability of biologic therapy in these patients.

## Materials and patients

### STUDY DESIGN

This exploratory, single-center, double-blinded and placebo-controlled randomized clinical trial registered under ClinicalTrials.gov Identifier NCT03688971 was performed from September 2020 until all mild patients and healthy controls had been recruited in January 2023. The study was conducted conform the Declaration of Helsinki principles at the Centre for Human Drug Research (CHDR), in Leiden, the Netherlands. Ethical approval was obtained from the institutional review board METC Brabant (Tilburg, the Netherlands). Written informed consent was obtained from participants before any study-related procedures were performed. General health was evaluated at screening and psoriasis-specific aspects were evaluated for patients. Patients were only included when presenting at screening with  $\geq 1$  lesion of lesion severity score (LSS)  $\geq 6$  and with a psoriasis area and severity (PASI) score of  $\leq 5$  (mild psoriasis group) or  $\geq 10$  (moderate-to-severe psoriasis group). All in- and exclusion requirements, including washouts, for healthy controls and patients are included in the supplemental material. Patients were randomized 3:1 to standard-of-care induction therapy with guselkumab 100mg (GUS) subcutaneously or placebo (PLA). Treatment allocation was performed by a study-independent statistician. Randomization was performed in blocks of four, separately for sex and severity. As placebo and guselkumab were supplied in visually different syringes, administration of guselkumab and placebo was performed by study-independent physicians that did not

partake in other clinical activities surrounding the trial, administration was performed in a separate room and subjects were instructed to look away during administration. Therefore, the study team and patients remained blinded, and the double blinded nature of the trial was upheld. No concomitant medication was allowed. Patients visited the CHDR for visits 2, 4, 8, 12, 16 and 24 weeks after first dose, with two more 100mg doses given at week 4 and 12. Clinical scoring and imaging were performed on the same lesion with LSS  $\geq 6$  at baseline at every visit.

### CLINICAL SCORING

Psoriasis severity was evaluated using PASI and Physicians Global Assessment (PGA) scoring as commonly applied.<sup>17,18</sup> The percentage body surface area affected (%BSA) was estimated per body region by referencing the patient's palm as 1% BSA. This enabled the use of the PASI-High Discrimination (PASI-HD) which subdivides the lowest categorical area value for the PASI ( $<10\%BSA=1$ ) in tenths (e.g.,  $8.5\%BSA=0.8$ ).<sup>11</sup> Single lesions were scored using a 5-point grading system for erythema, induration and scaling for psoriasis (0-4; none-very severe), with the sum representing the lesion severity score (LSS).<sup>19</sup>

### TOTAL BODY PHOTOGRAPHY

Automated total body photography was performed using the ATBM system (FotoFinder Systems GMBH, Bad BirnBach, Germany) with subjects photographed from all sides. Subjects were photographed from the sides, back and front while dressed in disposable underwear covering solely the genitalia. Subjects adopted standard poses as prompted by the ATBM system. Flash photography was performed in front of the same dark blue backdrop under standardized lighting conditions. The proprietary PASI-vision Universe software 2.0.41.20 was used to obtain digital PASI (DPASI) scores after minimal correction for affected surface area by the operator.

### OPTICAL COHERENCE TOMOGRAPHY

The Vivosight Dx Optical Coherence Tomography (OCT) was used to obtain a scan over a 6x6 mm area of skin. Skin roughness was extracted from measurement files after analysis through the proprietary Vivosight Tools analysis software (Michelson Diagnostics, Kent, United Kingdom). Epidermal thickness was determined by analysing the exported scans containing 120 frames using ImageJ and averaging 36 depth measurements at the centre and both sides every 10 frames.

## MULTISPECTRAL IMAGING

An Antera 3D (Miravex, Dublin, Ireland) was used to capture multispectral 3D images of the skin. Relevant parameters were extracted from the software after analysing a 40 mm diameter circle of skin using the Antera 3D proprietary software.

## COLORIMETRY

The degree of redness is determined using a Cortex DSM-3 (Aalborg, Denmark). Redness is determined by averaging the CIELAB A\*-value of three different overlapping measurements. The A\*-value represents the degree of redness from a scale of 0-60.<sup>20</sup>

## LASER SPECKLE CONTRAST IMAGING

The cutaneous microcirculation is captured using the Pericam PSI imager (Perimed, Järfälla, Sweden). The device is calibrated before the first measurement of the day. Perfusion is determined within a 40 mm diameter circular region of interest over a continuous recording of 30 seconds. Prior to measurement, subjects acclimatized a minimum of 15 minutes to the temperate and humidity controlled room (humidity < 60%, temperature 22 ± 2 °C).

## STATISTICS

Group sizes were determined based on PASI-90 responses from Phase III guselkumab trials.<sup>21,22</sup> Heat map and baseline comparisons using an unpaired one-way ANOVA with multiple comparisons with Tukey's post hoc tests were made in PRISM 9.0 (GraphPad, Software, Boston, Massachusetts, United States). Longitudinal effects were analysed with a mixed model of repeated measures (ANCOVA), with group (severity-treatment: mild-GUS, moderate-to-severe-GUS, mild-PLA), time, and group-by-time as fixed factors and patients as random factor, assuming a variance component variance-covariance matrix in SAS version 9.4 (SAS Institute, Cary, North Carolina, United States). Contrasts were reported in respect to changes from baseline for each group, and between the mild-GUS and Mild-PLA groups. Common within-individual associations for paired measures were determined using Rmcorr in R Statistical Software (version 4.1.2, R Core Team 2021).<sup>23</sup> For conciseness, associated means, confidence-intervals and p-values are listed in table s3. In-text values represent mean±standard deviations. P-values are denoted by \*: P≤0.05, -: P≤0.01, -: P≤0.001.

## Results

Of the 78 patients screened for eligibility, 21 mild with mild and 6 with moderate-to-severe psoriasis were included into the study (table 1, Supplemental Figure s1). One patient dropped out citing incompatibility with the protocol before randomization. 15/20 mild and 5/6 moderate-to-severe patients were allocated to guselkumab treatment. The single moderate-to-severe patient receiving placebo is only included in baseline comparisons with 10 healthy controls. All dosed subjects completed the study without any serious adverse events (Supplemental Table s1). Efficacy and tolerability in the mild study population was reported previously.<sup>24</sup>

### EFFICACY IN MILD AND MODERATE-TO-SEVERE PATIENTS AS ASSESSED BY CLINICAL SCORING

Clinician-reported endpoints show evident treatment effects (figure 1). Severity scoring with the simple 5-point PGA-scale showed 13/15 mild patients and 4/5 moderate-to-severe patients randomized to guselkumab obtained PGA 0/1 (clear/almost clear) compared to 1/5 mild patients in the placebo group with all patients having PGA≥2 at baseline.

PASI scoring showed was higher in the moderate-to-severe group compared to the mild group (12.82±2.7 vs 5.4±2.1, p<0.0001). PASI scores decreased significantly compared to baseline for both guselkumab groups, but not in the placebo group. Mild patients treated with guselkumab showed a significant decrease compared to those on placebo. PASI-75, PASI-90 and PASI-100 responses in the guselkumab groups were obtained by 15/15 (100%), 8/15 (53%) and 6/15 (40%) in the mild group and by 5/5 (80%), 4/5 (60%) and 1/5 (20%) in the moderate-to-severe group. Of note, the DPASI was able to detect a significant decrease from baseline in the treatment groups, but was unable to establish effects compared to placebo and correlated poorly with the physician-performed PASI ( $r_{tm}$ : 0.45, figure 2 and figure 3).

Tailoring the PASI score to the mild population by enhancing sensitivity at lower %BSA, the PASI-HD and PASI scores at baseline showed little difference in the moderate-to-severe group (PASI: 12.5±0.9, PASI-HD: 11.7±2.7) but was affected in the mild patient group (PASI: 5.6±2.0, PASI-HD: 2.2±2.4). In both groups, a significant treatment effect was observed upon guselkumab treatment. As with regular PASI scoring, a significant decrease compared to placebo was observed for mild patients. PASI-HD treatment responses exceeded those determined by PASI, with 15/15 (100%), 12/15 (80%) and 6/15 (40%)

of mild guselkumab-treated patients and 5/5 (100%), 4/5 (80%) and 1/5 (20%) of moderate-to-severe guselkumab treated patients obtaining PASI-HD-75, PASI-HD-90 and PASI-HD-100 scores, respectively.

When focussing on the resolution of a single lesion, the cumulative LSS was similar at baseline between both severity groups (mild: 7.1±1.0, moderate-to-severe: 6.7±1.2,  $p=0.97$ ) in contrast to PASI. After treatment, guselkumab significantly reduced LSS compared to baseline. For the mild patients, this decrease was significant compared to placebo.

**Figure 1** Clinical scoring of psoriasis severity. The number of subjects reaching a Physicians Global Assessment (PGA) rating of clear or almost clear (0/1) with the number of patients on the Y-axis and percentages in the graph indicating the fraction of patients reaching PGA 0/1 (A). The Psoriasis Area and Severity Index (PASI) (B) and the Psoriasis Area and Severity Index-High Discrimination (PASI-HD) which has a higher sensitivity below 10% involved body surface area (C) shows significant decreases in psoriasis severity in the guselkumab treated groups. This is reiterated by monitoring the Lesion Severity Score (LSS) of a representative but moderate target plaque of at least LSS ≥ 6 at baseline over time. Graphs show the mean and standard deviations.

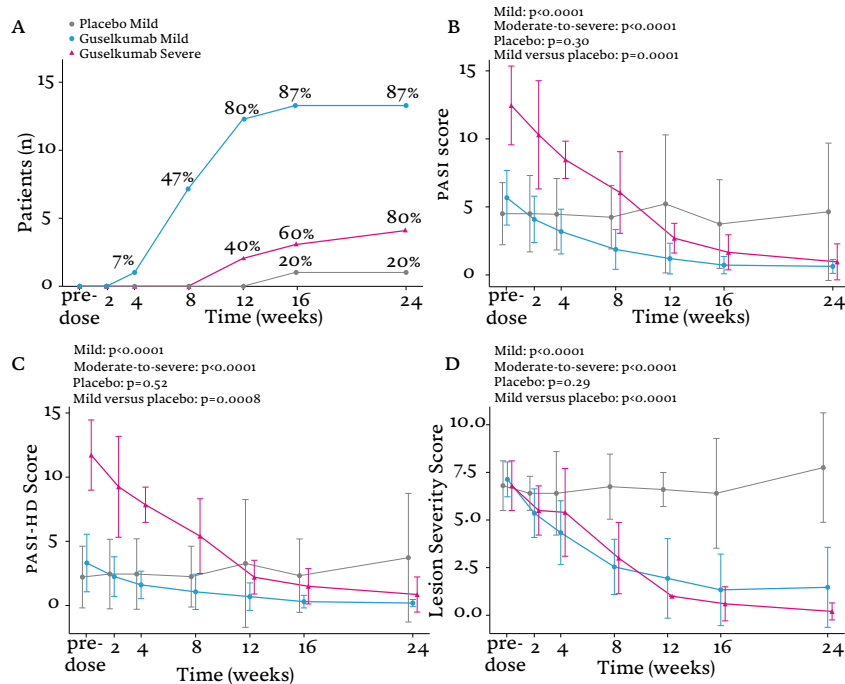


**Table 1** Baseline demographics of the study population. Significant differences in psoriasis severity between the groups is presented for the psoriasis area and severity index (PASI), digital PASI (DPASI) and lesion severity score, but not for the Physicians Global Assessment (PGA). Contrasts are made compared to the mild guselkumab group.

	Controls	Mild (placebo)	Mild (Guselkumab)	Moderate-to-severe (Guselkumab)
Total number of patients	10	5	15	5
Age at first dose	≤ 18 years	0 (0%)	0 (0%)	0 (0%)
	18-65 years	10 (100%)	5 (100%)	14 (93%)
	≥ 65 years	0 (0%)	0 (0%)	1 (7%)
Sex	Female	7 (70%)	1 (20%)	3 (20%)
	Male	3 (30%)	4 (80%)	12 (80%)
Race	White	9 (90%)	4 (80%)	13 (87%)
	Asian	0 (0%)	1 (20%)	0 (0%)
	Hispanic	1 (10%)	0 (0%)	0 (0%)
	More than one	0 (0%)	0 (0%)	2 (13%)
Fitzpatrick	I	0 (0%)	0 (0%)	1 (7%)
	II	5 (50%)	2 (40%)	5 (33%)
	III	4 (40%)	2 (40%)	9 (60%)
	IV	1 (10%)	0 (0%)	1 (20%)
	V	0 (0%)	0 (0%)	0 (0%)
	VI	0 (0%)	1 (20%)	0 (0%)
Baseline PASI (mean ± SD)	N.A.	4.5±2.3 <sup>ns</sup>	5.6±2.0	12.5±0.9 <sup>***</sup>
Baseline DPASI (mean ± SD)	N.A.	4.0±1.9 <sup>ns</sup>	4.6±1.5	6.8±1.7*
Baseline PASI-HD (mean ± SD)	N.A.	3.3±2.2 <sup>ns</sup>	2.2±2.4	11.7±2.7 <sup>***</sup>
Baseline Lesion Severity Score (mean ± SD)	N.A.	6.8±1.3 <sup>ns</sup>	7.1±0.9	6.8±1.3 <sup>ns</sup>
Baseline PGA	0 (Clear)	N.A.	0 (0%)	0 (0%)
	1 (Almost clear)	N.A.	0 (0%)	0 (0%)
	2 (Mild)	N.A.	3 (60%)	15 (100%)
	3 (Moderate)	N.A.	2 (40%)	0 (0%)
	4 (Severe)	N.A.	0 (0%)	0 (0%)

ns;  $p>0.05$ , \*;  $p<0.05$ , \*\*\*;  $p<0.0001$ .

**Figure 2** The digital Psoriasis Area and Severity Index (DPASI) over time. The mean and standard deviation is shown. Though clinician reported outcomes demonstrate significant differences compared to placebo, the DPASI is unable to replicate this.

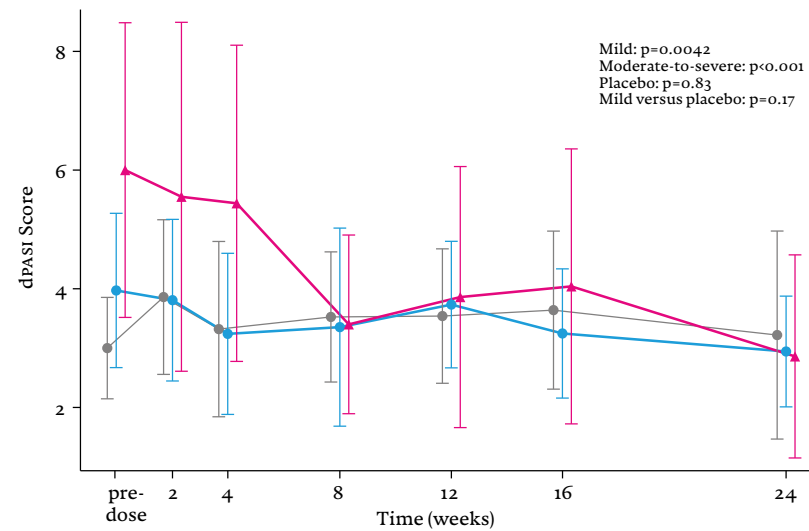
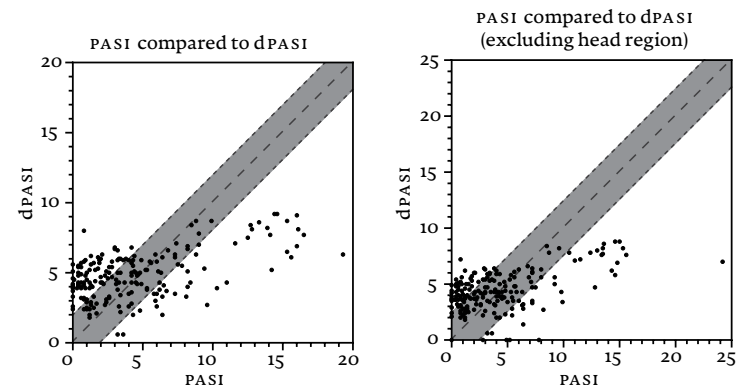


**Figure 3** All available datapoints of the physician-performed psoriasis area and severity index (PASI) plotted against their digital PASI (DPASI) counterpart. Note that both the full PASI scores and the PASI scores without the head and neck area have been plotted, which might introduce bias as the scalp can be obscured by hair and therefore impact the DPASI assessments. A band has been plotted indicating the same score with physician PASI and DPASI with a datapoint at the middle-dotted line. A  $\pm 2$ -point margin is indicated in grey. Note that a repeated measures correlation is indicated in Table 2.



## OBJECTIVE CONFIRMATION OF PHYSICIAN-BASED TREATMENT RESPONSES IN PATIENTS

Analysis of skin roughness (RA) by multispectral imaging and OCT showed a significantly higher roughness at lesional skin compared to non-lesional skin in mild patients, but no other significant baseline differences in skin roughness were observed compared to controls or within the moderate-to-severe group. Longitudinal monitoring showed roughness was significantly reduced after guselkumab treatment compared to baseline in both guselkumab groups for OCT and in the mild guselkumab group for multispectral imaging. However, no significant differences compared to placebo were observed for both analysis (Supplemental Figure s2).

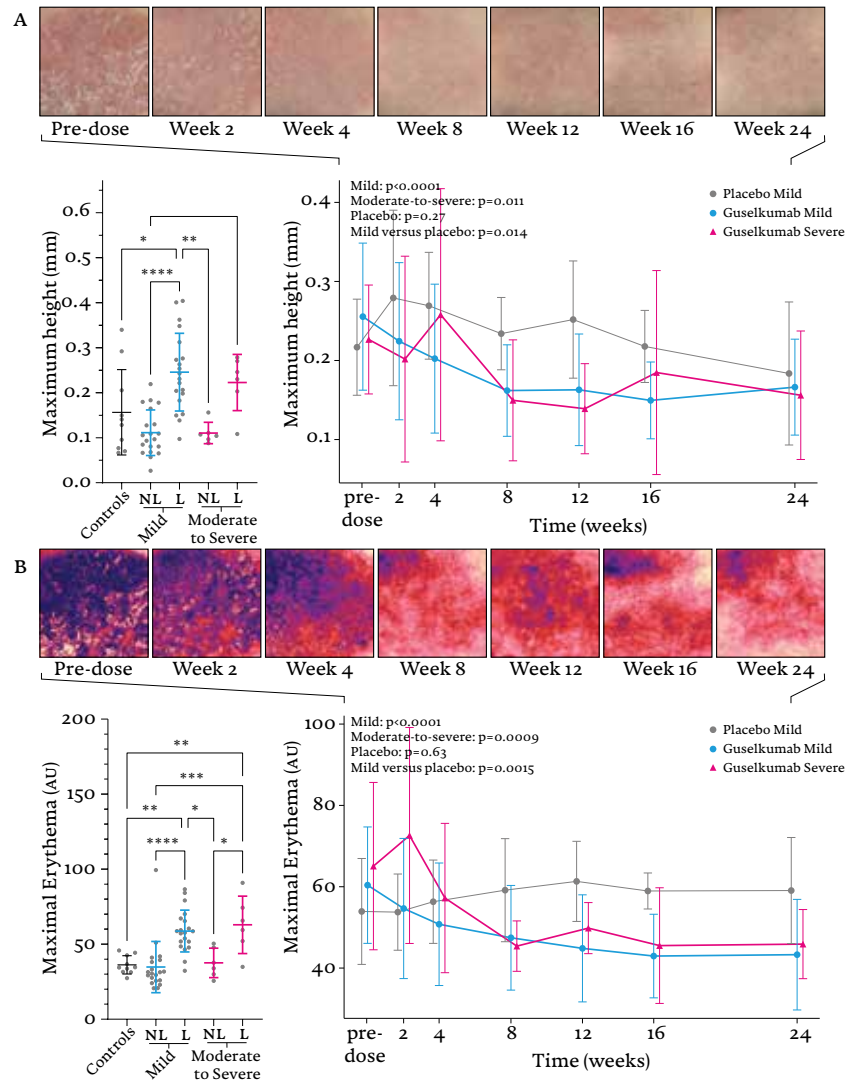
Maximum height (RT) within the analysed region proved significantly higher in lesional skin compared to non-lesional skin and that of controls for mild patients (figure 4). In moderate-to-severe patients, maximum height in lesional skin was neither increased compared to their non-lesional skin or that of controls. However, lesional skin showed evident decreases in maximal height over time for both guselkumab treated groups. After treatment, maximum height was significantly decreased compared to placebo in mild patients.

Comprising a pertinent part of clinical scoring, digitalization of erythema grading might constitute an applicable outcome measure. The  $A^*$ -CIELAB value from single-point colorimetry indicated significantly more erythema at lesional compared to non-lesional skin. However, no significant differences between controls and lesional skin were observed. Additionally, monitoring lesional  $A^*$  did not result in significant reductions compared to baseline or placebo (Supplemental Figure s3).

On the other hand, multispectral imaging was able to highlight increased maximum erythema over a bigger region of interest in lesional skin compared to controls and compared to non-lesional skin (figure 3). Lesional skin did not significantly differ between the two treatment groups at baseline. Maximal erythema decreased during guselkumab treatment, resulting in significantly lower erythema compared to baseline regardless of severity. This resulted in a significantly decreased erythema compared to placebo for mild patients. Similar results were obtained when monitoring the delta  $A^*$ -value but not with average  $A^*$  (figure s4).



**Figure 4** Multispectral imaging for the determination of superficial roughness (A) and erythema (B). Comparisons between healthy control skin, non-lesional skin and lesional skin are made at baseline, with the lesional skin of patients monitored further throughout the trial. The time course has been supplemented with visual output of the modalities, showing the effect of guselkumab in the same subject. Texture and erythema images of three additional subjects are presented in the supplemental material in figures s4 and s5. Graphs show the mean and standard deviations.



### SUBSURFACE CHANGES IN SKIN PERFUSION AND EPIDERMAL THICKNESS SUPPORT VISUALLY OBSERVED TREATMENT EFFECTS

Cutaneous perfusion is enhanced in lesional skin compared to non-lesional and control skin (figure 5). Lesional perfusion is not significantly higher in skin of moderate-to-severe patients compared to mild patients. During guselkumab treatment, basal flow declined significantly compared to baseline in both mild and moderate-to-severe patients but not in the placebo group. Compared directly to placebo in the mild group, this remained a significant decrease.

Optical coherence tomography showed epidermal thickness was increased in both mild and moderate-to-severe patients when compared to their non-lesional skin and controls at baseline (figure 5). Over time, epidermal thickness decreased significantly in both actively treated groups but not in the placebo group. However, no significant difference was observed when comparing mild patients on guselkumab to placebo.

### CLINICAL AND DIGITAL ENDPOINTS CORRELATE WITH EACH OTHER

Summarizing, evident treatment effects are observed throughout the mild and moderate-to-severe population (figure 6). As outlined in figure 1, clinical scoring by PASI, PASI-HD and LSS provides strong indications of disease remission in both treatment groups with decreases of >80%. With the exception of the maximal height which decreases below the average of healthy controls in moderate-to-severe patients, imaging endpoints show a smaller reduction compared to clinical scores and are indicative of a placebo effect as decreases are observed for epidermal thickness and maximal height in the placebo group. The repeated measures correlation was high among the different clinical endpoints ( $r_{rm} > 0.7$ ) but moderate between clinical scores and objective endpoints ( $0.37 < r_{rm} < 0.71$ ) (table 2, table 3). Coefficients increased marginally only for maximal height when using the applicable LSS sub-scores instead of total LSS (induration-epidermal thickness, erythema-maximal erythema and scaling-maximal height).

**Figure 5** Baseline differences and longitudinal monitoring of the cutaneous perfusion in target lesions by laser speckle contrast imaging (A) and epidermal thickness by optical coherence tomography (B). The effect over time is supplemented with the visual output of the device with the degree in cutaneous perfusion in a gradient from blue to green to red, with red indicating the highest degree of perfusion. The dermal-epidermal junction has been indicated with a dotted line in the optical coherence tomography images. Images shown pertain to the same lesion from the same patient on guselkumab as shown earlier, lesions of additional patients are included in the supplementary methods in figures s6 and s7. Graphs show the mean and standard deviations.

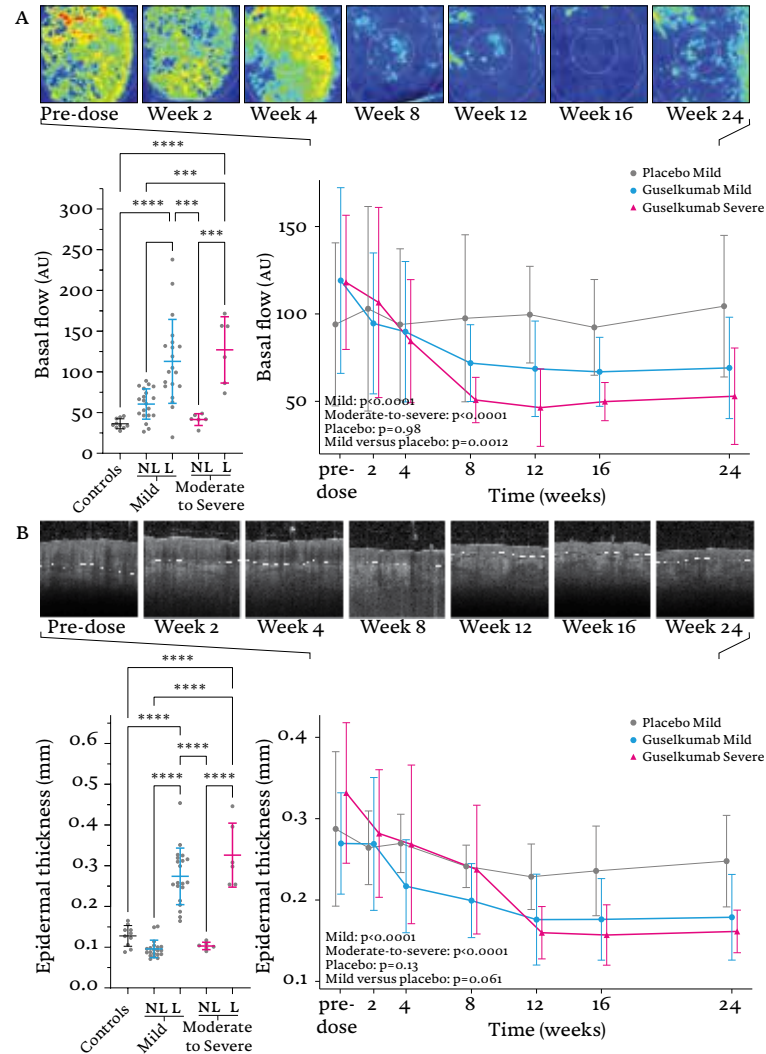


**Figure 6** Heat plot showing the percent change from baseline of endpoints at the end of study. Lesion imaging endpoints (cutaneous perfusion, epidermal thickness, maximal erythema and maximal height) are corrected with the average value of the healthy control cohort, meaning a 100% decrease indicates normalization of these parameters to the level observed in healthy controls.

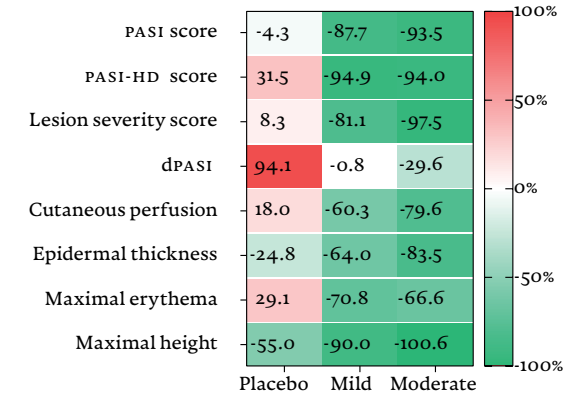


**Table 2** Correlations in the guselkumab treated group, both mild and moderate-to-severe, between all modalities. The clinical scores comprised of the Psoriasis Area and Severity Index (PASI), PASI-High Discrimination (PASI-HD) and the Lesion Severity Score (LSS) are emphasized. Numerical data represent the Repeated Measure Correlation ( $r_{rm}$ ).

	PASI	PASI-HD	Lesion Severity Score (LSS)	Digital PASI	Basal Flow (mm/sec)	Epidermal Thickness (mm)	Maximal Erythema	Maximal Height (mm)
<b>PASI</b>	1.00	0.95	0.85	0.45	0.63	0.71	0.58	0.45
<b>PASI-HD</b>	0.95	1.00	0.74	0.51	0.57	0.68	0.52	0.37
<b>Lesion Severity Score (LSS)</b>	0.85	0.74	1.00	0.33	0.67	0.68	0.69	0.56
<b>Digital PASI</b>	0.45	0.51	0.33	1.00	0.31	0.40	0.23	0.15
<b>Basal Flow (mm/sec)</b>	0.63	0.57	0.67	0.31	1.00	0.44	0.58	0.45
<b>Epidermal Thickness (mm)</b>	0.71	0.68	0.68	0.40	0.44	1.00	0.47	0.33
<b>Maximal Erythema</b>	0.58	0.52	0.69	0.23	0.58	0.47	1.00	0.49
<b>Maximal Height (mm)</b>	0.45	0.37	0.56	0.15	0.45	0.33	0.49	1.00

**Table 3** Correlations in the guselkumab treated group, both mild and moderate-to-severe, between subscores of the Lesion Severity Score (LSS) and the objective modalities. Plausible connections between specific endpoints and lesion severity subscores (e.g. LSS-Erythema and maximal erythema) are emphasized. Numerical data represent the Repeated Measure Correlation ( $r_{rm}$ ).

	Lesion Severity Score (LSS)	LSS-Erythema	LSS-Scaling	LSS-Induration
Lesion Severity Score (LSS)	1.00	0.91	0.94	0.93
Basal Flow (mm/sec)	0.67	0.54	0.64	0.68
Maximal Erythema	0.69	0.60	0.63	0.69
Maximal Height (mm)	0.56	0.41	0.60	0.53
Epidermal Thickness (mm)	0.68	0.59	0.64	0.66

## Discussion

By complementing traditional clinical endpoints with objective digitalized endpoints, we have shown how treatment responses can be readily observed in a cohort of 20 mild psoriasis patients and can differentiate between active treatment and placebo. Although this trial is not powered to compare the treatment response in mild patients directly with their moderate-to-severe counterparts, characterizing these populations at baseline and subsequently following guselkumab-induced treatment responses adequately indicated differences were small.

As a direct result from the in- and exclusion criteria, significant baseline differences in PASI-assessed disease severity were apparent between the mild and moderate-to-severe patients, in line with the EMA classification of these patient groups.<sup>25</sup> However, it has to be noted that the definition of mild patients is subject to debate and is influenced by more factors than PASI alone.<sup>26</sup> It has been described that insensitivity of the PASI at low disease severity might complicate the effective use of PASI-scoring in mild patients as low baseline scores require near-complete clearance to achieve PASI-75 and PASI-90 responses.<sup>11,12</sup> However, significant PASI-responses were observed for mild patients, indicating that this scoring system remains sufficiently powered to detect differences in populations with low baseline scores. Although PASI-75 and PASI-90 responses in our mild population were comparable to earlier phase III studies in moderate-to-severe patients,<sup>21,22</sup> implementation of the PASI-HD enhanced responses that might more appropriately reflect disease remission in this group as PASI has been shown to underrepresent actual clinical effects.<sup>27</sup> All patients in this study were recruited based on the presence

of at least one moderate psoriasis plaque to allow for an evident plaque to monitor during treatment. In practice, this resulted in a similar LSS at baseline for both severity groups with different total PASI scores which illustrates how the extend of psoriasis impacts the latter.<sup>27</sup> In terms of single lesions, additional measures did not show any significant differences between mild and moderate-to-severe patients and non-lesional skin appeared not significantly different from that of controls.

The cutaneous morphology of lesional skin normalized during treatment. Expected increases in lesional roughness, caused by the presence of scaling, were hard to establish and might have resulted from insufficient sensitivity to detect fine scaling.<sup>28</sup> Instead, maximum height proved to be a suitable endpoint that differentiated the patient and control groups at baseline and active treatment from placebo. Evidently tied to the psoriatic phenotype, redness decreased over time when expressed as maximal erythema and delta A\*. Objectively quantifying erythema has been exploited to monitor disease remission before in psoriasis<sup>29</sup> and other indications,<sup>16,30-32</sup> but not yet applied to placebo-controlled trials in psoriasis. Of note, simpler assessments based on single-point colorimetry and average A\* failed to show differences compared to placebo which highlights that internal controls might be warranted to limit intersubject variation. Indeed, using multispectral imaging to derive redness from haemoglobin levels instead of CIELAB values resulted in an evident treatment effect compared to placebo which might be attributed to a decreased influence of skin tone.<sup>33,34</sup> High superficial haemoglobin levels are well-supported by the observed increases in subcutaneous perfusion determined by LSCI at baseline and its subsequent normalization during guselkumab treatment. OCT measurements reiterated that acanthosis and rete ridges are observable through increased epidermal thickness and decreases during effective treatment,<sup>35,36</sup> now also in the target plaque of mild patients. However, epidermal thickness did not significantly decrease compared to placebo, which may be partly attributed to a small measurement surface and heterogeneity in the plaques themselves,<sup>37</sup> or to substantial distortion of the OCT signal by rete ridges making the dermal-epidermal junction harder to locate.<sup>38</sup> Together, these measures differentiate healthy and non-lesional skin from lesional skin and reflect treatment over time, thereby supporting their use in early clinical drug development.

Unfortunately, not all measures yielded favourable results as DPASI correlated poorly with the physician reported PASI despite previously having been validated in an observational study.<sup>39</sup> However, validation of the DPASI was

performed based on PASI-scoring of images post-hoc. Direct comparisons between the live physician-performed PASI and DPASI yielded differences exceeding 40%. Similar variation in this study might have obscured treatment effects in a population with mild disease. Disregarding the often-cited shortcomings of the physician-performed PASI in favour of computerized substitutes, it highlights that this method remains insufficiently powered to detect effects to a level that is expected in a clinical trial setting. However, the advance of deep learning might offer new opportunities for the conception of a fully automatized PASI, but remains challenging.<sup>40</sup>

Although this study demonstrated the feasibility of using a mild psoriasis population in clinical trials with IL-23 inhibition, the translatability to moderate-to-severe patients in future trials could be limited by differences in disease phenotype that could differentially affect outcomes. Although the genetic background has been shown to differ between mild and moderate-to-severe psoriasis,<sup>41</sup> the transcriptome still shows a high degree of similarity.<sup>42,43</sup> Although a more apparent immune signature around IL-17 was observed in mild disease, this did not seem to affect treatment responses.<sup>44</sup>

The ability to demonstrate treatment responses in a small cohort with low disease severity is promising for its application in early drug development. However, guselkumab is one of a variety of biologics that have collectively pushed the acceptable response rate in clinical care from PASI-75 to PASI-90.<sup>45,46</sup> Although target lesion monitoring would be ideal for following responses to topical therapies, these are often associated with weaker responses and might therefore not show such an evident effect as guselkumab therapy.<sup>8</sup> The sensitivity to detect less evident changes using this toolbox remains to be explored. However, novel drug candidates for psoriasis will have to demonstrate equal or higher responses to achieve market approval and reimbursement by medical insurance.

## Conclusion

Altogether, this study establishes mild psoriasis patients as a suitable and representative population for early phase clinical research. A high degree of confidence was obtained by bolstering traditional endpoints with novel objective outcomes. The possibility to conduct data-rich trials in this mild population will facilitate easier patient recruitment and provide earlier signs of efficacy of candidate drugs in proof-of-concept studies.

## REFERENCES

- Langley, R. G. B., Krueger, G. G. & Griffiths, C. E. M. Psoriasis: epidemiology, clinical features, and quality of life. *Ann Rheum Dis* **64**, ii8 (2005).
- Egeberg, A., See, K., Garrelts, A. & Burge, R. Epidemiology of psoriasis in hard-to-treat body locations: Data from the Danish skin cohort. *BMC Dermatol* **20**, 1-8 (2020).
- Sbidian, E. et al. Systemic pharmacological treatments for chronic plaque psoriasis: a network meta-analysis. *Cochrane Database Syst Rev* **2017**, (2017).
- Papp, K. A. et al. Psoriasis Prevalence and Severity by Expert Elicitation. *Dermatol Ther (Heidelb)* **11**, 1053 (2021).
- Stern, R. S., Nijsten, T., Feldman, S. R., Margolis, D. J. & Rolstad, T. Psoriasis Is Common, Carries a Substantial Burden Even When Not Extensive, and Is Associated with Widespread Treatment Dissatisfaction. *Journal of Investigative Dermatology Symposium Proceedings* **9**, 136-139 (2004).
- Lebwohl, M. A clinician's paradigm in the treatment of psoriasis. *J Am Acad Dermatol* **53**, S59-S69 (2005).
- Patel, D., Svoboda, R., Maczuga, S., Foulke, G. T. & Helm, M. A retrospective claims analysis confirms the cost of most biologic agents for psoriasis is increasing more rapidly than medical inflation. *J Am Acad Dermatol* **88**, 490-493 (2023).
- Samarasekera, E. J., Sawyer, L., Wonderling, D., Tucker, R. & Smith, C. H. Topical therapies for the treatment of plaque psoriasis: systematic review and network meta-analyses. *British Journal of Dermatology* **168**, 954-967 (2013).
- Kim, J. et al. The Spectrum of Mild to Severe Psoriasis Vulgaris Is Defined by a Common Activation of IL-17 Pathway Genes, but with Key Differences in Immune Regulatory Genes. *Journal of Investigative Dermatology* **136**, 2173-2182 (2016).
- Kim, J. et al. Secukinumab improves mild-to-moderate psoriasis: A randomized, placebo-controlled exploratory clinical trial. *J Am Acad Dermatol* **88**, 428-430 (2023).
- Papp, K. A. et al. The Proposed PASI-HD Provides More Precise Assessment of Plaque Psoriasis Severity in Anatomical Regions with a Low Area Score. *Dermatol Ther (Heidelb)* **11**, 1079-1083 (2021).
- Walsh, J. A. et al. Product of the Physician Global Assessment and body surface area: a simple static measure of psoriasis severity in a longitudinal cohort. *J Am Acad Dermatol* **69**, 931-937 (2013).
- Otero, M. E. et al. A pilot study on the Psoriasis Area and Severity Index (PASI) for small areas: Presentation and implications of the Low PASI score. *Journal of Dermatological Treatment* **26**, 314-317 (2015).
- Rissmann, R., Moerland, M. & van Doorn, M. B. A. Blueprint for mechanistic, data-rich early phase clinical pharmacology studies in dermatology. *Br J Clin Pharmacol* **86**, 1011 (2020).
- ten Voorde, W. et al. A Multimodal, Comprehensive Characterization of a Cutaneous Wound Model in Healthy Volunteers. *Exp Dermatol* (2023) DOI:10.1111/exd.14808.
- Logger, J. G. M., de Jong, E. M. G. J., Driessen, R. J. B. & van Erp, P. E. J. Evaluation of a simple image-based tool to quantify facial erythema in rosacea during treatment. *Skin Res Technol* **26**, 804-812 (2020).
- Ashcroft, D. M., Li Wan Po, A., Williams, H. C. & Griffiths, C. E. M. Clinical measures of disease severity and outcome in psoriasis: a critical appraisal of their quality. *British Journal of Dermatology* **141**, 185-191 (1999).
- Langley, R. G. & Ellis, C. N. Evaluating psoriasis with psoriasis area and severity index, psoriasis global assessment, and lattice system physician's global assessment. *J Am Acad Dermatol* **51**, 563-569 (2004).
- Glatt, S. et al. First-in-human randomized study of bimekizumab, a humanized monoclonal antibody and selective dual inhibitor of IL-17A and IL-17F, in mild psoriasis. *Br J Clin Pharmacol* **83**, 991-1001 (2017).
- Jaspers, M. E. H. & Moortgat, P. Objective Assessment Tools: Physical Parameters in Scar Assessment. *Textbook on Scar Management* 149-158 (2020) DOI:10.1007/978-3-030-44766-3\_17.
- Blauvelt, A. et al. Efficacy and safety of guselkumab, an anti-interleukin-23 monoclonal antibody, compared with adalimumab for the continuous treatment of patients with moderate to severe psoriasis: Results from the phase III, double-blinded, placebo- and active comparator-controlled Voyage 1 trial. *J Am Acad Dermatol* **76**, 405-417 (2017).
- Reich, K. et al. Efficacy and safety of guselkumab, an anti-interleukin-23 monoclonal antibody, compared with adalimumab for the treatment of patients with moderate to severe psoriasis with randomized withdrawal and retreatment: Results from the phase III, double-blind, placebo- and active comparator-controlled Voyage 2 trial. *J Am Acad Dermatol* **76**, 418-431 (2017).
- Bakdash, J. Z. & Marusich, L. R. Repeated measures correlation. *Front Psychol* **8**, 252904 (2017).
- Rousel, J. et al. Guselkumab induction therapy demonstrates long-lasting efficacy in patients with mild psoriasis, results from a randomized, placebo-controlled exploratory clinical trial. *J Am Acad Dermatol* **0**, (2023).
- Committee For Medicinal Products For Human Use. Clinical investigation of medicinal products indicated for the treatment of psoriasis - Scientific guideline. (2004).
- Strober, B. et al. Recategorization of psoriasis severity: Delphi consensus from the International Psoriasis Council. *J Am Acad Dermatol* **82**, 117-122 (2020).
- Jacobson, C. C. & Kimball, A. B. Rethinking the Psoriasis Area and Severity Index: the impact of area should be increased. *British Journal of Dermatology* **151**, 381-387 (2004).
- Ahmad Fadzil, M. H. et al. 3D surface roughness measurement for scaliness scoring of psoriasis lesions. *Comput Biol Med* **43**, 1987-2000 (2013).
- Iyatomi, H. et al. Computerized quantification of psoriasis lesions with colour calibration: preliminary results. *Clin Exp Dermatol* **34**, 830-833 (2009).
- Rousel, J. et al. Treatment with the Topical Antimicrobial Peptide Omiganan in Mild-to-Moderate Facial Seborrheic Dermatitis versus Ketoconazole and Placebo: Results of a Randomized Controlled Proof-of-Concept Trial. *Int J Mol Sci* **24**, 14315 (2023).
- Cantisani, C. et al. MAL Daylight Photodynamic Therapy for Actinic Keratosis: Clinical and Imaging Evaluation by 3D Camera. *Int J Mol Sci* **17**, (2016).
- Niemeyer-van der Kolk, T. et al. Topical antimicrobial peptide omiganan recovers cutaneous dysbiosis but does not improve clinical symptoms in patients with mild to moderate atopic dermatitis in a phase 2 randomized controlled trial. *J Am Acad Dermatol* **86**, 854-862 (2022).
- Baquie, M. & Kasraee, B. Discrimination between cutaneous pigmentation and erythema: Comparison of the skin colorimeters Dermacatch and Mexameter. *Skin Research and Technology* **20**, 218-227 (2014).

34 Matias, A. R., Ferreira, M., Costa, P. & Neto, P. Skin colour, skin redness and melanin biometric measurements: comparison study between Antera® 3D, Mexameter® and Colorimeter®. *Skin Research and Technology* **21**, 346-362 (2015).

35 Morsy, H. *et al.* Optical coherence tomography imaging of psoriasis vulgaris: Correlation with histology and disease severity. *Arch Dermatol Res* **302**, 105-111 (2010).

36 Ha-Wissel, L. *et al.* Case report: Optical coherence tomography for monitoring biologic therapy in psoriasis and atopic dermatitis. *Front Med (Lausanne)* **9**, (2022).

37 Griffin, T. D., Lattanand, A. & Vanscott, E. J. Clinical and Histologic Heterogeneity of Psoriatic Plaques: Therapeutic Relevance. *Arch Dermatol* **124**, 216-220 (1988).

38 Welzel, J., Bruhns, M. & Wolff, H. H. Optical coherence tomography in contact dermatitis and psoriasis. *Arch Dermatol Res* **295**, 50-55 (2003).

39 Fink, C. *et al.* Precision and reproducibility of automated computer-guided Psoriasis Area and Severity Index measurements in comparison with trained physicians. *British Journal of Dermatology* **180**, 390-396 (2019).

40 Schaap, M. J. *et al.* Image-based automated Psoriasis Area Severity Index scoring by Convolutional Neural Networks. *Journal of the European Academy of Dermatology and Venereology* **36**, 68-75 (2022).

41 Nikamo, P., Lysell, J. & Ståhle, M. Association with Genetic Variants in the IL-23 and NF- $\kappa$ B Pathways Discriminates between Mild and Severe Psoriasis Skin Disease. *Journal of Investigative Dermatology* **135**, 1969-1976 (2015).

42 Kim, J. *et al.* The Spectrum of Mild to Severe Psoriasis Vulgaris Is Defined by a Common Activation of IL-17 Pathway Genes, but with Key Differences in Immune Regulatory Genes. *Journal of Investigative Dermatology* **136**, 2173-2182 (2016).

43 Kim, J. *et al.* Histological Stratification of Thick and Thin Plaque Psoriasis Explores Molecular Phenotypes with Clinical Implications. *PLoS One* **10**, 132454 (2015).

44 Kim, J. *et al.* Secukinumab improves mild-to-moderate psoriasis: A randomized, placebo-controlled exploratory clinical trial. *J Am Acad Dermatol* **88**, 428-430 (2023).

45 Manalo, I. F., Gilbert, K. E. & Wu, J. J. Time to Raise the Bar to Psoriasis Area Severity Index 90 and 100 – JDDonline – Journal of Drugs in Dermatology. *Journal of Drugs in Dermatology* **14**, (2015).

46 Puig, L. PASI90 response: the new standard in therapeutic efficacy for psoriasis. *J Eur Acad Dermatol Venereol* **29**, 645-648 (2015).

## SUPPLEMENTAL MATERIAL

### OVERVIEW OF THE IN- AND EXCLUSION CRITERIA FOR THIS STUDY

*Eligible healthy controls must meet all of the following inclusion criteria at screening:*

- 1 Male or non-pregnant female subjects, 18 to 75 years of age (inclusive); during COVID-19 pandemic this is set to 18 to 69 year of age (inclusive)
- 2 Healthy as defined by the absence of any uncontrolled active or uncontrolled chronic disease following a medical and surgical history, documentation of general symptoms, and a symptom-directed physical examination including vital signs;
- 3 Willing to give written informed consent and willing and able to comply with the study protocol;

*And eligible healthy controls must meet none of the following exclusion criteria at screening:*

- 1 History or symptoms of any uncontrolled, significant disease including (but not limited to), neurological, psychiatric, endocrine, cardiovascular, respiratory, gastrointestinal, hepatic, or renal disorder that may interfere with the study objectives, in the opinion of the Investigator;
- 2 History of immunological abnormality (e.g., immune suppression, severe allergy or anaphylaxis) that may interfere with study objectives, in the opinion of the Investigator;
- 3 Known infection requiring antibiotic therapy within the last three months prior to the study;

- 4 Immunosuppressive or immunomodulatory treatment within 30 days prior to the study;
- 5 Body mass index (BMI)  $\leq 18.0$  or  $\geq 40.0$  kg/m<sup>2</sup>; during COVID-19 pandemic only  $\leq 18.0$  or  $> 33.0$  kg/m<sup>2</sup>
- 6 Participation in an investigational drug study within 3 months prior to screening or more than 4 times a year;
- 7 Previous participation in an investigational drug study involving the dosing of an investigational compound targeting an immune pathway within one year prior to screening;
- 8 Loss or donation of blood over 500 mL within three months prior to screening;
- 9 The use of any medication or vitamin/mineral/herbal/dietary supplement within less than 5 half-lives prior to study participation, if the Investigator judges that it may interfere with the study objectives. The use of paracetamol (up to 4 g/day) is allowed;
- 10 History of alcohol consumption exceeding 5 standard drinks per day on average within 3 months of screening. Alcohol consumption will be prohibited from at least 12 hours preceding each study visit;
- 11 Any other condition that could interfere with the conduct of the study or the study objectives, in the opinion of the Investigator.
- 12 During COVID-19 pandemic: presence of high risk comorbidities: such as cardiovascular, respiratory or immune system disorders.

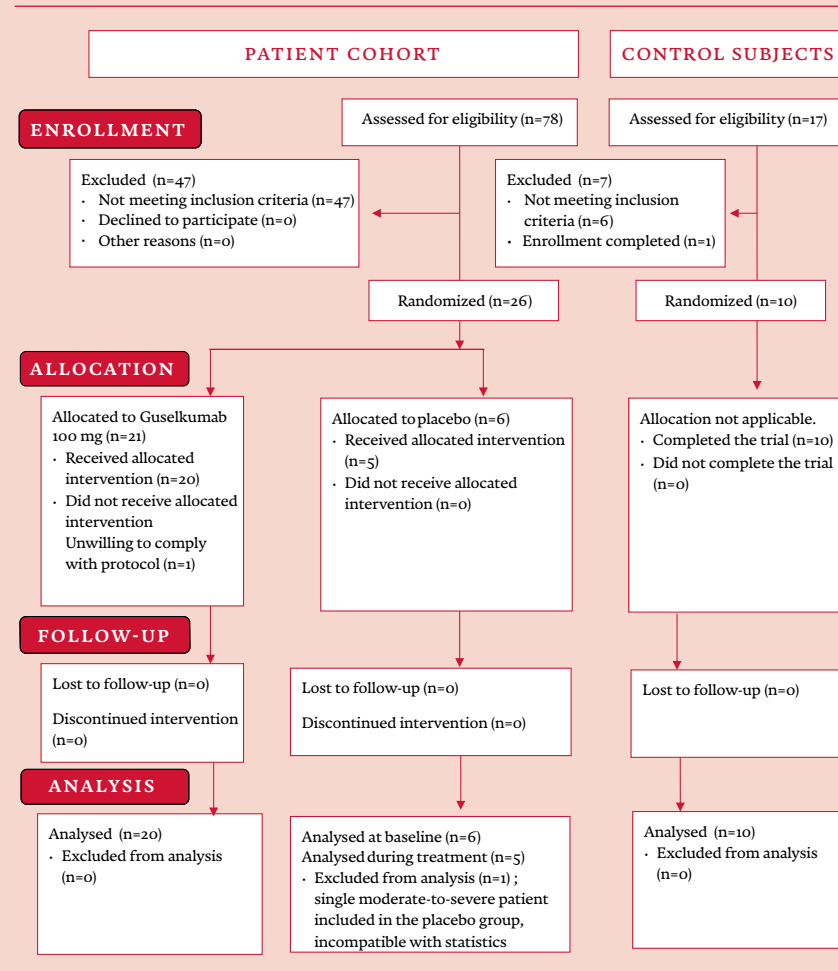
Eligible psoriasis patients must meet all of the following inclusion criteria at screening:

- 1 Male or non-pregnant female subjects, 18 to 75 years of age (inclusive); during COVID-19 pandemic this is set to 18 to 69 year of age (inclusive)
- 2 Diagnosed with plaque psoriasis at least 6 months prior to study participation
- 3 Willing to discontinue any psoriasis therapy other than emollients.
- 4 Having mild (PASI  $\geq 1$  and  $\leq 5$ ) or moderate-to-severe (PASI  $\geq 10$ ) plaque psoriasis;
- 5 Currently not using psoriasis medication and  $\geq 2$  plaques suitable for repeated biopsies and target lesion assessments. At least one of these lesions must be located on the extremities, preferably on the elbow or knee, with a minimal target lesion score between 6 and 9. Or, when currently using psoriasis medication and insufficient lesional skin is present, willing to discontinue treatment awaiting rescreening (see also exclusion criteria 3 for psoriatic patients);
- 6 Willing to give written informed consent and willing and able to comply with the study protocol;

And none of the following exclusion criteria at screening:

- 1 Having primarily erythrodermic, pustular or guttate psoriasis;
- 2 Having medication-induced psoriasis;
- 3 Having previously failed on ANTI-IL23 therapy;
- 4 Having received treatments for psoriasis within the following intervals prior to the start of the study:
  - a  $< 2$  weeks for topical treatment, e.g. retinoids, corticosteroids, vitamin D analogs
  - b  $< 4$  weeks for phototherapy, e.g. PUVA, PDT
  - c  $< 4$  weeks for non-biologic systemic treatment, e.g. retinoids, methotrexate, cyclosporine, fumaric acid esters
  - d  $< 4$  weeks for etanercept
  - e  $< 8$  weeks for adalimumab
  - f  $< 3$  months for ANTI-IL17, ANTI-IL12(/23) and ANTI-IL23 treatments
- 5 History or symptoms of any significant uncontrolled disease including (but not limited to), neurological, psychiatric, endocrine, cardiovascular, respiratory, gastrointestinal, hepatic, or renal disorder that may interfere with the study objectives, in the opinion of the Investigator, excluding psoriasis and conditions that are related to psoriasis;
- 6 History of immunological abnormality (e.g., immune suppression, severe allergy or anaphylaxis) that may interfere with study objectives, in the opinion of the Investigator;
- 7 Known infection requiring antibiotic therapy within the last 3 months prior to the study, including latent tuberculosis;
- 8 Systemic immunosuppressive or immunomodulatory treatment within 30 days prior to the study;
- 9 Body mass index (BMI)  $\leq 18.0$  or  $\geq 40.0$  kg/m<sup>2</sup>; during COVID-19 pandemic only  $\leq 18.0$  or  $> 33.0$  kg/m<sup>2</sup>
- 10 Participation in an investigational drug study within 3 months prior to screening or more than 4 times a year;
- 11 Loss or donation of blood over 500 mL within three months prior to screening;
- 12 The use of any medication or vitamin/mineral/herbal/dietary supplement within less than 5 half-lives prior to study participation, if the Investigator judges that it may interfere with the study objectives.
- 13 History of alcohol consumption exceeding 5 standard drinks per day on average within 3 months of screening. Alcohol consumption will be prohibited from at least 12 hours preceding each study visit;
- 14 Any other condition that could interfere with the conduct of the study or the study objectives, in the opinion of the Investigator.
- 15 During COVID-19 pandemic: presence of high risk comorbidities: such as cardiovascular, respiratory or immune system disorders other than psoriasis and psoriasis arthritis.

**Supplemental Figure 1** Completed PRISM flowchart showing the number of patients screened, included and analyzed.



**Supplemental Table 1** Overview of adverse effects recorded during the study.

		Mild (Placebo)	Mild (Guselkumab)	Moderate-to-severe (Guselkumab)
Total Adverse Events		16 (5/5)	22 (11/15)	5 (4/5)
Eye disorders	Glaucoma	0 (0/5)	1 (1/15)	0 (0/5)
Gastrointestinal disorders	Gastrointestinal viral infection	1 (1/15)	1 (1/15)	1 (1/5)
	Diarrhea	3 (2/5)	1 (1/15)	0 (0/5)
	Abdominal pain	0 (0/5)	1 (1/15)	0 (0/5)
General disorders and administration site conditions	Fatigue	0 (0/5)	2 (2/15)	0 (0/5)
	Fever	0 (0/5)	1 (1/15)	0 (0/5)
	Injection site erythema	0 (0/5)	1 (1/15)	0 (0/5)
Infections and infestations	SARS-COV-2 infection	4 (4/5)	3 (3/15)	1 (1/5)
	Influenza	2 (2/5)	0 (0/15)	0 (0/5)
	Upper respiratory tract infections	1 (1/5)	2 (2/15)	1 (1/5)
	Vaginal yeast infection	1 (1/5)	0 (0/15)	0 (0/5)
	Impetigo	0 (0/5)	1 (1/15)	0 (0/5)
Injury poisoning and procedural complications	Scapula fracture	0 (0/15)	0 (0/15)	1 (1/5)
	Rib contusion	0 (0/15)	0 (0/15)	1 (1/5)
	Traumatic hematoma	1 (1/5)	0 (0/15)	0 (0/5)
	Post vaccination syndrome	0 (0/5)	1 (1/15)	0 (0/5)
	Scarring	0 (0/5)	1 (1/15)	0 (0/5)
Musculoskeletal and connective tissue disorders	Muscular back pain	0 (0/5)	0 (0/5)	1 (1/5)
Nervous systems disorders	Headache	1 (1/5)	4 (4/15)	0 (0/5)
Skin and subcutaneous tissue disorders	Alopecia	1 (1/5)	1 (1/15)	0 (0/5)
	Allergic dermatitis	0 (0/5)	1 (1/15)	0 (0/5)
	Pruritus	1 (1/5)	1 (1/15)	0 (0/5)
Surgical and medical procedures	Dental operation	1 (1/5)	0 (0/15)	0 (0/5)

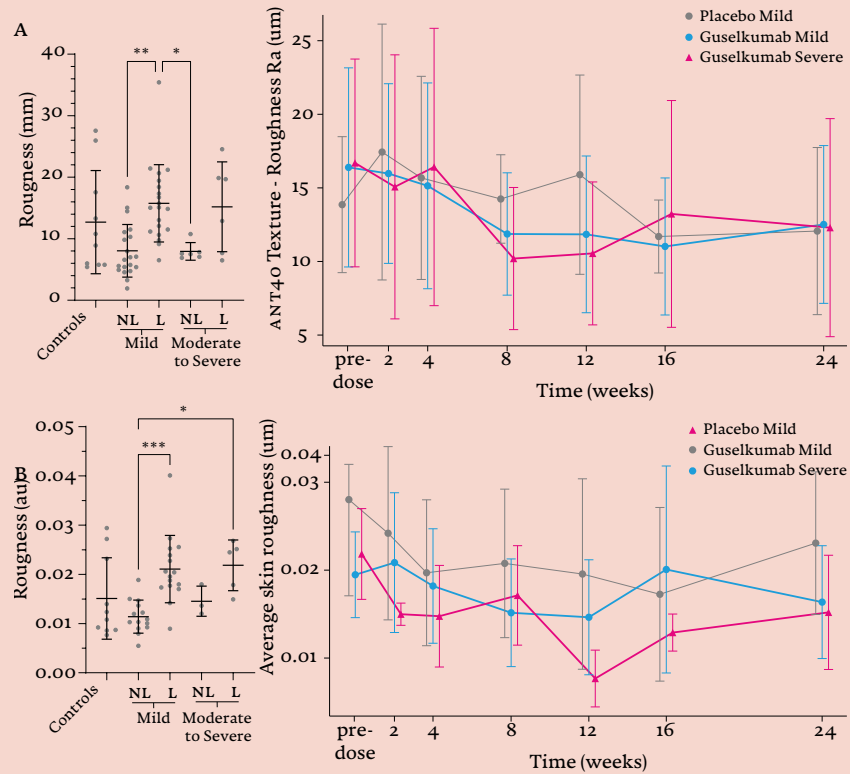
**Supplemental Table 2** Statistical output of all longitudinal scores and assessments mentioned in the main text for change to baseline (all groups) and compared to placebo (mild-GUS versus mild-PLA), separately. For change from baseline: the least square mean (LSM) change from baseline, followed by the 95% confidence interval and p-value are shown. For comparisons between Mild-GUS versus Mild-PLA, the LSM of Mild-GUS is contrasted with that of Mild-PLA, 95% confidence interval and the p-value.

	Change from baseline			End of study
	Mild patients (GUS)	Moderate-to-severe patients (GUS)	Mild patients (PLA)	Mild patients (GUS) vs mild patients (PLA)
<b>CLINICAL SCORING</b>				
PASI	-5.52 (-6.43 to -4.60) p<0.0001	-9.03 (-11.12 to -6.93) p<0.0001	-0.84 (-2.45 to 0.77) p=0.30	2.56 vs 5.75 (-4.61 to -1.75) p=0.0001
PASI-HD	-3.71 (-4.53 to -2.90) p<0.0001	-7.96 (-9.96 to -5.97) p<0.0001	0.46 (-0.96 to 1.87) p=0.52	1.84 vs 4.21 (-3.64 to -1.11) p=0.0008
Lesion severity score	-5.62 (-6.47 to -4.77) p<0.0001	-6.67 (-8.14 to -5.20) p<0.0001	0.84 (-0.72 to 2.41) p=0.29	2.7 vs 6.8 (-5.4 to -2.7) p<0.0001
DPASI	-0.92 (-1.53 to -0.30) p=0.0042	-2.59 (-3.70 to -1.48) p<0.0001	-0.11 (-1.16 to 0.93) p=0.83	3.61 to 4.27 (-1.63 to 0.30) p=0.17
<b>COLORIMETER</b>				
Average A* (AU)	-0.29 (-2.32 to 1.74) p=0.78	-2.26 (-5.83 to 1.30) p=0.21	-0.33 (-3.83 to 3.17) p=0.85	18.62 vs 17.67 (-1.81 to 3.71) p=0.48
<b>MULTISPECTRAL IMAGING</b>				
Roughness (mm)	3.54 (-6.27 to -0.81) p=0.012	-3.89 (-8.61 to 0.83) p=0.11	-2.88 (-7.62 to 1.86) p=0.23	12.85 vs 15.35 (-6.45 to 1.45) p=0.20
Maximal Height (mm)	-0.083 (-0.12 to -0.043) p<0.0001	-0.089 (-0.16 to -0.021) p=0.011	-0.039 (-0.11 to 0.031) p=0.27	0.19 vs 0.27 (-0.15 to -0.18) p=0.014
Average A* (AU)	-1.00 (-2.00 to 0.00) p=0.051	-2.49 (-4.25 to -0.73) p=0.0063	-0.75 (-2.49 to 1.00) p=0.40	11.15 to 11.41 (-1.82 to 1.28) p=0.72
Delta A* (AU)	-1.21 (-1.60 to 0.82) p<0.0001	-1.20 (-1.87 to -0.53) p=0.0006	-0.36 (-1.04 to 0.31) p=0.28	2.37 vs 3.14 (-1.28 to -0.25) p=0.0055
Maximal Erythema (AU)	-16.85 (-22.36 to -11.34) p<0.0001	-16.72 (-26.32 to -7.12) p=0.0009	2.34 (-7.28 to 11.96) p=0.6294	47.17 vs 61.23 (-22.10 to -6.02) p=0.0015

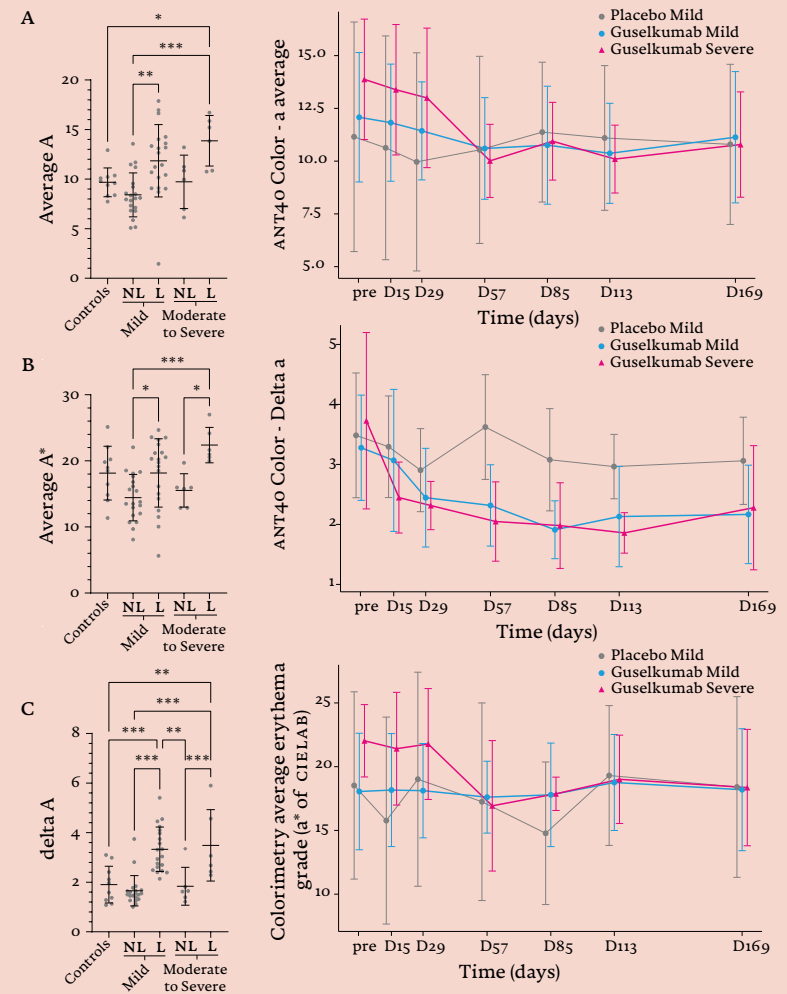
	Change from baseline			End of study
	Mild patients (GUS)	Moderate-to-severe patients (GUS)	Mild patients (PLA)	Mild patients (GUS) vs mild patients (PLA)
<b>OPTICAL COHERENCE TOMOGRAPHY</b>				
Roughness (µm)	-0.0045 (-0.0085 to -0.00045) p=0.030	-0.0064 (-0.012 to -0.00078) p=0.026	-0.0027 (-0.016 to 0.010) p=0.68	0.018 to 0.22 (-0.011 to 0.0023) p=0.20
Epidermal thickness (mm)	-0.10 (-0.13 to -0.074) p<0.0001	-0.13 (-0.18 to -0.084) p<0.0001	-0.038 (-0.087 to 0.011) p=0.13	0.21 vs 0.25 (-0.084 to 0.002) p=0.061
<b>LASER SPECKLE CONTRAST IMAGING</b>				
Perfusion (AU)	-46.57 (-58.97 to -34.18) p<0.0001	-62.29 (-83.72 to -40.86) p<0.0001	0.34 (-21.25 to 21.93) p=0.98	74.41 vs 107.12 (-50.87 to 14.55) p=0.0012
<b>THERMOGRAPHY</b>				
Skin temperature (°C)	-0.30 (-1.06 to 0.46) p=0.44	-0.18 (-1.41 to 1.05) p=0.77	-0.46 (-1.78 to 0.86) p=0.49	32.05 vs 32.26 (-1.32 to 0.89) p=0.69



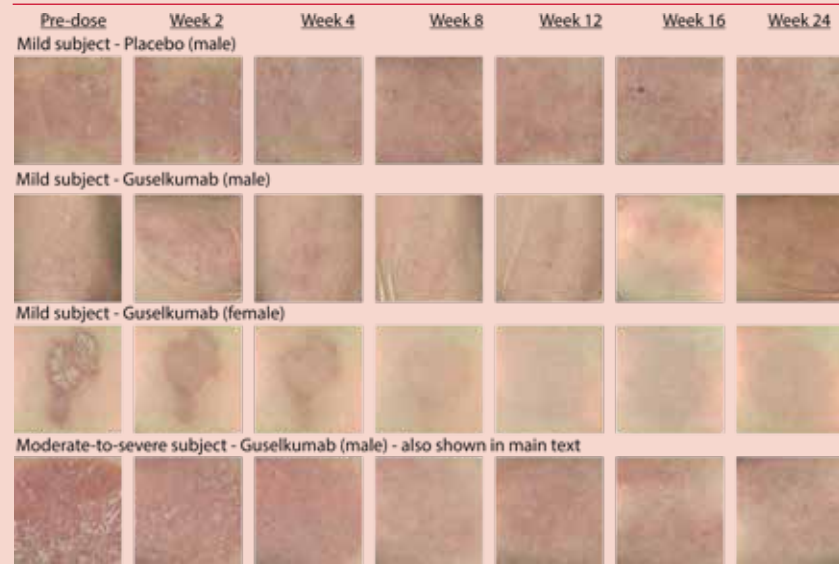
**Supplemental Figure 2** Results of superficial roughness analysis by multispectral imaging (A) and optical coherence tomography (B). Graphs show mean and standard deviation.



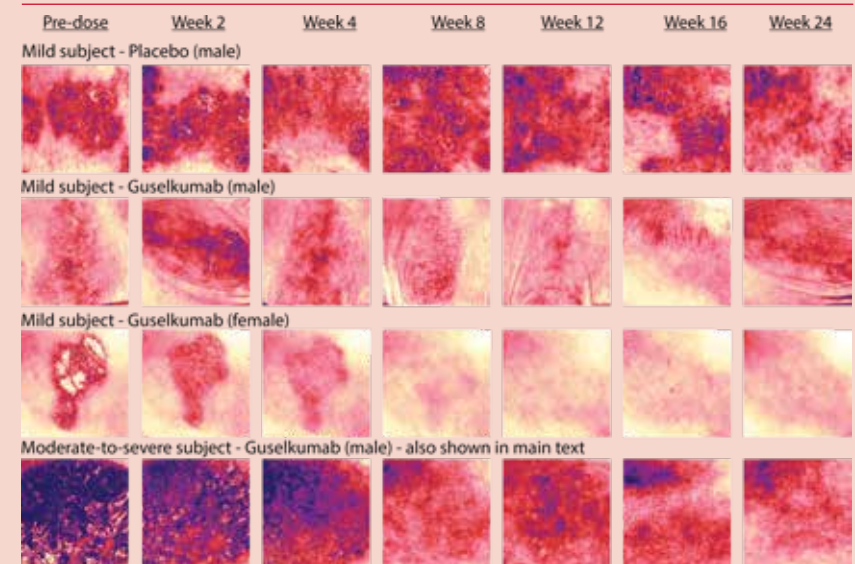
**Supplemental Figure 3** Baseline differences and longitudinal time course during the trial of the degree of redness based on the CIELAB A\* value determined by colorimetry (A), the average CIELAB A\* value by multispectral imaging (B) and the delta CIELAB A\*, being the difference between the lowest and highest recorded value within the region of interest, by multispectral imaging (C). Colorimetry did not indicate a difference compared to baseline and not compared to placebo. Average A\* was significantly lower compared to baseline in both guselkumab treated groups but not compared to placebo. Delta A\* showed a significant decrease compared to baseline and also compared to placebo.



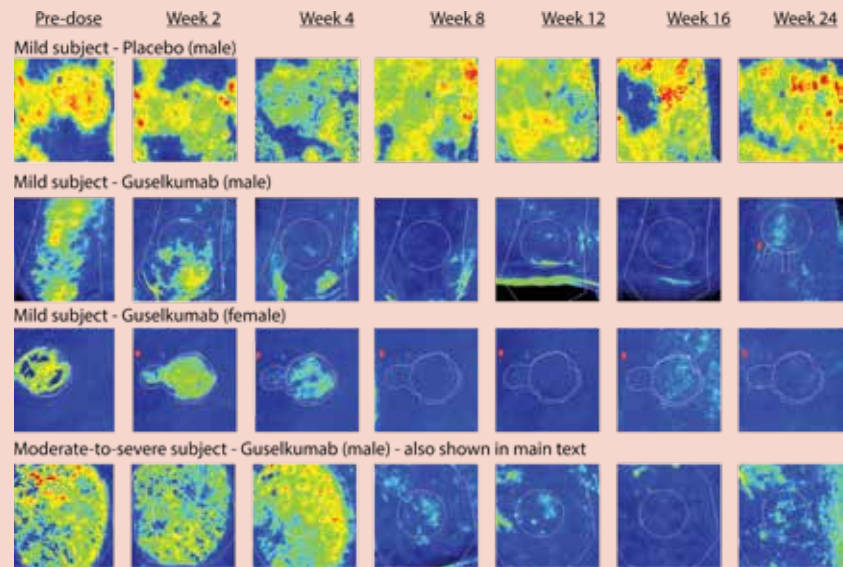
**Supplemental Figure 4** Overview of the superficial texture as recorded with multispectral imaging of additional patients.



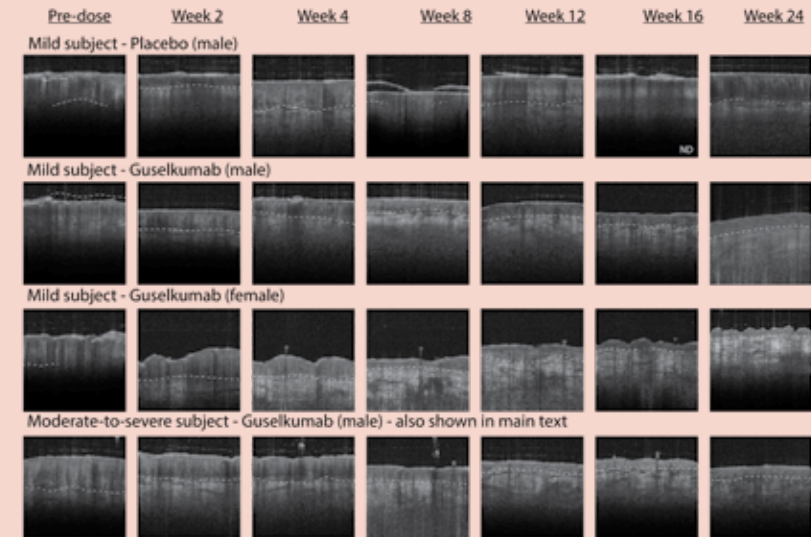
**Supplemental Figure 5** Overview of erythema as recorded with multispectral imaging of additional patients.



**Supplemental Figure 6** Overview of cutaneous perfusions as recorded with Laser Speckle Contrast Imaging of additional patients.



**Supplemental Figure 7** Overview of a frame from an optical biopsy as recorded with optical coherence tomography of additional patients. A dotted line indicates the dermal-epidermal junction. 'ND' indicates the basal-epidermal junction could not be reliably determined in that frame of the scan.



## SECTION 3

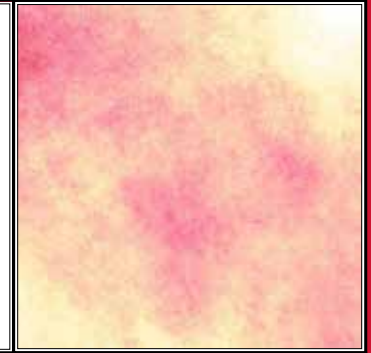
---

The stratum corneum  
ceramide profile as  
biomarker and therapeutic  
target

## CHAPTER 6

### SIMILAR ALTERATIONS OF THE STRATUM CORNEUM CERAMIDE PROFILE IN ATOPIC DERMATITIS, PSORIASIS, ICHTHYOSIS AND OTHER DERMATOSES, RESULTS FROM A SYSTEMATIC REVIEW AND META-ANALYSIS

Adapted from: The Journal of Investigative Dermatology (2024). (DOI: <https://doi.org/10.1016/j.jid.2024.02.010>)



Jannik Rousel,<sup>1,2,\*</sup> Catherine Mergen,<sup>2,\*</sup> Jan W. Schoones,<sup>3</sup> Tessa Niemeyer-van der Kolk,<sup>1</sup> Martijn B.A. van Doorn,<sup>1,4</sup> Joke A. Bouwstra,<sup>2</sup> Jeroen van Smeden<sup>1,2,5</sup> and Robert Rissmann<sup>1,2,5</sup> \*These authors contributed equally.

1. Centre for Human Drug Research, Leiden, NL / 2. Leiden Academic Centre for Drug Research, Leiden University, Leiden, NL / 3. Directorate of Research Policy, Leiden University Medical Centre, Leiden, NL / 4. Department of Dermatology, Erasmus Medical Centre, Rotterdam, NL / 5. Leiden University Medical Centre, Leiden, NL

## Abstract

**INTRODUCTION:** Ceramides form an integral part of the extracellular lipid matrix in the stratum corneum and are indispensable for a proper skin barrier function. The specific composition of ceramide subclasses is altered in many cutaneous diseases. This review systematically characterizes ceramide profiles throughout different dermatoses and evaluates their consistency.

**METHODS:** A systematic search was performed according to the PRISMA guidelines for studies that evaluated the stratum corneum ceramide profile of cutaneous diseases on 4 July 2023. The search yielded 2309 articles of which 76 were included comprising 1329 patients and 852 controls. An overview of ceramide profile alterations compared to healthy volunteers and average ceramide profiles were compiled per indication.

**RESULTS:** Most literature was available for atopic dermatitis, ichthyosis and psoriasis. Here, a large consensus in literature on increased CER[S] abundances, decreased CER[P] abundances and decreased ceramide chain length in lesional skin is observed. Although literature on palmoplantar hyperkeratosis and acne vulgaris was scarce, meta-analysis highlighted similar changes in their ceramide profiles.

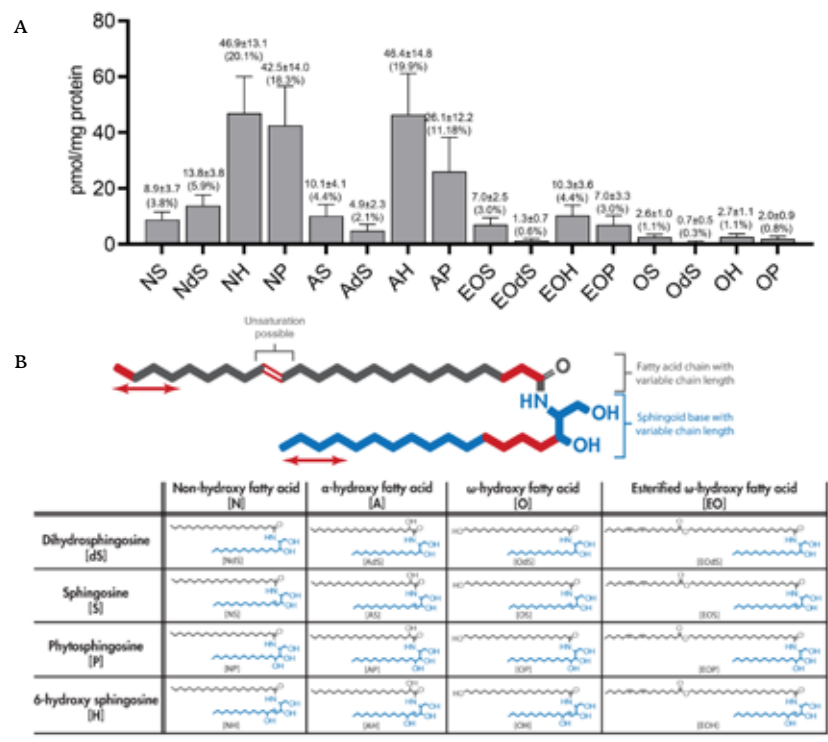
**CONCLUSIONS:** Similar alterations in the ceramide profile are observed throughout different dermatoses and might therefore highlight that these not primarily relate to specific disease mechanisms but general epidermal deregulation. Monitoring these alterations may be exploited as a biomarker for disease severity and treatment responses.

## Introduction

The skin barrier represents the physical interface between the human body and the external environment. It is vital in maintaining proper homeostasis and prevents the penetration of foreign substances and pathogens into the body.<sup>1</sup> Much of the barrier function is dependent on the stratum corneum (SC), where layers of near-impermeable corneocytes are embedded in a complex lipid matrix. This matrix is essential for the barrier as it represents the only continuous pathway through intact skin that allergens and other exogenous compounds need to overcome.<sup>2</sup> The lipid matrix contains a vast variety of lipids. During terminal differentiation, keratinocytes readily synthesize cholesterol, fatty acids and ceramides in a highly regulated manner. These lipids are eventually extruded to the extracellular space where they form a tight and well-organized matrix around the corneocytes.<sup>3</sup>

Ceramides represent a complex fraction of barrier lipids with over 1000 different species identified in human SC using modern liquid chromatography-mass spectrometry (LC-MS) techniques.<sup>4</sup> These ceramides can be categorized based on their fatty acid and sphingoid base moiety (figure 1). Based on this classification, a total of 25 different subclasses have been identified in the healthy SC ceramide profile of which CER[NH], CER[NP] and CER[AH] are most abundantly present.<sup>5</sup> Although grouped by a single abbreviation, each ceramide class comprises ceramides with varying degrees of unsaturation and chain length, generally between 42 to 52 total carbons or between 70 to 80 total carbons in the case of CER[EO].<sup>6</sup> These longer ceramide species are critical in anchoring the lipid matrix to the cornified envelope as they can be covalently bound to structural proteins upon conversion to CER[O].<sup>7</sup>

**Figure 1** Ceramides of the human skin stratum corneum. (A) Overview of a representative absolute stratum corneum ceramide composition of 19 healthy controls which comprises the 12 subclasses that are frequently reported. Specific quantities of ceramide classes are presented in pmol/mg protein with its relative abundance in parenthesis above their respective bar. Adapted from Kawana et al. (2020). (B) An example of a ceramide, in this case CER(NDS), is shown with areas of variation with in a subclass highlighted. Below, a structural overview of the major subclasses of relevance in this review. Ceramides are abbreviated based on their sphingoid base (dihydro sphingosine: DS, sphingosine: S, phytosphingosine: P and 6-hydroxy sphingosine: H) and fatty acid chain (non-hydroxy: N,  $\alpha$ -hydroxy: A,  $\omega$ -hydroxy: O and esterified  $\omega$ -hydroxy: EO). Note these can still differ in chain length and degree of unsaturation. Adapted from van Smeden et al. (2014).



The specific composition of the ceramide fraction has shown to be important in maintaining a proper barrier function. In atopic dermatitis, barrier dysfunction has been attributed a major role in disease pathophysiology and SC barrier impairment appears well correlated with changes in the ceramide profile of lesional skin.<sup>8,9</sup> Direct relation between changes in ceramide

composition and permeability has been demonstrated using model systems that mimic the lipid matrix of inflamed skin<sup>10-12</sup> and has been contributed as a causative factor of the poor barrier function of in-vitro cultured human skin equivalents.<sup>13,14</sup> However, it remains unclear whether these alterations are a causative factor, aggravate the existing disease or are merely a symptom of disease. Although the fatty acid fraction has also shown to be altered concomitantly with ceramides in disease<sup>15</sup> and changes in this fraction have also shown to be important for barrier function,<sup>16,17</sup> their significance to the SC in disease has been reviewed in-depth elsewhere.<sup>18,19</sup>

Up to now, integrative approaches to SC profiling in disease have been limited to non-systematic scholarly reviews without meta-analysis. By performing a systematic search and meta-analysis, research on the ceramide profiles from single indications is intuitively compiled and contrasted with all available literature. This might enable an increased understanding of barrier impairment in skin diseases, which might be relevant in the development of therapies focused on barrier restoration.

## Methods

This systematic review adhered to the Preferred Reporting Items for Systematic Reviews and Meta-analysis (PRISMA) guidelines<sup>20</sup> and was registered under CRD42023440867 in the PROSPERO database. A comprehensive search query was composed by a trained librarian (JWS) which combined ceramides, skin compartment and dermatological conditions. All relevant keywords and associated free text word variations within these components were included in the search strategy (see supplementary information). The search strategy was optimized for PubMed, Embase (OVID version), Web Of Science, Cochrane Library and Emcare (OVID version). The final search was performed on 4 July 2023. Review articles were excluded, as were studies solely reporting animal or *in-vitro* studies as they fell outside the objective of the review. All retrieved articles were independently screened by two reviewers by title and abstract before critically assessing the full text for inclusion. Reviewers were blinded from each other's decisions and discrepancies were resolved by consensus.

For the meta-analysis numerical data was retrieved from (supplemental) results or extracted from figures using WebPlotDigitizer<sup>21,22</sup> and indication and group size were listed. Relative ceramide profiles were extracted from studies that reported at least 11 predefined subclasses for healthy and diseased

skin and a forest plot was generated showing the weighted average change compared to control. Weighing was performed based on the fraction of subjects per extracted profile compared to all subjects included per indication.

## Results

The final search returned 2309 titles, of which 1007 were identified as duplicates (figure 2). Of the 1302 manuscripts, 1124 were excluded after reviewing the abstract and another 102 were excluded after reviewing the full text. Exclusions were mostly based on the absence of ceramide classes (752) or did not primarily relate to human skin disease samples (290). The remaining 76 included articles contained information on SC ceramides in atopic dermatitis (40 articles, 849 patients), psoriasis (10 articles, 85 patients), ichthyosis (13 articles, 121 patients), xerosis (7 articles, 170 patients), acne vulgaris (3 articles, 43 patients), palmoplantar hyperkeratosis (2 articles, 4 patients), dandruff (2 articles, 63 patients), pruritus (1 article, 20 patients), melasma (1 article, 21 patients), scarring (article 1, 9 patients) and hypohidrotic ectodermal dysplasia (1 article, 7 patients). Additionally, 852 healthy controls were included in 55 of these articles. Sections 3.1 to 3.11 systematically describe all observations on ceramide classes in disease. Those that compare findings with healthy controls are thereafter compiled in table 1. Furthermore, a meta-analysis is performed on extracted ceramide profiles and compared to the average ceramide profile of all collected healthy volunteer profiles (figure 3).

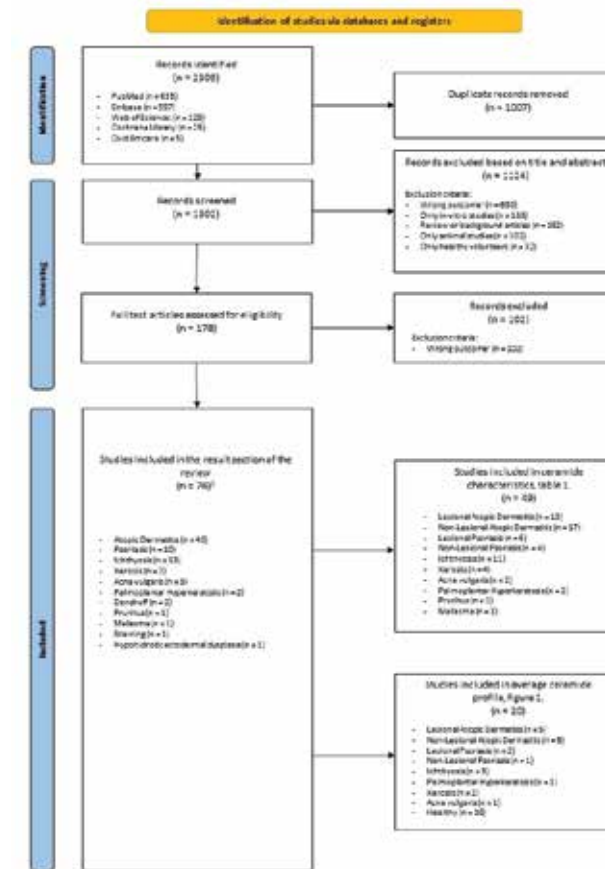
### ATOPIC DERMATITIS

#### Lesional Skin of Atopic Dermatitis

Ceramide profiling has been extensively reported in atopic dermatitis. Firstly, the amount of total ceramides was reported to be lower in lesional skin compared to healthy volunteers.<sup>8,9,23,24</sup> On the level of subclass composition, decreased CER[NDS],<sup>8,9</sup> CER[NP],<sup>8,9,15,25</sup> CER[NH],<sup>8,9</sup> CER[AP]<sup>25</sup> and CER[OS]<sup>25</sup> were observed. Furthermore, the abundance of CER[EOS],<sup>8,9,15,24-27</sup> CER[EODS],<sup>9</sup> CER[EOP],<sup>8,9,15,25</sup> CER[EOH],<sup>8,9,15</sup> or CER[EO]<sup>9,28</sup> in general was reported to be decreased in lesional skin compared to healthy controls. On the other hand, the amount of CER[S] was commonly increased in lesional skin based on reported increases of CER[NS],<sup>9,15,27-29</sup> CER[AS]<sup>8,9,15,28</sup> or CER[DS] in general.<sup>30</sup> A study comparing lesional and non-lesional skin of patients showed decreased total ceramide abundance with decreased

CER[NDS], CER[NP], CER[NH], CER[ADS], CER[AP], CER[AH], CER[EOS], CER[EOP] and CER[EOH] in lesional skin<sup>31</sup>. This is supported by *in vitro* observations showing that the rate at which CER[NP], CER[EO], and ratio of CER[AP/AH] were synthesized was decreased in excised lesional skin.<sup>32</sup> High Performance Thin-layer Chromatography (HPTLC) analysis showed a reduction in CER[EOS] abundance<sup>23,33-35</sup> and an increased CER[AH/AP] ratio.<sup>36</sup>

**Figure 2** PRISMA flowchart showing the process of the systematic search and eventual inclusion based on indication. Single articles can contain multiple different indications. Wrong outcome indicates no information about the ceramide composition in diseased human stratum corneum was present in the study.





### **Ceramide Chain Length in Lesional Skin of Atopic Dermatitis**

Compared to controls, ceramide chain length was decreased in lesional skin as the abundance of short-chain ceramides was increased,<sup>8,15,24,29,37</sup> long-chain ceramides were decreased<sup>8,15,24,25,29,37</sup> or the average length.<sup>9,15,38</sup> Especially the abundance of CER[NS] with a total chain length of 34 carbons, detected in full or based on its fatty acid or sphingoid constituents, was increased in lesional skin.<sup>8,9,15,24,28,29,39</sup> However, this was not observed in CER[NP] and CER[AP].<sup>25,39</sup> Additionally, lesional skin showed increased unsaturation in specific CER[NS] and throughout CER[EO].<sup>27,39</sup> However, increased unsaturation of selected ceramides or subclasses might not necessarily translate to all SC ceramides.<sup>26,39</sup>

### **The Bound Lipid Fraction in Lesional Skin of Atopic Dermatitis**

Conflicting reports are present on ceramides covalently bound to the cornified envelope, which were both reported to be lower<sup>32</sup> or unaffected<sup>26</sup> in lesional skin. The bound CER[O] fraction showed similar changes to the free fraction described above as an increased proportion of CER[S], a decreased ceramide chain length and increased unsaturation was observed at lesional sites.<sup>26</sup>

### **Non-Lesional Skin of Atopic Dermatitis**

Of note, the ceramide profile of non-lesional skin was also affected. Compared to healthy volunteers, non-lesional skin demonstrated decreased<sup>9,23,40,41</sup> or similar<sup>24,36</sup> abundance of total ceramides, decreased abundances of CER[NH],<sup>8,42</sup> CER[NP],<sup>8,43</sup> CER[EOS],<sup>26,27,40,42,44</sup> CER[EOP],<sup>9</sup> CER[EODS],<sup>9</sup> CER[EOH]<sup>9</sup> or CER[EO],<sup>28,43,45</sup> but also increased abundances of CER[S],<sup>9,26,29,30,42,45</sup> degree of unsaturation<sup>26</sup> and amount of CER[NSC34].<sup>9,44,45</sup> Contrarily, increases in CER[NP] and CER[EOH] were observed in one study, but were ultimately decreased when corrected for the overall decrease in total ceramides.<sup>40</sup> However, other studies using HPTLC did not report clear changes between non-lesional atopic dermatitis skin and healthy controls.<sup>46,47</sup>

The total abundance of protein-bound ceramides in non-lesional was lower<sup>32</sup> or similar to controls.<sup>26,44</sup> However, increased CER[S] and unsaturation was observed within this fraction.<sup>26</sup> In contrast, a study quantifying the acyl-chain remnant produced in binding of CER[EO] to the cornified envelope found this to be increased, indicating more CER[EO] was converted. However, they did not verify their results by determining the abundance of CER[EO] or CER[O].<sup>48</sup>

Several studies observe a decreased average ceramide chain length in non-lesional skin compared to controls,<sup>15,41,42,44,45</sup> but the chain length has also shown not to significantly differ.<sup>9,39</sup>

### **Application of the Ceramide Profile in Atopic Dermatitis as Biomarker**

Interestingly, the ceramide profile has been used as a biomarker and showed to be directly affected by therapy. Monitoring lesional skin during efficacious treatment with the IL-4/IL-13 inhibitor dupilumab showed that aberrant levels of C18-sphingosine containing CER[NS] and CER[EOS] species in lesional skin were restored.<sup>27</sup> Additionally, the abundance of longer ceramide species increased compared to baseline<sup>27,49</sup> and the abundance of CER[NSC34] decreased significantly in only one report,<sup>27</sup> therewith normalizing these levels towards those of controls. Head-to-head comparisons between the calcineurin-inhibitor tacrolimus and the corticosteroid mometasone showed that clinical improvements were reflected in the ceramide profile with increased CER[NP] and CER[NH], but also showed a concomitant increase in overall SC lipids.<sup>50</sup> However, an earlier study investigating tacrolimus did not observe significant changes to the ceramide profile, but neither did it report whether treatment was effective.<sup>51</sup> Treatment with a novel topical cannabinoid receptor agonist resulted in increased CER[EOS] but did not explicitly report the clinical effects in these subjects.<sup>52</sup> Of note, the use of an assay comprising only selected subclasses might only partially capture changes to the ceramide profile and thereby skew results.<sup>50,52</sup> Normalization of the CER[EOS] abundance and chain length was also observed in non-lesional skin after dupilumab treatment,<sup>27</sup> despite the generally smaller changes observed in the non-lesional ceramide profile. Another study showed that a topical synthetic pseudoceramide capable of alleviating atopic dermatitis symptoms altered the ceramide profile of non-lesional skin with increased CER[ADS], CER[AH], CER[AP] but decreased CER[EOS], CER[EOH], CER[EOP] abundances.<sup>53</sup> Additionally, average chain length increased in CER[NS] and CER[ADS] while chain lengths in CER[AS], CER[AH], CER[AP], CER[EOS], CER[EOS], CER[EOH] and CER[EOP] decreased. The amounts of ceramides with 34 carbons remained unaltered throughout.<sup>53</sup> Comparing the non-lesional skin of patients before and after UV-therapy showed only an increase in CER[NH], but might not properly reflect the overall treatment response as the more subtle changes in non-lesional skin might not be detected using HPTLC.<sup>54</sup> A biomarker approach has also been employed prospectively, showing healthy

children that will develop atopic dermatitis in the future are characterized by minimally higher CER[NSC34] and CER[ASC34] abundances, reduction in ceramide chain length and decrease in protein-bound CER[OS], while CER[EOS] remained unaltered.<sup>55</sup> A report including the analysis of selected ceramide species reiterated the ability to aid in the prediction of future atopic dermatitis development based on increased CER[DS] and decreased monounsaturated CER[S] species, or ratios based thereon.<sup>56</sup> In a clinical setting, maintaining remission after topical corticosteroid treatment was associated with significantly increased CER[AH] and ceramide chain length compared to patients that experiences a flare-up within 8 weeks.<sup>57</sup> Levels of CER[NP] and CER[NH] were additionally elevated, but this was not statistically significant.<sup>57</sup>

## PSORIASIS

Although psoriasis is a frequently occurring condition, only 9 publications were identified that investigated the ceramide profile in psoriasis patients and compared these to healthy controls. An absolute quantitative approach showed that more CER[NS] and CER[AS] was present in lesional skin compared to that of controls, despite a decrease in total ceramide content and concomitant decreases in CER[NDS], CER[NP], CER[NH], CER[AH], CER[AP], CER[EOS], CER[EOP] and CER[EOH].<sup>58</sup> When expressed as relative to the total ceramides detected, the abundance of CER[NDS],<sup>59</sup> CER[ADS]<sup>59</sup> and CER[AH]<sup>59</sup> showed to be increased in addition to that of CER[NS]<sup>59-61</sup> and CER[AS].<sup>59,61</sup> Comparable to an absolute approach, the abundance of CER[NP],<sup>59-61</sup> CER[AP],<sup>59,61</sup> CER[EOS],<sup>59,61,62</sup> CER[EOP]<sup>59</sup> and CER[EOH]<sup>59</sup> remained decreased. The decreased lesional CER[NP]:CER[NS] ratio is specifically reported on.<sup>63</sup> Of note, analysis of non-lesional skin showed similar<sup>38,60</sup> or smaller<sup>63</sup> changes than lesional skin compared to healthy controls. All articles containing relative CER[EOS] abundances showed a decrease of CER[EOS] in lesional skin.<sup>59,61,62</sup> In contrast, Tyrrell *et al.* showed increased absolute abundances of specific CER[EOS], CER[EOP] and CER[EOH] species in both lesional and non-lesional skin compared to healthy controls, but this study did not correct for the amount of SC removed and its focus on selective CER[EO] species might not be representative for entire subclasses.<sup>64</sup> However, this study still showed that the ratio between selected longer versus shorter chain CER[EOS], CER[EOP] and CER[EOH] species was decreased in lesional skin compared to non-lesional skin.<sup>64</sup> Indeed, analysis of the ceramide chain length in lesional

skin showed an average decrease compared to controls, along with increased abundances of non-CER[EO] with 34 carbons and CER[EO] of 62 carbons.<sup>59</sup> This is supported by other studies which observed that shorter ceramides were increased compared to their further elongated counterparts throughout CER[NH], CER[ADS], CER[NP] and CER[AP]<sup>37</sup> or showed a decreased average chain length within CER[NDS]<sup>38</sup> in lesional skin. This effect seems to be less pronounced in a study where these comparisons were made based on only the length of solely the ceramide fatty-acid tail.<sup>60</sup> HPTLC analysis showed increased CER[S] abundances<sup>61</sup> and a decrease in CER[EOS]<sup>61,62</sup> and CER[P]<sup>61</sup> in lesional skin compared to healthy controls. Another study using HPTLC reported no compositional changes between non-lesional psoriatic skin and healthy controls.<sup>46</sup> High similarity between non-lesional psoriatic and healthy stratum corneum is reiterated by more recent work using LC-MS which showed only a significant increase in CER[NH] abundance.<sup>58</sup>

## ICHTHYOSES AND OTHER MENDELIAN DISORDERS

The spectrum of ichthyoses is diverse, with different mutations underlying various phenotypes. Though it might be appropriate to stratify ceramide profiles per genotype based on the specific defects in ceramide processing, they have been summarized together for conciseness. We have included a more elaborate section on ceramide changes per mutation in the supplementary information. Pioneering work using HPTLC showed a reduction in total ceramide levels and CER[EOS] amongst 80 patients with different ichthyoses.<sup>65</sup> Another HPTLC study reported an increased abundance of CER[NS] and CER[NP] and a decrease of CER[AS].<sup>66</sup>

More specifically, the ceramide profile of ichthyosis patients has shown a reduction in total ceramides<sup>15,67-69</sup> with a relative increase in CER[NS],<sup>69-72</sup> CER[NDS],<sup>71</sup> CER[AS],<sup>70-72</sup> CER[AP],<sup>71</sup> CER[ADS]<sup>71</sup> and CER[OS]<sup>73</sup> and a relative decrease in CER[NP],<sup>15,69-71</sup> CER[NH]<sup>71</sup> and CER[AH]<sup>71</sup> compared to healthy controls. When absolute abundances were determined, increased CER[NS],<sup>68,69,74</sup> CER[AS],<sup>74</sup> CER[OS],<sup>69</sup> CER[OP]<sup>69</sup> and CER[OH]<sup>69</sup> and decreased CER[NP],<sup>68,69,74,75</sup> CER[NH],<sup>68,69,74,75</sup> CER[AP],<sup>68,69</sup> CER[ADS]<sup>69,75</sup> and CER[AH]<sup>68,69</sup> were observed compared to healthy controls. CER[EO] is commonly altered with reported absolute and relative decreases in CER[EOS],<sup>68,69,71,73-76</sup> CER[EOH],<sup>15,68,69,71,72,74,75</sup> CER[EODS]<sup>15,71,75</sup> and CER[EOP].<sup>68-71,74,75</sup> In the single report that showed increased CER[EOS] abundances, this could be linked to genetic defects in the binding of ceramides to

the cornified envelope resulting in its accumulation.<sup>72</sup> The amount of protein-bound CER[OS]<sup>72,77</sup> and CER[OH]<sup>72</sup> were reported to be decreased in ichthyosis patients, but the protein-bound fraction has also shown not to be affected in other studies even though CER[EOS] levels were depleted.<sup>69,71,75</sup> Although unsaturation in the CER[EO] or CER[O] fraction did not show to be increased,<sup>69,71,75</sup> an evident increase in unsaturated ceramides, especially within CER[NP], was observed in ichthyosis linearis circumflexa patients.<sup>76</sup>

Ceramide chain length was shown to be decreased in ichthyosis patients,<sup>15,68,69,71,75</sup> but ceramide chain lengths comparable with controls have also been observed.<sup>72</sup> Of note, evident overabundances of very short-chain ceramides CER[NSC34],<sup>15,68,71</sup> CER[ASC34]<sup>71,76</sup> and CER[AHC34]<sup>15</sup> were observed.

Interestingly, treatment with oral retinoids partly restored the level of CER[NH], CER[EOH] and CER[EOP] and seemed to slightly restore the impaired chain elongation.<sup>68</sup>

More severe cases include that of a collodion baby that showed a near-depletion of all ceramides in the SC and did not survive past six weeks.<sup>67</sup> Cases of collodion babies which resolved into very mild cases of ichthyosis have shown to exhibit ceramide profiles comparable to other ichthyosis patients with increased CER[NS] and CER[AS] but decreased CER[NP], CER[AP], CER[EOS], CER[EOP], CER[EOH], protein-bound CER[OS] and protein-bound CER[OH]. Additionally, ceramide species showed a decreased average chain length.<sup>78</sup>

## XEROSIS

Studies on the ceramide subclass composition in xerosis mainly monitor dry skin over time without comparisons to healthy controls. The total abundance of ceramide increased compared to baseline upon the clinical improvement of dry skin.<sup>79,80</sup> This increase was reflected in the ceramide subclass profile with increased abundances throughout all classes, except for CER[NDS], CER[EODS] and CER[EOP].<sup>79</sup> However, increases were proportionate to the overall increase in ceramides resulting in a relative ceramide profile comparable to baseline.<sup>79</sup> A more targeted analysis supported a differential effect on subclass synthesis with increased CER[AH] but comparable CER[NP] and CER[EOS] levels after treatment.<sup>80</sup> Another longitudinal study showed no effect on total ceramide abundances after treatment with an investigative humectant containing eucalyptus extract but demonstrated increased

CER[NP] abundances when compared to baseline. However, this remained similar when compared to placebo. Additionally, clinical improvements compared to both baseline and placebo were inconclusive and reporting on other ceramide parameters determined during the study was sparse.<sup>81</sup> Chemotherapy with the epidermal growth factor inhibitor erlotinib, of which dry skin is a common adverse effect, resulted in significant decreases of CER[AP] and CER[AH], even though this included samples from patients under erlotinib treatment regardless of the presence of dry skin.<sup>82</sup> Conflicting results are reported by studies using HPTLC. One study reported no compositional changes compared to normal skin and no meaningful correlations between the severity of xerosis and ceramide composition could be observed.<sup>83</sup> Another study observed an increase in CER[NS], CER[NP], CER[AP] and decrease in CER[EOS] and CER[AS] in dry skin compared to controls.<sup>84</sup> The induction of dry skin showed to alter the ceramide profile compared to healthy volunteers leading to an increase in CER[NS] and CER[AS] and a decrease in CER[AP].<sup>85</sup>

## ACNE VULGARIS

Comprehensive profiling of cheek samples from acne patients at four different moments throughout the year showed season-dependent changes in the ceramide composition compared to controls. Decreased absolute abundances of CER[NH] and CER[AH] were observed in February and April, decreased CER[EOS] in February, April and November, and a decrease in CER[EOH] was observed only in February.<sup>86</sup> Changes to the relative ceramide composition appeared smaller, but no statistics were reported.<sup>86</sup> While this study did not report average carbon chain lengths, another study showed these were not necessarily altered when comparing lesional and non-lesional samples.<sup>87</sup> HPTLC analysis showed that the ceramide profile in comedones differed from surface lipids from non-lesional sites with increased CER[NS] and CER[EOS] and decreased CER[AS] and CER[AP].<sup>88</sup>

## PALMOPLANTAR HYPERKERATOSIS

The affected palms of two patients with hyperkeratosis showed only small differences in the total ceramide content, ceramide composition and ceramide chain length, partly due to high variation within the patient- and (related) control-group.<sup>89</sup> However, two other patients demonstrated increased CER[NS] and decreased CER[NP] abundances along with a reduction in CER[NDS] chain length on lesional skin compared to controls.<sup>38</sup>

## DANDRUFF

The literature search returned two publications on the ceramide profile in dandruff.<sup>90,91</sup> A decrease in total ceramides was observed between healthy and affected study groups, but changes in the ceramide profile remained inconclusive.<sup>90</sup> The amount of bound lipids was unaltered.<sup>90</sup> In a randomized trial, ceramide levels increased in patients allocated to anti-dandruff shampoo with concurrent changes on the subclass profile.<sup>91</sup> Unfortunately, translation from old nomenclature based on HPTLC retention times to the nomenclature of Motta *et al.* is not unequivocally. This hinders a more detailed interpretation of the results.

## PRURITUS

Skin surface lipid profiling in senile pruritis patients showed an increase in CER[NS], CER[NDS], CER[NP], CER[EOS] and CER[OS] on the lower leg. Interestingly, the abundance of CER[OS] exceeded that of CER[EOS] in this study. It has to be noted that the collection method used was tailored towards sebum lipids, although this procedure does also collect superficial SC layers.<sup>92</sup>

## MELASMA

Differential analysis of the non-lesional and lesional skin of melasma patients showed that lesional skin was characterized by an increase in total ceramides with specific increases in CER[NP], CER[NDS], CER[AH], CER[EOS], and CER[EOH]. Additionally, an absolute significantly increased amount of ceramides was observed with a fatty acid-tail of over 20 carbons in length. While those with a length of 12 to 19 carbons were also elevated, this increase was not significant. However, only fold-changes of lesional compared to non-lesional skin instead of abundances were reported.<sup>93</sup>

## SCARRING

Using HPTLC Kunii *et al.* report a relative increase in CER[AS] and decrease in CER[NP] in the year following scar formation compared to healthy controls, while CER[EOS] abundances remained unaltered.<sup>94</sup>

## HYPHIDROTIC ECTODERMAL DYSPLASIA

Lastly, non-lesional skin of patients with hypohidrotic ectodermal dysplasia was directly compared to that of atopic dermatitis. Compared to non-lesional atopic dermatitis skin, an increased abundance of CER[EOS] was observed.<sup>95</sup>

However, the omission of a healthy control group prevents any conclusions from being drawn as atopic dermatitis is associated with decreased CER[EOS] levels.<sup>8,9,15,24-27</sup>

## SYNTHESIS

The degree of agreement on alterations in the ceramide profile of diseased skin compared to healthy controls throughout all studies is shown in table 1. In atopic dermatitis sources are well aligned on alterations in subclass abundance, chain length impairment and unsaturation. Disagreement is observed on the bound lipid fraction which might in part be due to the lack of attention as only two publications report on this. Similar changes in chain length impairment and subclass abundance are also reported in psoriasis, except for CER[NDS], CER[NH], CER[ADS] and CER[AH], which might be partly due to a much smaller amount of studies performed. Non-lesional skin of atopic dermatitis and psoriasis is attributed similar compositional changes as lesional skin, but literature appears inconclusive, and many subclasses remain unaltered when compared to healthy skin. Interestingly, similar alterations are also observed in ichthyosis, despite consisting of varying phenotypes resulting from different mutations. Common changes are a reduction in chain length and a decrease in CER[EO]. However, disagreements are present in CER[EOS] abundance and in the bound lipid fraction, which might also be due to the fact that, despite a large number of studies, only a relatively small number of patients and controls were included in total. Despite a limited amount of sources, the ceramide profile in palmoplantar hyperkeratosis shows resemblance to that of atopic dermatitis, psoriasis and ichthyosis. The low number of papers available on acne vulgaris, dandruff, pruritus, melasma, scar formation and hypohidrotic ectodermal dysplasia makes comparisons and general conclusions difficult. This is also the case for xerosis, where most studies only report changes to baseline within the same subject.

To further visualize the ceramide profile in disease and healthy skin, a meta-analysis of the average relative ceramide profile has been performed using literature that reports on at least 11 defined subclasses (figure 2). The weighted profiles of lesional atopic dermatitis (AD-L), lesional psoriasis (PSO-L), ichthyosis, palmoplantar hyperkeratosis (PHK) and acne show a evidently decreased CER[NP] abundance compared to controls (AD-L: -6.1±2.3%, PSO-L: -12.3±1.7%, ichthyosis: -8.2±4.4%, PHK: -6.4±4.9%, acne: 13.7±0.6%). These changes appear relatively small expressed as percentage of the total ceramide

profile, but they amount to a 26%, 52%, 35%, 28% and 59% reduction in CER[NP] abundance, respectively. Although increases in CER[NS] appear smaller, the lower abundance of CER[NS] makes these changes even more drastic (AD-L: +2.7±4.9% (+37%), PSO-L: +9.3±0.2% (+127%), ichthyosis: +7.7±4.9% (+105%), PHK: +4.9±3.8% (+66%), acne: +6.8±1.2% (+92%). Apart from small changes in CER[H] ceramide for psoriasis and acne, no other evident changes compared to control are observed. Though more powerful, we opted not to report the percentage change of a percentage as that might entice one to overestimate the effect. It has to be noted that data retrieved from PHK and acne is sourced from a single article. Changes to the non-lesional skin in atopic dermatitis and psoriasis appear less pronounced and fall within the standard deviation of healthy volunteers together with the ceramide profile of xerosis.

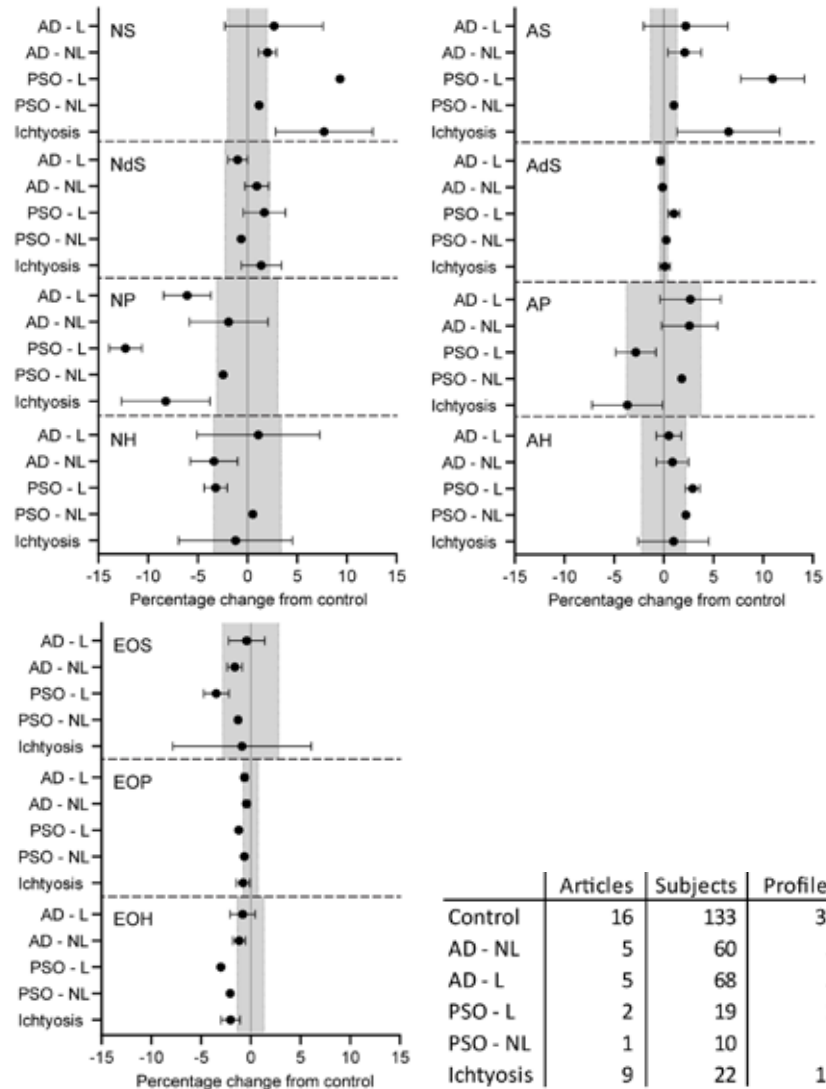
## Discussion

In total, this systematic review and meta-analysis identified articles on 11 different diseases in which ceramide profiling has been performed. This review affirmed that different diseases share common alterations in the ceramide profile using a systematic approach and meta-analysis. Decreased CER[NP] abundances, increased CER[NS] and CER[AS] abundances, and a reduction in ceramide chain length are frequently observed in atopic dermatitis, psoriasis and ichthyosis. Reports on the ceramide profile in palmoplantar hyperkeratosis, acne vulgaris, melasma, dandruff and xerosis were sparse and

**Table 1 (next page)** Alterations in the ceramide profile in disease with increases (↑), decreases (↓) or no significant differences (↔) indicated compared to controls with the fraction of articles showing similar changes reported. Differences in ceramide chain length (CCL) are defined based on changed average CCL and changes in the abundance of short or long ceramide species. The total subjects and number of articles represent the fraction included in the table of all literature identified through the systematic search. Note that <sup>31,93</sup> are compared to non-lesional skin of the same disease and <sup>79-82</sup> represent changes associated with dry skin after or before treatment. Not all articles in the review have been included in this overview as they lack comparisons with healthy controls, <sup>36,47,49-54,95</sup> present data in wrong format <sup>48,63</sup> or are prospective biomarker studies. <sup>55-57</sup> Please note studies performed using HPTLC are excluded from the table. <sup>23,32-35,40,61,62,65,66,83-85,88,90,91,94</sup>

Articles (n)	Patients (n)	TotalCer	[NS]	[NP]	[NH]	[AS]	[ADS]	[AP]	[AH]	[EOS]	[EODS]	[EOP]	[EOH]	[EO]	other	CCL	C34	MUCER	Bound lipids	Conclusive evidence <sup>33</sup> sources	
Lesional/Atopic Dermatitis 13/29	176/575	4/4±8.9, 24,31	5/8↑ 3/4±8, 9/15, 9/31	5/1±8, 8/3↓ 9/15, 8/9, 31	3/3↓ 4/6±8, 8/9, 31	4/6±8, 9/15, 27-29	3/4↔ 8/9, 25 1/4↓ 2/4↓	2/4↔ 8/9, 25 1/4↓ 2/4↓	2/3↓ 8/8±8.9, 9/31	8/8±8.9, 15, 24, 27, 9	5/5±8, 9/15, 25, 31	4/4↓ 9/15, 8/9, 15, 9, 28	2/2↓ 8/9, 15, 9, 28	1/1↑ 1/10±1.25, 1/10±1.25, 25, 31	1/10±1.25, 1/10±1.25, 24, 25, 27, 29, 31	10/10↓ 9/9↑	2/2±26, 39	1/2↔ 26	TC34 ↓[NP]	TC34 ↑[NP]	
Non-Lesional Atopic Dermatitis 17/28	295/529	2/5↔ 24,46	4/4↔ 8/25, 25, 42, 43, 47	2/4↔ 4/3, 47 2/4±8, 46, 47	3/3↓ 2/4±8, 42, 43, 45, 46	4/4↔ 8/25, 28, 40, 42, 43	4/4↔ 8/25, 8, 25, 8, 25, 8, 40, 26, 27, 40, 43	7/7↔ 8/25, 8, 25, 8, 40, 26, 27, 40, 43	5/5↔ 6/12±9, 1/1↔ 8, 25, 8, 42, 28, 43, 43, 46, 45	6/12±9, 1/1↔ 43, 46, 46	3/3↔ 8, 25, 43	5/6↔ 43, 46, 45	3/3↓ 47	1/10±1.25, 1/10±1.25, 25, 44, 45	5/7±1.5, 2/2↑	1/1↑ 26	3/3↔ 44	↔[NS] ↔[AS] ↔[ADS] ↔[AP] ↔[AH] ↔[EOP]	↔[NS] ↔[AS] ↔[ADS] ↔[AP] ↔[AH] ↔[EOP]		
Lesional Psoriasis 6/9	57/79	2/3↔ 59,61	1/2↑ 58	1/3↓ 58	1/3↓ 61	1/2↔ 58	1/2↑ 58	1/2↔ 58	1/2↑ 58	3/4±58, 59	59,61	58,59	58,59	1/2↓ 1/4↑	6/6↓ 2/2↑	6/6↓ 2/2↑	37,38, 58,59	3/3↔	↑[NS] ↑[AS] ↓[NP] ↓[AP]	↑[NS] ↑[AS] ↓[NP] ↓[AP]	
Non-lesional Psoriasis 4/5	37/47	2/2↔ 46,58	1/3↑ 58	1/2↑ 58	1/2↑ 58	1/1↔ 58	1/1↔ 58	2/2↔ 46,58	2/2↔ 46,58	2/2↔ 46,58	1/3↑ 58	1/3↑ 58	1/3↑ 58	1/3↑ 58	1/2↔ 64	1/2↔ 58	1/1↔ 58	3/5↔	In- conclusive	In- conclusive	
Ichthyosis 11/13	38/121	4/5↓ 67,69,76	7/9↑ 68,71, 68,72, 69,71, 74,78	7/7↓ 68,71, 69,71, 74,75, 74	6/7↓ 68,71, 69,71, 74,75, 74	3/6↔ 70,72, 70,72, 72	3/6↔ 68,69, 68,69, 69,71, 71,75, 76	3/6↔ 68,69, 68,69, 69,71, 71,75, 76	3/6↓ 68,69, 68,69, 69,71, 71,75, 76	7/9±68, 3/5↓ 70,72, 72	7/8↓ 78,82	7/8↓ 78,82	5/5↓ 69,71, 75,76	3/3↑ 69,71, 73,76	7/9↓ 68,71, 71,76	3/3↑ 68, 1/1↑ 76	69,71, 75, 76	3/5↔ 69,71, 75	TC34 ↓[NP]	TC34 ↓[NP]	
Xerosis 4/7	71/170	3/4↓ 79,80,82	2/2↔ 79,81	2/2↓ 80	2/2↓ 79,82	1/2↓ 79,82	2/2↔ 79,82	2/2↔ 79,82	2/2↔ 79,82	2/2↔ 79,82	2/2↔ 79,82	2/2↔ 79,82	2/2↔ 79,82	1/1↔ 82	1/1↔ 82	1/1↔ 82	1/1↔ 82	1/1↔ 82	1/1↔ 82	↓[AH]	↓[AH]
Acne vulgaris 2/3	37/43	1/1↑ 86	1/1↔ 86	1/1↑ 86	1/1↔ 86	1/1↔ 86	1/1↔ 86	1/1↔ 86	1/1↔ 86	1/1↔ 86	1/1↔ 86	1/1↔ 86	1/1↔ 86	1/1↔ 86	1/1↔ 86	1/1↔ 86	1/1↔ 86	1/1↔ 86	Not enough evidence	Not enough evidence	
Palmoplantar Hyperkeratosis 2/2	4/4	1/1↔ 89	2/2↑ 89	2/2↑ 89	1/1↔ 89	1/1↔ 89	1/1↔ 89	1/1↔ 89	1/1↔ 89	1/1↔ 89	1/1↔ 89	1/1↔ 89	1/1↔ 89	1/1↔ 89	1/1↔ 89	1/1↔ 89	1/1↔ 89	1/1↔ 89	Not enough evidence	Not enough evidence	
Pruritus 1/1	20/20	1/1↑ 92	1/1↑ 92	1/1↑ 92	1/1↔ 92	1/1↔ 92	1/1↔ 92	1/1↔ 92	1/1↔ 92	1/1↔ 92	1/1↔ 92	1/1↔ 92	1/1↔ 92	1/1↔ 92	1/1↑ 92	1/1↔ 92	1/1↔ 92	1/1↔ 92	Not enough evidence	Not enough evidence	
Melasma 1/1	21/21	1/1↑ 93	1/1↑ 93	1/1↑ 93	1/1↑ 93	1/1↑ 93	1/1↑ 93	1/1↑ 93	1/1↑ 93	1/1↑ 93	1/1↑ 93	1/1↑ 93	1/1↑ 93	1/1↑ 93	1/1↑ 93	1/1↑ 93	1/1↑ 93	1/1↑ 93	Not enough evidence	Not enough evidence	

**Figure 2** Forest plot showing the percentage change compared to healthy controls of the weighted relative ceramide profile in disease synthesised from articles that report a complete ceramide profile. The number of articles, subjects and profiles are indicated in the table for each indication. Error bars represent the standard deviation. References included per indication are listed in the supplementary table 1. AD: Atopic Dermatitis, NL: non-lesional, L: Lesional, PSO: Psoriasis, PHK: Palmoplantar Hyperkeratosis.



necessitate additional studies before conclusions can be made. However, the synthesized profile in palmoplantar hyperkeratosis and acne vulgaris strongly resembles that of atopic dermatitis, psoriasis and ichthyosis.

In some indications, discord is present between results obtained using LC-MS and HPTLC.<sup>46,47,54,84</sup> HPTLC analysis is less sensitive and lower resolution compared to LC-MS and incapable of sufficiently separating and detecting all ceramide subclasses.<sup>96,97</sup> This is illustrated by the ability of LC-MS to consistently detect decreased CER[NP] compared to healthy volunteers in settings where HPTLC-based studies often shows no significant difference.<sup>23,33,35,62,65</sup> Additionally, HPTLC provides less detailed output and necessitates the hyphenation with additional techniques to determine ceramide chain length and degree of unsaturation.<sup>98</sup> However, methods for SC lipidomics by LC-MS analysis differ widely and include methods that might not detect all ceramides.<sup>99</sup> One should therefore consider that changes observed using a targeted approach might not necessarily be representative for the entire ceramide profile.

The striking similarity of alterations in the ceramide profile between different indications might indicate that these are not inherently associated with specific diseases but induced by general epidermal dysregulation. Indeed, these changes extend past the well-defined causative mutations that underlie ichthyosis and are similar in atopic dermatitis and psoriasis despite two different immunological backgrounds.<sup>100</sup> The mechanistic basis for the altered subclass profile remains unclear. Based on the differential changes on subclass level, especially CER[S] and CER[P], dihydroceramide desaturase (DES)-1 and -2 activity might be affected as this enzyme mediates conversion of CER[DS] to CER[S] or CER[P], respectively.<sup>6</sup> Decreased DES-2 expression was observed in the lesional SC of atopic dermatitis patients.<sup>101</sup> However, other enzymes might differentially contribute to CER[P] synthesis<sup>102</sup> and aberrant expression and activity of acid sphingomyelinase showed to correlate to increased CER[S] abundance observed in atopic dermatitis.<sup>9,28</sup>

Besides differences in subclass composition, lipid elongation is frequently impacted. In ichthyosis this is related to mutations in CER[EO] synthesis. However, the CER[NON-EO] moiety is altered concurrently which might be caused by impairments in fatty acid elongation. Altered expression of fatty acid elongases ELOVL1, -3 and -6<sup>28,29,60</sup> and Ceramide Synthases 3 and -4<sup>28,31,60</sup> have provided some basis for impaired ceramide elongation in atopic dermatitis or psoriasis. This also emphasizes the interplay between ceramide and

fatty acid synthesis for the SC lipid profile which might also explain the increased degree of unsaturated ceramides.<sup>26,39,76,103</sup>

The altered enzymatic expression and activity may be linked to abnormal differentiation.<sup>63</sup> *In vitro* skin models show similar alterations compared to disease and these could be ameliorated by blocking the liver X-receptor which concurrently decreased epidermal differentiation in these models.<sup>104</sup> Indeed, abnormal differentiation is observed throughout the aforementioned indications.<sup>105,106</sup> Nevertheless, the role of inflammation cannot be overlooked in this process as supplementation of these models with pro-inflammatory cytokines aggravated these alterations together with changes to the expression of enzymes involved in the synthesis of CER[S], CER[EOS] and lipid elongation.<sup>28,37,107</sup> Additionally, anti-inflammatory treatment in atopic dermatitis patients ameliorated the altered ceramide profile.<sup>27,49</sup>

This review demonstrated a high amount of conformity between studies. This is reiterated by the acceptable standard deviations in the synthesized average ceramide profile of controls, which comprises data of 31 profiles. However, relatively high discord is observed among studies on non-lesional atopic dermatitis and psoriasis<sup>8,24,40,42,43</sup>. Although studies in atopic dermatitis source might have sampled close to lesional skin and thereby capture a partial lesional profile, psoriasis is characterized by sharply demarcated lesions which makes this unlikely. Based on the systemic inflammatory character of these diseases, it is therefore probable that the ceramide profile of non-lesional skin is indeed impacted to some extent.<sup>108</sup> However, the meta-analysis shows that these changes do not result in a high degree of differentiation at the level of subclass profile. Alternatively, many factors contribute to differences in the ceramide profile which could have skewed results observed throughout the review. The ceramide profile has shown to be subject to anatomical differences,<sup>42,89,109-112</sup> seasonal variations,<sup>86,90,109,110,113</sup> ethnicity<sup>114,115</sup> and age.<sup>84,110,113</sup> Additionally, conditions such as obesity and pregnancy appear to impact the composition.<sup>116,117</sup> The fact that control samples in this analysis are predominantly sourced from limbs might explain why a difference between acne and healthy skin is observed in this meta-analysis but not by the original authors.<sup>86</sup> It might therefore be advisable to perform proper matching when including a healthy control group.

Alterations in ceramide composition have occasionally been correlated to the extent of disease. Indeed, studies in atopic dermatitis and ichthyosis have adopted ceramide profiling in a biomarker capacity and showed that subclass

skewing and chain length impairment was alleviated in response to treatment.<sup>27,49,50,52,53</sup> Additionally, ceramides biomarkers have helped predict the development of atopic dermatitis in children<sup>55,56</sup> and disease exacerbation after remission.<sup>57</sup> Although this prospective application is promising, the high similarity between profiles in different indications would disqualify its use as a classical diagnostic biomarker. Nevertheless, the ability to monitor a treatment response using selected ceramides<sup>27</sup> might be useful throughout dermatology,<sup>28,49,50</sup> although their use outside atopic dermatitis, psoriasis and ichthyosis remains to be explored.

## Conclusion

To conclude, this article systemically evaluated alterations in ceramide profiles throughout various dermatoses and showed that results on ceramide alterations are well-aligned for atopic dermatitis, psoriasis and ichthyosis judged by the high degree of similarity among patients and control groups over multiple sources. The observation that many diseases share similar changes in the ceramide profile might indicate that these are only secondarily induced by specific disease-related mechanisms, but primarily by general epidermal dysregulation. However, results also show the dynamics of the ceramide profile with age, ethnicity, seasons and anatomical sites underlining the selection of proper controls in future studies which might focus on further elucidating the ceramide profile in acne vulgaris, melasma, dandruff and xerosis.

## REFERENCES

- 1 Proksch, E., Brandner, J. M. & Jensen, J. M. The skin: an indispensable barrier. *Exp Dermatol* **17**, 1063-1072 (2008).
- 2 van Smeden, J., Janssens, M., Gooris, G. S. & Bouwstra, J. A. The important role of stratum corneum lipids for the cutaneous barrier function. *Biochimica et Biophysica Acta (BBA) – Molecular and Cell Biology of Lipids* **1841**, 295-313 (2014).
- 3 Feingold, K. R. & Elias, P. M. Role of lipids in the formation and maintenance of the cutaneous permeability barrier. *Biochim Biophys Acta Mol Cell Biol Lipids* **1841**, 280-294 (2014).
- 4 Suzuki, M., Ohno, Y. & Kihara, A. Whole picture of human stratum corneum ceramides, including the chain-length diversity of long-chain bases. *J Lipid Res* **63**, (2022).
- 5 Kawana, M., Miyamoto, M., Ohno, Y. & Kihara, A. Comparative profiling and comprehensive quantification of stratum corneum ceramides in humans and mice by LC/MS/MS. *J Lipid Res* **61**, 884-895 (2020).
- 6 Kihara, A. Synthesis and degradation pathways, functions, and pathology of ceramides and epidermal acylceramides. *Prog Lipid Res* **63**, 50-69 (2016).
- 7 Elias, P. M. et al. Formation and functions of the corneocyte lipid envelope (CLE). *Biochim Biophys Acta* **1841**, 314-318 (2014).
- 8 Ishikawa, J. et al. Changes in the ceramide profile of atopic dermatitis patients. *Journal of Investigative Dermatology* vol. 130 2511-2514. Preprint at <https://doi.org/10.1038/jid.2010.161> (2010).
- 9 Boer, D. E. C. et al. Skin of atopic dermatitis patients shows disturbed -glucocerebrosidase and acid sphingomyelinase activity that relates to changes in stratum corneum lipid composition. *Biochim Biophys Acta Mol Cell Biol Lipids* **1865**, (2020).
- 10 Pullmannová, P. et al. Permeability and microstructure of model stratum corneum lipid membranes containing ceramides with long (C16) and very long (C24) acyl chains. *Biophys Chem* **224**, 20-31 (2017).
- 11 Uche, Lorretta, E., Gooris, Gerrit, S., Bouwstra, Joke, A. & Beddoes, Charlotte, M. Barrier Capability of Skin Lipid Models: Effect of Ceramides and Free Fatty Acid Composition. *Langmuir* **35**, 15376-15388 (2019).
- 12 Nádabán, A. et al. Effect of sphingosine and phytosphingosine ceramide ratio on lipid arrangement and barrier function in skin lipid models. *J Lipid Res* **64**, 100400 (2023).
- 13 Thakoersing, V. S. et al. Unraveling barrier properties of three different in-house human skin equivalents. *Tissue Eng Part C Methods* **18**, 1-11 (2012).
- 14 Mieremet, A. et al. Multitargeted approach for the optimization of morphogenesis and barrier formation in human skin equivalents. *Int J Mol Sci* **22**, (2021).
- 15 van Smeden, J. et al. The importance of free fatty acid chain length for the skin barrier function in atopic eczema patients. *Exp Dermatol* **23**, 45-52 (2014).
- 16 Mojumdar, E. H., Helder, R. W. J., Gooris, G. S. & Bouwstra, J. A. Monounsaturated Fatty Acids Reduce the Barrier of Stratum Corneum Lipid Membranes by Enhancing the Formation of a Hexagonal Lateral Packing. *Langmuir* **30**, 6534-6543 (2014).
- 17 Uchiyama, M., Oguri, M., Mojumdar, E. H., Gooris, G. S. & Bouwstra, J. A. Free fatty acids chain length distribution affects the permeability of skin lipid model membranes. *Biochimica et Biophysica Acta (BBA) – Biomembranes* **1858**, 2050-2059 (2016).
- 18 Bouwstra, J. A. et al. The skin barrier: An extraordinary interface with an exceptional lipid organization. *Prog Lipid Res* **101252** (2023) DOI:10.1016/j.plipres.2023.101252.
- 19 Mijaljica, D., Townley, J. P., Spada, F. & Harrison, I. P. The heterogeneity and complexity of skin surface lipids in human skin health and disease. *Prog Lipid Res* **93**, 101264 (2024).
- 20 Page, M. J. et al. The PRISMA 2020 statement: an updated guideline for reporting systematic reviews. *BMJ* **372**, (2021).
- 21 Rohatgi, A. WebPlotDigitizer: Version 4.6. <https://automeris.io/WebPlotDigitizer> (2022).
- 22 Drevon, D., Fursa, S. R. & Malcolm, A. L. Intercoder Reliability and Validity of WebPlotDigitizer in Extracting Graphed Data. *Behav Modif* **41**, 323-339 (2017).
- 23 Imokawa, G. et al. Decreased Level of Ceramides in Stratum Corneum of Atopic Dermatitis: An Etiologic Factor in Atopic Dry Skin? *Journal of Investigative Dermatology* **96**, 523-526 (1991).
- 24 Kim, J. et al. Alterations of Epidermal Lipid Profiles and Skin Microbiome in Children with Atopic Dermatitis. *Allergy Asthma Immunol Res* **15**, 186-200 (2023).
- 25 Chu, H. et al. Head and neck dermatitis is exacerbated by Malassezia furfur colonization, skin barrier disruption, and immune dysregulation. *Front Immunol* **14**, (2023).
- 26 Boiten, W., van Smeden, J. & Bouwstra, J. The Cornified Envelope-Bound Ceramide Fraction Is Altered in Patients with Atopic Dermatitis. *Journal of Investigative Dermatology* **140**, 1097-1100.e4 (2020).
- 27 Berdyshev, E. et al. Dupilumab significantly improves skin barrier function in patients with moderate-to-severe atopic dermatitis. *Allergy* **77**, 3388-3397 (2022).
- 28 Danso, M. et al. Altered expression of epidermal lipid bio-synthesis enzymes in atopic dermatitis skin is accompanied by changes in stratum corneum lipid composition. *J Dermatol Sci* **88**, 57-66 (2017).
- 29 Berdyshev, E. et al. Lipid abnormalities in atopic skin are driven by type 2 cytokines. *JCI Insight* **3**, (2018).
- 30 Toncic, R. J. et al. Altered levels of sphingosine, sphinganine and their ceramides in atopic dermatitis are related to skin barrier function, disease severity and local cytokine milieu. *Int J Mol Sci* **21**, (2020).
- 31 Ito, S. et al. Ceramide synthase 4 is highly expressed in involved skin of patients with atopic dermatitis. *Journal of the European Academy of Dermatology and Venereology* **31**, 135-141 (2017).
- 32 Macheleidt, O., Kaiser, H. W. & Sandhoff, K. Deficiency of Epidermal Protein-Bound w-Hydroxyceramides in Atopic Dermatitis. *J Invest Dermatol* vol. 119 (2002).
- 33 Yamamoto, A., Serizawa, S., Ito, M. & Sato, Y. Stratum corneum lipid abnormalities in atopic dermatitis. *Arch Dermatol Res* **283**, 219-223 (1991).
- 34 Di Nardo, A., Wertz, P., Giannetti, A. & Seidenari, S. Ceramide and cholesterol composition of the skin of patients with atopic dermatitis. *Acta Derm Venereol* **78**, 27-30 (1998).
- 35 Matsumoto, N. U. H. S. M. Difference in Ceramide Composition between 'Dry' and 'Normal' Skin in Patients with Atopic Dermatitis. *Acta Derm Venereol* **79**, 246-247 (1999).
- 36 Angelova-Fischer, I. et al. Distinct barrier integrity phenotypes in filaggrin-related atopic eczema following sequential tape stripping and lipid profiling. *Exp Dermatol* **20**, 351-356 (2011).
- 37 Tawada, C. et al. Interferon-decreases ceramides with long-chain fatty acids: Possible involvement in atopic dermatitis and psoriasis. *Journal of Investigative Dermatology* **134**, 712-718 (2014).
- 38 Pilz, R. et al. Formation of keto-Type ceramides in palmoplantar keratoderma based on biallelic KDSR mutations in patients. *Hum Mol Genet* **31**, 1105-1114 (2022).
- 39 Joo, K.-M. et al. Relationship of ceramide-, and free fatty acid-cholesterol ratios in the stratum corneum with skin barrier function of normal, atopic dermatitis lesional and non-lesional skins. *J Dermatol Sci* **77**, 71-74 (2015).
- 40 Bleck, O. et al. Two Ceramide Subfractions Detectable in Cer(AS) Position by HPTLC in Skin Surface Lipids of Non-Lesional Skin of Atopic Eczema. *J Invest Dermatol* vol. 113 (1999).
- 41 Kim, D. et al. As in Atopic Dermatitis, Nonlesional Skin in Allergic Contact Dermatitis Displays Abnormalities in Barrier Function and Ceramide Content. *Journal of Investigative Dermatology* **137**, 748-750 (2017).
- 42 Emmert, H. et al. Stratum corneum lipidomics analysis reveals altered ceramide profile in atopic dermatitis patients across body sites with correlated changes in skin microbiome. *Exp Dermatol* **30**, 1398-1408 (2021).
- 43 Janssens, M. et al. Lamellar lipid organization and ceramide composition in the stratum corneum of patients with atopic eczema. *Journal of Investigative Dermatology* **131**, 2136-2138 (2011).
- 44 Berdyshev, E. et al. Unique skin abnormality in patients with peanut allergy but no atopic dermatitis. *Journal of Allergy and Clinical Immunology* **147**, 361-367.e1 (2021).
- 45 Janssens, M. et al. Increase in short-chain ceramides correlates with an altered lipid organization and decreased barrier function in atopic eczema patients. *J Lipid Res* **53**, 2755-2766 (2012).
- 46 Farwanah, H., Raith, K., Neubert, R. H. H. & Wohlrab, J. Ceramide profiles of the uninvolved skin in atopic dermatitis and psoriasis are comparable to those of healthy skin. *Arch Dermatol Res* **296**, 514-521 (2005).
- 47 Jungersted, J. M. et al. Stratum corneum lipids, skin barrier function and filaggrin mutations in patients with atopic eczema. *Allergy: European Journal of Allergy and Clinical Immunology* **65**, 911-918 (2010).
- 48 Chiba, T. et al. Measurement of trihydroxy-linoleic acids in stratum corneum by tape-stripping: Possible biomarker of barrier function in atopic dermatitis. *PLoS One* **14**, (2019).
- 49 Lee, S. J., Kim, S. E., Shin, K. O., Park, K. & Lee, S. E. Dupilumab therapy improves stratum corneum hydration and skin dysbiosis in patients with atopic dermatitis. *Allergy Asthma Immunol Res* **13**, 762-775 (2021).
- 50 Dähnhardt, D., Bastian, M., Dähnhardt-Pfeiffer, S., Buchner, M. & Fölster-Holst, R. Comparing the effects of proactive treatment with tacrolimus ointment and mometasone furoate on the epidermal barrier structure and ceramide levels of patients with atopic dermatitis. *Journal of Dermatological Treatment* **32**, 721-729 (2021).
- 51 Paslin, D. & Wertz, P. A study to determine the effect of tacrolimus on ceramide levels in the stratum corneum of patients with atopic dermatitis. *Int J Dermatol* **45**, 352-356 (2006).
- 52 Oláh, A. et al. Echinacea purpurea-derived alkylamides exhibit potent anti-inflammatory effects and alleviate clinical symptoms of atopic eczema. *J Dermatol Sci* **88**, 67-77 (2017).
- 53 Ishida, K., Takahashi, A., Bito, K., Draelos, Z. & Imokawa, G. Treatment with Synthetic Pseudoceramide Improves Atopic Skin, Switching the Ceramide Profile to a Healthy Skin Phenotype. *Journal of Investigative Dermatology* **140**, 1762-1770.e8 (2020).
- 54 Jungersted, J. M., Høgh, J. K., Hellgren, L. I., Jemec, G. B. E. & Agner, T. The impact of ultraviolet therapy on stratum corneum ceramides and barrier function. *Photodermatol Photoimmunol Photomed* **27**, 331-333 (2011).
- 55 Berdyshev, E. et al. Stratum corneum lipid and cytokine biomarkers at age 2 months predict the future onset of atopic dermatitis. *Journal of Allergy and Clinical Immunology* **151**, 1307-1316 (2023).
- 56 Rinnov, M. R. et al. Skin biomarkers predict development of atopic dermatitis in infancy. *Allergy: European Journal of Allergy and Clinical Immunology* **78**, 791-802 (2023).
- 57 Sho, Y. et al. Stratum Corneum Ceramide Profiles Provide Reliable Indicators of Remission and Potential Flares in Atopic Dermatitis. *Journal of Investigative Dermatology* **142**, 3184-3191.e7 (2022).
- 58 KOYANO, S. et al. Psoriasis Patients Have Abnormal Ceramide Profile in Stratum Corneum. *Nishi Nihon Hifuka* **72**, 494-499 (2010).
- 59 Uchino, T. et al. Comparative analysis of intercellular lipid organization and composition between psoriatic and healthy stratum corneum. *Chem Phys Lipids* **254**, 105305 (2023).
- 60 Kim, B. K. et al. Decrease of ceramides with long-chain fatty acids in psoriasis: Possible inhibitory effect of interferon gamma on chain elongation. *Exp Dermatol* **31**, 122-132 (2022).
- 61 Motta, S. et al. Ceramide Composition of the Psoriatic Scale. *Biochimica et Biophysica Acta* vol. 1182 (1993).
- 62 Motta, S. Abnormality of Water Barrier Function in Psoriasis. *Arch Dermatol* **130**, 452 (1994).
- 63 Yokose, U. et al. The ceramide [NP]/[NS] ratio in the stratum corneum is a potential marker for skin properties and epidermal differentiation. *BMC Dermatol* **20**, (2020).
- 64 Tyrrell, V. J. et al. Lipidomic and transcriptional Analysis of the linoleoyl-omega-hydroxyceramide biosynthetic Pathway in human Psoriatic lesions. *J Lipid Res* **62**, (2021).
- 65 Paige, D. G., Morse-Fisher, N. & Harper, J. I. Quantification of Stratum Corneum Ceramides and Lipid Envelope Ceramides in the Hereditary Ichthyoses. *British Journal of Dermatology* vol. 131 (1994).
- 66 Lavrijsen, A. P. M. et al. Reduced Skin Barrier Function Parallels Abnormal Stratum Corneum Lipid Organization in Patients with Lamellar Ichthyosis. *Journal of Investigative Dermatology* **105**, 619-624 (1995).
- 67 Takeichi, T. et al. Reduction of stratum corneum ceramides in Neu-Laxova syndrome caused by phosphoglycerate dehydrogenase deficiency. *J Lipid Res* **59**, 2413-2420 (2018).
- 68 Murase, Y. et al. Reduced stratum corneum acylceramides in autosomal recessive congenital ichthyosis with a NIPAL4 mutation. *J Dermatol Sci* **97**, 50-56 (2020).
- 69 Arai, A. et al. Ceramide profiling of stratum corneum in Sjögren-Larsson syndrome. *J Dermatol Sci* **107**, 114-122 (2022).
- 70 van Smeden, J. et al. Skin barrier lipid enzyme activity in Netherton patients is associated with protease activity and ceramide abnormalities. *J Lipid Res* **61**, 859-869 (2020).
- 71 Yamamoto, M. et al. Comprehensive stratum corneum ceramide profiling reveals reduced acylceramides in ichthyosis patient with CERS3 mutations. *Journal of Dermatology* **48**, 447-456 (2021).
- 72 Takeichi, T. et al. SDR9C7 catalyzes critical dehydrogenation of acylceramides for skin barrier formation. *Journal of Clinical Investigation* **130**, 890-903 (2020).
- 73 Pichery, M. et al. PNPLA1 defects in patients with



- autosomal recessive congenital ichthyosis and KO mice sustain PNPLA1 irreplaceable function in epidermal omega-Oacylceramide synthesis and skin permeability barrier. *Hum Mol Genet* **26**, 1787-1800 (2017).
- 74 Ohno, Y. *et al.* Essential role of the cytochrome P450 CYP4F22 in the production of acylceramide, the key lipid for skin permeability barrier formation. *Proc Natl Acad Sci U S A* **112**, 7707-7712 (2015).
- 75 Takahashi, T. *et al.* Hypomyelinating spastic dyskinesia and ichthyosis caused by a homozygous splice site mutation leading to exon skipping in ELOVL1. *Brain Dev* **44**, 391-400 (2022).
- 76 Van Smeden, J. *et al.* Intercellular skin barrier lipid composition and organization in netherton syndrome patients. *Journal of Investigative Dermatology* **134**, 1238-1245 (2014).
- 77 Dick, A. *et al.* Diminished protein-bound -hydroxylated ceramides in the skin of patients with ichthyosis with 12R-lipoxygenase (LOX) or eLOX-3 deficiency. *British Journal of Dermatology* vol. 177 e119-e121 Preprint at <https://doi.org/10.1111/bjd.15406> (2017).
- 78 Takeichi, T. *et al.* Ceramide Analysis in Combination with Genetic Testing May Provide a Precise Diagnosis for Self-Healing Collodion Babies. *J Lipid Res* **63**, (2022).
- 79 Murphy, B. *et al.* Alteration of barrier properties, stratum corneum ceramides and microbiome composition in response to lotion application on cosmetic dry skin. *Sci Rep* **12**, (2022).
- 80 Stettler, H. *et al.* Targeted dry skin treatment using a multifunctional topical moisturizer. *Int J Cosmet Sci* **43**, 191-200 (2021).
- 81 Ishikawa, J. *et al.* Dry skin in the winter is related to the ceramide profile in the stratum corneum and can be improved by treatment with a Eucalyptus extract. *J Cosmet Dermatol* **12**, 3-11 (2013).
- 82 Uchino, T. *et al.* Association of dry skin with intercellular lipid composition of stratum corneum after erlotinib administration. *Cancer Chemother Pharmacol* **86**, 233-243 (2020).
- 83 Saint-Léger, D. *et al.* Stratum corneum Lipids in Skin Xerosis. *Dermatology* **178**, 151-155 (1989).
- 84 Akimoto, K., Yoshikawa, N., Higaki, Y., Kawashima, M. & Imokawa, G. Quantitative Analysis of Stratum Corneum Lipids in Xerosis and Asteatotic Eczema. *J Dermatol* **20**, 1-6 (1993).
- 85 Fulmer, A. W. & Kramer, G. J. Stratum Corneum Lipid Abnormalities in Surfactant-Induced Dry Scaly Skin. *Journal of Investigative Dermatology* **86**, 598-602 (1986).
- 86 Pappas, A., Kendall, A. C., Brownbridge, L. C., Batchvarova, N. & Nicolaou, A. Seasonal changes in epidermal ceramides are linked to impaired barrier function in acne patients. *Exp Dermatol* **27**, 833-836 (2018).
- 87 Zhou, M. *et al.* Skin surface lipidomics revealed the correlation between lipidomic profile and grade in adolescent acne. *J Cosmet Dermatol* **19**, 3349-3356 (2020).
- 88 Perisho, Kathy., Wertz, P. W., Madison, K. C., Stewart, M. Ellen. & Downing, D. T. Fatty Acids of Acylceramides From Comedones and From the Skin Surface of Acne Patients and Control Subjects. *Journal of Investigative Dermatology* **90**, 350-353 (1988).
- 89 Takeichi, T. *et al.* Biallelic Mutations in KDSR Disrupt Ceramide Synthesis and Result in a Spectrum of Keratinization Disorders Associated with Thrombocytopenia. *Journal of Investigative Dermatology* **137**, 2344-2353 (2017).
- 90 Harding, C. R. *et al.* Dandruff: A condition characterized by decreased levels of intercellular lipids in scalp stratum corneum and impaired barrier function. *Arch Dermatol Res* **294**, 221-230 (2002).
- 91 Rogers, J. S., Moore, A. E., Meldrum, H. & Harding, C. R. Increased scalp skin lipids in response to antidandruff treatment containing zinc pyrithione. *Arch Dermatol Res* **295**, 127-129 (2003).
- 92 Ma, X. *et al.* Lipidomics profiling of skin surface lipids in senile pruritus. *Lipids Health Dis* **19**, (2020).
- 93 Xu, J. *et al.* Tape stripping and lipidomics reveal skin surface lipid abnormality in female melasma. *Pigment Cell Melanoma Res* **34**, 1105-1111 (2021).
- 94 Kunii, T., Hirao, T., Kikuchi, K. & Tagami, H. Stratum corneum lipid profile and maturation pattern of corneocytes in the outermost layer of fresh scars: the presence of immature corneocytes plays a much more important role in the barrier dysfunction than do changes in intercellular lipids. *British Journal of Dermatology* **149**, 749-756 (2003).
- 95 Jungersted, J. M., Høgh, J. K., Høllgren, L. I., Agner, T. & Jemec, G. B. E. Ceramide profile in hypohidrotic ectodermal dysplasia. *Clin Exp Dermatol* **37**, 153-155 (2012).
- 96 Vietzke, J. *et al.* Comparative investigation of human stratum corneum ceramides. *Lipids* **36**, 299-304 (2001).
- 97 van Smeden, J. *et al.* Combined LC/MS-platform for analysis of all major stratum corneum lipids, and the profiling of skin substitutes. *Biochim Biophys Acta Mol Cell Biol Lipids* **1841**, 70-79 (2014).
- 98 Wertz, P. W., Miethke, M. C., Long, S. A., Strauss, J. S. & Downing, D. T. The Composition of the Ceramides from Human Stratum Corneum and from Comedones. *Journal of Investigative Dermatology* **84**, 410-412 (1985).
- 99 Boiten, W., Absalah, S., Vreeken, R., Bouwstra, J. & van Smeden, J. Quantitative analysis of ceramides using a novel lipidomics approach with three dimensional response modelling. *Biochim Biophys Acta Mol Cell Biol Lipids* **1861**, 1652-1661 (2016).
- 100 Hosack, T. *et al.* Inflammation across tissues: can shared cell biology help design smarter trials? *Nature Reviews Rheumatology* Preprint at <https://doi.org/10.1038/s41584-023-01007-2> (2023).
- 101 Duca, E. Del *et al.* Intra-patient comparison of atopic dermatitis skin transcriptome shows differences between tape-strips and biopsies. *Allergy* (2023) DOI:10.22541/au.167945946.65926819/v1.
- 102 Ota, A. *et al.* Bifunctional DEGS2 has higher hydroxylase activity toward substrates with very-long-chain fatty acids in the production of phytosphingosine ceramides. *Journal of Biological Chemistry* **299**, (2023).
- 103 Helder, R. W. J. *et al.* Improved organotypic skin model with reduced quantity of monounsaturated ceramides by inhibiting stearoyl-CoA desaturase-1. *Biochim Biophys Acta Mol Cell Biol Lipids* **1866**, (2021).
- 104 Helder, R. W. J. *et al.* The effects of LXR agonist T0901317 and LXR antagonist GSK2033 on morphogenesis and lipid properties in full thickness skin models. *Biochim Biophys Acta Mol Cell Biol Lipids* **1865**, (2020).
- 105 Hoffjan, S. & Stemmler, S. On the role of the epidermal differentiation complex in ichthyosis vulgaris, atopic dermatitis and psoriasis. *British Journal of Dermatology* vol. 157 441-449 Preprint at <https://doi.org/10.1111/j.1365-2133.2007.07999.x> (2007).
- 106 Engelke, M., Jensen, J.-M., Ekanayake-Mudiyanselage, S. & Proksch, E. Effects of Xerosis and Ageing on Epidermal Proliferation and Differentiation. *British Journal of Dermatology* vol. 137 <https://academic.oup.com/bjd/article/137/2/219/6682242> (1997).
- 107 Danso, M. O. *et al.* TNF- and Th2 cytokines induce atopic dermatitis-like features on epidermal differentiation proteins and stratum corneum lipids in human skin equivalents. *Journal of Investigative Dermatology* **134**, 1941-1950 (2014).
- 108 He, H. *et al.* Tape strips detect distinct immune and barrier profiles in atopic dermatitis and psoriasis. *Journal of Allergy and Clinical Immunology* **147**, 199-212 (2021).
- 109 Ishikawa, J. *et al.* Variations in the ceramide profile in different seasons and regions of the body contribute to stratum corneum functions. *Arch Dermatol Res* **305**, 151-162 (2013).
- 110 Rogers, J., Harding, C., Mayo, A., Banks, J. & Rawlings, A. Stratum corneum lipids: the effect of ageing and the seasons. *Arch Dermatol Res* **288**, 765-770 (1996).
- 111 Watkinson, A. *et al.* Reduced barrier efficiency in axillary stratum corneum. *Int J Cosmet Sci* **24**, 151-161 (2002).
- 112 Masukawa, Y. *et al.* Characterization of overall ceramide species in human stratum corneum. *J Lipid Res* **49**, 1466-1476 (2008).
- 113 Fujiwara, A. *et al.* Age-related and seasonal changes in covalently bound ceramide content in forearm stratum corneum of Japanese subjects: determination of molecular species of ceramides. *Arch Dermatol Res* **310**, 729-735 (2018).
- 114 Jungersted, J. M., Høgh, J. K., Høllgren, L. I., Jemec, G. B. E. & Agner, T. Ethnicity and stratum corneum ceramides. *British Journal of Dermatology* **163**, 1169-1173 (2010).
- 115 Muizzuddin, N. *et al.* Structural and functional differences in barrier properties of African American, Caucasian and East Asian skin. *J Dermatol Sci* **59**, 123-128 (2010).
- 116 Chen, F. & Huang, D. Study on the skin status of mid-pregnancy women based on lipidomics. *J Cosmet Dermatol* **20**, 955-963 (2021).
- 117 Mori, S. *et al.* Characterization of skin function associated with obesity and specific correlation to local/systemic parameters in American women. *Lipids Health Dis* **16**, 214 (2017).

## SUPPLEMENTAL MATERIAL

**Supplementary table 1** Overview of articles used to extract data for the average ceramide profile for figure 2. See reference section for the full title.

Lesional Atopic Dermatitis	8,9,15,31,53
Non-Lesional Atopic Dermatitis	8,9,15,31,43
Lesional Psoriasis	58,82
Non-Lesional Psoriasis	58
Ichthyosis	67-72,74,75,78
Palmoplantar Hyperkeratosis	89
Xerosis	79,82
Acne vulgaris	86
Healthy	8,9,15,43,58,59,67-72,74,75,78,89

### Additional descriptive information about the articles included on congenital Ichthyosis and other mendelian disorders stratified per mutation

#### Ceramide Synthase 3 (CERS3) mutations

CERS3 catalyzes the linking of the sphingoid- and fatty acid-moiety of ceramides, with higher specificity towards further elongated species. Yamamoto *et al.* demonstrated evident changes in the ceramide profile from the back of a 1-year-old ichthyosis patient with a CERS3 mutation compared to healthy controls marked by an increase in the relative abundance of CER[NS], CER[ADS], CER[AS], CER[AP] and a decrease in CER[NP], CER[NH] and CER[AH]. In line with Cers3 involvement in CER[EO] production, the CER[EO] abundance was both absolutely and relatively decreased compared to healthy controls, but the abundance of protein-bound ceramides seemed unaltered. Ceramide chain length was decreased based on analysis of the ceramide fatty acid moiety of CER[NS] and CER[AS]. However, this decrease in average chain length could be stemming from the overabundance of fatty-acid moieties with 16-carbons or both 16- and 18- carbons observed in CER[AS] and CER[NS], respectively.<sup>71</sup>

#### Short chain dehydrogenase/reductase family 9C member 7 (SDR9C7) mutations

A patient with autosomal recessive congenital ichthyosis stemming from a mutation in SDR9C7 demonstrated impairment of lipid envelope formation. In this article, the authors narrow down the function of SDR9C7 to

the processing of CER[EO] to allow the covalent binding of CER[EO] to proteins. Total ceramide levels were not affected compared to controls, but the relative abundance of CER[NS], CER[AS] and CER[EOS] were increased. Conversely, CER[NP], CER[EOH], protein-bound CER[OS] and protein-bound CER[OH] were decreased in line with the mechanism of SDR9C7. Ceramide chain length appeared not to be affected.<sup>72</sup>

#### Nipa-Like Domain-Containing 4 (NIPAL4) mutations

The function of NIPAL4 and its contribution to ichthyosis remain unclear, but effects on the ceramide profile of one patient were established. Lacking relative data, differences in the absolute ceramide profile between two skin sites was observed in a case of autosomal recessive congenital ichthyosis due to a NIPAL4 mutation. While CER[NS] was increased and CER[AH], CER[AP], CER[EOH] and CER[EOP] were decreased in samples from both the forearm and upper arm compared to healthy volunteers, samples from the upper arm showed that CER[NP], CER[NH] and CER[EOS] were additionally reduced. No CER[O] or protein bound CER[O] levels were reported. The ceramide chain length within CER[NS] was decreased and an evident increase in CER[NSC34] was observed compared to healthy volunteers. Interestingly, treatment with oral retinoids partly restored the level of CER[NH], CER[EOH] and CER[EOP] and seemed to slightly restore the impaired chain elongation.<sup>68</sup>

#### Elongation Of Very Long Chain Fatty Acids 1 (ELOVL1) mutations

ELOVL1 mediates the elongation of fatty acids past 21 carbons in length, which are essential for the formation of CER[EO] species. Mutations the ELOVL1 gene resulted in changes throughout the ceramide profile despite its well-defined role fatty acid elongation. Two siblings showed decreased CER[NP], CER[NH] and CER[ADS] abundances compared to their older parents. The amount of CER[EO] was negligible, but levels of protein bound CER[EO] were not significantly altered. Corresponding to ELOVL1 substrate specificity, ceramides with a fatty acid tail exceeding 26 carbons were significantly reduced and those of 24 carbons and shorter increased.<sup>75</sup>

#### Arachidonate lipoxygenase mutations (ALOX) mutations

ALOX enzymes are involved in the formation of terminal hydroxyl groups that facilitate the binding of ceramides to the cornified envelope. A concise report on 7 autosomal recessive congenital ichthyoses patients contrasted

the amount of protein-bound CER[OS] to the amount of free CER[NON-EO] which showed to be decreased compared to adult and age-matched juvenile controls. Interestingly, the 5 patients with an ALOXE3 mutation showed smaller changes compared to the 2 patients with ALOX12B mutation, corresponding to the milder phenotype in this group. Furthermore, it showed a lower protein-to-ceramide ratio and level of protein-bound CER[OS] in the older compared to the juvenile control group.<sup>77</sup>

### ***Patatin-like phospholipase containing 1 (PNPLA1) mutations***

On another occasion, a limited ceramide profile of two older siblings over 50-year-old with autosomal recessive congenital ichthyosis caused by a mutation in PNPLA1 was determined. The involvement in ceramide processing of PNPLA1 was not elucidated. However, a dramatic reduction of CER[EOS] abundance and an increased CER[OS] abundance was observed compared to healthy controls. No change in the combined abundance of CER[NS] and CER[AS] was observed.<sup>73</sup>

### ***Aldehyde dehydrogenase 3 family member A2 (ALDH3A2) mutations***

The ceramide profile of a Sjögren-Larsson Syndrome patient, caused by mutations in ALDH3A2, showed an increased absolute abundance of CER[NS] and CER[O] despite lower total ceramide levels compared to healthy controls. A decrease in total ceramide was reflected by a reduction in CER[NP], CER[NH], CER[AP], CER[AH] and CER[EO]. Bound CER[O] remained unaltered. Decreases in the average ceramide fatty-acid tail lengths compared to controls was observed throughout CER[NON-EO], but primarily in CER[NDS], CER[AS] and CER[ADS].<sup>69</sup>

### ***3-Ketodihydrospingosine reductase (KDSR) mutations***

Mutations in the gene for KDSR, which catalyzes the formation of the ceramide sphingoid-base, gives rise to hyperkeratosis. Analysis of the affected palm, affected wrist and non-affected forearm of two patients and their respective mothers showed only small changes in total ceramide content, ceramide composition and ceramide chain length partly due to high variation within the patient- and control-group.<sup>89</sup> Pilz *et al.* demonstrated that ceramide synthesis was not necessarily impaired in two patients with KDSR mutations as unreduced 3-ketodihydrospingosine could also be incorporated in ceramides. While not the primary scope of the authors, they do report

increased CER[NS] and decreased CER[NP] abundances in the affected skin of both patients and slightly increased CER[NS] but markedly decreased CER[NP] in the non-affected skin of one patient. Although compositional changes were apparent in both affected and non-affected skin, the chain lengths of CER[NDS] was reduced in the affected skin only.<sup>38</sup>

### ***Serine protease inhibitor Kazal-type 5 (SPINK5) mutation***

Two studies from the same group describe the ceramide composition of Netherton patients, a hereditary disease arising from mutations in SPINK5 which directly results in abnormal desquamation but also affects other epidermal processes. Both studies show an increase in the relative abundances of CER[NS] and CER[AS] and decrease in CER[NP].<sup>70,76</sup> A detailed overview does not show other significant changes in the abundance of specific subclasses between lesional and control stratum corneum.<sup>70</sup> However, the combined fraction of CER[EO] was decreased in the majority of subjects.<sup>70,76</sup> Notably, the abundance of the CER[EO] precursors glucosyl-CER[EO] remained similar to controls.<sup>76</sup> Follow-up studies demonstrated enzymes responsible for glucosyl-Cer[EO] to CER[EO] conversion and CER[S] synthesis were dysregulated, corresponding to disease severity.<sup>16</sup> While they remained undetected in healthy controls, unsaturated ceramides were present throughout all subclasses of Netherton patients.<sup>76</sup> The variety in ceramide chain lengths was smaller and decreased on average in Netherton patients compared to controls. Increases in the amount of ceramides with 34 carbons was noted in CER[NS], CER[AS] and CER[AH].<sup>76</sup>

### ***CYP4F22 mutations***

CYP4F22 catalyzes the  $\omega$ -hydroxylation of ultra-long chain fatty acids and is therefore responsible for the synthesis of CER[EO]. Two cases of self-healing collodion babies, resulting from mutations in the CYP4F22 gene, have shown to exhibit ceramide profiles comparable to other ichthyosis patients with increased CER[NS] and CER[AS] but decreased CER[NP], CER[AP], CER[EOS], CER[EOP] and CER[EOH] abundance. Additionally, the levels of protein-bound CER[OS] and CER[OH] and the average ceramide chain length were reduced.<sup>78</sup> Another ichthyosis patient with a mutation in the CYP4F22 gene showed similar changes with increased absolute abundance of CER[NS] and CER[AS] and reduction of CER[EOS], CER[EOH] and CER[EOP] compared to controls.<sup>74</sup>

### Phosphoglycerate dehydrogenase (PHGDH) mutation

PHGDH is one of the enzymes involved in the de-novo synthesis of L-serine and therefore essential for the formation of sphingolipids. Mutations in the PHGDH gene cause Neu-Laxova syndrome, characterized by many anomalies including ichthyosis. The severe case of a collodion baby with Neu-Laxova syndrome showed a drastic reduction of all ceramide classes and did not survive past six weeks.<sup>67</sup>

### SYSTEMATIC LITERATURE SEARCH TERM

The search term used for the systematic search. The search term is optimized for PubMed, Embase, Web Of Science, Cochrane Library and Ovid Emcare separately. All searches were conducted on 04-July-2023. A high number of hits were generated on the subject of breast cancer when optimizing the search terms. Therefore, this indication was explicitly excluded from the systematic search.

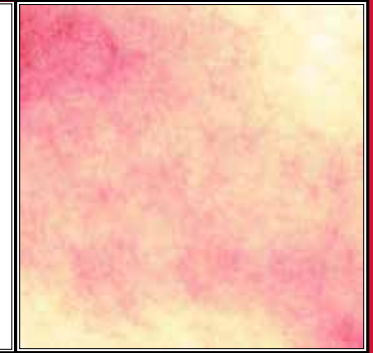


The full search term can be retrieved from the supplemental material provided with the published version of this chapter at the *Journal of Investigative Dermatology* by using the QR-code.

## CHAPTER 7

### GUSELKUMAB TREATMENT ALLEVIATES BARRIER DYSFUNCTION AND NORMALIZES THE ALTERED STRATUM CORNEUM CERAMIDE PROFILE IN LESIONAL PSORIASIS: RESULTS OF A RANDOMIZED, PLACEBO-CONTROLLED TRIAL

Adapted from: Journal of Lipid Research  
(J Lipid Res, 2024, DOI: 10.1016/j.jlr.2024.100591)



Jannik Rousel,<sup>1,2,\*</sup> Catherine Mergen,<sup>2,\*</sup> Menthe E. Bergmans,<sup>1,3</sup> Lisa J. Buijninx<sup>1</sup>, Marieke L. de Kam,<sup>1</sup> Naomi B. Klarenbeek,<sup>1</sup> Tessa Niemeyer-van der Kolk,<sup>1</sup> Martijn B.A. van Doorn,<sup>1,4</sup> Joke A. Bouwstra,<sup>2</sup> and Robert Rissmann,<sup>1,2,3</sup> on behalf of the Next-Generation Immunodermatology (NGID) Consortium. \*These authors contributed equally.  
1. Centre for Human Drug Research, Leiden, NL / 2. Leiden Academic Centre for Drug Research, Leiden University, Leiden, NL / 3. Department of Dermatology, Leiden University Medical Center, Leiden, NL / 4. Department of Dermatology, Erasmus Medical Centre, Rotterdam, NL



## Abstract

**BACKGROUND:** The epidermal inflammation associated with psoriasis drives skin barrier perturbations. The skin barrier function is dependent on the stratum corneum lipid matrix of which ceramides constitute important components. Changes in the ceramide profile are directly related to barrier function. In this study, we set out to characterize the barrier function and ceramide profile of psoriatic skin before and during treatment with guselkumab.

**METHODS:** A double-blind, randomized controlled trial was performed in which the barrier function and ceramide profile of 26 patients was assessed before and after 3:1 randomization to 100mg guselkumab or placebo for 16 weeks. Barrier function was measured by trans-epidermal Water loss measurements. Ceramide profiling was performed using liquid chromatography-mass spectrometry after stratum corneum was harvested using tape-stripping.

**RESULTS:** Barrier function was significantly decreased and the ceramide profile significantly different in lesional skin compared to non-lesional skin and that of healthy controls. Barrier function and the ceramide profile of lesional skin normalized to that of controls during treatment with guselkumab, but not placebo. This resulted in significant differences compared to placebo at the end of treatment. Changes in the lesional ceramide profile during treatment correlated with barrier function and the target lesion severity. Non-lesional skin was similar to controls at baseline and did not change during treatment.

**CONCLUSION:** Skin barrier function and the ceramide profile are altered in lesional psoriatic skin. Alterations in the ceramide profile normalize in response to guselkumab treatment and correlate with clinical severity. Monitoring the ceramide profile might be exploited as an objective biomarker for treatment responses.

## Introduction

Psoriasis is a chronic inflammatory skin disease characterized by erythematous, indurated, and scaly lesions. Psoriasis can be increasingly well-managed in clinical practice, but the presence of any residual lesions can still remain a significant burden to patients.<sup>1</sup> While being primarily an inflammatory condition, cutaneous barrier perturbations allows exogenous substances to cross the skin barrier and enhance epidermal dysregulation.<sup>2</sup> Indeed, barrier dysfunction is observed in lesional skin and, although not observed consistently throughout all studies, also in non-lesional skin.<sup>3-6</sup>

Proper barrier function is in part regulated by the specific composition of ceramides present in the stratum corneum (sc).<sup>7</sup> Ceramides are incorporated in a highly organized lipid matrix together with mainly fatty acids and cholesterol. This matrix presents the only continuous penetration pathway for substances crossing the intact sc. The ceramide fraction is composed of many different species which can be categorized into as many as 25 different subclasses (figure s1).<sup>8</sup> Alterations in the ceramide composition and concomitant decreases in skin barrier function have been observed in psoriasis and other inflammatory dermatological conditions.<sup>9</sup> In atopic dermatitis (AD), these appear correlated to barrier function.<sup>10-13</sup> Additionally, *in vitro* studies have highlighted the potential of inflammation to affect the ceramide lipid biosynthesis and thereby aggravate barrier dysfunction.<sup>14,15</sup> Understanding barrier dysfunction in psoriasis might provide further targets for therapy and prevent the formation of new lesions.<sup>16</sup>

Pathomechanistic insights have identified the interleukin (IL)-23 and -17 axis as main driver of the aberrant immunological responses in psoriasis which enabled the use of targeted immunosuppressing therapies to great success.<sup>17</sup> Guselkumab is an ANTI-IL23P19 monoclonal antibody which has shown high and lasting efficacy in clinical practice.<sup>18,19</sup> Besides its pronounced anti-inflammatory effect, ANTI-IL-23 therapy has shown to also improve barrier function in a preclinical psoriasis mouse model.<sup>20</sup>

Although studies have already characterized barrier dysfunction and the lipid composition in psoriasis, their integration and association with measures for disease severity are lacking and warrant further investigation.<sup>21-23</sup> In this study, we set out to characterize the ceramide profile in psoriasis and investigate the dynamics of barrier function and ceramide profile in response to biologic therapy. Differences between healthy and (non-)lesional

psoriatic skin were evaluated at baseline, after which barrier function and ceramide composition were monitored during disease regression induced by guselkumab in a randomized, placebo-controlled trial.

## Patients and methods

Extended methods are present in the supplementary information.

### STUDY DESIGN

The SKINERGY-PP study was an exploratory, single-center, double-blinded and placebo controlled randomized trial conducted from September 2020 to January 2023 at the Centre for Human Drug Research (Leiden, the Netherlands) and registered under NCT04394936. The study included plaque psoriasis patients that were not undergoing active treatment, or with appropriate wash-out, and had at least one active lesion of sufficient size to allow for sampling and with a minimal lesion severity score <sup>36</sup>. The use of medication prior and during the study was prohibited, including the application of any topical products on lesions subjected to assessment. Control subjects without any dermatological conditions and otherwise healthy were included and matched for average sex, age and tape-stripping location to the patient group. Baseline measurements were obtained from patients and controls 2 weeks apart. Afterwards, 26 patients were randomized 3:1 to subcutaneous injections at week 0, 4 and 12 with guselkumab 100 mg or placebo, respectively. The full inclusion and exclusion criteria, demographics of the study population at baseline and locations of the assessments are presented in the supplementary information.

### TRANS-EPIDERMAL WATER LOSS

Assessments were performed under controlled environmental conditions of <60% humidity and 22±2 °C. Cutaneous water loss was determined using an AquaFlux AF200 (Biox Systems Ltd., London, United Kingdom) over 180 seconds or until steady state was reached.

### TAPE-STRIPPING

Subsequently, a total of 8 tapes (Nichiban, Tokyo, Japan) were pressed onto the skin using a D500-pressure instrument (D-squame, Cuderm Corporation, Dallas, TX, USA) and measured using a SquameScan 850A (Heiland

Electronic, Wetzlar, Germany) to obtain the SquameScan value (SQV) as a measure for SC removed.<sup>24</sup> A 16 mm diameter circle was punched out and stored in chloroform:methanol (2:1) awaiting extraction.

### LIPID EXTRACTION AND ANALYSIS

Tapes were extracted using a modified 4-step Bligh and Dyer extraction at elevated temperature as described by Boiten *et al.* (2016).<sup>25</sup> Extracts from tape strips 5-8 were pooled for analysis. Lipidomics was performed using Liquid Chromatography-Mass Spectrometry as described in the supplemental materials. The amount of ceramide per sample was normalized by the cumulative SQV of the extracted tapes after correction with the average signal of 2 blank tapes to obtain absolute amounts of ceramides in pm/SQV value.

### CLINICAL SCORING OF PSORIASIS SEVERITY

Severity was scored using the Psoriasis Area and Severity Index (PASI).<sup>26</sup> Additionally, the lesion severity score (LSS) of the target lesion was obtained by summing erythema, scaling and induration graded on a 5-point scale (0; clear-4; severe).<sup>27,28</sup>

### STATISTICS

Statistical testing at baseline was performed using one or two-way ANOVA with Tukey's test for multiple comparisons in PRISM 9.0 (GraphPad, Software, Boston, United States). Longitudinal analysis was performed using a least-squares method in SAS 9.4 (SAS Institute Inc., Cary, North Carolina, United States). Repeated Measures Correlation was performed using Rmcorr in R Statistical Software (version 4.1.2, R Core Team 2021).<sup>29</sup> Statistical significance is shown as: P<0.05: \*, P<0.005: - and P<0.005: -\*.

## Results

A total of 26 patients with plaque psoriasis and 10 healthy controls were included in the study (figure S2). Demographics are listed in table S1 and the adverse events associated with guselkumab or placebo treatment have been reported previously.<sup>30,31</sup>

## THE CERAMIDE PROFILE IS ALTERED IN LESIONAL PSORIATIC SKIN

Correcting with the sqv as a measure for the amount of SC removed, quantitative analysis showed a significant decrease in total saturated ceramides in lesional skin compared to non-lesional skin and controls (figure 1A). On the level of subclass composition, a significantly decreased CER[NDS], CER[NP], CER[NH], CER[AP], CER[OS] and CER[OH] abundance is observed in lesional skin compared to non-lesional skin and controls (figure 1B). The abundances of CER[ADS] and CER[AH] were additionally decreased in lesional skin compared to non-lesional skin. Contrarily, non-lesional skin shows a significantly increased CER[NP] abundance compared to control skin. There were no significant differences in abundances within the CER[EO] fraction.

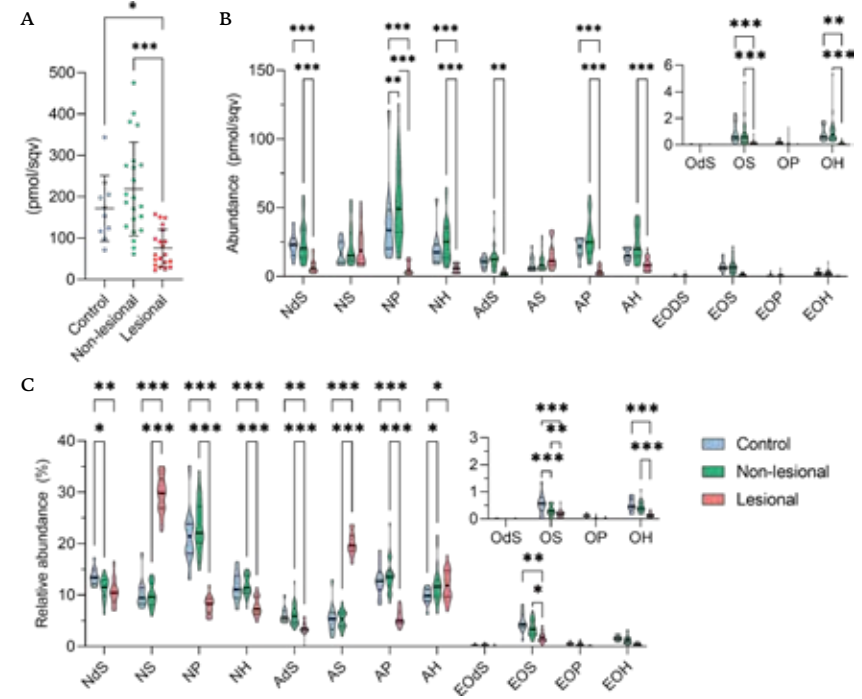
Compositional display of the data shows that decreased CER[NDS], CER[NP], CER[NH], CER[ADS], CER[AP], CER[OS] and CER[OH] abundances are maintained in lesional skin compared to control skin (figure 1C). However, significant increases in CER[NS], CER[AS], CER[AH] and CER[EOS] were observed which were not observed for the absolute profile.

Trans-epidermal water loss (TEWL) represents a surrogate marker for barrier integrity and was significantly higher in lesional compared to non-lesional skin and controls (figure 2A). Skewing of ceramide subclass synthesis is reiterated by the significantly increased CER[NS]:CER[NP] ratio in lesional skin (figure 2B). Additionally, the fraction of monounsaturated ceramides (MUCER) in CER[NS], as an indication for the degree of unsaturation throughout the entire profile, was significantly higher in lesional skin (figure 2C).

Ceramides can be divided in three groups based on their average ceramide chain length (CCL): the CER[A] and CER[N] (CER[N,A]) fraction, the CER[EO] fraction which contains an additional linoleic acid moiety, and the CER[O] fraction which resemble CER[EO] without linoleic acid moiety. Ceramide elongation appears impacted as the average ceramide chain length (CCL) in the CER[N,A], CER[EO] and CER[O] fraction is significantly decreased in lesional compared to non-lesional and control skin (figure 2E). However, the decrease in the CCL of CER[O] in lesional skin was small and only significant compared to non-lesional skin. Additionally, the abundance of short-chain CER[NS]-species totaling 34 carbons, CER[NSC34], was increased significantly in lesional skin (figure 2D). When the ceramide profile was measured two weeks before the initiation of treatment, an small but significant increased

in the relative abundance of CER[NDS] and CER[NS] was observed compared to baseline of controls (Supplemental Figure s3). No other differences were observed in the relative and absolute profile, nor in TEWL, CER[NS]:CER[NP] ratio, percentage MUCER[NS], abundance CER[NSC34] nor average CCL of control and patients (Supplemental Figure s4), indicating the ceramide profile in psoriasis was stable in the two weeks prior to baseline.

**Figure 1** The ceramide profile of the stratum corneum in controls, non-lesional psoriasis and lesional psoriasis. The total sum of the detected saturated ceramides (A) and the ceramide profile (B) are shown with absolute display of the data using the squamescan value (sqv) as a measure for stratum corneum removed. Additionally, the ceramide profile is shown relative to the total detected ceramides (C).



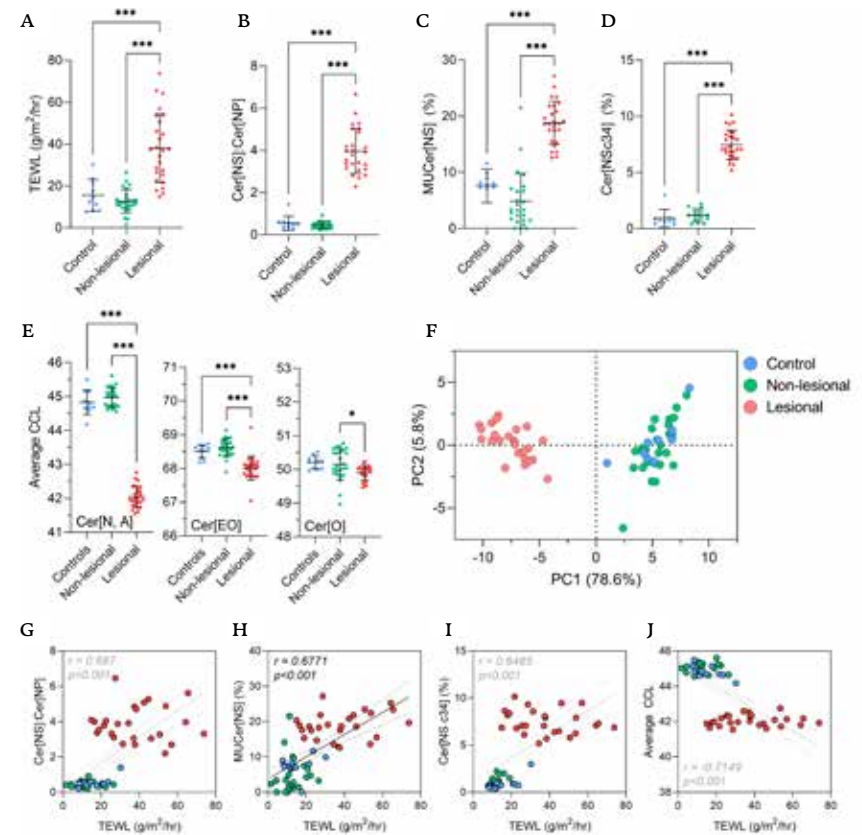
Using dimension reduction analysis to visualize the full ceramide profile, lesional skin forms a separately defined cluster compared to the overlapping non-lesional and control datapoints (figure 2F). This indicates a high degree of difference between the ceramide profile of lesional skin compared to non-

lesional and control skin. A high degree of similarity between non-lesional and control skin is supported by the aforementioned features (figure 2B-E) which do not appear significantly altered in non-lesional skin compared to controls.

Although the study included mild and moderate-to-severe patients, as defined by a PASI  $\leq 5$  or  $\geq 10$  at screening, no evident differences in the ceramide profile were observed between these two groups. However, a slight but significant decreased relative CER[NP] abundance and increased relative CER[NH] abundance in the moderate-to-severe group was present compared to mild patients (figure s5). This might have resulted in the significantly increased CER[NS]:CER[NP] ratio observed in the moderate-to-severe patients. Additionally, a significant increase in the average CCL of the CER[O] fraction is observed in moderate-to-severe patients compared to mild patients. However, these changes did not result in a markedly different ceramide profile as seen by the overlap with mild patients from principal component analysis (figure s6)

Ceramide parameters were correlated to barrier function (figure 2G-J). TEWL correlated positively with CER[NS]:CER[NP] ( $r=0.0687$ ), fraction MUCER[NS] ( $r=0.6771$ ) and abundance CER[NSC34] ( $r=0.6485$ ) and negatively with the average CCL in CER[N,A] ( $r=-0.7149$ ). However, linearity appears limited as lesional skin is markedly different compared to control and non-lesional skin in terms of both TEWL and ceramide composition.

**Figure 2 (next page)** Specific features of the stratum corneum ceramide profile in lesional psoriasis, non-lesional psoriasis and control skin. Skin barrier functionality is determined by the Trans-epidermal Water Loss (TEWL) (A). Compositional changes of the ceramide profile are summarized by calculating the ratio between CER[NS] and CER[NP] abundances as a measure for subclass synthesis skewing (B), fraction of monounsaturated ceramide (MUCER) in CER[NS] (C), the percentage of very short-chain ceramide CER[NSC34] (D) and the ceramide chain length (CCL) of CER[N] and CER[A] (CER[N,A]), CER[EO] and CER[O] separately (E). For the CCL per subclass, see figure s7. Graphs show mean and standard deviation. The (dis)similarity of the different ceramide profiles is visualized by Principal Component Analysis (PCA) of the full profile, containing the relative abundance of all individually detected saturated ceramides, with the amount of variance explained by the respective components on either axis (F). The relationship between barrier function as measured by TEWL and CER[NS]:Cer[NP] (G), fraction MUCER[NS] (H), percentage of CER[NSC34] (I) and CCL in CER[N,A] (J) are demonstrated with a line representing the best fit of a linear regression through all data points with its 95% confidence intervals shown together with the Pearson correlation coefficient ( $r$ ) and associated p-value. Lines and values in grey indicate linear regression is unsuitable for those parameters.



### ALTERATIONS IN THE CERAMIDE PROFILE NORMALIZE DURING TREATMENT WITH GUSELKUMAB BUT NOT PLACEBO

After establishing differences in untreated lesional and non-lesional skin compared to controls, their dynamics under guselkumab or placebo treatment were investigated during a 16-week treatment period. As reported previously in this cohort,<sup>30,31</sup> treatment with guselkumab effectively induced disease remission compared to placebo based on the PASI score (figure s8).

All subclasses that were decreased compared to controls at baseline normalized during guselkumab treatment (figure 3). Of note, the abundance of CER[AH] appeared to exceed that observed in controls. In the placebo group,



abundances of CER[OH] also appeared to recover to the level observed in controls as no significant difference was present when comparing the abundance of CER[OH] in controls with that of patients receiving placebo at week 16. However, the apparent variation in the CER[OH] abundance in controls was substantial and might have contributed to this as the abundance of CER[OH] remained low. All other subclasses remained significantly decreased.

As total-body PASI scoring does not necessarily correspond to target plaque severity, the LSS is used as an alternative to allow correlation between barrier characteristics and severity, and demonstrates a significant decrease compared to placebo in line with PASI scores (figure 4A). Complete skin clearance was not obtained based on PASI and LSS scores >0 after 16 weeks of guselkumab treatment. Barrier function of lesional skin improved significantly in the guselkumab group but remained comparable to baseline for patients receiving placebo (figure 4B). In line with the reduction in TEWL, ceramide parameters distilled from the overall profile ameliorated (figure 4C-F).

**Figure 3** The absolute ceramide subclass profile in lesional skin of psoriasis patients after 16 weeks of guselkumab or placebo treatment compared to controls at baseline. The ceramide subclass profile determined at baseline for controls and patients, and for patients after 16 weeks of guselkumab or placebo treatment. Pairwise comparisons are only reported between controls at baseline and patients at week 16. Grey pairwise comparisons indicate no significant difference was observed between lesional skin and control skin at baseline. ns indicates there is no significant difference ( $P > 0.05$ ).

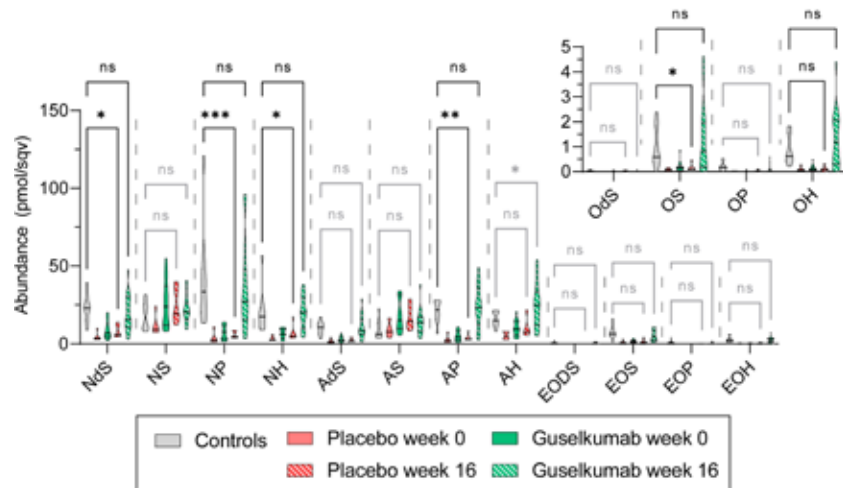
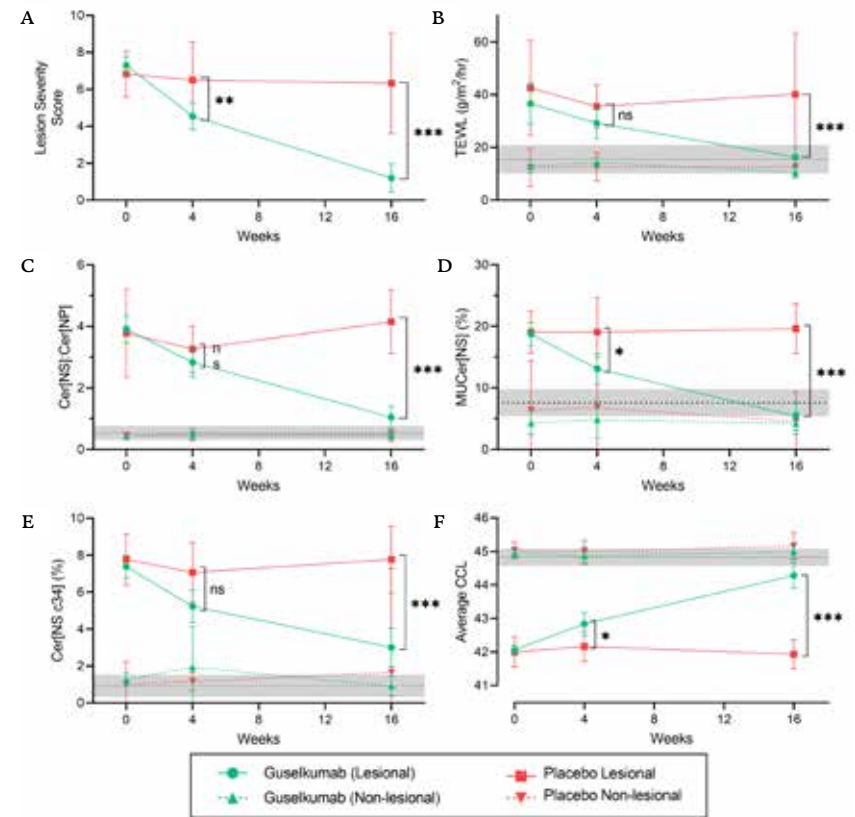


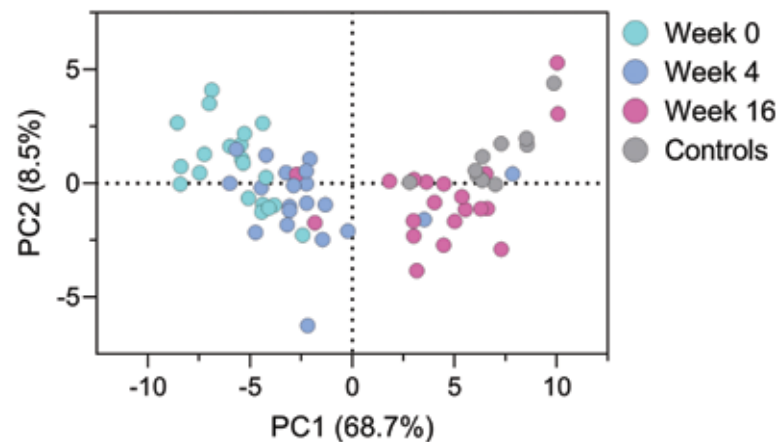
**Figure 4** The effect of guselkumab treatment on disease severity and ceramide parameters over time. Non-lesional and non-lesional skin is followed over time. Disease severity of the target plaque is determined using the lesion severity score (LSS) (A). The same plaque was monitored using the Trans-epidermal Water Loss (TEWL) as a measure for barrier function (B) and subsequently assessed with ceramide profiling yielding the the CER[NS]:CER[NP] ratio (C), percentage monounsaturated CER[NS] (MUCer[NS]) of total CER[NS] (D), percentage CER[N34] of total CER[NS] (E) and the average ceramide chain length (CCL) of the CER[A] and CER[N] fraction (F) as representative parameters of the altered ceramide profile at baseline. Graphs represent the mean and 95% Confidence Interval. The dotted black line and grey band represents the mean and 95% confidence interval of the control group at baseline. P-values are indicated when comparing lesional skin of the guselkumab group with the lesional skin of the placebo group. No significant changes were present when comparing non-lesional skin in the placebo group with non-lesional skin in the guselkumab group.



Compared to placebo, a significant decrease in the CER[NS]:CER[NP] ratio, fraction MUCER[NS] and percentage CER[NSC34] was observed to the level observed in healthy controls and non-lesional skin. The CCL in the CER[N,A] fraction increased as well but remained slightly lower compared to controls and non-lesional skin. No significant changes between the placebo and guselkumab group was observed in the CCL of the CER[EO] and CER[O] fractions (figure s9). Parameters in non-lesional skin remained consistent over time and comparable to those observed in controls at baseline.

Visualization of the ceramide profile using dimension reduction analysis indicates normalization of the ceramide profile over time to that of healthy controls (figure 5). The ceramide profile of lesional skin is markedly different from controls at baseline but shifts towards that of healthy volunteers already after 4 weeks of treatment. After 16 weeks, all lesional samples but two have become separated from those obtained at baseline and overlap fully with those from healthy controls indicating a high degree of similarity between samples of lesional and control skin.

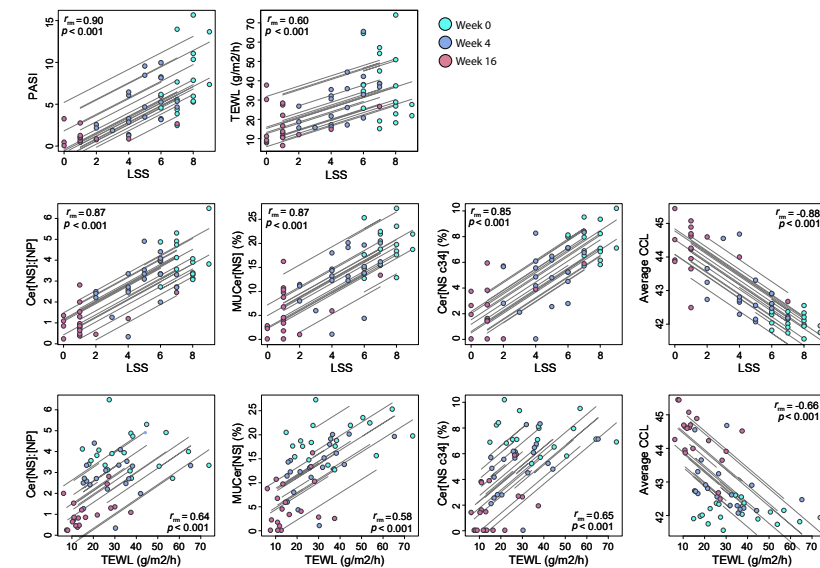
**Figure 5** The lesional ceramide profile of patients during guselkumab treatment and the ceramide profile of healthy controls at baseline visualized by Principal Component Analysis (PCA). The relative composition of all detected saturated ceramides is used for each datapoint. Profiles of healthy controls are added as a reference for a normal ceramide profile, and a high proximity to these datapoints indicates a high degree of similarity. The amount of variance explained per principal component (PC) is displayed on the axis.



## BARRIER FUNCTION AND CERAMIDE PARAMETERS CORRELATE WITH DISEASE SEVERITY

The high similarity in LSS before treatment disqualifies its use in correlation analysis at baseline. However, the repeated assessment of disease severity, barrier function and the ceramide profile during guselkumab treatment allows for the use of repeated measures correlations (figure 6). Local LSS and total-body PASI correlated strongly ( $r_{rm}=0.90$ ). Repeated measures correlations between LSS and the CER[NS]:Cer[NP] ratio ( $r_{rm}=0.87$ ), abundance MUCER[NS] ( $r_{rm}=0.87$ ), CER[NSC34] ( $r_{rm}=0.85$ ) and average CCL ( $r_{rm}=-0.88$ ) were high. However, coefficients of TEWL with LSS ( $r_{rm}=0.60$ ), CER[NS]:CER[NP] ratio ( $r_{rm}=0.64$ ), abundance MUCER[NS] ( $r_{rm}=0.58$ ), CER[NSC34] ( $r_{rm}=0.65$ ) and average CCL in CER[N,A] ( $r_{rm}=-0.66$ ) were generally lower.

**Figure 6** Correlation between disease severity and barrier function or ceramide parameters from patients receiving guselkumab treatment. Repeated measures correlation coefficients ( $r_{rm}$ ) between local lesion severity (LSS) score and the psoriasis area and severity index (PASI) and Trans-epidermal Water Loss (TEWL) are plotted. Additionally, the CER[NS]:Cer[NP] ratio, monounsaturated CER[NS] (MUCER[NS]), percentage CER[NSC34] and the average ceramide chain length (CCL) of CER[A] and CER[N] are contrasted with the LSS. Lastly, these ceramide parameters are correlated with Trans-epidermal Water Loss (TEWL). Lines indicate the common within-individual association per subject and directly relate to the  $r_{rm}$  coefficient.



## Discussion

In this study, we expand the knowledge on the SC ceramide profile in psoriasis by the in-depth profiling of lesional and non-lesional skin compared to controls and were able to correlate these alterations in the ceramide profile to barrier function. Additionally, we demonstrate how barrier impairment is alleviated during guselkumab treatment and how the observed alterations in the ceramide profile normalize throughout a randomized controlled trial.

### *The ceramide profile of lesional psoriasis is defined by altered subclass composition, increased unsaturation and decreased average ceramide chain lengths*

The baseline characterization of this cohort is in good agreement with previously published work where relative increased CER[S] and decreased amount of CER[P] and CER[EO] were observed in lesional skin compared to healthy controls, resulting in a skewed CER[S]:Cer[P] ratio.<sup>21,22,32-34</sup> However, absolute values indicates a decrease in total ceramides with a major decrease in CER[P] instead of increased CER[S]. Reflecting on the ceramide composition of lesional AD skin which has been described more extensively, increased levels of CER[S] were observed in relative profiles<sup>35,36</sup> rather than absolute profiles.<sup>37-39</sup> It should therefore be considered that increased relative CER[S] abundances merely reflect the interdependency of compositional data and results from strong reductions in absolute CER[P] abundances. However, the molar ratio between lipid classes dictates the organization of the extracellular lipid matrix and subsequently affects the barrier function.<sup>7</sup>

Decrease ceramide synthesis in lesional psoriasis has been observed, which is in line with the lower abundance of ceramides observed in the present study.<sup>40</sup> Although alterations in the activity of dihydroceramide desaturase 2 might explain the skewed CER[NS]:CER[NP] ratio as it mediates the final step in CER[P] synthesis and is downregulated in SC of lesional AD,<sup>41,42</sup> an overall decrease in ceramides, including precursor CER[NDS], indicates a more upstream inhibition. Indeed, a psoriasis mouse model indicated other enzymes might differentially contribute to CER[P] synthesis as CER[P] was still present despite knocking out dihydroceramide desaturase 2.<sup>43</sup> Presumably, decreases in the expression of acid sphingomyelinase and its activators as observed in psoriatic skin prevents sufficient sphingomyelin to be converted to ceramide.<sup>44</sup> Aberrant acid sphingomyelinase expression and activity has previously been observed in AD.<sup>35,36</sup>

Furthermore, the amount of CER[OS] and CER[OH] is decreased in lesional skin. CER[O] is a precursor of CER[EO] but may also represent CER[EO] after loss of its linoleic acid moiety. This linoleic acid moiety is required for covalent binding of ceramides to the cornified envelope.<sup>45-47</sup> However, the relevance of decreased CER[OS] and CER[OH] abundances might be questioned as their abundance is already low in controls and even their complete absence did not lead to increased permeability of model membranes.<sup>48</sup> Their relation to the bound lipid fraction might warrant its analysis in future studies.

In addition, the fraction MUCER[NS] was increased in lesional skin as has also been observed in Netherton syndrome, AD and seborrheic dermatitis.<sup>49-51</sup> A causative reason for this increase remains unknown, but might relate to increased Stearyl-CoA-9-desaturase activity.<sup>41,52</sup> Although the degree of unsaturation is only determined for CER[NS], increased MUCER has been linked to increased monounsaturated fatty acids which are incorporated in ceramides regardless of subclass and appear especially prevalent in CER[EO].<sup>8</sup> Therefore, it might be expected that increased unsaturation extends past CER[NS] and is present in other subclasses.

Besides compositional changes, ceramide elongation is impaired in lesional skin with an evident reduction in CCL observed in CER[N] and CER[A] with a more limited reduction in the CCL of CER[EO] and CER[O] fractions. An murine psoriasis model showed decreases in fatty acid elongases ELOVL1, -3 and -4, as well as in Ceramide Synthases 3 which are all involved in the synthesis of ceramides exceeding 24 carbons.<sup>21</sup> These findings are supported by studies in AD where comparable changes were observed in patients and after inducing inflammation in models.<sup>36,38,53</sup> Of note, the presence of short-chain CER[NSC34] is increased in lesional skin as indicated priorly in AD, ichthyosis and psoriasis.<sup>30</sup> These specific ceramides are associated with cellular stress and might therefore reflect the dysregulated homeostasis in psoriasis instead of impaired lipid elongation.<sup>54,55</sup> The high similarity in the ceramide profile of psoriasis and AD might reflect more general state of epidermal dysregulation rather than being primarily related to distinct pathogenic mechanisms.

### *Association of the altered ceramide profile with barrier dysfunction*

In this study, alterations in the ceramide composition, unsaturation and CCL of lesional skin are paired with decreased barrier function. Correlations between changes in ceramide composition and permeability have been demonstrated using model systems that mimic the lipid matrix of inflamed skin

with a skewed CER[NS]:CER[NP],<sup>56,57</sup> decreased CCL58,<sup>59</sup> and increased unsaturation<sup>60</sup> resulting in a decreased barrier function. Moreover, the altered ceramide profile is implicated in barrier impairment of in-vitro cultured human skin equivalents.<sup>61,62</sup> Despite these associations, linearity between ceramide alterations and barrier dysfunction within lesional skin at baseline appears limited in this study and might indicate co-occurrence rather than correlation. In AD and seborrheic dermatitis, alterations in the ceramide profile and barrier function follow a more gradual transition from non-lesional to lesional skin.<sup>33,35,37,49,63</sup> However, the lesions assessed in this study are all moderate in baseline severity which might explain the marked differences between lesional and non-lesional skin. Indeed, monitoring TEWL and lesion severity during treatment suggest a more gradual normalization instead of strict dichotomy.

Altogether, in-depth characterization of lesional psoriatic ceramide profile yields a markedly different profile compared to non-lesional and control skin. The non-inflammatory phenotype of uninvolved psoriasis is reiterated by a high similarity to control skin as reported priorly.<sup>34,64</sup> This differentiates psoriasis from AD where non-lesional barrier defects are cemented in its pathogenesis.<sup>65</sup> Variation in the study is controlled by matching the controls with patients for approximate age, sex, assessment location and recruitment throughout seasons. The robustness of the results is substantiated by their consistency when measured two weeks apart, which exceeds the turnover time of the SC in psoriasis.<sup>66</sup>

### ***Correlation of the altered ceramide profile with disease severity during guselkumab treatment***

We performed a double-blind, randomized, placebo-controlled trial to solidly affirm the relationship between alterations in the ceramide profile, barrier dysfunction and psoriasis. Priorly, a smaller cross-sectional study linked barrier dysfunction to alterations in the ceramide profile but did not evaluate the same patients barring direct correlations.<sup>23</sup> Guselkumab treatment effectively decreased disease severity as expected based on several studies including real-world evidence.<sup>18,19,67</sup> Concurrently, barrier dysfunction and alterations in the ceramide profile associated with lesional skin resolved. The ceramide profile was similar in mild and moderate-to-severe patients (PASI $\leq$ 5 or PASI $\geq$ 10 at screening), in line with pathomechanistic studies that demonstrated a high degree of similarity in the lesional transcriptomic profiles

between these groups.<sup>68,69</sup> Instead, the ceramide profile primarily relates to the target lesion severity. The narrow range of lesion severity at baseline, as a direct result of the inclusion criteria, precluded any correlation to severity pre-dose. However, variability in local severity increased during guselkumab treatment and allowed for its association with barrier parameters which were strongly correlated. Of note, the association between local severity and barrier parameters was affirmed by two patients who showed incomplete remission despite a decrease in PASI score and maintained a ceramide profile closer to baseline despite receiving guselkumab.

### ***Ceramide profiling as a biomarker for treatment monitoring***

The relationship between treatment effect and ceramide profiles might allow for exploitation in a biomarker capacity. Indeed, CER[NSC34] constitutes a single biomarker that is able to discern lesional from non-lesional skin and gradually decreases during treatment. Traditional clinical endpoints, such as the PASI, have become commonplace but are associated with poor sensitivity, bias and interrater variability.<sup>26,70,71</sup> Expanding clinical endpoints with objective measures might increase confidence in these results.<sup>72</sup> Earlier, normalization of the ceramide profile was observed in a more concise analysis during dupilumab treatment in AD patients.<sup>73,74</sup> Considering the similarity of the ceramide profile in psoriasis and AD, together with its comparable response to effective treatment, ceramide profiling might also be applied to other indications where similar alterations are observed such as ichthyosis.<sup>9</sup> However, treatment responses of plaques within the patient might differ which should be considered when only selected lesions are monitored.<sup>75</sup> Although TEWL and ceramides are both markers of skin barrier function, ceramide readouts from lesional skin seem less variable. TEWL can be impacted by personal factors, environmental factors and differ between measurement locations.<sup>76,77</sup> Although these factors can also impact the ceramide profile, their influences might be more limited.<sup>78-82</sup> Tape-stripping has already been applied to obtain protein and transcriptome-based biomarkers that are able to reflect the specific inflammatory component of specific diseases.<sup>83,84</sup> In contrast, ceramides represent more distal biomarkers that might be more primarily related to overall epidermal differentiation.<sup>85</sup> Although this disconnect might invalidate their use in a diagnostic manner, their more general relationship to disease provide a more holistic view of the response to treatment.

## Conclusion

In this study, we show that guselkumab therapy alleviates skin barrier dysfunction and normalizes the underlying ceramide profile in psoriasis patients. We showed barrier dysfunction and concurrent alterations in the ceramide profile are limited to the lesional skin of patients. Correlations between the ceramide profile and barrier function underline their interdependency, and the effective clinical response towards guselkumab therapy further establishes their relationship with disease severity. Ceramide profiling might represent a suitable biomarker for treatment monitoring.

## REFERENCES

- 1 Van Den Reek, J. M. P. A. *et al.* Satisfaction of treatment with biologics is high in psoriasis: results from the Bio-CAPTURE network. *Br J Dermatol* **170**, 1158-1165 (2014).
- 2 Elias, P. M. *et al.* Epidermal Vascular Endothelial Growth Factor Production Is Required for Permeability Barrier Homeostasis, Dermal Angiogenesis, and the Development of Epidermal Hyperplasia: Implications for the Pathogenesis of Psoriasis. *Am J Pathol* **173**, 689-699 (2008).
- 3 Nosbaum, A. *et al.* Psoriasis is a disease of the entire skin: non-lesional skin displays a prepsoriasis phenotype. *Eur J Dermatol* **31**, 143-154 (2021).
- 4 Bergboer, J. G. M., Zeeuwen, P. L. J. M. & Schalkwijk, J. Genetics of Psoriasis: Evidence for Epistatic Interaction between Skin Barrier Abnormalities and Immune Deviation. *Journal of Investigative Dermatology* **132**, 2320-2331 (2012).
- 5 Pershing, L. K., Bakhtian, S., Wright, E. D. & Rallis, T. M. Differentiation of involved and uninvolved psoriatic skin from healthy skin using noninvasive visual, colorimeter and evaporimeter methods. *Skin Res Technol* **1**, 140-144 (1995).
- 6 Takahashi, H., Tsuji, H., Minami-Hori, M., Miyauchi, Y. & Iizuka, H. Defective barrier function accompanied by structural changes of psoriatic stratum corneum. *J Dermatol* **41**, 144-148 (2014).
- 7 Bouwstra, J. A. *et al.* The skin barrier: An extraordinary interface with an exceptional lipid organization. *Prog Lipid Res* **92**, 101252 (2023).
- 8 Kawana, M., Miyamoto, M., Ohno, Y. & Kihara, A. Comparative profiling and comprehensive quantification of stratum corneum ceramides in humans and mice by LC/MS/MS. *J Lipid Res* **61**, 884 (2020).
- 9 Rousel, J. *et al.* Similar alterations of the stratum corneum ceramide profile in atopic dermatitis, psoriasis and ichthyosis: results from a systematic review and meta-analysis. *Journal of Investigative Dermatology* (2024)
- 10 Van Smeden, J., Janssens, M., Vreeken, R., Lavrijsen, A. & Bouwstra, J. Free fatty acids and lipid chain length correlate with the impaired skin barrier of atopic eczema patients. *Journal of Investigative Dermatology* **133**, S123 (2013).
- 11 Janssens, M. *et al.* Increase in short-chain ceramides correlates with an altered lipid organization and decreased barrier function in atopic eczema patients. *J Lipid Res* **53**, 2755 (2012).
- 12 Janssens, M. *et al.* Non-lesional skin in atopic eczema patients shows a change in lipid organization that correlates with a decreased barrier function. *Journal of Investigative Dermatology* **132**, S77 (2012).
- 13 Van Smeden, J. *et al.* Lipid chain length reduction correlates with the skin barrier function in atopic eczema patients and inflammation plays a role in the altered epidermal lipid biosynthesis. *Journal of Investigative Dermatology* **135**, S59 (2015).
- 14 Tawada, C. *et al.* Interferon-Decreases Ceramides with Long-Chain Fatty Acids: Possible Involvement in Atopic Dermatitis and Psoriasis. *Journal of Investigative Dermatology* **134**, 712-718 (2014).
- 15 Danso, M. O. *et al.* TNF- and Th2 cytokines induce atopic dermatitis-like features on epidermal differentiation proteins and stratum corneum lipids in human skin equivalents. *J Invest Dermatol* **134**, 1941-1950 (2014).
- 16 Orsmond, A., Bereza-Malcolm, L., Lynch, T., March, L. & Xue, M. Skin Barrier Dysregulation in Psoriasis. *Int J Mol Sci* **22**, (2021).
- 17 Hawkes, J. E., Chan, T. C. & Krueger, J. G. Psoriasis Pathogenesis and the Development of Novel, Targeted Immune Therapies. *J Allergy Clin Immunol* **140**, 645 (2017).
- 18 Puig, L., Daudén, E., Cuervas-Mons, M., Novella, C. & Guisado, C. Persistence and effectiveness of guselkumab treatment in patients with moderate-to-severe plaque psoriasis in a non-interventional real-world setting: The SPRING study. *Journal of the European Academy of Dermatology and Venerology* **00**, 1-11 (2023).
- 19 Reich, K. *et al.* Efficacy and safety of guselkumab, an anti-interleukin-23 monoclonal antibody, compared with adalimumab for the treatment of patients with moderate to severe psoriasis with randomized withdrawal and retreatment: Results from the phase III, double-blind, placebo- and active comparator-controlled Voyage 2 trial. *J Am Acad Dermatol* **76**, 418-431 (2017).
- 20 Takahashi, T., Koga, Y. & Kainoh, M. Anti-IL-12/IL-23p40 antibody ameliorates dermatitis and skin barrier dysfunction in mice with imiquimod-induced psoriasis-like dermatitis. *Eur J Pharmacol* **828**, 26-30 (2018).
- 21 Kim, B. K. *et al.* Decrease of ceramides with long-chain fatty acids in psoriasis: Possible inhibitory effect of interferon gamma on chain elongation. *Exp Dermatol* **31**, 122-132 (2022).
- 22 Uchino, T. *et al.* Comparative analysis of intercellular lipid organization and composition between psoriatic and healthy stratum corneum. *Chem Phys Lipids* **254**, (2023).
- 23 Motta, S. *et al.* Abnormality of water barrier function in psoriasis. Role of ceramide fractions. *Arch Dermatol* **130**, 452-456 (1994).
- 24 Keurentjes, A. J., Jakasa, I. & Kezic, S. Research Techniques Made Simple: Stratum Corneum Tape Stripping. *Journal of Investigative Dermatology* **141**, 1129-1133.e1 (2021).
- 25 Boiten, W., Absalah, S., Vreeken, R., Bouwstra, J. & van Smeden, J. Quantitative analysis of ceramides using a novel lipidomics approach with three dimensional response modelling. *Biochimica et Biophysica Acta (BBA) - Molecular and Cell Biology of Lipids* **1861**, 1652-1661 (2016).
- 26 Ashcroft, D. M., Li Wan Po, A., Williams, H. C. & Griffiths, C. E. M. Clinical measures of disease severity and outcome in psoriasis: a critical appraisal of their quality. *Br J Dermatol* **141**, 185-191 (1999).
- 27 Vissers, W. H. P. M., Van Vlijmen, I., Van Erp, P. E. J., De Jong, E. M. G. J. & Van De Kerkhof, P. C. M. Topical treatment of mild to moderate plaque psoriasis with 0.3% tacrolimus gel and 0.5% tacrolimus cream: the effect on SUM score, epidermal proliferation, keratinization, T-cell subsets and HLA-DR expression. *British Journal of Dermatology* **158**, 705-712 (2008).
- 28 Glatt, S. *et al.* First-in-human randomized study of bimekizumab, a humanized monoclonal antibody and selective dual inhibitor of IL-17A and IL-17F, in mild psoriasis. *Br J Clin Pharmacol* **83**, 991-1001 (2017).
- 29 Bakdash, J. Z. & Marusch, L. R. Repeated measures correlation. *Front Psychol* **8**, 252904 (2017).
- 30 Rousel, J. *et al.* Mild Psoriasis Patients are Suitable Alternatives for Moderate-To-Severe Psoriasis Patients in Early-Phase Clinical Trials: Results of a Randomized Controlled Trial with Guselkumab. *Submitted* (2024).
- 31 Rousel, J. *et al.* Guselkumab induction therapy demonstrates long-lasting efficacy in patients with mild psoriasis, results from a randomized, placebo-controlled

- exploratory clinical trial. *J Am Acad Dermatol* **0**, (2023).
- 32 Motta, S. *et al.* Ceramide composition of the psoriatic scale. *Biochim Biophys Acta* **1182**, 147-151 (1993).
- 33 Yokose, U. *et al.* The ceramide [NP]/[NS] ratio in the stratum corneum is a potential marker for skin properties and epidermal differentiation. *BMC Dermatol* **20**, (2020).
- 34 Koyano, S. *et al.* Psoriasis patients have abnormal ceramide profile in stratum corneum. *Nishinihon Journal of Dermatology* **72**, 494-499 (2010).
- 35 Boer, D. E. C. *et al.* Skin of atopic dermatitis patients shows disturbed -glucocerebrosidase and acid sphingomyelinase activity that relates to changes in stratum corneum lipid composition. *Biochimica et Biophysica Acta (BBA) - Molecular and Cell Biology of Lipids* **1865**, 158673 (2020).
- 36 Danso, M. *et al.* Altered expression of epidermal lipid bio-synthesis enzymes in atopic dermatitis skin is accompanied by changes in stratum corneum lipid composition. *J Dermatol Sci* **88**, 57-66 (2017).
- 37 Ishikawa, J. *et al.* Changes in the Ceramide Profile of Atopic Dermatitis Patients. *Journal of Investigative Dermatology* **130**, 2511-2514 (2010).
- 38 Ito, S. *et al.* Ceramide synthase 4 is highly expressed in involved skin of patients with atopic dermatitis. *Journal of the European Academy of Dermatology and Venereology* **31**, 135-141 (2017).
- 39 Chu, H. *et al.* Head and neck dermatitis is exacerbated by *Malassezia furfur* colonization, skin barrier disruption, and immune dysregulation. *Front Immunol* **14**, (2023).
- 40 Cho, Y., Lew, B. L., Seong, K. & Kim, N. I. An Inverse Relationship Between Ceramide Synthesis and Clinical Severity in Patients with Psoriasis. *J Korean Med Sci* **19**, 859 (2004).
- 41 Kihara, A. Synthesis and degradation pathways, functions, and pathology of ceramides and epidermal acylceramides. *Progress in Lipid Research* vol. 63 50-69 Preprint at <https://doi.org/10.1016/j.plipres.2016.04.001> (2016).
- 42 Del Duca, E. *et al.* Inpatient comparison of atopic dermatitis skin transcriptome shows differences between tape-strips and biopsies. *Allergy* **00**, 1-13 (2023).
- 43 Ota, A. *et al.* Bifunctional DEGS2 has higher hydroxylase activity toward substrates with very-long-chain fatty acids in the production of phytosphingosine ceramides. *Journal of Biological Chemistry* **299**, (2023).
- 44 Alessandrini, F., Stachowitz, S., Ring, J. & Behrendt, H. The Level of Prosaposin is Decreased in the Skin of Patients with Psoriasis Vulgaris. *Journal of Investigative Dermatology* **116**, 394-400 (2001).
- 45 Ohno, Y. *et al.* Determining the structure of protein-bound ceramides, essential lipids for skin barrier function. *iScience* **26**, 108248 (2023).
- 46 Takeichi, T. *et al.* SDR9C7 catalyzes critical dehydrogenation of acylceramides for skin barrier formation. *J Clin Invest* **130**, 890 (2020).
- 47 Ohno, Y., Kamiyama, N., Nakamichi, S. & Kihara, A. PNPLA1 is a transacylase essential for the generation of the skin barrier lipid -O-acylceramide. *Nat Commun* **8**, 14610 (2017).
- 48 Opálka, L. *et al.* -O-Acylceramides but not -hydroxy ceramides are required for healthy lamellar phase architecture of skin barrier lipids. *J Lipid Res* **63**, 100226 (2022).
- 49 Rousel, J. *et al.* Lesional skin of seborrheic dermatitis patients is characterized by skin barrier dysfunction and correlating alterations in the stratum corneum ceramide composition. *Exp Dermatol* **00**, 1-12 (2023).
- 50 Van Smeden, J. *et al.* Intercellular skin barrier lipid composition and organization in netherton syndrome patients. *Journal of Investigative Dermatology* **134**, 1238-1245 (2014).
- 51 Boiten, W., van Smeden, J. & Bouwstra, J. The Cornified Envelope-Bound Ceramide Fraction Is Altered in Patients with Atopic Dermatitis. *Journal of Investigative Dermatology* **140**, 1097-1100.e4 (2020).
- 52 Helder, R. W. J. *et al.* Improved organotypic skin model with reduced quantity of monounsaturated ceramides by inhibiting stearyl-CoA desaturase-1. *Biochimica et Biophysica Acta (BBA) - Molecular and Cell Biology of Lipids* **1866**, 158885 (2021).
- 53 Berdyshev, E. *et al.* Lipid abnormalities in atopic skin are driven by type 2 cytokines. *JCI Insight* **3**, (2018).
- 54 Gaggini, M., Ndreu, R., Michelucci, E., Rocchiccioli, S. & Vassalle, C. Ceramides as Mediators of Oxidative Stress and Inflammation in Cardiometabolic Disease. *Int J Mol Sci* **23**, (2022).
- 55 Fekry, B. *et al.* C16-ceramide is a natural regulatory ligand of p53 in cellular stress response. *Nature Communications* **2018** 9:1 9, 1-12 (2018).
- 56 Uche, L. E., Gooris, G. S., Bouwstra, J. A. & Beddoes, C. M. Barrier Capability of Skin Lipid Models: Effect of Ceramides and Free Fatty Acid Composition. *Langmuir* **35**, 15376-15388 (2019).
- 57 Nádabán, A. *et al.* Effect of sphingosine and phytosphingosine ceramide ratio on lipid arrangement and barrier function in skin lipid models. *J Lipid Res* **64**, 100400 (2023).
- 58 Pullmannová, P. *et al.* Permeability and microstructure of model stratum corneum lipid membranes containing ceramides with long (C16) and very long (C24) acyl chains. *Biophys Chem* **224**, 20-31 (2017).
- 59 Mojumdar, E. H., Kariman, Z., van Kerckhove, L., Gooris, G. S. & Bouwstra, J. A. The role of ceramide chain length distribution on the barrier properties of the skin lipid membranes. *Biochimica et Biophysica Acta (BBA) - Biomembranes* **1838**, 2473-2483 (2014).
- 60 Mojumdar, E. H., Helder, R. W. J., Gooris, G. S. & Bouwstra, J. A. Monounsaturated fatty acids reduce the barrier of stratum corneum lipid membranes by enhancing the formation of a hexagonal lateral packing. *Langmuir* **30**, 6534-6543 (2014).
- 61 Mieremet, A. *et al.* Multitargeted approach for the optimization of morphogenesis and barrier formation in human skin equivalents. *Int J Mol Sci* **22**, (2021).
- 62 Thakoersing, V. S. *et al.* Unraveling Barrier Properties of Three Different In-House Human Skin Equivalents. *Tissue Eng Part C Methods* **18**, 1-11 (2012).
- 63 van Smeden, J. *et al.* The importance of free fatty acid chain length for the skin barrier function in atopic eczema patients. *Exp Dermatol* **23**, 45-52 (2014).
- 64 Farwanah, H., Raith, K., Neubert, R. H. & Wohlrab, J. Ceramide profiles of the uninvolved skin in atopic dermatitis and psoriasis are comparable to those of healthy skin. *Arch Dermatol Res* **296**, 514-521 (2005).
- 65 Yoshida, T., Beck, L. A. & De Benedetto, A. Skin barrier defects in atopic dermatitis: From old idea to new opportunity. *Allergology International* **71**, 3-13 (2022).
- 66 Weinstein, G. D. & Van Scott, E. J. Autoradiographic Analysis of Turnover Times of Normal and Psoriatic Epidermis. *Journal of Investigative Dermatology* **45**, 257-262 (1965).
- 67 Reich, K. *et al.* Guselkumab versus secukinumab for the treatment of moderate-to-severe psoriasis (ECLIPSE): results from a phase 3, randomised controlled trial. *The Lancet* **394**, 831-839 (2019).
- 68 Kim, J. *et al.* The Spectrum of Mild to Severe Psoriasis Vulgaris Is Defined by a Common Activation of IL-17 Pathway Genes, but with Key Differences in Immune Regulatory Genes. *Journal of Investigative Dermatology* **136**, 2173-2182 (2016).
- 69 Castillo, R. L. *et al.* Spatial transcriptomics stratifies psoriasis disease severity by emergent cellular ecosystems. *Sci Immunol* **8**, eabq7991 (2023).
- 70 Langley, R. G. & Ellis, C. N. Evaluating psoriasis with psoriasis area and severity index, psoriasis global assessment, and lattice system physician's global assessment. *J Am Acad Dermatol* **51**, 563-569 (2004).
- 71 Gourraud, P. A. *et al.* Why Statistics Matter: Limited Inter-Rater Agreement Prevents Using the Psoriasis Area and Severity Index as a Unique Determinant of Therapeutic Decision in Psoriasis. *Journal of Investigative Dermatology* **132**, 2171-2175 (2012).
- 72 Rissmann, R., Moerland, M. & van Doorn, M. B. A. Blueprint for mechanistic, data-rich early phase clinical pharmacology studies in dermatology. *Br J Clin Pharmacol* **86**, 1011 (2020).
- 73 Berdyshev, E. *et al.* Dupilumab significantly improves skin barrier function in patients with moderate-to-severe atopic dermatitis. *Allergy* **77**, 3388-3397 (2022).
- 74 Lee, S. J., Kim, S. E., Shin, K. O., Park, K. & Lee, S. E. Dupilumab Therapy Improves Stratum Corneum Hydration and Skin Dysbiosis in Patients With Atopic Dermatitis. *Allergy Asthma Immunol Res* **13**, 762 (2021).
- 75 Haidari, W., Pona, A. & Feldman, S. R. Management of Residual Psoriasis in Patients on Biologic Treatment. *J Drugs Dermatol* **19**, 188-194 (2020).
- 76 Akdeniz, M., Gabriel, S., Lichterfeld-Kottner, A., Blume-Peytavi, U. & Kottner, J. Transepidermal water loss in healthy adults: a systematic review and meta-analysis update. *British Journal of Dermatology* **179**, 1049-1055 (2018).
- 77 Peer, R. P., Burli, A. & Maibach, H. I. Unbearable transepidermal water loss (TEWL) experimental variability: why? *Arch Dermatol Res* **314**, 99-119 (2022).
- 78 Fujiwara, A. *et al.* Age-related and seasonal changes in covalently bound ceramide content in forearm stratum corneum of Japanese subjects: determination of molecular species of ceramides. *Arch Dermatol Res* **310**, 729-735 (2018).
- 79 Rogers, J., Harding, C., Mayo, A., Banks, J. & Rawlings, A. Stratum corneum lipids: the effect of ageing and the seasons. *Arch Dermatol Res* **288**, 765-770 (1996).
- 80 Muizzuddin, N. *et al.* Structural and functional differences in barrier properties of African American, Caucasian and East Asian skin. *J Dermatol Sci* **59**, 123-128 (2010).
- 81 Pappas, A., Kendall, A. C., Brownbridge, L. C., Batchvarova, N. & Nicolaou, A. Seasonal changes in epidermal ceramides are linked to impaired barrier function in acne patients. *Exp Dermatol* **27**, 833-836 (2018).
- 82 Ishikawa, J. *et al.* Variations in the ceramide profile in different seasons and regions of the body contribute to stratum corneum functions. *Arch Dermatol Res* **305**, 151-162 (2013).
- 83 He, H. *et al.* Tape strips detect distinct immune and barrier profiles in atopic dermatitis and psoriasis. *Journal of Allergy and Clinical Immunology* **147**, 199-212 (2021).
- 84 He, H. *et al.* Tape-Strip Proteomic Profiling of Atopic Dermatitis on Dupilumab Identifies Minimally Invasive Biomarkers. *Front Immunol* **11**, 565656 (2020).
- 85 Yokose, U. *et al.* The ceramide [NP]/[NS] ratio in the stratum corneum is a potential marker for skin properties and epidermal differentiation. *BMC Dermatol* **20**, (2020).

**SUPPLEMENTAL MATERIAL**

**Figure s1** An overview of the variety in ceramides Adapted from Janssens *et al.* (2012). A general structure with the structural differences highlighted such as differences in headgroup architecture, chain length and degree of unsaturation. Additionally, it presents the structure of all ceramide classes used in this study according to the nomenclature by Motta *et al.* (1993).

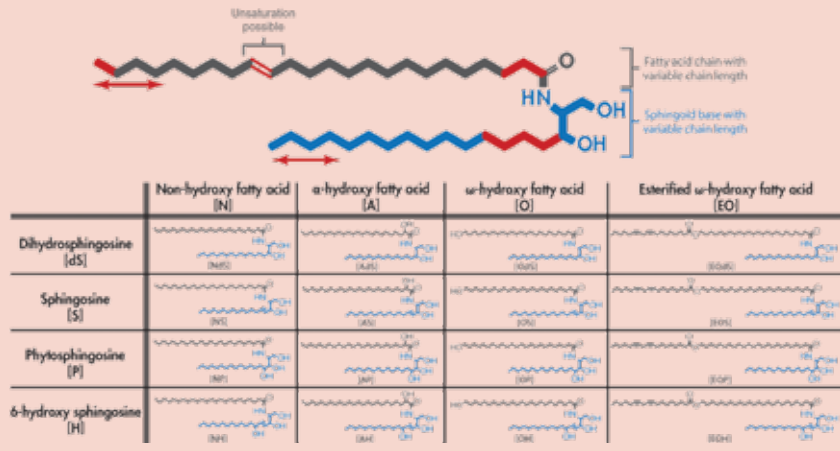


**Figure s2** Consort flow chart of the study population.

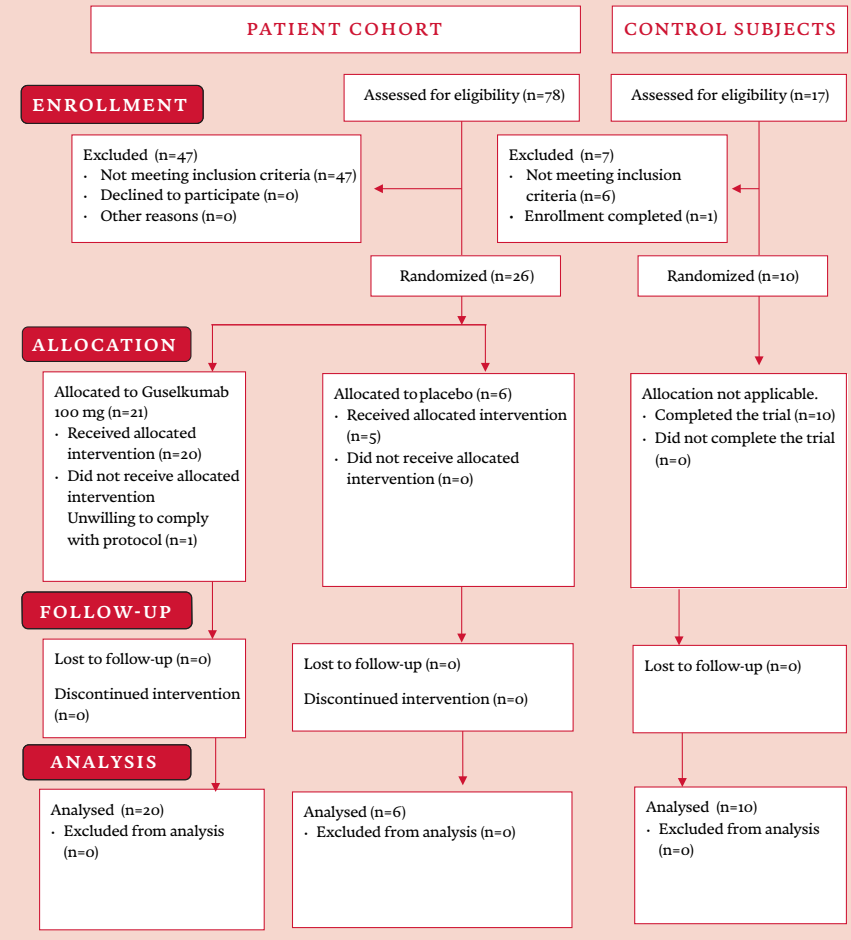


**Table s1** Baseline demographics.

		Controls	Placebo	Guselkumab
Total number of patients		10	6	20
Age at first dose	≤ 18 years	0 (0%)	0 (0%)	0 (0%)
	18-65 years	10 (100%)	6 (100%)	19 (95%)
	≥ 65 years	0 (0%)	0 (0%)	1 (5%)
	Average age (years ± SD)	42.6±9.8	44.4±12.5	40.2±6.9
Gender	Female	7 (70%)	1 (17%)	5 (25%)
	Male	3 (30%)	5 (83%)	15 (75%)
Race	White	9 (90%)	5 (83%)	17 (85%)
	Asian	0 (0%)	1 (17%)	0 (0%)
	Hispanic	1 (10%)	0 (0%)	1 (5%)
	More than one	0 (0%)	0 (0%)	2 (10%)
Fitzpatrick	I	0 (0%)	0 (0%)	1 (5%)
	II	5 (50%)	3 (50%)	8 (40%)
	III	4 (40%)	2 (33%)	10 (50%)
	IV	1 (10%)	0 (0%)	0 (0%)
	V	0 (0%)	0 (0%)	0 (0%)
	VI	0 (0%)	1 (17%)	1 (5%)

## OVERVIEW OF THE IN- AND EXCLUSION CRITERIA FOR THIS STUDY

Eligible healthy controls must meet all of the following inclusion criteria at screening:

- 1 Male or non-pregnant female subjects, 18 to 75 years of age (inclusive); during COVID-19 pandemic this is set to 18 to 69 year of age (inclusive)
- 2 Healthy as defined by the absence of any uncontrolled active or uncontrolled chronic disease following a medical and surgical history, documentation of general symptoms, and a symptom-directed physical examination including vital signs;
- 3 Willing to give written informed consent and willing and able to comply with the study protocol;

And eligible healthy controls must meet none of the following exclusion criteria at screening:

- 1 History or symptoms of any uncontrolled, significant disease including (but not limited to), neurological, psychiatric, endocrine, cardiovascular, respiratory, gastrointestinal, hepatic, or renal disorder that may interfere with the study objectives, in the opinion of the Investigator;
- 2 History of immunological abnormality (e.g., immune suppression, severe allergy or anaphylaxis) that may interfere with study objectives, in the opinion of the Investigator;
- 3 Known infection requiring antibiotic therapy within the last three months prior to the study;

- 4 Immunosuppressive or immunomodulatory treatment within 30 days prior to the study;
- 5 Body mass index (BMI) ≤ 18.0 or ≥ 40.0 kg/m<sup>2</sup>; during COVID-19 pandemic only ≤ 18.0 or > 33.0 kg/m<sup>2</sup>
- 6 Participation in an investigational drug study within 3 months prior to screening or more than 4 times a year;
- 7 Previous participation in an investigational drug study involving the dosing of an investigational compound targeting an immune pathway within one year prior to screening;
- 8 Loss or donation of blood over 500 mL within three months prior to screening;
- 9 The use of any medication or vitamin/mineral/herbal/dietary supplement within less than 5 half-lives prior to study participation, if the Investigator judges that it may interfere with the study objectives. The use of paracetamol (up to 4 g/day) is allowed;
- 10 History of alcohol consumption exceeding 5 standard drinks per day on average within 3 months of screening. Alcohol consumption will be prohibited from at least 12 hours preceding each study visit;
- 11 Any other condition that could interfere with the conduct of the study or the study objectives, in the opinion of the Investigator.
- 12 During COVID-19 pandemic: presence of high risk comorbidities: such as cardiovascular, respiratory or immune system disorders

Eligible psoriasis patients must meet all of the following inclusion criteria at screening:

- 1 Male or non-pregnant female subjects, 18 to 75 years of age (inclusive); during

- COVID-19 pandemic this is set to 18 to 69 year of age (inclusive)
- 2 Diagnosed with plaque psoriasis at least 6 months prior to study participation
  - 3 Willing to discontinue any psoriasis therapy other than emollients.
  - 4 Having mild (PASI ≥ 1 and ≤ 5) or moderate-to-severe (PASI ≥ 10) plaque psoriasis;
  - 5 Currently not using psoriasis medication and ≥ 2 plaques suitable for repeated biopsies and target lesion assessments. At least one of these lesions must be located on the extremities, preferably on the elbow or knee, with a minimal target lesion score between 6 and 9. Or, when currently using psoriasis medication and insufficient lesional skin is present, willing to discontinue treatment awaiting rescreening (see also exclusion criteria 3 for psoriatic patients);
  - 6 Willing to give written informed consent and willing and able to comply with the study protocol;

And none of the following exclusion criteria at screening:

- 1 Having primarily erythrodermic, pustular or guttate psoriasis;
- 2 Having medication-induced psoriasis;
- 3 Having previously failed on ANTI-IL23 therapy;
- 4 Having received treatments for psoriasis within the following intervals prior to the start of the study:
  - a < 2 weeks for topical treatment, e.g. retinoids, corticosteroids, vitamin D analogs
  - b < 4 weeks for phototherapy, e.g. PUVA, PDT



- c < 4 weeks for non-biologic systemic treatment, e.g. retinoids, methotrexate, cyclosporine, fumaric acid esters
  - d < 4 weeks for etanercept
  - e < 8 weeks for adalimumab
  - f < 3 months for anti-IL17, anti-IL12(/23) and anti-IL23 treatments
- 5 History or symptoms of any significant uncontrolled disease including (but not limited to), neurological, psychiatric, endocrine, cardiovascular, respiratory, gastrointestinal, hepatic, or renal disorder that may interfere with the study objectives, in the opinion of the Investigator, excluding psoriasis and conditions that are related to psoriasis;
  - 6 History of immunological abnormality (e.g., immune suppression, severe allergy or anaphylaxis) that may interfere with study objectives, in the opinion of the Investigator;
  - 7 Known infection requiring antibiotic therapy within the last 3 months prior to the study, including latent tuberculosis;
  - 8 Systemic immunosuppressive or immunomodulatory treatment within 30 days prior to the study;
  - 9 Body mass index (BMI)  $\leq 18.0$  or  $\geq 40.0$  kg/m<sup>2</sup>; during COVID-19 pandemic only  $\leq 18.0$  or  $> 33.0$  kg/m<sup>2</sup>
  - 10 Participation in an investigational drug study within 3 months prior to screening or more than 4 times a year;
  - 11 Loss or donation of blood over 500 mL within three months prior to screening;
  - 12 The use of any medication or vitamin/mineral/herbal/dietary supplement within less than 5 half-lives prior to study participation, if the Investigator judges that it may interfere with the study objectives. The use of paracetamol (up to 4 g/day) and is allowed;
  - 13 History of alcohol consumption exceeding 5 standard drinks per day on average within 3 months of screening. Alcohol consumption will be prohibited from at least 12 hours preceding each study visit;
  - 14 Any other condition that could interfere with the conduct of the study or the study objectives, in the opinion of the Investigator.
  - 15 During COVID-19 pandemic: presence of high risk comorbidities: such as cardiovascular, respiratory or immune system disorders other than psoriasis and psoriasis arthritis.

## SUPPLEMENTAL MATERIALS AND METHODS

### Chemicals

HPLC-grade chloroform (Honeywell, Charlotte, North Carolina, United States), UPLC grade ethanol (Biosolve, Valkenswaard, the Netherlands), UPLC grade heptane (LiChorSolv, Merck, Darmstadt, Germany), UPLC grade isopropyl alcohol (Biosolve, Valkenswaard, the Netherlands), UPLC grade Methanol (Biosolve, Valkenswaard, the Netherlands) were used. The 0.25M potassium chloride solution was prepared by dissolving reagent grade potassium chloride (Sigma Aldrich, Saint-Louis, Missouri, USA) in ultrapure water from a Milli-Q Advantage A10 system (Merck, Darmstadt, Germany). Deuterated internal standard and ceramide standards were bought from Avanti Polar Lipids (Alabaster, Alabama, United States) or received from Evonik (Darmstadt, Germany). Polyphenylene sulfide tape (Nichiban, Tokyo, Japan) was used for tape stripping.

Tape stripping was performed after TEWL was determined and at the same location. Tapes 5, 6, 7, 8 were measured using a SquameScan 850A (Heiland Electronic, Wetzlar, Germany) to obtain the squame scan value (SQV) before a 16 diameter circle was punched out. The circles of tape were stored in a 20 ml glass vial with chloroform:methanol (2:1) at  $-40$  °C prior to extraction. Tapes were extracted in three batches. Tapes were agitated by rotary shaker using an IKA S4000 at 120 rounds per minute at 40 °C for one hour. The solvent was collected and shaking repeated with 1 ml of chloroform:methanol:water (1:2:0.5), chloroform:methanol (1:1) and heptane:isopropylalcohol (1:1), sequentially, pooling the solvent of the 4 tapes per assessment together between each round of shaking. A liquid-liquid extraction was performed by the addition of 4 ml 0.25M KCL and the samples stored overnight at 4 °C to allow for phase separation. The organic layer was collected and the aqueous layer washed with 4 ml of chloroform. Organic layers were combined and filtered through 0.45  $\mu$ m PVDF syringe filters (Grace, Deerfield, Illinois, United States). After filtration, a aliquot of the samples were dried and reconstituted in 60  $\mu$ l heptane:chloroform:methanol (95:2.5:2.5) with containing 10  $\mu$ M CER[N(24DEU)S(18)] for analysis by ultra-performance liquid chromatography-mass spectrometry on a Acquity UPLC H-class (Waters, Milford, Massachusetts, United States) with a PVA-silica column (5  $\mu$ m particles, 100  $\times$  2.1 mm i.d.) (YMC, Kyoto, Japan) hyphenated to a XEVO TQ-S mass spectrometer (Waters, Milford, MA, USA) operating with atmospheric pressure chemical

ionization in positive mode. Samples were analyzed in three runs and each contained quality control samples from the same from combined stratum corneum extract pool and calibration curves. All patient samples at baseline showed sufficient responses and were used for relative analysis. Peak picking was performed using TargetLynx V4.1 (Waters, Milford, Massachusetts, United States). The monoisotopic response of ceramides corrected with the internal standard was used for corrections including adduct formation as determined from quality control samples and calibration curves,  $^{13}\text{C}$  isotope abundance, difference in response based on molecular weight determined from calibration curves and, if applicable, the SQV. 6 samples did not show any analytes. Absolute quantification using the SQV resulted in 2 non-lesional samples and 3 lesional baseline samples identified as outliers (ROUT method) which were excluded from analysis. Full details and validation of the method is described by Boiten, *et al.* (2016).

### Statistical analysis

Analysis of baseline data, including Pearson correlations, between groups was performed using PRISM 9.0 (GraphPad, Software, Boston, Massachusetts, United States). Profiles of controls, non-lesional psoriasis and lesional psoriasis were compared using One or Two-Way Analysis of Variance (ANOVA). Multiple comparisons were conducted with Tukey's test. Longitudinal analysis were performed in SAS 9.4 (SAS Institute Inc., Cary, North Carolina, United States). A repeated measures mixed effects model with treatment, time and the interaction as fixed factors, and time as a repeated factor is used. The baseline measurement is used as covariate. Any log-normal distributed data is log transformed before analysis, whereby ana are treated as missing. Analysis results are back transformed. Treatment graphs show the mean and 95% Confidence Interval and are reported by p-value. Common within-individual associations for paired measures were determined using Rmcorr in R Statistical Software (version 4.1.2, R Core Team 2021). Statistical significance is shown as:  $P < 0.05$ ; \*,  $P < 0.005$ ; - and  $P < 0.005$ ; -\*.

**Figure s3** Stability of the ceramide profile over two weeks. The relative ceramide profile (A) and absolute ceramide profile (B) from lesional psoriasis, non-lesional psoriasis and matched locations of controls. Displayed data shows the ceramide profile at baseline (week 0) and two weeks before baseline (week -2). Statistical testing is performed with a two-way ANOVA comparing week -2 and week 0. Significance is only indicated for comparisons yielding  $p < 0.05$ .

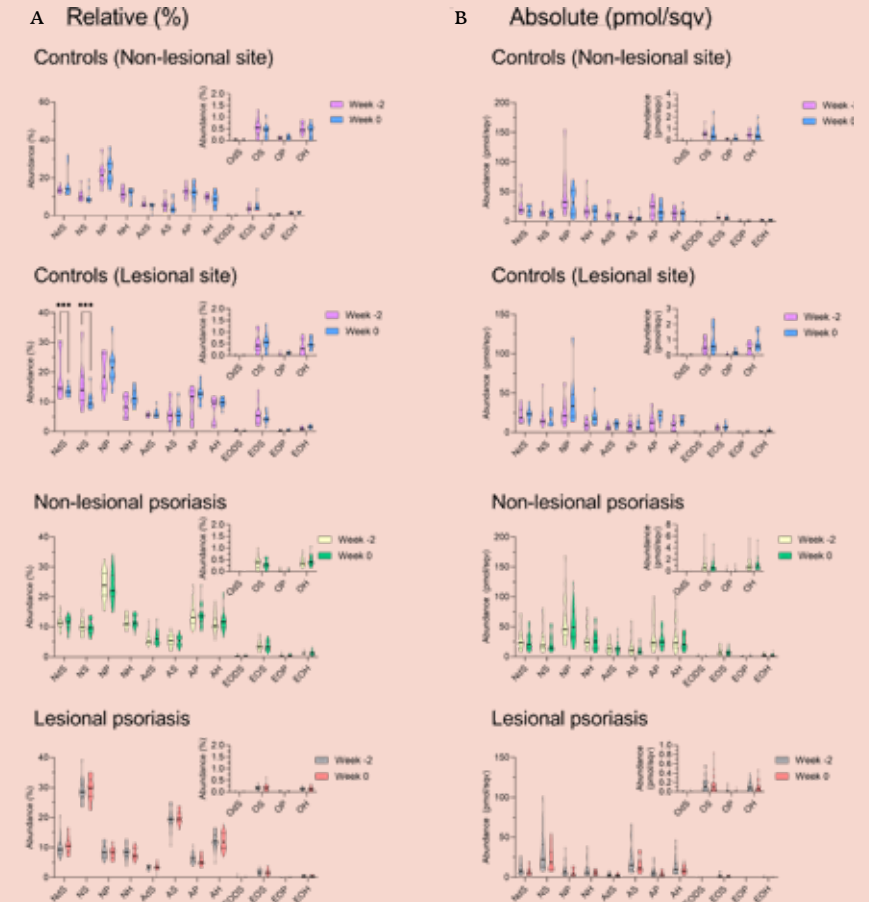


**Figure s4** Stability of barrier function (A) and selected characteristics of the ceramide profile from lesional psoriasis, non-lesional psoriasis and matched locations of controls. The ratio between the abundance of CER[NS] and CER[NP] (B) and abundance of monounsaturated MUCER[NS] from the entire CER[NS] fraction (C) are shown. Specifics on the ceramide chain length (CCL) are shown with the abundance of CER[NSC34] of total CER[NS] (D), the average CCL of the CER[N] and CER[A] fraction (Cer[N,A]) (E), the CER[EO] fraction (F) and the CER[O] fraction (G). Displayed data shows the features at baseline (week 0) and two weeks before baseline (week -2) of the same location. Statistical testing is performed with a two-way ANOVA with “NS” indicating  $p > 0.05$ .

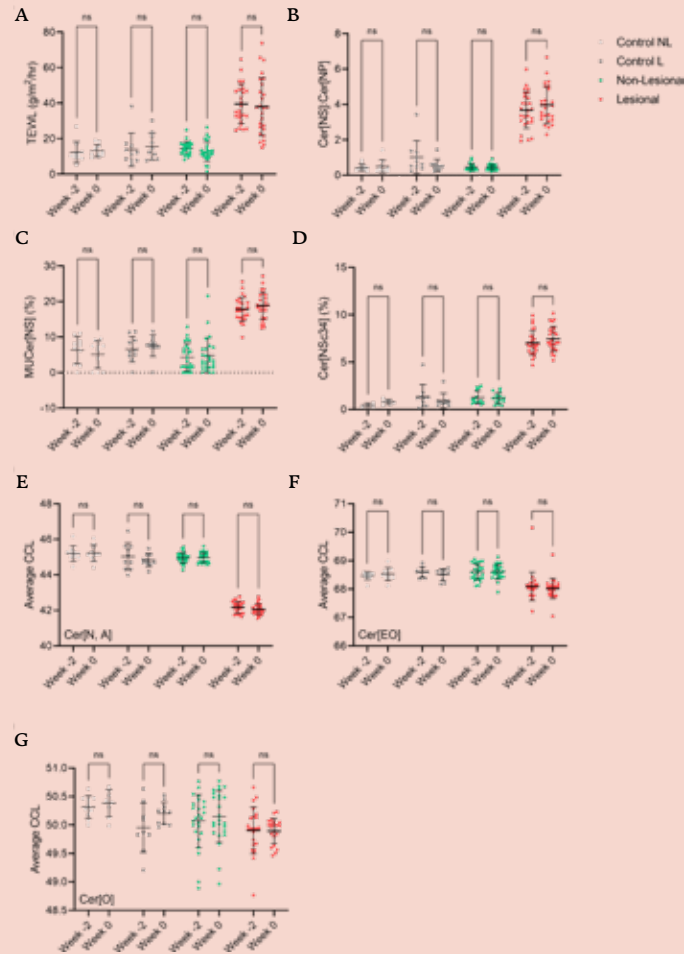


**Figure s5** Stratification of the patient cohort based on PASI scores at baseline. Patients are assigned to the mild or moderate-to-severe group based on a PASI score of  $\leq 5$  or  $\geq 10$ , respectively. Comparisons of disease severity based on PASI score (A) or Lesion Severity Score (B) showing target lesion severity is scored similarly despite a higher overall PASI in the moderate-to-severe group. Additionally, the ceramide characteristics in lesional skin are shown with the total ceramides after correction with the squamescan value (C), relative ceramide subclass profile (D), abundance of CER[NS C34] of total CER[NS] (E), ratio between the abundance of CER[NS] and CER[NP] (F), the fraction of monounsaturated ceramides in CER[NS] (G) and the average ceramide chain length (H) of CER[N, A], CER[EO] and CER[O], respectively. Statistical testing is performed with a two-way ANOVA, “NS” indicated  $p > 0.05$  and is not shown for panel (D).

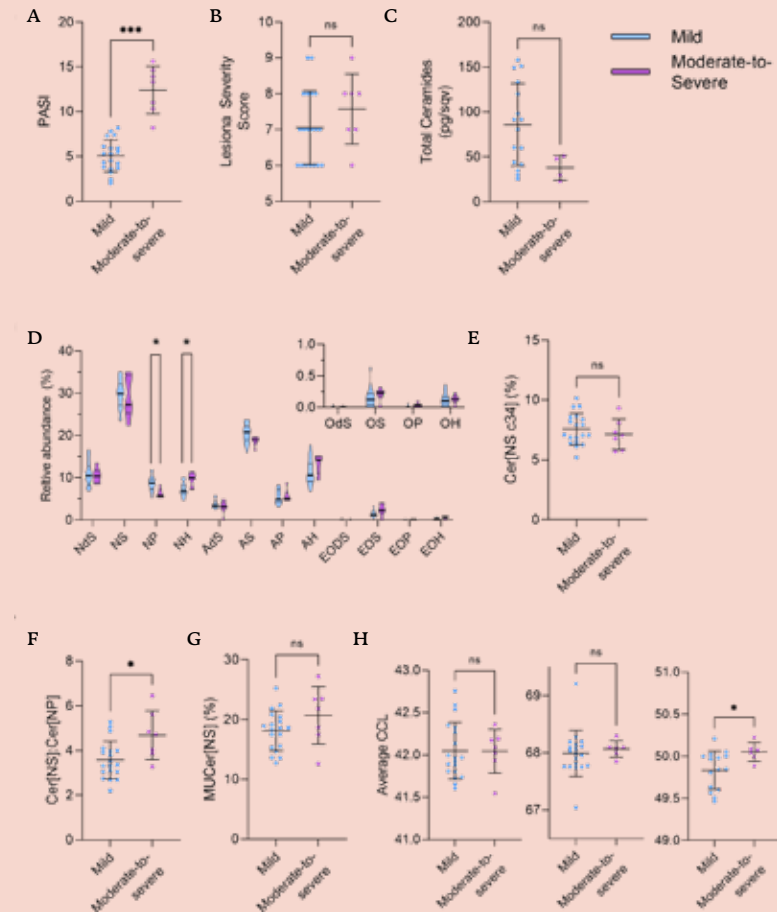


**Figure s6** Principal component analysis of the ceramide profile at baseline of mild and moderate-to-severe patients as defined by a PASI score of  $\leq 5$  or  $\geq 10$ , respectively. The high degree of overlap between the two severity groups indicates the ceramide profile is similar.

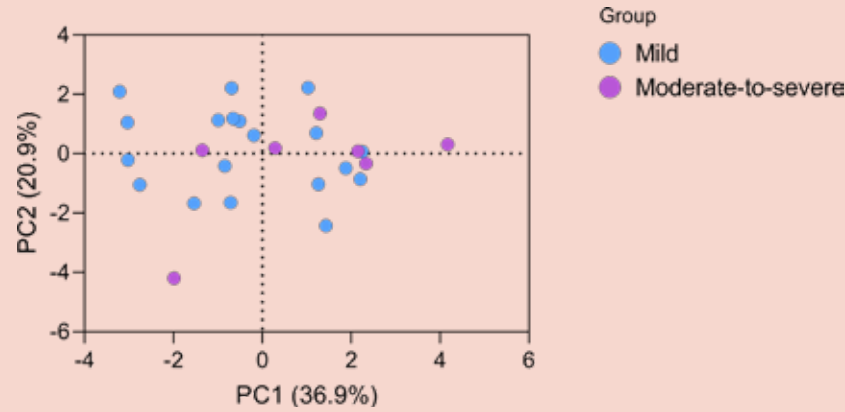


**Figure s7** The ceramide chain length per subclass indicates that the decrease in Ceramide Chain Length (CCL) in lesional skin is seen throughout all subclasses, except for CER[EOP], CER[EOH] and CER[OH]. Of note, decreased CCLs in lesional skin are maintained when ceramides of  $\leq 34$  carbons in lengths are excluded from the analysis (data not shown).

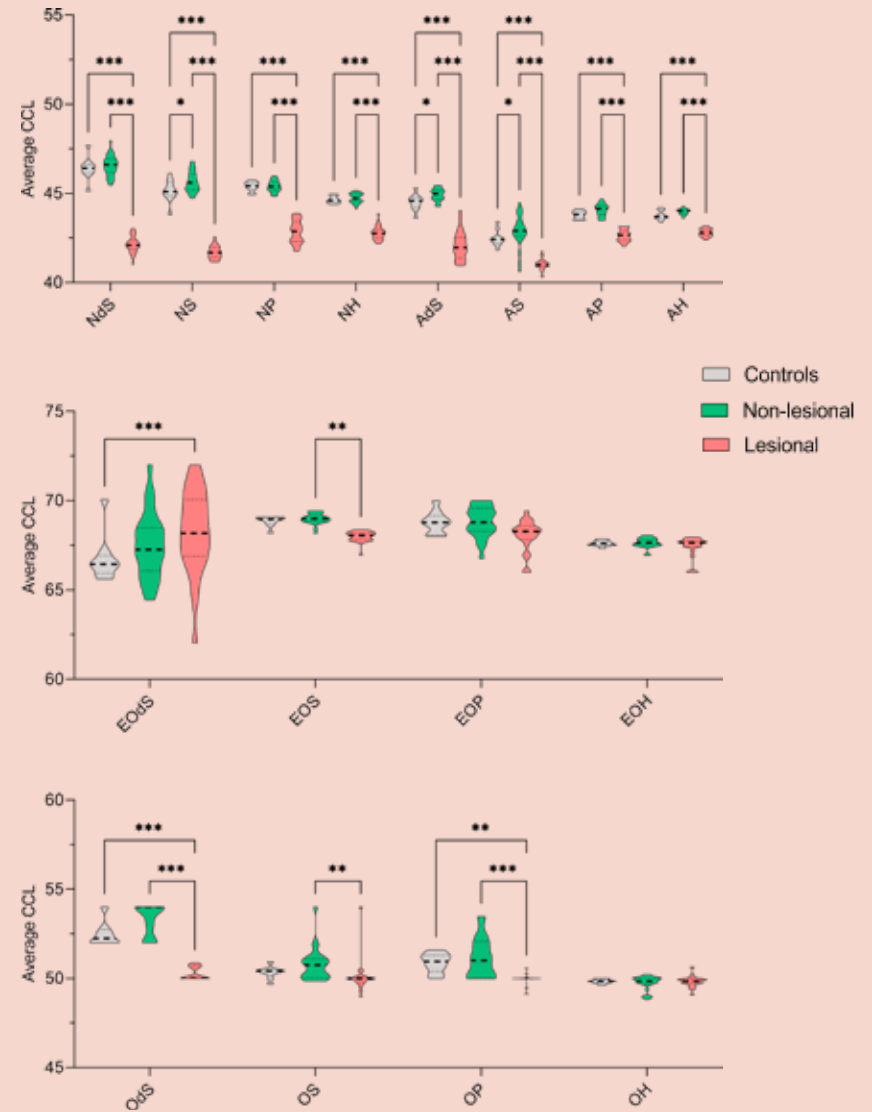


**Figure s8** The Psoriasis Area and Severity Index (PASI) score over time in the guselkumab and placebo group.

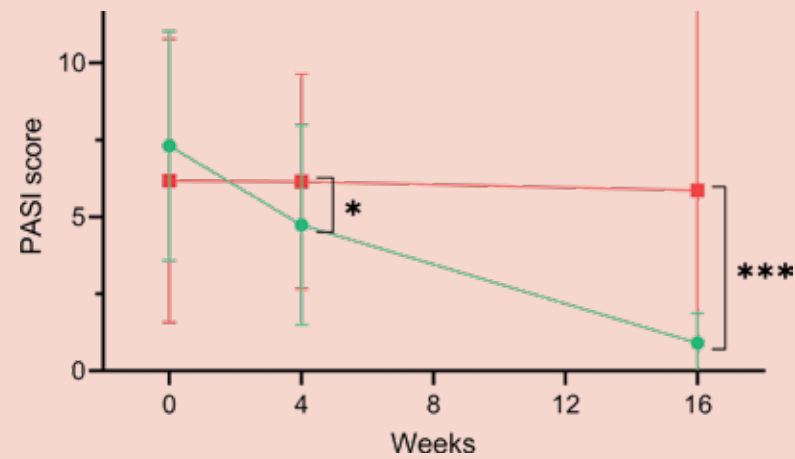
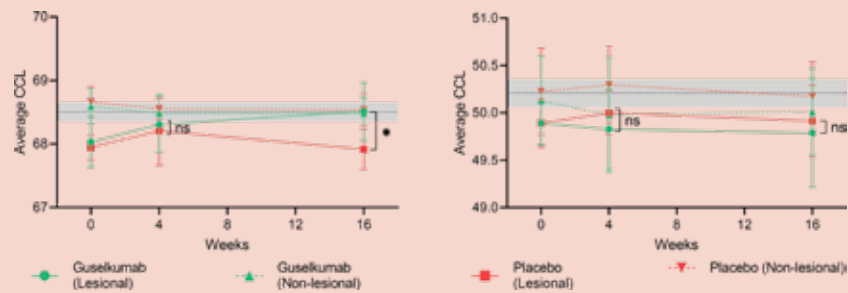


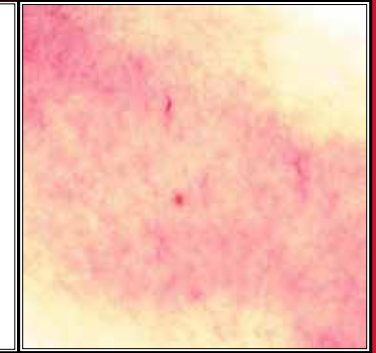
**Figure s9** Ceramide chain length (CCL) over time during the treatment period. No significant differences are observed in the CCL of the CER[EO] fraction (left) nor CER[O] fraction (right) during treatment with guselkumab and placebo.



## CHAPTER 8

### IMPROVED ORGANOTYPIC SKIN MODEL WITH REDUCED QUANTITY OF MONOUNSATURATED CERAMIDES BY INHIBITING STEAROYL-COA DESATURASE-1

Adapted from: Biochimica et Biophysica Acta-Molecular and Cell Biology of Lipids (1866 (2021), 158885, DOI: 10.1016/j.bbaliip.2021.158885)



Richard W. J. Helder,<sup>1</sup> Jannik Rousel,<sup>1,2</sup> Walter A. Boiten,<sup>1</sup> Gerrit S. Gooris,<sup>1</sup> Andreea Nadaban,<sup>1</sup> Abdoelwaheb El Ghalbzouri,<sup>3</sup> and Joke A. Bouwstra<sup>1</sup>

1. Leiden Academic Centre for Drug Research, Leiden University, Leiden, NL / 2. Centre for Human Drug Research, Leiden, NL / 3. Department of Dermatology, Leiden University Medical Center, Leiden, NL

## Abstract

**INTRODUCTION:** Full thickness models (FTM) are 3D *in vitro* skin cultures that resemble the native human skin (NHS) to a great extent. However, the barrier function of these skin models is reduced. The skin barrier is located in the stratum corneum (SC) and consists of corneocytes embedded in a lipid matrix. In this matrix, deviations in the composition of the FTMS lipid matrix may contribute to the impaired skin barrier compared to NHS. One of the most abundant changes in lipid composition is an increase in mono-unsaturated lipids for which Stearoyl-CoA desaturase-1 (SCD-1) might be responsible. In here, we investigate if SCD-1 inhibition results in an improved barrier function of FTMS.

**METHODS:** FTMS were cultured with and without SCD-1 antagonist supplementation to the culturing medium. These FTMS were subsequently assessed on all major aspects, including epidermal homeostasis, lipid composition, lipid organization, and barrier functionality.

**RESULTS:** SCD-1 inhibition successfully reduced the amount of monounsaturated lipids. However, the reduced monounsaturated lipid content did not result in changes to the lipid organization or barrier function of the FTMS.

**CONCLUSION:** This study demonstrates that inhibition of SCD-1 activity is an effective approach for decreasing the monounsaturated lipid content in the SC of our FTM models. Combining SCD-1 inhibition with other targeted approaches might be a valuable approach for optimizing the FTMS.

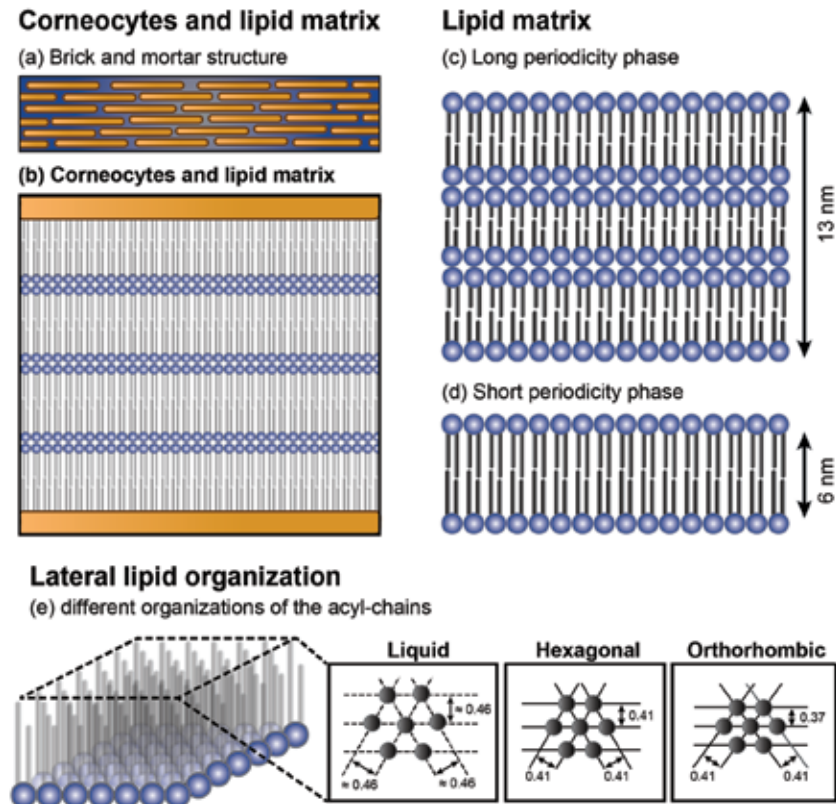
## Introduction

Full thickness skin models (FTMS) are *in vitro* skin models that mimic native human skin (NHS) in many aspects and serve as a valuable tool to unravel biological processes in healthy and diseased skin.<sup>1</sup> In addition, FTMS serve as an excellent tool for the prediction of toxicity screenings and diffusion of novel compounds as an alternative for animal experiments.<sup>1-4</sup> However, the most important drawback is the reduced barrier function of the FTMS.<sup>5-8</sup> This limits the use of FTMS in the prediction of novel pharmaceutical compounds on their diffusion across the skin. Therefore, there is an urgent need for a new generation of FTMS that mimic the NHS barrier properties more closely. To improve the skin barrier of the FTMS, normalization of the stratum corneum (SC) lipid composition is considered to be crucial.<sup>9-11</sup>

The outside-in NHS barrier is primarily located in the SC, which consists of corneocytes embedded in a lipid matrix.<sup>12</sup> In this lipid matrix, three main lipid classes are present: cholesterol, free fatty acids (FFAS), and ceramides (CERS). The ceramides are the most complex of these lipids and over 16 subclasses have been identified.<sup>13-15</sup> In addition to different subclasses, each subclass has a broad distribution in their total chain length as well (combined sphingoid base and acyl chain length).<sup>16-17</sup> Although less variety in subclasses, the FFAS also have a broad distribution of chain length. Together with cholesterol, these lipids can organize themselves into two lamellar phases, the short periodicity phase (SPP) with a repeat distance of around 6 nm and the long periodicity phase (LPP) with a repeat distance of approximately 13 nm.<sup>18-19</sup> Within the lamellae, the lipids can adopt a very dense (orthorhombic), a less dense (hexagonal) packing or even a fluid phase. The lipid organization is depicted schematically in figure 1 and the molecular structure of the various ceramide subclasses are described in chapter 6, figure 1.

Differences in lipid composition and organization have been reported between the FTMS and NHS. One of the most prevalent differences is a high level of monounsaturated ceramides (MUCERS) and monounsaturated FFAS (MUFFAS). Besides this major difference, other differences are observed as well: 1) an altered ceramide subclass profile, 2) a strong reduction in the FFA amount, 3) a reduction in the mean chain length (MCL) of the ceramides and FFAS.<sup>5,16,21</sup> These changes in lipid composition lead to changes in the lipid organization. The most predominant ones include a shorter repeat distance of the LPP, the absence of the SPP and a less dense lipid packing: lipids adopt mainly a less dense hexagonal packing. Ultimately, these changes contribute to a reduced barrier function in the FTMS.<sup>16,20</sup>

**Figure 1** Schematic presentation of the organization in the lipid matrix between corneocytes. The SC is organized in a brick-and-mortar structure (A), between the corneocytes lipid lamellae are present (B). Two different lamellar phases are identified; the long periodicity phase (LPP) (C), and the short periodicity phase (SPP) (D). The hydrocarbon chains can assemble in different types of packing referred to as the lateral organization (E), which is either liquid (loose packing), hexagonal (dense packing) or orthorhombic (very dense packing).



The aim in this study was to improve the lipid composition by reducing the level of MUCERS and MUFFAS in our in-house FTM model. This in-house model displays the alteration in lipid composition and organization as described above, such as an increase in monounsaturations of the lipids.<sup>16</sup> A possible underlying factor for this is the enzyme stearoyl-CoA desaturase-1 (SCD-1).

Studies have reported that this enzyme is overexpressed and is also present in the suprabasal layers, whereas in NHS, SCD-1 is mainly expressed in the basal layer.<sup>16,21</sup>

SCD-1 serves as a catalyst for creating a double bond at the  $\Delta 9$  carbon in saturated FFAs (C16:0 and C18:0) to convert them in their monounsaturated counterparts (C16:1, and C18:1), respectively.<sup>22</sup> Subsequently, these saturated FFAs (SAFFAS) and MUFFAS are elongated by a group of elongases referred to as ELOVLs and finally incorporated into the SC lipid matrix.<sup>23</sup> Next, these (MU)FFAS are also building blocks for ceramides and are linked to a sphingoid base by the group of ceramide synthases leading to the more complex ceramide subclasses.<sup>24-26</sup> However, this means that a higher quantity of both ceramides and FFAs that contain monounsaturated bonds in their acyl chains are synthesized. These MUCERS and MUFFAS are key factors that contribute to the formation of a less dense hexagonal organization.<sup>9</sup> To reduce the level of monounsaturations in the SC lipids, the culture medium of our in-house developed FTM was supplemented with an SCD-1 inhibitor to normalize the lipid monounsaturations.

After generation of FTMS, the lipid composition was analyzed and a drastic reduction in the amount of MUCERS and MUFFAS were observed. This demonstrates that the SCD-1 inhibitor successfully inhibited the SCD-1 activity. In addition, changes were observed in the lipid synthesis, such as the increase in CER[DS] and the overall reduction in CER[EO] subclasses.

## Materials and methods

### PRIMARY CELL ISOLATION AND MONOLAYER CULTURES

To study the effects of SCD-1 inhibition, all studies were performed in triplicate using keratinocytes from three female donors (3 Caucasian female skin donors aged between 18-26 years old).

Within 24 hours of plastic surgery, the skin was processed. After cleaning the skin by removing the excess of subcutaneous fat tissue, the skin was stretched on styrofoam and the skin surface was cleaned with demineralized H<sub>2</sub>O, ethanol and again with demineralized H<sub>2</sub>O prior to dermatoming to a thickness of 400  $\mu$ m. Subsequently, the skin was placed overnight in 2.4 U/ml dispase II (Roche, Almere, the Netherlands). After overnight incubation, the epidermis and dermis were separated and further used for the keratinocyte and fibroblast isolation as described elsewhere.<sup>5</sup>

## GENERATION OF THE FULL THICKNESS SKIN MODELS

Prior to the SCD-1 study, two concentrations of SCD-1 inhibitor were tested: 45 nM and 450 nM. However, the 450 nM did not result in viable FTMS, therefore this study was performed with 45 nM as concentration for the SCD-1 inhibitor. Two out of three originating NHS keratinocyte donor samples were also used as a control in the following subsequent studies (liquid-chromatography-mass spectrometry (LC-MS), quantitative polymerase chain reaction (QPCR), small angle X-ray diffraction (SAXD)). Due to limit of sample material the third control was from an additional donor. Using each donor, the FTMS were generated in triplicate. First, the dermal compartment was prepared as reported in detail previously.<sup>5,27</sup> To this end, rattail-collagen was populated with fibroblasts ( $4 \times 10^4$  fibroblasts/ml) as described before.<sup>5</sup> After 7 days of culturing the dermal compartment, keratinocytes ( $2.5 \times 10^5$  cells) were seeded onto each dermal compartment and subsequently cultured for another four days under submerged conditions. Then the FTMS were lifted to the air-liquid interface and the SCD-1 inhibitor was supplemented to the culture medium. The FTM conditions were: 1) FTM<sub>CONTROL</sub>, that contained normal culture medium as described elsewhere,<sup>20</sup> 2) FTM<sub>SCD-1</sub> that contained in addition to the normal culture medium, 45 nM of SCD-1 inhibitor AB142089 (Sigma-Aldrich, Zwijndrecht, the Netherlands) dissolved in 0.05% DMSO of the culture medium (v/v), 3) FTM<sub>DMSO</sub> supplemented with 0.05% DMSO in the medium was cultured to serve as a second control. The results obtained in this study for FTM<sub>DMSO</sub> and the FTM<sub>CONTROL</sub> were similar in all features, therefore, the FTM<sub>DMSO</sub> are not shown in the result section. The FTMS were cultured air exposed for a period of 14-17 days and medium was refreshed twice a week with freshly prepared supplements.<sup>27,28</sup>

## IMMUNO-HISTOCHEMICAL STAINING AND VISUALIZATION

After harvesting the FTMS, tissue samples were fixed in biopsy pads soaked in 4% paraformaldehyde (Pharma B.V., Oss, the Netherlands) for 24 hours. Subsequently, the samples were dehydrated in a series of ethanol solutions before embedding in paraffin. Sections of the sample were cut at 5 µm and collected on SuperFrost®Plus slides (VWR international B.V., Leuven, Belgium). This was left overnight at 60 °C in an oven. After rehydration, heat-induced antigen retrieval was performed in a citrate buffer in the waterbath or autoclave depending on the primary antibody (see Supplemental Table 1). After cooling to room temperature, the sections were blocked with normal human

serum (2%, Sanquin, Leiden, The Netherlands). Subsequently, the blocking was removed and primary antibodies were added. Then the streptavidin-biotin-peroxidase complex (GE Healthcare, Buckinghamshire, United Kingdom) was placed on the sections. Subsequently, the staining was visualized by using 3-amino-9-ethylcarbazole (AEC, Sigma Aldrich Chemie, Zwijndrecht, The Netherlands), and counter staining with Haematoxylin (Klinipath B.V., Duiven, The Netherlands). The slides were sealed with Kaiser's glycerine (Boom B.V., Meppel, The Netherlands). Microscopic images were taken with a light microscope (Zeiss Axioplan 2, Zeiss, The Netherlands). The proliferation index was calculated for KI67 using the following method. A minimum of 100 cells at the basal layer were counted for four sections of each slide and the stained nuclei were divided by the total number of counted cells (e.g. 12 stained from a total of 100 means 12% proliferation index). This was performed FTM of 3 donors.

## STRATUM CORNEUM ISOLATION

Isolated SC was used for the LC-MS, SAXD, FTIR and TEWL measurements. SC isolation was performed by placing dermatomed skin (in case of NHS) or the FTMS on a cotton pad soaked in an 0.1% (w/v) trypsin (Sigma Aldrich Chemie, Zwijndrecht, The Netherlands) in PBS solution. 0.1M PBS (pH 7.4) was used and consisted of NaCl (8.13g), Na<sub>2</sub>HPO<sub>4</sub> (2.87g), KHPO<sub>4</sub> (0.20g) and KCl (0.19g) in 1L of MilliQ. The samples were placed in the fridge at 4 °C overnight, subsequently, the skin was placed in an oven for 37 °C for 1 hour. This allowed the SC to separate from the epidermis. The SC was washed after separation with 0.1% (w/v) trypsin inhibitor (Sigma Aldrich Chemie, Zwijndrecht, The Netherlands) in PBS and subsequently washed twice with MILLIQ. After washing, the SC was air dried and stored in a dark environment under argon and over silica prior to use.

## LIPID EXTRACTION FROM ISOLATED STRATUM CORNEUM

Extraction of the SC lipids was performed using an adapted Blight and Dyer method. This method has been described elsewhere.<sup>14</sup> After the extraction, the samples were stored in a glass vial under argon at 4 °C until ceramide and FFA analysis was performed. For NHS, the SC originated from 3 Caucasian female skin donors aged 18-26. Furthermore, for each of the ceramide or FFA runs, a Quality Control sample that consisted out of multiple NHS samples pooled together was added to ensure reproducibility between and during the run.



## CERAMIDE ANALYSIS USING LIQUID CHROMATOGRAPHY-MASS SPECTROMETRY

Ceramide analysis was performed as reported elsewhere.<sup>14</sup> In short, the solvent in the samples was evaporated and reconstituted in 95:2<sub>1/2</sub>:2<sub>1/2</sub> (v/v/v) heptane:chloroform:methanol to a concentration of 0.3 mg/ml. An injection standard, deuterated CER[NS] (C<sub>24</sub> deuterated; C<sub>18</sub> protonated, Evonik Industries, Essen, Germany for abbreviations see Supplemental Figure S1) was added. From the reconstituted sample, 5 µl was injected into the UPLC. The UPLC-MS setup consisted of an Acquity UPLC H-class (Waters, Milford, MA, USA) coupled to an XEVO TQ-S mass spectrometer (waters, Milford, MA, USA) with an atmospheric pressure chemical ionization (APCI) chamber. Detection occurred in full scan m/z between 350 and 1200 atmospheric mass units (AMU) in positive ion mode. Separation of ceramides was performed on a PVA-SIL column (5 µm particles size, 100x2.1 mm I.D., YMC, Kyoto, Japan).

Data analysis was performed by Waters Masslynx 4.1 and area under the curve (AUC) was used for the detection of the ceramide species. 15 ceramide subclasses were analyzed. For the ceramide class containing CER[N] non-hydroxy and CER[A] α-hydroxy (belonging to the CER[NON-EO]), the subclasses CER[NDS], CER[NS], CER[NP], CER[NH], CER[ADS], CER[AS], CER[AP], and CER[AH] were quantified. For the ceramide class containing the linoleic acid esterified to an ω-hydroxy (belonging to the CER[EO]), the subclasses CER[EODS], CER[EOS], CER[EOP], and CER[EOH] were analyzed. For the CER class containing the ω-hydroxy (CER[O]) the subclasses CER[OS], CER[OP], and CER[OH] were examined. The subclasses classification and abbreviations are explained in Supplemental Figure S1. The abbreviations are according to Motta *et al.* (1993).<sup>13</sup> AUCs were corrected according to the processing method.<sup>14</sup> After data corrections, areas were converted to nmol and plotted in absolute values (ceramide in nmol / mg SC) or ceramide mol (%).

## FATTY ACID ANALYSIS USING LIQUID CHROMATOGRAPHY-MASS SPECTROMETRY

Samples were evaporated under a gentle stream of nitrogen and reconstituted in isopropanol to a concentration of 0.75 mg/ml. After adding the deuterated C<sub>24</sub> (C<sub>24</sub>D<sub>47</sub>) internal standard (purchased at Sigma-Aldrich Zwijndrecht, The Netherlands), 2 µl was injected into a UPLC. UPLC-MS setup consisted of a Waters Acquity UPLC H-class system (Waters, Milford, Massachusetts, Unites States) coupled to a XEVO TQ-S mass spectrometer (waters, Milford,

Massachusetts, Unites States) connected to an atmospheric pressure chemical ionization (APCI) chamber (probe temperature: 425°C, discharge current 3 µA). Detection occurred in negative ion mode measuring full scan m/z between 200 and 550 AMU. FFAS were separated using a Purospher Star LiChroCART reverse phase column (3 µm particle size, 55x2 mm i.d., Merck, Darmstadt, Germany) between 0-6 min with a flow rate of 0.5 ml/min. The gradient started at acetonitrile/water/chloroform/acetic acid (90:10:2:0.005(v/v/v/v)) and shifted to methanol/heptane/chloroform/acetic acid (90:10:2:0.005). Data analysis was performed by Waters Masslynx 4.1 and the area under the curve (AUC) was calculated. FFA analysis included the following: monounsaturated FFA: (C<sub>20:1</sub>, C<sub>22:1</sub>, and C<sub>24:1</sub>) and saturated FFAS: (C<sub>20</sub>, C<sub>22</sub>, C<sub>23</sub>, C<sub>24</sub>, C<sub>25</sub>, C<sub>26</sub>, C<sub>28</sub>, and C<sub>30</sub>). As chloroform was manufacturer contaminated with FFA C<sub>16</sub> and C<sub>18</sub>, these FFA could not be determined accurately and were therefore excluded in the analysis. Subsequently the AUCs were corrected for the internal standard (C<sub>24</sub>D<sub>47</sub>) and corrected for response using FFA standards calibration curves for: C<sub>20:0</sub>, C<sub>20:1</sub>, C<sub>22:0</sub>, C<sub>22:1</sub>, C<sub>23:0</sub>, C<sub>24:0</sub>, C<sub>24:1</sub>, C<sub>25:0</sub>, C<sub>26:0</sub>, C<sub>28:0</sub>, and C<sub>30:0</sub> (Sigma-Aldrich, Zwijndrecht, The Netherlands).

## QUANTITATIVE POLYMERASE CHAIN REACTION

Isolation of RNA was performed with the Favorprep Tissue total RNA mini kit (Bio-connect B.V., Huissen, The Netherlands). The concentration and purity of the RNA was determined with the NanoDrop One (Thermo Scientific). cDNA was synthesized using C1000 touch thermal cycler (Biorad). The cDNA mixture contained 4 µL of 5x iScript reaction mix, 1 µL iScript reverse transcriptase, and 500 ng cDNA in 15 µL RNA-free H<sub>2</sub>O. The run was performed by a CFX384 real time system (Biorad) and each well contained 3.5 µL SYBR green, 2.275 µL RNA-free H<sub>2</sub>O, 0.875 cDNA, and 0.35 µL of Primer work solution (10 µM forward and reverse primer in RNA-free H<sub>2</sub>O). The following primers were used: SREBP-1C, ACC1, FAS, ELOVL1, ELOVL4, SCD-1, ABCA1, CERS2, CERS3, CERS4, CERS5, CERS6, DES1, and DES2. The forward and reverse sequence of these primers are listed in Supplemental Table 2.

## LAMELLAR ORGANIZATION BY SMALL ANGLE X-RAY DIFFRACTION ANALYSIS

X-ray diffraction studies were performed at BM26B at the European Synchrotron Radiation Facility (ESRF, Grenoble, France). The setup of this analysis is described elsewhere.<sup>9</sup> Prior to measurement, isolated SC sheets were

equilibrated for 24 hours in a humidity chamber at room temperature using 27% NABR solution (w/v). The Pilatus 1M detector was calibrated using AGBR and cholesterol. Measurements were performed at room temperature (24 °C) in 2x90 sec and dual images were merged in the sample processing. The distance between the sample and detector was 2.1 m. After acquiring the scattering profile, the 2D images were converted to a 1D image by converting the Cartesian (x,y) to polar (r,θ) coordinates by integrating over θ. A diffraction pattern attributed to a lamellar phase is characterised by diffraction peaks at equidistant position from each other. From the position of these peaks the repeat distance or spacing (D) is calculated by  $d = 2\pi/q$ . In this formula, the scattering vector  $q = 4\pi \sin \theta/\lambda$ , where θ is the scattering angle, and λ, the X-ray wavelength, was 0.1033 nm.

#### LATERAL ORGANIZATION BY FOURIER TRANSFORMED INFRARED SPECTROSCOPY ANALYSIS

Fourier transformed infrared spectroscopy (FTIR) measurements were performed on a Varian 670-IR spectrometer (Varian Inc., Santa Clara, CA) equipped with a broad band Mercury-Cadmium-Telluride (MCT) detector. Before the measurement, SC was hydrated for 24 hours in a humidity chamber containing deuterated water. After hydration, the SC was placed between two AGBR windows and was subsequently heated to 24 °C. The temperature gradient was 0.25 °C/min and spectra were collected with 2 cm<sup>-1</sup> resolution. In the acquired spectra, the rocking area (710-740 cm<sup>-1</sup>) was analyzed by the Varian Resolution Pro software (v4.1).

#### TRANS EPIDERMAL WATER LOSS

Trans epidermal water loss (TEWL) was measured using isolated SC from NHS and the FTMS. The SC was placed on a polycarbonate filter (Diachema, Munich, Germany) and mounted in a Permeagor inline diffusion cell (Bethlehem, Pennsylvania, United States). The donor compartment was empty and the acceptor compartment was filled with milliQ water to hydrate the sample. After 15 min hydration, the TEWL was measured by an evaporimeter (Aqua Flux AF200, Biox Systems Ltd, London, UK) connected to a modified nozzle to close the donor compartment. Measurements were performed each 10 sec for a period of 15 minutes. The data points used in the graph are the average of the final three minutes (28-30 minutes) when the TEWL was stabilized.

#### STATISTICAL ANALYSIS

Statistical analysis was performed in Graphpad 7 (Graphpad Software, San Diego, California, United States). For statistical analysis, an unpaired t-test was performed between the FTM<sub>CONTROL</sub> and FTM<sub>SCD-1</sub>. To compare the FTM<sub>CONTROL</sub> against NHS, an unpaired t-test was used. Significant differences are indicated by \* for p<0.05, - for p<0.01, and -\* for p<0.001.

## Results

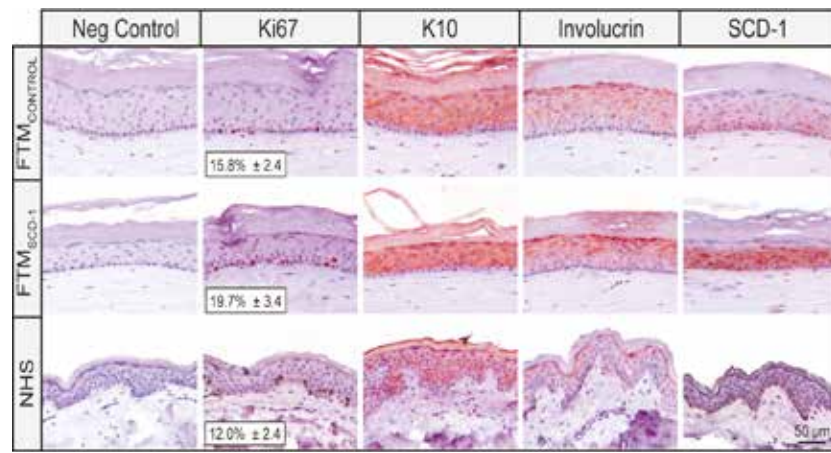
#### SUPPLEMENTATION OF THE SCD-1 INHIBITOR LED TO MINOR CHANGES IN THE EPIDERMAL HOMEOSTASIS BUT DRASTICALLY INCREASED SCD-1 PROTEIN EXPRESSION

Before the initial study on FTMS, a small pilot was performed to determine the effects of the SCD-1 inhibitor in two different concentrations; 45 nM and 450 nM. The concentration of 45 nM is based on the reported IC<sub>50</sub> of AB142089, which was 4.5 nM.<sup>21</sup> In addition to a 10 times increase, that would already demonstrate an effect without causing toxicity to the FTMS, we also wanted to include a higher concentration of the inhibitor (450 nM). This was initiated due to the high percentage of monounsaturated lipids in the lipids of FTMS and to determine whether it would be more beneficial. However, the inhibitor concentration of 450 nM did not lead to a viable FTM (Supplemental Figure S2). Therefore, the study was performed with inhibitor SCD-1 concentration of 45 nM (referred to as the FTM<sub>SCD-1</sub>), which was supplemented to the culture medium.

After culturing, FTMS and NHS were investigated on basal cell proliferation, early, and late differentiation by several epidermal homeostasis proteins markers (figure 2). Basal cell proliferation was examined by a KI67 protein staining. As shown, no significant changes in KI67 expression was observed, irrespective the condition tested. Next, the early differentiation was investigated by staining for keratin 10 (K10). K10, which stains the suprabasal cell layers, showed no changes in expression, indicating a normal execution of the early differentiation program. Next the late differentiation protein involucrin was stained. This protein was similarly expressed in FTM<sub>CONTROL</sub> and FTM<sub>SCD-1</sub> and equally present in the stratum granulosum as well as the stratum spinosum, whereas in NHS, involucrin was restricted to the stratum granulosum. When examining the SCD-1 expression, a significant difference

was observed: The  $FTM_{SCD-1}$  displayed a drastic increase in SCD-1 expression compared to  $FTM_{CONTROL}$ , but both displayed expression throughout the epidermis. In NHS, SCD-1 expression was less prominently present and more restricted to the basal layer.

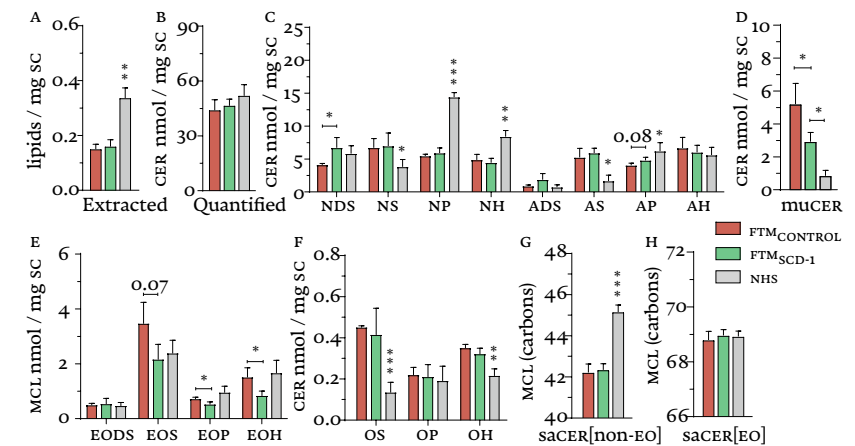
**Figure 2** Different epidermal homeostasis markers and SCD-1 were examined in FTMS and NHS. Expression of protein markers in  $FTM_{CONTROL}$ ,  $FTM_{SCD-1}$  and NHS from left to right: negative control, proliferation (K167), early differentiation (K10), late differentiation (involucrin), and lipid monounsaturase enzyme SCD-1. K167 proliferation index determination. Scale bar: 50  $\mu$ m.



### SCD-1 INHIBITION LED TO REDUCTION OF MONOUNSATURATED CERAMIDES

To determine whether SCD-1 inhibition led to changes in the SC lipid composition, the ceramide profile in FTMS and NHS was examined. First, the extracted amount of SC lipids was determined (figure 3A). The amount of extracted lipids was similar between FTMS, but was significantly increased in NHS compared to the FTMS. After the lipid extraction, the peaks of all ceramide subclasses (SACER+MUCER) in the LC-MS spectrum were integrated, processed and converted to ceramide amounts in nmol/mg SC (figure 3B). No differences in the total amount of ceramides in nmol/mg SC between the FTMS and NHS were observed. Next, the absolute amounts of the ceramide subclasses were analyzed.

**Figure 3** SCD-1 inhibition alters lipid composition by reducing the monounsaturase, reducing the CER[EO] subclasses, and by increasing the CER[DS] fraction. During sample preparation, the amount of extracted lipids was determined (A). The total amount of ceramides (SACER+MUCER) in nmol/mg SC (B). The subclasses of the CER[NON-EO] (SACER+MUCER) (C). The total amount of MUCER[NON-EO] (MUCERS in nmol/mg SC) (D). Subclasses in CER[EO] (SACER+MUCER) (E). Subclasses in CER[O] (SACER+MUCER) (F). The mean chain lengths for SACER[NON-EO] (G) and CER[EO] main peak (SACER[EO-18:2]+MUCER[EO-18:1]) (H).



### QUANTIFIED CERAMIDE VSUBCLASS COMPOSITION

The individual subclasses of CER[NON-EO], CER[EO], and CER[O] were plotted in absolute amounts (figure 3C, 3E, 3F, respectively). Individual analysis of the quantified subclasses of CER[NON-EO] revealed a similar subclass profile after SCD-1 inhibition compared to  $FTM_{CONTROL}$ , except for an increased amount of CER[DS] subclass in  $FTM_{SCD-1}$ . Compared to NHS, in both  $FTM_{CONTROL}$  and  $FTM_{SCD-1}$  an altered amount of CER[NS], CER[AS], CER[NH], CER[NP] and CER[NH] subclasses was observed. More drastic changes were observed when examining the amount of MUCERS after SCD-1 inhibition (figure 3D). This demonstrated that the SCD-1 inhibitor successfully reduced the amount of MUCERS to a level more closely to that in NHS.

In addition to the CER[NON-EO], the CER[EO] subclasses were also quantified (figure 3E). The total amount of CER[EO] was reduced in  $FTM_{SCD-1}$ , this was mainly caused by the reduction in CER[EOS] ( $p=0.07$ ) and a significant

reduction in CER[EOP] and CER[EOH] subclasses. To study the underlying factor of this reduction, the individual monounsaturated and saturated subclasses of CER[EO] with either oleic (C18:1) or linoleic (C18:2) acid chain were analyzed (Supplemental Figure S3). This displayed that it was not one individual CER[EO] subset that was reduced, but all subsets were reduced. This reduction was most prevalent in the CER[EOS], where the combined amount of MUCER[EO-18:1]/ SACER[EO-18:2] was decreased (Supplemental Figure S3A,  $p=0.06$ ). Similar results were observed for the MUCER[EO-18:2] (Supplemental Figure S3B,  $p=0.11$ ) and SACER[EO-18:1] (Supplemental Figure S3C,  $p=0.07$ ).

Next, to determine whether the decrease in amount of CER[EO] was due to a change in the CER[O] content as these have a common synthetic pathway, the amount of CER[O] (SACER+MUCER) was determined (figure 3F). The amount of CER[O] was similar between the FTM conditions tested. However, when studying the SACER[O] and MUCER[O] composition separately (Supplemental Figure S4), an increase (but not significant) in subclasses of SACER[O] in the FTM<sub>SCD-1</sub> was observed more comparable to NHS, although NHS still has significantly higher amount of SACER[O].

Another important aspect for the barrier is the mean chain length (MCL) of the lipids. This was determined for both SACER[NON-EO] (figure 3g) and the main CER[EO] subclass (figure 2H) subclasses. Inhibition of SCD-1 did not have an impact on the MCL of the CER[NON-EO]; The MCL was still shorter compared to that of NHS.<sup>21,29</sup> The MCL of CER[EO] were comparable between the FTMS and NHS groups and did not change in the FTM<sub>SCD-1</sub> compared to FTM. In addition, to determine whether some ceramide chain lengths were more abundantly present in FTM<sub>SCD-1</sub> than in FTM, the chain length distribution was determined in absolute and relative amounts (Supplemental Figure S5). The absolute chain length distribution displayed some minor but significant differences between the FTM conditions for CER[NON-EO] subclasses. The amount of ceramides with a chain length of C36, C38, C44 and C46 were increased in FTM<sub>SCD-1</sub> compared to FTM<sub>CONTROL</sub>. When comparing the ceramide chain length profile of the FTMS to NHS, there is still a large amount of ceramides of <C42 present in FTMS, where in NHS most ceramides contain >C42. Next, the absolute CER[EO] chain length distribution was investigated. For most of the chain lengths (with the exception of C68, and C74) the chain length distribution of CER[EO] in FTM<sub>SCD-1</sub> mimicked closely the distribution in NHS. However, this was mainly due to the decreased total amount of CER[EO] in FTM<sub>SCD-1</sub>.

When examining the relative chain length distribution, hardly no difference in chain length distribution was present between FTM<sub>SCD-1</sub> and FTM<sub>CONTROL</sub>.

### RELATIVE CERAMIDE SUBCLASS COMPOSITION

In order to relate changes in lipid composition to lipid organization, relative amounts of ceramide subclasses are important. The composition of the relative amounts of CER[NON-EO] and CER[EO] are reported in Supplemental Figure S6 and S7, respectively. Briefly, the ceramide changes reported in figure 2 became more prominent when determining the percentage of ceramide subclasses. Such as the higher percentage of CER[DS] subclass and a significant reduction of most of the CER[EO] subclasses: CER[EOS], [EOH], and [EOP]. Finally, when examining the level of CER[NON-EO] monounsaturated, the difference was more abundant ( $p=0.007$  vs  $p=0.05$ ) when the amount of Cers (%) was calculated for each FTM donor.

### SCD-1 INHIBITION REDUCED MONOUNSATURATED FATTY ACIDS IN FULL THICKNESS SKIN MODELS

The total amount of FFA in FTMS (SAFFA+MUFFA) did not change upon SCD-1 inhibition (figure 4A). Inhibition of SCD-1 did not change the chain length distribution of SAFFA either (figure 4B). The amount of all SAFFA irrespective of their chain length was strongly reduced compared to NHS as observed in earlier studies.<sup>21,29</sup> Next, the MUFFA profile was determined (figure 4C). Inhibition of SCD-1 reduced the amount of MUFFA C16:1, C18:1, and C24:1 in the FTM<sub>SCD-1</sub> compared to FTM<sub>CONTROL</sub>. This was also reflected in the total amount of MUFFA (figure 4D) and resulted in a reduced percentage of MUFFA in FTM<sub>SCD-1</sub> (figure 4E). This percentage indicates that the MUFFA content in FTMS were higher than in NHS and SCD-1 inhibition was a valuable approach to reduce the MUFFA content to mimic more closely the level in NHS. In addition, the FFA MCL was determined (figure 4F), SCD-1 inhibition did not affect the MCL.

In order to relate changes in FFA composition to lipid organization, percentages of FFA subclasses were also calculated (Supplemental Figure S8). These results demonstrate that especially long chain FFAs (>C24) were reduced and the short chain FFAs (<C22) were increased in FTMS compared to NHS. Although no significant effects were observed by SCD-1 inhibition on the MCL of the lipids, the MUFFA content was significantly reduced in the FTM<sub>SCD-1</sub>.

**Figure 4** SCD-1 inhibition led to a reduction in the amount of monounsaturated FFAs. Amount of FFA in nMol/mg SC (A). Absolute SAFFAS as function of chain length (B); Absolute amount of MUFFAs as function of chain length (C); Absolute amount of MUFA in nmol/mg SC (D); The percentage of MUFA (E); the SAFFA MCL (F). For statistical analysis, an unpaired t-test was performed between the FTMC<sub>CONTROL</sub> and FTMS<sub>SCD-1</sub>.

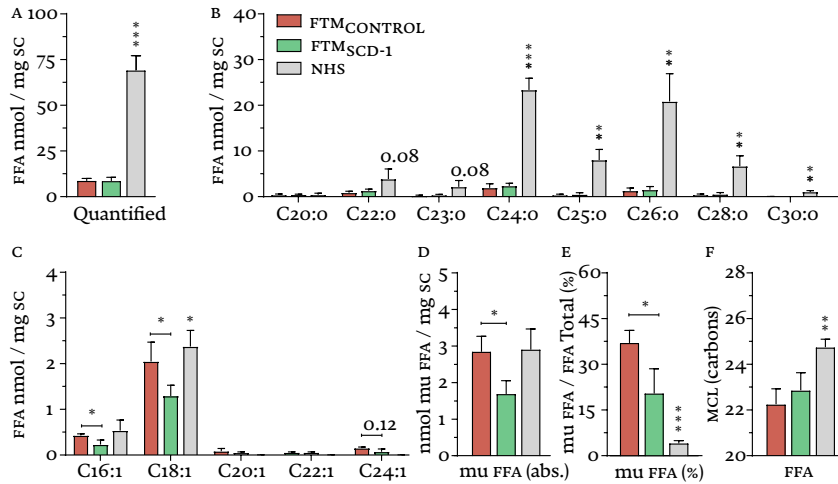
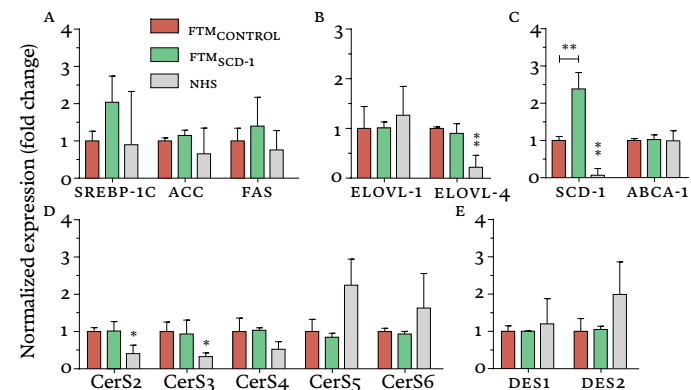


**Figure 5** Minor changes in the expression of genes involved in lipid synthesis, lipid processing, or ceramide synthesis after SCD-1 inhibition. Lipid synthesis genes investigated for FTMC<sub>CONTROL</sub>, FTMS<sub>SCD-1</sub>, and NHS. Lipid synthesis genes SREBP-1C, ACC, and FAS (A). Lipid elongases ELOVL-1 and ELOVL-4 (B). Lipid desaturase SCD-1 and LXR downstream target ABCA1 (C). Ceramide synthases 2-6 (D), and ceramide processing enzymes DES1 and DES2 (E).



## EFFECT OF THE SCD-1 INHIBITION ON THE LIPID SYNTHESIS GENES

To obtain information on the underlying factors that might explain the lipid composition changes after SCD-1 inhibition, several genes that are involved in lipid synthesis, elongation of FFA, and the ceramide synthesis were investigated (figure 5).

For the lipid processing genes (SREBP-1C, ACC, and FAS), no difference in gene expression between the FTMS<sub>SCD-1</sub> and FTMC<sub>CONTROL</sub> was observed. This was also observed for the lipid elongation genes ELOVL-1 and ELOVL-4 (figure 5B). However, an increased ELOVL-4 expression was observed in FTMS when compared to NHS. The next gene that was investigated was SCD-1 (figure 5C). This gene was drastically increased in the FTMS<sub>SCD-1</sub> when compared to the FTMC<sub>CONTROL</sub>. FTMC<sub>CONTROL</sub> already expressed significantly higher SCD-1 compared to NHS. To examine whether this increase was driven by LXR activation, ABCA1 gene expression (figure 5C) was investigated. However, no change in this gene was observed, excluding LXR activation as underlying factor. Next, the ceramide synthesis genes were investigated. No differences in expression of the Ceramide Synthases (CERS) were observed between FTMS (figure 5D). However, a higher expression for CERS2 and CERS3 were observed in FTMS compared to NHS. Finally, the gene expression of the enzymes that play a role in the head group synthesis were examined (figure 5E). DES1 and DES2 convert the CER[DS] subclass to CER[S] and CER[P], respectively. No differences were observed for these genes in FTMC<sub>CONTROL</sub> and FTMS<sub>SCD-1</sub>. However, DES2 was slightly decreased in FTMS compared to NHS.

## EFFECT OF SCD-1 INHIBITION ON THE LIPID ORGANIZATION AND TRANS-EPIDERMAL WATER LOSS

To investigate whether the changes in lipid composition affected lipid organization and subsequently SC barrier, the lipid organization and SC barrier function were examined (figure 6). For comparison all presented data were measured at 24 °C.

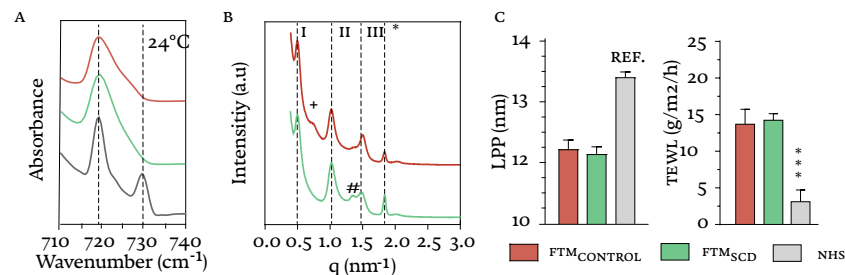
FTIR was used to determine the lateral organization of the lipids (figure 6A). We present the rocking vibrations at 24 °C, the temperature at which the TEWL measurement was performed (see below). The high peak intensity of the vibration located at 719 cm<sup>-1</sup> together with a small shoulder located at 730 cm<sup>-1</sup> in the FTIR spectrum of FTMC<sub>CONTROL</sub> indicates that most lipids adopt a hexagonal packing. A similar rocking pattern was observed for FTMS<sub>SCD-1</sub>.

In the spectrum of NHS, the intensity of the vibrations at  $730\text{ cm}^{-1}$  was much stronger indicating that a higher fraction of lipids adopt to an orthorhombic organization. This demonstrates a less dense lipid organization in the FTMS compared to that in NHS.

Next, we determined the lamellar organization using X-ray diffraction (figure 6B), the peak positions, indicated by *I*, *II* and *III* refer to the various orders of a lamellar phase with a repeat distance of 12.1 nm and 12.2 nm for the  $\text{FTM}_{\text{SCD-1}}$  and  $\text{FTM}_{\text{CONTROL}}$ , respectively. Besides this diffraction pattern two additional small peaks were observed in the SAXD profile, indicated by + and #.

To determine whether the changes in lipid organization led to a change in the barrier function of  $\text{FTM}_{\text{SCD-1}}$  compared to  $\text{FTM}_{\text{CONTROL}}$  the TEWL was measured for FTMS and NHS (figure 6C). No differences were observed after SCD-1 inhibition in the FTMS. However, the TEWL of NHS was approximately 4.5 times lower than that of the  $\text{FTM}_{\text{CONTROL}}$ .

**Figure 6** SCD-1 inhibition does not change lipid organizations or lipid permeation. The lipid organization was analyzed at  $24^\circ\text{C}$  for both the FTMS and NHS. The lateral organization is shown by displaying the rocking region (A) and the X-ray diffraction profiles for only FTMS with associated LPP repeat distances (B). Diffraction order of the LPP is indicated by *I*, *II*, and *III*. The cholesterol phase is indicated by the asterisk (\*). Unknown phases are indicated by + and #. The repeat distance is provided in the bar plot, with NHS as a reference.<sup>18</sup> The trans-epidermal water loss (TEWL) values are plotted in a barplot (c).



## Discussion

Our aim was to improve the lipid composition and organization in the FTM model by modulating the activity of SCD-1. By inhibiting SCD-1, several modifications were observed on the lipid composition. The most important

modification was the reduction in the amount of MUCERS and MUFFAS in the SC of the  $\text{FTM}_{\text{SCD-1}}$ , which resembles the lipid composition in NHS more closely. Another important finding was that the quantity of lipids remained similar after SCD-1 inhibition, which indicates that the total amount of lipids synthesized was unaffected by the SCD-1 inhibition and thus the synthesis of SACERS and SAFFAS was increased at the expense of the monounsaturated variant. In addition, several other lipid compositional changes were observed.

First, there was a strong decrease in the amount of CER[EO] observed in the  $\text{FTM}_{\text{SCD-1}}$ . Interestingly, when displaying the individual CER[EO] subsets, both MUCER[EO-18:2] and SACER[EO-18:1] are reduced, together with the main CER[EO] peak composed of two ceramide subclasses: MUCER[EO-18:1]/SACER[EO-18:2]. This reveals that not only the MUCER[EO] contributed to this reduction, but the CER[EO-18:1] as well. To understand why the CER[EO] was reduced, as a first possible underlying factor, enzymes responsible for the synthesis of CER[EO] were investigated. For this synthesis CERS3 and ELOVL-4 are required,<sup>30</sup> but the gene level for ELOVL4 and CERS3 did not change between  $\text{FTM}_{\text{CONTROL}}$  and  $\text{FTM}_{\text{SCD-1}}$ . A second possible factor is an increase in CER[O], since CER[EO] is a precursor for CER[O].<sup>31,32</sup> However, similar amounts of CER[O] were observed in the FTMS. A third explanation is a reduction in the amount of oleic acid (C18:1) for the synthesis of the CER[EO-18:1]. The amount of C18:1 was reduced in the  $\text{FTM}_{\text{SCD-1}}$  and therefore might be an underlying factor of the reduction of CER[EO-18:1]. When comparing FTMS to NHS, the amount of CER[EO] in FTMS is increased. Both CERS3 and ELOVL-4 are known to play a key role in the synthesis of ceramides,<sup>4,30</sup> the increased mRNA expression of these genes in FTMS might explain why the amount of CER[EO] is higher in FTMS.

Second, we observed an increase in the absolute amount of CER[DS] in the  $\text{FTM}_{\text{SCD-1}}$  compared to the  $\text{FTM}_{\text{CONTROL}}$ . This effect was even more prevalent when relative amounts of ceramides were calculated. To investigate whether the increase in the amount of CER[DS] was due to a reduction in the ceramide head group synthesis genes, the ceramide subclass synthases DES1 and DES2 that are responsible for the conversion of CER[DS] to CER[S] and CER[P], respectively, were investigated on gene level. As both FTMS had similar mRNA level for DES1 and DES2, there is no indication that these genes are an underlying factor of the shift towards more CER[DS]. However, when observing the morphology of the  $\text{FTM}_{\text{SCD-1}}$ , the epidermis does appear thinner. Perhaps, the differentiation is performed more rapidly, giving the ceramide

processing enzymes less time to convert the head groups resulting in a higher level of CER[DS]. In addition, higher levels of CER[DS] were also observed in mouse skin, which also has a very thin epidermis.<sup>33</sup> Indicating that the thickness of the epidermis might have an impact on the subclasses.

When studying epidermal morphology and protein expression, an interesting observation is that SCD-1 inhibition resulted in a drastic increase in SCD-1 expression on both protein and RNA level. Even with an increased expression, the SCD-1 inhibitor still inhibited the majority of the protein, since there was a significant reduction in MUCERS observed. This increase in SCD-1 protein level was likely due to the necessity to maintain several crucial biological processes, such as regulating cell survival, membrane integrity, or preventing lipotoxicity in the cells.<sup>34-39</sup>

Although the effects of SCD-1 inhibiting resulted in an improved lipid composition, the observed changes ultimately did not lead to alterations in the lateral organization and both FTMS adopted a hexagonal lipid organization. In order to advance the lipid organization of FTMS, several key-changes may be an important next step to generate FTMS with normalized barrier function: 1) Perhaps the most crucial change, is the increase in the quantity of FFAS. In NHS, the ratio between CER:FFA in this study is approximately 0.8:1, whereas the ratio in FTMS is approximately 1:0.125. Normalization of this ratio would promote the lipids to adopt an orthorhombic packing in FTMS.<sup>40</sup> 2) An increase in the MCL of both CERAMIDES and FFAS would enhance SC lipids to adopt an orthorhombic organization.<sup>21</sup> Another study demonstrated that LXR inhibition reduced the MUCERS, but at the same time also an increase in chain length was observed.<sup>21</sup> This subsequently also led to an improved lipid organization, demonstrating the importance of targeting both the monounsaturated and lipid chain length. 3) A further reduction in the amount of MUCERS and MUFFAS would likely result in a higher fraction of lipids forming an orthorhombic organization as shown in previous studies.<sup>9</sup>

SCD-1 inhibition did not alter the lamellar organization. The diffraction patterns of the FTMS revealed lamellar phases in the FTMS. Although it remains to be elucidated why the phases + and # formed, these small changes are most probably observed due to the ceramide subclass composition as this composition is crucial for the formation of the lamellar phases.<sup>41</sup> In the FTMS<sub>SCD-1</sub>, the fraction of CER[EO] is reduced and the additional phase + is no longer present, which could indicate that the abundant presence of CER[EO] contributes to this peak as suggested in previous studies.<sup>42</sup> The phase #

might be attributed to the increased amounts of CER[DS] in the FTMS<sub>SCD-1</sub>, since the FTMS<sub>CONTROL</sub> does not contain this phase.

To conclude, this study demonstrates that SCD-1 activity could be successfully reduced and that SCD-1 modulation can be a tool to lower the amount of MUCERS and MUFFAS in our FTMS models. However, although a reduced SCD-1 activity improved the lipid composition, it did not result in an improved barrier function. This demonstrates the complexity of the lipid synthesis and the subsequent formation of the lipid organization. Nevertheless, it is important to know that the approach to reduce the monounsaturated lipids is useful, it should be combined with other targeted approaches to improve the lipid composition in order to generate the next generation of FTMS that even better mimic NHS.

## REFERENCES

- 1 Niehues, H., et al., 3D skin models for 3R research: The potential of 3D reconstructed skin models to study skin barrier function. *Exp Dermatol.*, 2018. 27(5): p. 501-511.
- 2 El Ghalbzouri, A., et al., Leiden reconstructed human epidermal model as a tool for the evaluation of the skin corrosion and irritation potential according to the ECVAM guidelines. *Toxicol In Vitro.*, 2008. 22(5): p. 1311-20.
- 3 Lilienblum, W., et al., Alternative methods to safety studies in experimental animals: role in the risk assessment of chemicals under the new European Chemicals Legislation (REACH). *Archives of Toxicology*, 2008. 82(4): p. 211-236.
- 4 Schäfer-Korting, M., et al., The use of reconstructed human epidermis for skin absorption testing: Results of the validation study. *Alternatives to laboratory animals: ATLA*, 2008. 36(2): p. 161-187.
- 5 Thakoersing, V.S., et al., Unraveling barrier properties of three different in-house human skin equivalents. *Tissue Eng Part C Methods.*, 2012. 18(1): p. 1-11.
- 6 Schäfer-Korting, M., et al., Reconstructed human epidermis for skin absorption testing: results of the German prevalidation study. *Altern Lab Anim.*, 2006 34: p. 283-94.
- 7 M., van Gele, et al., Three-dimensional skin models as tools for transdermal drug delivery: challenges and limitations. *Expert Opin Drug Deliv.*, 2011 8(6): p. 705-20.
- 8 Flaten, G.E., et al., In vitro skin models as a tool in optimization of drug formulation. *Eur J Pharm Sci.*, 2015 30(75): p. 10-24.
- 9 Mojumdar, E.H., et al., Monounsaturated Fatty Acids Reduce the Barrier of Stratum Corneum Lipid Membranes by Enhancing the Formation of a Hexagonal Lateral Packing. *Langmuir.*, 2014. 30(22): p. 6534-43.
- 10 van Smeden, J., et al., The importance of free fatty acid chain length for the skin barrier function in atopic eczema patients. *Exp Dermatol.*, 2014. 23(1): p. 45-52.
- 11 J., Van Smeden and J.A. Bouwstra, Stratum Corneum Lipids: Their Role for the Skin Barrier Function in Healthy Subjects and Atopic Dermatitis Patients. *Curr Probl Dermatol.*, 2016. 49: p. 8-26.
- 12 Proksch, E., J.M. Brandner, and J.M. Jensen, The skin: an indispensable barrier. *Exp Dermatol.*, 2008 17(12): p. 1063-72.
- 13 Motta, S., et al., Ceramide composition of the psoriatic scale. *Biochim Biophys Acta.*, 1993. 1182(2): p. 147-51.
- 14 Boiten, W., et al., Quantitative analysis of ceramides using a novel lipidomics approach with three dimensional response modelling. *Biochimica et Biophysica Acta (BBA) - Molecular and Cell Biology of Lipids*, 2016. 1861(11): p. 1652-1661.
- 15 t'Kindt, R., et al., Profiling and Characterizing Skin Ceramides Using Reversed-Phase Liquid Chromatography-Quadrupole Time-of-Flight Mass Spectrometry. *Analytical Chemistry*, 2012. 84(1): p. 403-411.
- 16 Thakoersing, V.S., et al., Increased Presence of Monounsaturated Fatty Acids in the Stratum Corneum of Human Skin Equivalents. *J Invest Dermatol.*, 2013. 133(1): p. 59-67.
- 17 van Smeden, J., et al., LC/MS analysis of stratum corneum lipids: ceramide profiling and discovery. *J Lipid Res.*, 2011. 52(6): p. 1211-21.
- 18 Bouwstra, J.A., et al., Structural investigations of human stratum corneum by small-angle X-ray scattering. *J Invest Dermatol.*, 1991. Dec(6): p. 1005-12.
- 19 Boncheva, M., The physical chemistry of the stratum corneum lipids. *International journal of cosmetic science*, 2014. 36(6): p. 505-515.
- 20 Thakoersing, V.S., et al., Unraveling barrier properties of three different in-house human skin equivalents. *Tissue Engineering Part C: Methods*, 2011. 18(1): p. 1-11.
- 21 Helder, R.W.J., et al., The effects of LXR agonist T0901317 and LXR antagonist GSK2033 on morphogenesis and lipid properties in full thickness skin models. *Biochim Biophys Acta Mol Cell Biol Lipids.*, 2019. 1865.
- 22 Paton, C.M. and J.M. Ntambi, Biochemical and physiological function of stearyl-CoA desaturase. *Am J Physiol Endocrinol Metab.*, 2009. 297(1): p. E28-E37.
- 23 Rabionet, M., K. Gorgas, and R. Sandhoff, Ceramide synthesis in the epidermis. *Biochim Biophys Acta.*, 2014. 1841(3): p. 422-434.
- 24 Kihara, A., Synthesis and degradation pathways, functions, and pathology of ceramides and epidermal acylceramides. *Progress in Lipid Research*, 2016. 63: p. 50-69.
- 25 Mizutani, Y., et al., Ceramide biosynthesis in keratinocyte and its role in skin function. *Biochimie*, 2009. 91: p. 784-790.
- 26 Masukawa, Y., et al., Comprehensive quantification of ceramide species in human stratum corneum. *J. Lipid Res.*, 2009. 50(8): p. 1708-19.
- 27 van Drongelen, V., et al., Barrier Properties of an N/TERT-Based Human Skin Equivalent. *Tissue Eng Part A.*, 2014. 20(21-22): p. 3041-9.
- 28 Ponec, M., et al., The Formation of Competent Barrier Lipids in Reconstructed Human Epidermis Requires the Presence of Vitamin C. *J Invest Dermatol.*, 1997. 109(3): p. 348-55.
- 29 Helder, R.W.J., et al., Contribution of Palmitic Acid to Epidermal Morphogenesis and Lipid Barrier Formation in Human Skin Equivalents. *Int J Mol Sci.*, 2019. 20(23).
- 30 Mizutani, Y., et al., Cooperative Synthesis of Ultra Long-Chain Fatty Acid and Ceramide during Keratinocyte Differentiation. *PLoS One*, 2013. 8.
- 31 Zheng, Y., et al., Lipoxigenases mediate the effect of essential fatty acid in skin barrier formation: A proposed role in releasing omega-hydroxyceramide for construction of the corneocyte lipid envelope. *J Biol Chem.*, 2011. 286(27): p. 24046-56.
- 32 Krieg, P. and G. Fürstenberger, The role of lipoxigenases in epidermis. *Biochim Biophys Acta*, 2014. 1841: p. 390-400.
- 33 Martins Cardoso, R., et al., Barrier lipid composition and response to plasma lipids: A direct comparison of mouse dorsal back and ear skin. *Exp Dermatol.* 2020: p. 548-555.
- 34 Miyazaki, M., W.C. Man, and J.M. Ntambi, Targeted disruption of stearyl-CoA desaturase1 gene in mice causes atrophy of sebaceous and meibomian glands and depletion of wax esters in the eyelid. *J Nutr.*, 2001 131: p. 2260-8.
- 35 Jackowski, S., Cell cycle regulation of membrane phospholipid metabolism. *J. Biol. Chem.*, 1996. 1271: p. 20219-20222.
- 36 Sampath, H., et al., Skin-specific Deletion of Stearyl-CoA Desaturase-1 Alters Skin Lipid Composition and Protects Mice from High Fat Diet-induced Obesity. *J Biol Chem.*, 2009. 284(30): p. 19961-19973.
- 37 Golfman, L.S., M. Bakovic, and D.E. Vance, Transcription of the CTP: phosphocholine cytidylyltransferase alpha gene is enhanced during the S phase of the cell cycle. *J. Biol. Chem.*, 2001. 276: p. 43688-43692.
- 38 Miyazaki, M., W.C. Man, and J.M. Ntambi, Targeted disruption of stearyl-CoA desaturase1 gene in mice causes atrophy of sebaceous and meibomian glands and depletion of wax esters in the eyelid. *J Nutr.*, 2001. 131: p. 2260-2268.
- 39 Li, L.O., E.L. Klett, and R.A. Coleman, Acyl-CoA synthesis, lipid metabolism and lipotoxicity. *Biochim Biophys Acta.*, 2010. 1801: p. 246-51.
- 40 Bouwstra, J.A., et al., Phase behavior of lipid mixtures based on human ceramides: coexistence of crystalline and liquid phases. *J Lipid Res.*, 2001. 42: p. 1759-70.
- 41 Smeden, J.v., et al., The important role of stratum corneum lipids for the cutaneous barrier function. *Biochim Biophys Acta.*, 2014. 1841: p. 295-313.
- 42 Groen, D., G.S. Gooris, and J.A. Bouwstra, Model membranes prepared with ceramide EOS, cholesterol and free fatty acids form a very unique lamellar phase. *Langmuir*, 2010. 26: p. 4168-75.



**SUPPLEMENTAL MATERIAL**

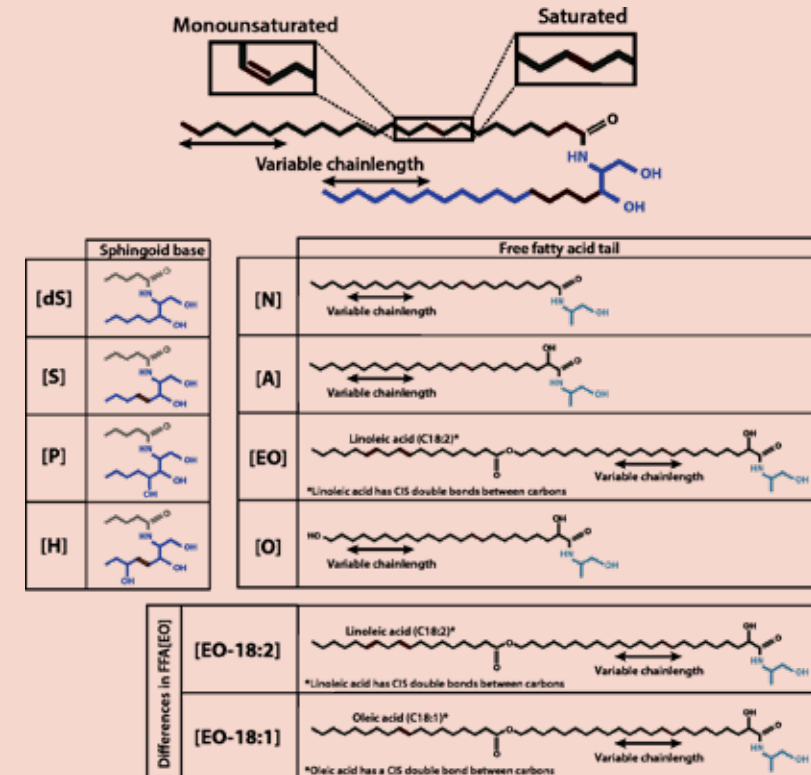
**Supplemental Table s1** Immunohistochemistry antibody list and specific methods.

Immunohistochemistry	Origin	Clone	Dilution	Antigen retrieval	Secondary antibody	Manufacturer
<b>PRIMARY ANTIBODY</b>						
Ki67	Mouse	MIB1	1:100	Autoclave	A	DAKO, Denmark
Cytokeratin 10	Mouse	DE-K10	1:50	Autoclave	A	Labvision/ Neomarkers, USA
Involucrin	Mouse	SY5	1:1200	Autoclave	A	Sanbio, NL
Stearoyl-CoA Desaturase	Mouse	CD.E10	1:300	Water Bath	A	Abcam, UK
<b>SECONDARY ANTIBODY</b>						
Biotinylated Goat anti-mouse (A)	Goat		1:200			Southern Biotechnology

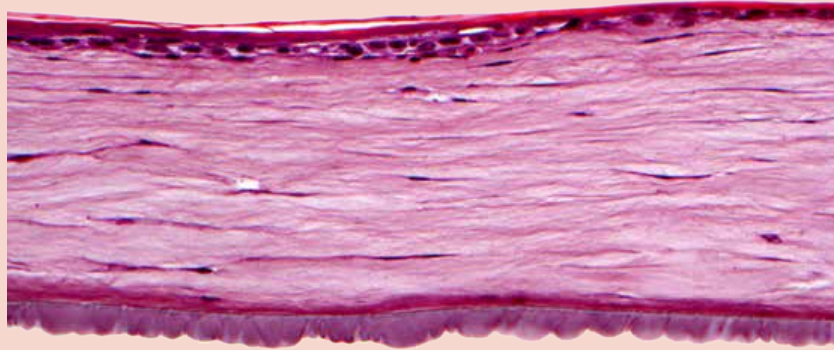
**Supplemental Table s2** Primer and housekeeping sequences.

TARGET GENE	SEQUENCE	TARGET GENE	SEQUENCE
SREBP1C_F	GGAGGGGTAGGGCCAACGGCCT	CERS4_F	GTGCTGCTGTTACACGATTCC
SREBP1C_R	CATGTCCTTCGAAAGTGCAATCC	CERS4_R	GTGGCACACTTGCTGATACTG
ACCI_F	CATATCCAGTCCATGCTGGCT	CERS5_F	CGGCTCTGTGACACCCTTT
ACCI_R	GTTCAGCCACTGCACAACC	CERS5_R	TCTCAAAGAGGGTCGTGTTC
FASN_F2	CATCCCACCTATGGCCTGC	CERS6_F	TGTTTGTATGTTGCCGTGGT
FASN_R2	GCCTGATGCAGTCGATGTAGTA	CERS6_R	CCAACGATCTCCCAGCTTCA
ELOVL1_F1	GGCTCTTCCTCTTCCAGTT	DES1_F	TCCCCAACATTCCTGGAAAAAG
ELOVL1_R1	TCCAGGAAGCACAGAGTGAT	DES1_R	CAGGAATTGTAGTGAGGGAGGT
ELOVL4_F	TTAGAGCCCAGTGCATCCAT	DES2_F	CGCATCCGGGCTACAACCT
ELOVL4_R	TTAGAGCCAGTGCATCCAT	DES2_R	CCAGGGAGTCTCAAACACAA
SCD-1_F	ACAGTGTGCCACCTCTTCG	<b>HOUSEKEEPING GENE</b>	
SCD-1_R	CCCTCACCCAGCTCCAAGTG	SDHA_F	AACCAAACGCTGGGAAGGAA
ABCA1_F	TGGCTCTCTAATTTGTCTGGGA	SDHA_R	GGAACACGGCAGCAGATT
ABCA1_R	TAGCACAGGCAGATTGGTGG	ZNF410_F	GCTGTGGTAAGCAGTTTACTACAG
CERS2_F	CTTCATCGTCTTCGCCATGTT	ZNF410_R	CTTGGGCTTCACAAAGGAAAGG
CERS2_R	AGGATAGAGTCCAGTGGGTA	ARCP2_F	TCCGGGACTACCTGCCTAC
CERS3_F	CCCTGTTTTTCATCTTCCACC	ARCP2_R	GGTTCAGCACCTTGAGGAAAG
CERS3_R	TAGGCAAGATCAGCGTGCAA		

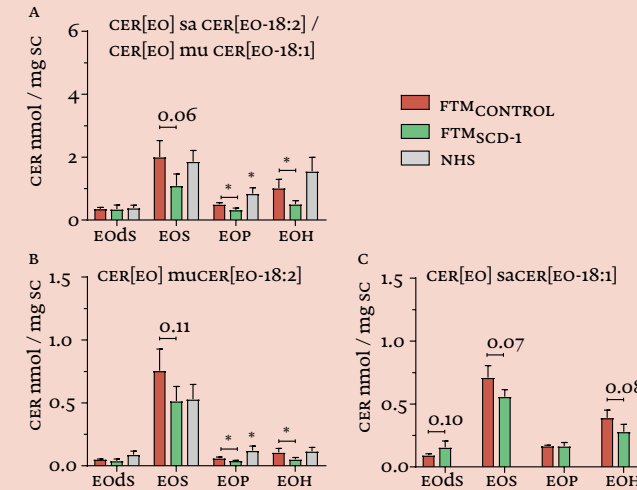
**Supplemental Figure s1** Molecular structure of the ceramide subclasses. The 16 ceramide subclasses that were analyzed are shown in the ion map. Ceramides consist of an acyl tail: [N]; non-hydroxy, [A];  $\alpha$ -hydroxy, [EO]; linoleic acid esterified to an  $\omega$ -hydroxy or [O];  $\omega$ -hydroxy. The acyl-chain is linked to a sphingoid base: [DS]; dihydro-sphingosine, [S]; sphingosine, [P]; phytosphingosine or [H]; 6-hydroxysphingosine. There are three ceramide fractions i) CER[NON-EO] with subclasses [NDS], [NS], [NP], [NH], [ADS], [AS], [AP], and [AH], ii) CER[EO] with subclasses [EODS], [EOS], [EOP], and [EOH] and iii) CER[O] with subclasses [OS], [OP], and [OH]. In each subclass fraction, CERs vary in chain length and can be either saturated or monounsaturated. In addition, CER[EO] structure containing an esterified-oleic acid rather than linoleic acid is also shown.



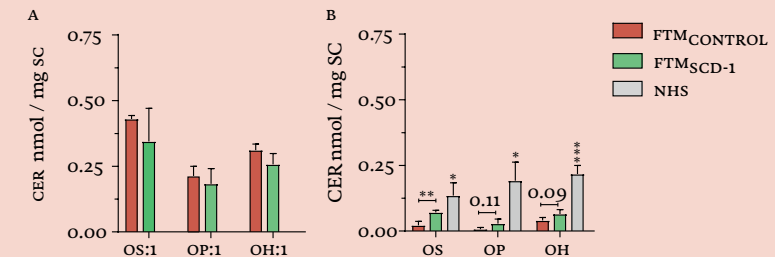
**Supplemental Figure s2** High concentrations of SCD-1 antagonist prevented the formation of a viable epidermis. H&E staining of the FTM cultured with 450 nM concentration did not result in a viable epidermis.



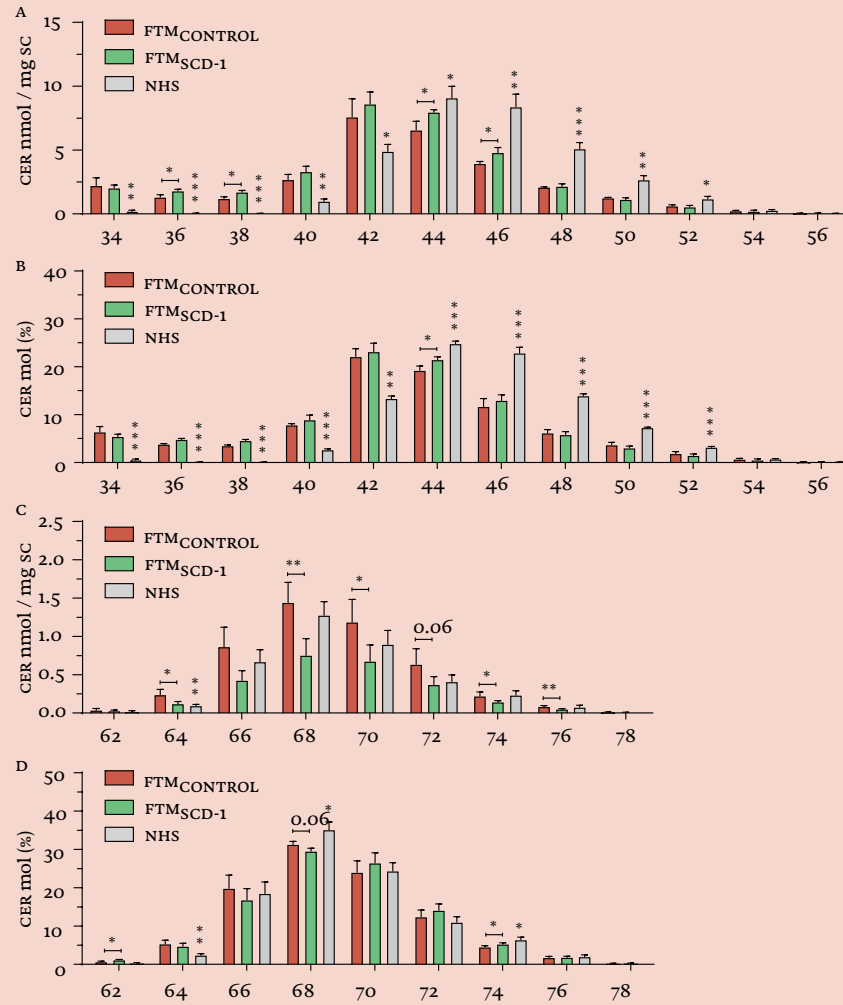
**Supplemental Figure s3** SCD-1 inhibition led to a reduction in the level of CER[EO] in the FTMS. The profile of the absolute amount of the subclasses of CER[EO] was determined for NHS, FTM<sub>CONTROL</sub> and FTM<sub>SCD-1</sub>; Amount of subclasses of CER[EO] was determined for NHS, FTM<sub>CONTROL</sub> and FTM<sub>SCD-1</sub>; Amount of subclasses of MUCER[EO-18:2] (A); Amount of subclasses of MUCER[EO-18:1]/ SACER[EO-18:2] (B); amount of subclasses of SACER[EO-18:1] (C). For statistical analysis, an unpaired t-test was performed between the FTM<sub>CONTROL</sub> and FTM<sub>SCD-1</sub>. The amounts of MUCER[EO-18:1]/SACER[EO-18:2] cannot be separately determined in the LC-MS method employed and are therefore grouped together. To compare the FTM<sub>CONTROL</sub> vs NHS, an unpaired t-test was used. Significant differences are indicated by \* for p<0.05.



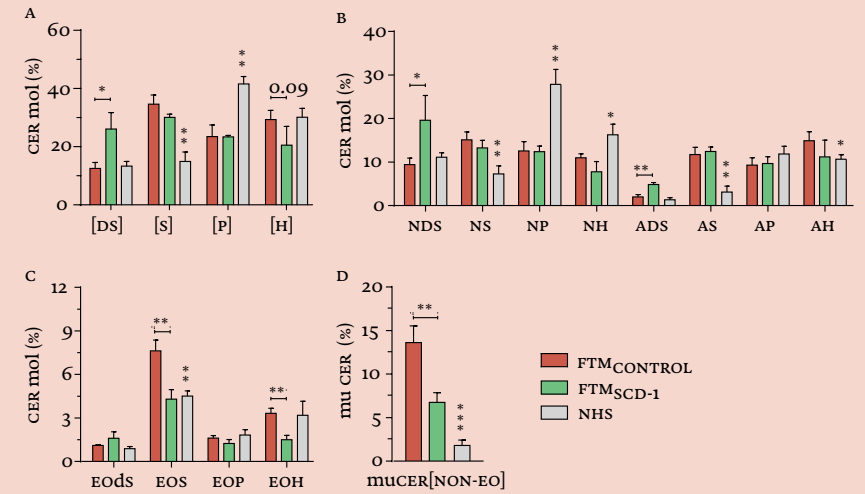
**Supplemental Figure s4** SCD-1 inhibition led an increased level of SACer[O] in the FTMS. The absolute CER[O] profile was calculated for NHS, FTM<sub>CONTROL</sub> and FTM<sub>SCD-1</sub>; Amount of all MUCER[O] subclasses (A); Amount of SACER[O] subclasses (B). For statistical analysis, an unpaired t-test was performed between the FTM<sub>CONTROL</sub> and FTM<sub>SCD-1</sub>. To compare the FTM<sub>CONTROL</sub> vs NHS, an unpaired t-test was used. Significant differences are indicated by \* for p<0.05, for p<0.01, and \*\*\* for p<0.001.



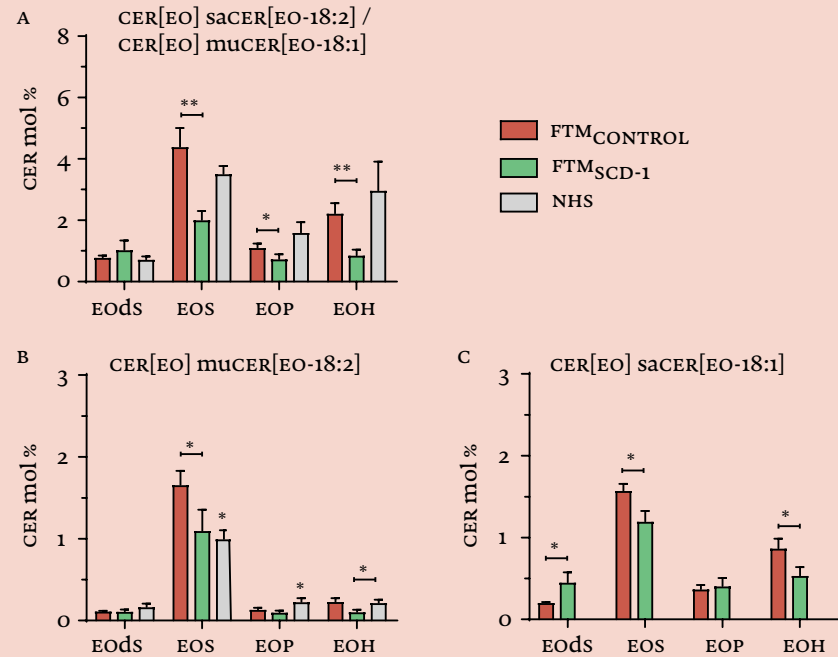
**Supplemental Figure s5** Inhibition of SCD-1 led to similar chain length distribution. The chain length profile of CER[NON-EO] were calculated in absolute amounts (A) and relative amounts (B). This was also done for CER[EO] in absolute amounts (C) and in relative amounts (D). For statistical analysis, an unpaired t-test was performed between the FTM<sub>CONTROL</sub> and FTM<sub>SCD-1</sub>. To compare the FTM<sub>CONTROL</sub> vs NHS, an unpaired t-test was used. Significant differences are indicated by \* for  $p < 0.05$ , for  $p < 0.01$ , and -\* for  $p < 0.001$ .



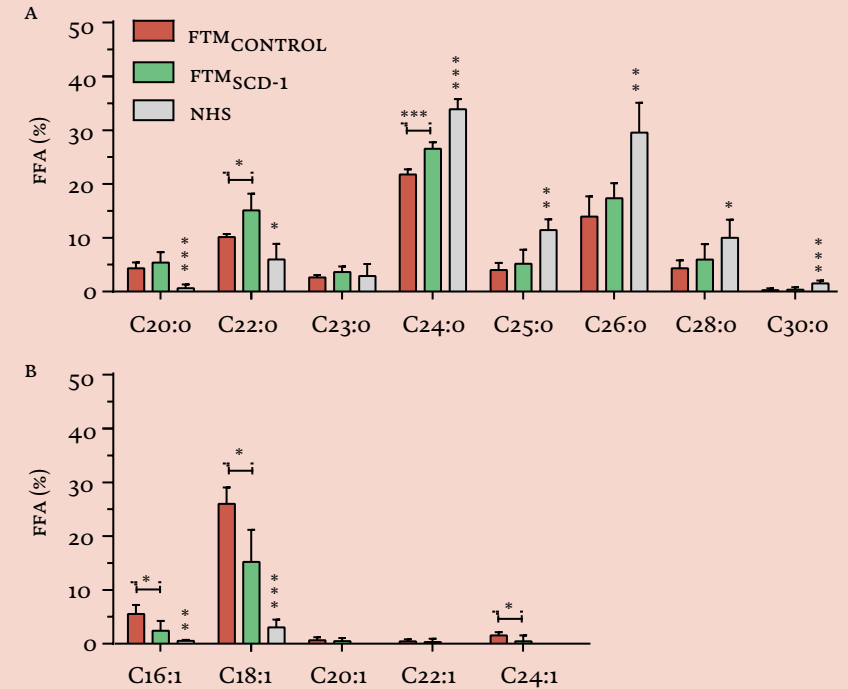
**Supplemental Figure s6** SCD-1 inhibition alters lipid composition by reducing the monounsaturations, reducing the CER[EO] subclasses, and by increasing the CER[DS] fraction. The percentage of the CER[NON-EO] head groups (SACER+MUCER) (A); The percentage amount of individual CER[NON-EO] subclasses (SACER+MUCER) (B); The percentage of the CER[EO] subclasses (SACER+MUCER) (C); The total percentage of MUCER[NON-EO] subclasses compared to the total amount of CER[NON-EO] (D). For statistical analysis, an unpaired t-test was performed between the FTM<sub>CONTROL</sub> and FTM<sub>SCD-1</sub>. After, to compare the FTM<sub>CONTROL</sub> and NHS, an unpaired t-test was used. Significant differences are indicated by \* for  $p < 0.05$ , for  $p < 0.01$ , and -\* for  $p < 0.001$ .



**Supplemental Figure s7** SCD-1 inhibition led to a strong reduction in the level of CER[EOS] in the FTMS. The relative CER[EO] profile for NHS and FTM<sub>CONTROL</sub> and FTM<sub>SCD-1</sub> percentage of all CER[EO] subclasses and compositions (A); Percentage of MUCER[EO-18:2] subclasses (B); Percentage of MUCER[EO-18:1]/SACER[EO-18:2] subclasses (C); Percentage of SACER[EO-18:1] subclasses (D). For statistical analysis, an unpaired t-test was performed between the FTM<sub>CONTROL</sub> and FTM<sub>SCD-1</sub>. To compare the FTM<sub>CONTROL</sub> vs NHS, an unpaired t-test was used. Significant differences are indicated by \* for p<0.05 and \*\* for p<0.01.



**Supplemental Figure s8** FFA composition after SCD-1 inhibition reduced the level of MUFA. Relative SAFA chain length distribution (A). Relative MUFA chain length distribution (B). For statistical analysis, an unpaired t-test was performed between the FTM<sub>CONTROL</sub> and FTM<sub>SCD-1</sub>. To compare the FTM<sub>CONTROL</sub> vs NHS, an unpaired t-test was used. Significant differences are indicated by \* for p<0.05 and \*\* for p<0.01.



**CHAPTER 9**  
**SUMMARY AND PERSPECTIVES**

Despite the advance of targeted therapy with biologics, an unmet medical need persists for patients with chronic inflammatory skin diseases. Early-phase clinical drug development in dermatology remains focused on traditional clinician reported outcomes to establish proof-of-pharmacology. However, it is possible that drug effects are not accurately captured as the optimal dosage has not yet been reached or the induction of endpoints are too variable or lack sensitivity. This could potentially lead to the misguided and false termination of clinical development programs.<sup>1</sup> However, a shift towards a more rational approach in clinical drug development which evaluates important pharmacokinetic and -dynamic hallmarks of candidate drugs is gaining momentum.<sup>2,3</sup> In dermatology, this question-based approach can benefit hugely from a “systems dermatology” methodology in which objective biomarkers can support clinical findings and advance drug development.<sup>1</sup> The scope of this thesis was to advance early clinical drug development by providing and applying new modalities that, without discarding traditional endpoints, enable rational and data-rich early-phase clinical trials.

This thesis comprises three sections that exemplify the added value of a data-rich approach to early-phase clinical drug development. The first section describes the characterization of seborrheic dermatitis using a multimodal approach and applies it to an interventional trial with a novel compound. The second section reports a model trial in psoriasis where multimodal technologies enhanced the confidence in clinical outcomes, which are less reliable in patients with low disease severity. The last section defines the stratum corneum ceramide profile as a useful biomarker and potential target for the optimization of the skin barrier. Finally, this chapter shortly delineates the main findings from this thesis and provides an outlook on its application in future early-phase clinical drug development of therapies for chronic inflammatory skin diseases.

### **Section 1 Multimodal characterization of the skin of seborrheic dermatitis patients**

Seborrheic dermatitis is a chronic inflammatory skin condition that is characterized by the presence of erythematous and scaly lesions primarily located in the face, scalp and upper chest, which are skin areas with increased sebaceous gland activity. Its pathophysiology is multifaceted, but much emphasis has been put on colonisation with the communal yeast *Malassezia*.<sup>4</sup> Using a multimodal approach, chapter 2 highlighted how the micro- and mycobiome,

cutaneous barrier function and inflammation contribute to the clinical phenotype in seborrheic dermatitis. By first imaging lesional sites and thereby capturing the degree of erythema and the cutaneous morphology, the presence of inflammation could be firmly established. Hereafter, the cutaneous microbiome and barrier function were characterized. Mycobial analysis showed that *Malassezia* was not differentially abundant on lesional skin compared to non-lesional skin. However, the lesional microbiome showed increased abundances of *Staphylococcus*. This constitutes a relevant finding considering the pro-inflammatory properties attributed to *Staphylococcus aureus* in other skin diseases such as atopic dermatitis.<sup>5</sup> However, the limited phylogenetic resolution prevented the identification of specific *Staphylococcus* species. A high degree of barrier impairment was observed in lesional skin, but this could also be attributed to the generally increased trans-epidermal water loss of the facial areas that are commonly affected by seborrheic dermatitis.<sup>6</sup> Therefore, analysis of the stratum corneum ceramide profile was performed. This showed that skin sites marked by excessive water loss showed concomitant alteration in the stratum corneum ceramide profile. These alterations were similar to those observed in atopic dermatitis where barrier dysfunction has been strongly established.<sup>7</sup> Showing the presence of barrier dysfunction in the pathophysiology of seborrheic dermatitis, which traditionally was mostly attributed *Malassezia* colonization, exemplifies how a multimodal approach can yield new insights in pathophysiology and therapy.

This multimodal approach was also applied to a randomized controlled clinical trial evaluating the antimicrobial peptide omiganan for the treatment of mild-to-moderate seborrheic dermatitis described in chapter 3. Taking the observed dysbiosis marked by increased *Staphylococcus* abundances as a possible target, the effect of topical omiganan 1.75% gel versus placebo and ketoconazole 2.00% cream was investigated. Ketoconazole is a first-line antifungal topical treatment for seborrheic dermatitis and functioned as a comparator drug in this trial. Omiganan was safe and well tolerated but did not decrease disease severity as defined by clinical scoring nor did it exhibit any effect on imaging, patient reported, microbial or skin barrier outcomes compared to placebo. In contrast, the efficacy of ketoconazole was reaffirmed by significant decreases in clinical scores compared to placebo. Moreover, we found a pronounced significant decrease in the abundance of *Malassezia* and a significant improvement in barrier function with concomitant normalization of markers of the stratum corneum ceramide profile. Of note, the

abundances of *Staphylococcus* decreased compared to baseline in the omiganan, ketoconazole and placebo groups. This indicated that *Staphylococcus* abundances do not seem to correlate with (changes in) disease severity of lesional skin, as treatment effects were solely apparent in patients receiving ketoconazole and downplays the importance of increased *Staphylococcus* abundances presented in the previous chapter. However, this study highlights the dynamics of barrier function upon treatment and its connection to the stratum corneum ceramide profile which further establishes the presence of barrier dysfunction in seborrheic dermatitis. Ultimately, this section highlights the added value of a multimodal approach in elucidating disease pathophysiology and how treatment-related effects contribute to a better understanding of disease.

### ***Section 2 Enabling the potential of mild psoriasis patients for early clinical drug development using a multimodal imaging approach***

This section concerns a model trial in chronic plaque psoriasis. Psoriasis is a common chronic inflammatory skin disease that affects up to 3% of the population worldwide. Psoriasis has a significant impact on patients' quality of life but can be increasingly well managed with the use of biologic therapy.<sup>8,9</sup> In this trial, mild and moderate-to-severe psoriasis patients were randomized to induction treatment with guselkumab or placebo. Guselkumab is a monoclonal antibody directed against interleukine-23 and is approved for the treatment of moderate-to-severe plaque psoriasis for which it is highly efficacious.<sup>10,11</sup>

In chapter 4, we demonstrated how our cohort of mild patients benefitted from a short regimen of guselkumab. This group, that comprises up to 80% of all psoriasis patients, is usually not considered for biological treatment considering the high costs associated with biologic treatment.<sup>12</sup> However, the potential to induce permanent disease remission in this group of patients with limited disease severity has been contemplated and might render biologic therapy cost-effective in this population.<sup>13</sup> Unfortunately, in our study all patients relapsed after cessation of guselkumab treatment. Nevertheless, this relapse extended up to 1 year after the last dose which exemplifies that mild patients benefit immensely from guselkumab therapy and may be considered more often for biological therapies in the future as these drugs become more affordable, possibly through the development of biosimilars and adoption of patient-centered dose-sparing regimens for this selected population.<sup>14</sup> Assured of an evident treatment effect, the response was further characterized in chapter 5 and compared to that of moderate-to-severe

patients given the same induction therapy. Although shown to be effective in establishing treatment effects in mild patients, clinical scoring with low disease severity is hampered by lower sensitivity of the commonly used Psoriasis Area And Severity Index.<sup>15</sup> Therefore, a multimodal imaging toolbox was applied to support the observed clinical effects in an objective manner through monitoring a target plaque with multispectral imaging, laser speckle contrast imaging and optical coherence tomography. This approach showed, in agreement with significantly decreasing (total body) clinical scores, a significantly decreased erythema and roughness with a significantly decreased perfusion and epidermal thickness of the target plaque. Although an evident clinical response could be established by clinical scoring in the mild population, the addition of objective imaging biomarkers substantiated this outcome. Additionally, it showed that mild patients demonstrate a similar clinical response to guselkumab compared to moderate-to-severe patients. Together, this opens up the possibility to include this more easily recruitable population of mild psoriasis patients in future trials as a representative surrogate population for moderate-to-severe psoriasis patients and might thereby accelerate early phase drug development in psoriasis.

### ***Section 3 The stratum corneum ceramide profile as biomarker and therapeutic target***

This last section focusses on the rationale and application of stratum corneum ceramide profiling for use in clinical development programs. The skin barrier function has been implicated in the pathogenesis of atopic dermatitis and has been linked to abnormalities in the lipid profile of the stratum corneum.<sup>7,16</sup> Recently, stratum corneum ceramides have been shown to function as a treatment response biomarker in observational trials in atopic dermatitis.<sup>17,18</sup> These results hold potential for its application in randomized controlled trials in other immune-mediated inflammatory skin diseases.

To scope the therapeutic area in which ceramide profiling might be applied, a systematic review and meta-analysis has been conducted in chapter 6 that compiled the available literature on the ceramide profiles in skin diseases. After selecting articles that contrast findings directly to that of healthy volunteers, it showed that the stratum corneum ceramide profile in atopic dermatitis, plaque psoriasis, ichthyosis, xerosis, acne vulgaris and palmoplantar hyperkeratosis shared many of the same alterations; mainly decreased CER[NP] abundances and decreased total carbon chain length. Interestingly,

the abundance of a very short ceramide CER[NSC34], a CER[NS] species with a total carbon chain length of 34 carbons, was increased consistently in lesional skin compared to healthy controls. These results were further supported by a meta-analysis comprised of 31 ceramide profiles from healthy controls and 68 ceramide profiles from dermatoses covering 11 subclasses. This showed that the relative abundances of CER[NS], CER[NP] and CER[AS] were predominantly affected in lesional atopic dermatitis, lesional psoriasis, ichthyosis, palmoplantar hyperkeratosis and acne vulgaris. Notably, the ceramide profile in stratum corneum of non-lesional atopic dermatitis and non-lesional psoriasis showed a high degree of similarity compared to healthy controls, indicating that the alterations in the non-lesional ceramide profile that are described in literature are not as evident as those of lesional skin. The potential for the ceramide profile to distinguish between lesional and non-lesional or healthy skin was thereafter evaluated in the aforementioned psoriasis trial in chapter 7. Indeed, results were in line with the systematic literature review from chapter 6 with significantly increased CER[NS], CER[NP] and decreased CER[NP] and CER[AP] abundances in lesional skin compared to non-lesional skin and healthy controls. Additionally, the average chain length was significantly decreased and the abundance of unsaturated CER[NS] and CER[NSC34] were significantly increased in lesional skin. These alterations correlated with barrier dysfunction measured by trans-epidermal water loss. As in chapter 6, no major differences were observed between mild and moderate-to-severe patients. Exploiting these alterations in the ceramide profile as biomarkers showed them to differentiate between guselkumab treatment and placebo and correlate with decreases in clinical disease severity and trans-epidermal water loss. This confirms the usefulness of ceramide profiling as biomarker in dermatology.

The correlations between barrier dysfunction and alterations in the ceramide profile as observed in atopic dermatitis, seborrheic dermatitis and psoriasis along with their implication in disease pathophysiology, also highlight the skin barrier as a potential therapeutic target for novel therapies.<sup>19,20</sup> In chapter 8, the possibility to influence specific components of skin barrier lipid synthesis is described using *in vitro* cultured human skin equivalents. Despite bearing a high resemblance to native human skin, their barrier function is decreased and the ceramide profile is marked by similar changes as observed in dermatoses as discussed in chapter 6.<sup>21</sup> In trying to reduce the increased amount of monounsaturated lipids, these models are supplemented

with an inhibitor for stearoyl-CoA desaturase-1 (SCD-1), the enzyme responsible for the conversion of saturated fatty acids to monounsaturated fatty acids.<sup>22</sup> Supplementation of SCD-1 inhibitor successfully reduced the degree of unsaturation in the fatty acids and ceramide fractions, but was still higher compared to that of native human skin. Additionally, the organization of the stratum corneum lipid matrix and barrier function remained similar to that of models without SCD-1 inhibition. The persisting presence of monounsaturated lipids may be explained by the strong upregulation of SCD-1 upon its inhibition, as baseline SCD-1 activity may remain necessary because of its vital function in other biological processes. Although the presence of residual monounsaturated lipid content might explain the negligible impact on barrier function, it could also highlight that the skin barrier function depends on more factors in the lipid matrix than solely the amount of unsaturation. Nevertheless, it indicates that alterations in the ceramide profile can be restored by pharmacological intervention. In the future, restoring the impaired skin barrier of inflammatory skin diseases by correcting alterations in the stratum corneum lipid profile could be explored and may eventually be integrated in existing maintenance therapy to prevent flares and relapses.

Concluding, this section describes that alterations in the ceramide profile are present throughout dermatological condition, can be exploited as a useful biomarker in support of a multimodal drug development approach and might represent a druggable target.

## Perspectives

### THE DATA-RICH EXPANSION OF FUTURE EARLY-PHASE CLINICAL TRIALS

Endpoints in early-phase clinical trials in patients are currently very similar to those of Phase I first-in-human trials in healthy volunteers. They predominantly evaluate safety and try to establish a suitable dosing regimen for patients based on pharmacodynamic effects before moving to larger cohorts. The process of dose-selection is frequently guided by leveraging the occurrence of adverse events and decreases in disease severity, mostly based on traditional endpoints. However, traditional endpoints such as the Seborrheic Dermatitis Area and Severity Index or Psoriasis Area and Severity Index as used in this thesis are associated with limited objectivity and sensitivity because they are performed based on a visual assessment by physicians



and are of a categorical nature. Combined with the possibility that a perceivable remission might only be apparent after a longer period of treatment; potentials drug effects might be overlooked. The integration of a multimodal approach offers additional endpoints that can facilitate the objective characterization of the treatment response in patients and might rescue a drug candidate that is not sufficiently effective as it is not dosed sufficiently to reach the peak of its pharmacodynamic effect. Additionally, implementing the technologies set out in this thesis might aid in the determination of minimum anticipated biological effect level with therapies that show adverse effects through exaggerated efficacy rather than off-target adverse effects, such as can be observed for monoclonal antibodies.<sup>23</sup> Ultimately, the biomarkers set out in this thesis can advance early clinical drug development by providing a solid basis for dose escalation and selection.

Besides the implementation in early-stage drug development, such an approach might also be applied at later stages of drug development to compare responses between different treatments. For moderate-to-severe psoriasis patients, various monoclonal antibody therapies have become available that all show a high degree of efficacy. In finding the most beneficial therapy for patients, comparator controlled clinical trials can be conducted in Phase III late-stage development to compare a novel treatment with that of the standard-of-care. However, these are often conducted with an exceedingly large number of patients.<sup>24</sup> Instead, trials as presented in this thesis might be employed to evaluate the 'head-to-head' response in a smaller cohort but with the support of more comprehensive data spanning multiple modalities. Additionally, the use of this approach in showing the non-inferiority of biosimilars might accelerate market access and reduce their development costs, the latter being pertinent to the reimbursement of therapies and biosimilars especially.

Of note, the assessments performed in this trial are all minimally or non-invasive in nature. Neither imaging, swabs nor tape strips leave a lasting mark on subjects which enables their intensive and repeated use during longitudinal studies. Additionally, they form a complementary set of measures that might even be able to replace invasive measures such as skin biopsies. Optical coherence tomography as used in this thesis, and its more high-resolution alternative reflectance confocal microscopy and line-field confocal optical coherence tomography, are able to provide clinicians with detailed and instant readouts on epidermal morphology.<sup>25,26</sup> Although these do not allow

for the determination of specific proteins and immune cells into the epidermis, the combination of tape stripping with sequencing and proteomics have highlighted the ability to detect the immune signature of atopic dermatitis and psoriasis similarly to biopsies.<sup>27,28</sup> This might render the use of skin biopsies redundant in the future. In seborrheic dermatitis, such an approach would be of high interest considering the preferential location of lesions in the face, disqualifying the use of biopsies for repeated monitoring of disease. Additionally, the immune signature of seborrheic dermatitis remains poorly elucidated. It is well possible that this signature bears resemblance to that of atopic dermatitis and, if proven, might be grounds to initiate studies in drug repurposing. This might represent a cost-saving alternative for the development of entirely new treatment modalities.

Altogether, the adoption of a multimodal toolbox in dermatology trials is promising. This thesis offers multiple different modalities that can be further developed and validated in order to meet the regulatory requirements for their use in drug development and clinical practice.<sup>29,30</sup>

## **THE BARRIER AS AN ACCOMPLICE TO CHRONIC INFLAMMATORY SKIN DISEASES**

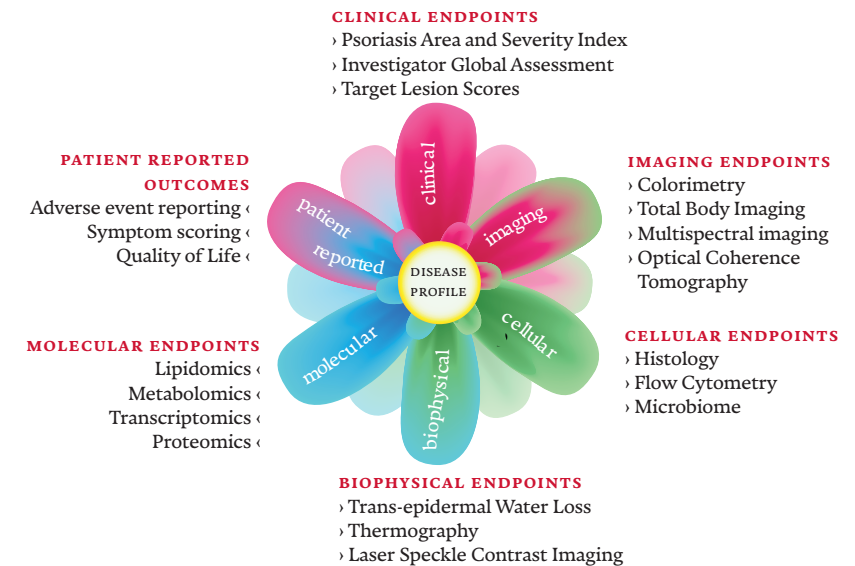
The impaired cutaneous barrier function has long been considered as an aggravating factor for atopic dermatitis.<sup>20</sup> Resulting from this thesis, a similar role might be attributed to barrier dysfunction seborrheic dermatitis. In atopic dermatitis, emollients are being used to a high extent with the goal to reinforce the compromised skin barrier and control disease.<sup>31</sup> However, moisturizers are not often considered for the treatment of seborrheic dermatitis, possibly due to the assumption that their use might be redundant based on the excessive production of lipids associated with lesional sites. Concomitant use of emollients has shown to boost the efficacy of existing topical therapies in atopic dermatitis and might do so for seborrheic dermatitis as well. As a medical need persists in patients with seborrheic dermatitis,<sup>32</sup> it might be a viable and cost-effective approach to evaluate the combination of existing medication for seborrheic dermatitis with emollients. Additionally, this approach might be applied to more dermatoses as the systematic literature review in chapter 6 highlights that changes in the stratum corneum ceramide profile, a major component of the skin barrier, are apparent throughout dermatology.

Although this is a promising result, the review also indicates that there remains a gap in literature outside of the stratum corneum ceramide profile in atopic dermatitis, psoriasis and ichthyosis that warrants further studies. Not only can the knowledge on the ceramide profile in various skin diseases benefit from an additional comprehensive characterization as performed for psoriasis as in chapter 7, but the ceramide profile remains unknown for many other cutaneous disorders. Properly characterizing the ceramide profile of all dermatoses could pave the way for their use as a biomarker in clinical trials. Although the platform used in this thesis is expansive and its high degree of detail is warranted for these first exploratory steps in elucidating unknown ceramide profiles, miniaturization might be needed before it can be widely applied as a clinical research tool. Widespread adaptation might be facilitated by reducing the number of tapes needed down to one and supplying this to clinicians or patients in ready-made kits. Furthermore, a primary detailed analysis of the ceramide profile allows for a more targeted approach thereafter which might significantly reduce sample preparation and data analysis.

### CONTRIBUTION OF SYSTEMS DERMATOLOGY IN EARLY-PHASE CLINICAL TRIALS TO UNDERSTANDING OF DISEASE

The value of a multimodal approach in early-phase drug development for the fundamental understanding of disease is exemplified in section 1, where evaluating multiple characteristics highlighted the multifaceted pathophysiology of seborrheic dermatitis. Indeed, the multimodality of chronic inflammatory skin diseases is becoming apparent as the first biologics that have been developed for atopic dermatitis, do not seem to be as broadly effective as those developed for psoriasis.<sup>33</sup> Multimodal profiling of diseases might enable the elucidation of various disease endotypes or highlight the differential contribution of different modalities to disease. With respect to inflammatory skin diseases, this might range from multiple targets within the immune system to synergistic action of the immune system and microbiome. To accomplish this, patients should be further characterized as a whole using a complete multimodal and, where possible, untargeted approach to capture all drivers of disease (figure 1). On their own, these modalities can yield additional information on disease pathogenesis. Combined, this vast amount of data might be condensed into a single readout by machine learning and highlight the different disease endotypes and might be employed in a precision medicine setting for treatment selection or to evaluate whether a selected treatment still represents the optimal choice for a patient as time goes on.<sup>34</sup>

**Figure 1** Visualization of the ideal multimodal approach. Applicable assessments are listed next to their respective modality and can be integrated into a single disease profile.



## Overall conclusion

This thesis describes the application of a biomarker-oriented multimodal approach to drug development in chronic inflammatory skin diseases. It exemplifies how this data-driven profiling approach can enhance the understanding of disease pathophysiology and substantiate the clinical effects that are observed using traditional endpoints in clinical trials focused on proof-of-pharmacology. Additionally, it demonstrates the applicability of ceramide profiling as a biomarker in clinical research and the potential for its use in other inflammatory skin conditions or dermatology in general. Ultimately, findings from this thesis can be implemented into upcoming clinical trials where it will facilitate a more rational approach to early clinical drug development in dermatology.

## REFERENCES

- 1 Rissmann, R., Moerland, M. & van Doorn, M. B. A. Blueprint for mechanistic, data-rich early phase clinical pharmacology studies in dermatology. *Br J Clin Pharmacol* **86**, 1011 (2020).
- 2 Cohen, A. F., Burggraaf, J., Van Gerven, J. M. A., Moerland, M. & Groeneveld, G. J. The Use of Biomarkers in Human Pharmacology (Phase I) Studies. <https://doi.org/10.1146/annurev-pharmtox-011613-135918> **55**, 55-74 (2015).
- 3 Visser, S. J. de. A question based approach to drug development. *Doctoral Thesis* (Leiden University, 2003).
- 4 Wikramanayake, T. C., Borda, L. J., Miteva, M. & Paus, R. Seborrheic dermatitis—Looking beyond Malassezia. *Exp Dermatol* **28**, 991-1001 (2019).
- 5 Geoghegan, J. A., Irvine, A. D. & Foster, T. J. Staphylococcus aureus and Atopic Dermatitis: A Complex and Evolving Relationship. *Trends Microbiol* **26**, 484-497 (2018).
- 6 Voegeli, R., Gierschendorf, J., Summers, B. & Rawlings, A. V. Facial skin mapping: from single point bio-instrumental evaluation to continuous visualization of skin hydration, barrier function, skin surface pH, and sebum in different ethnic skin types. *Int J Cosmet Sci* **41**, 411-424 (2019).
- 7 Kim, B. E. & Leung, D. Y. M. Significance of Skin Barrier Dysfunction in Atopic Dermatitis. *Allergy Asthma Immunol Res* **10**, 207 (2018).
- 8 Langley, R. G. B., Krueger, G. G. & Griffiths, C. E. M. Psoriasis: epidemiology, clinical features, and quality of life. *Ann Rheum Dis* **64**, ii18 (2005).
- 9 Sbidian, E. *et al.* Systemic pharmacological treatments for chronic plaque psoriasis: a network meta-analysis. *Cochrane Database of Systematic Reviews* **2022**, (2022).
- 10 Puig, L., Daudén, E., Cuervas-Mons, M., Novella, C. & Guisado, C. Persistence and effectiveness of guselkumab treatment in patients with moderate-to-severe plaque psoriasis in a non-interventional real-world setting: The SPRING study. *Journal of the European Academy of Dermatology and Venereology* **00**, 1-11 (2023).
- 11 Blauvelt, A. *et al.* Efficacy and safety of guselkumab, an anti-interleukin-23 monoclonal antibody, compared with adalimumab for the continuous treatment of patients with moderate to severe psoriasis: Results from the phase III, double-blinded, placebo- and active comparator-controlled Voyage 1 trial. *J Am Acad Dermatol* **76**, 405-417 (2017).
- 12 Papp, K. A. *et al.* Psoriasis Prevalence and Severity by Expert Elicitation. *Dermatol Ther (Heidelb)* **11**, 1053 (2021).
- 13 Eyerich, K. *et al.* IL-23 blockade with guselkumab potentially modifies psoriasis pathogenesis: rationale and study protocol of a phase 3b, randomised, double-blind, multicentre study in participants with moderate-to-severe plaque-type psoriasis (Guide). *BMJ Open* **11**, (2021).
- 14 Michielsens, C. A. J., van Muijen, M. E., Verhoef, L. M., van den Reek, J. M. P. A. & de Jong, E. M. G. J. Dose Tapering of Biologics in Patients with Psoriasis: A Scoping Review. *Drugs* **81**, 349-366 (2021).
- 15 Papp, K. A. *et al.* The Proposed PASI-HD Provides More Precise Assessment of Plaque Psoriasis Severity in Anatomical Regions with a Low Area Score. *Dermatol Ther (Heidelb)* **11**, 1079-1083 (2021).
- 16 Van Smeden, J., Janssens, M., Gooris, G. S. & Bouwstra, J. A. The important role of stratum corneum lipids for the cutaneous barrier function. *Biochim Biophys Acta Mol Cell Biol Lipids* **1841**, 295-313 (2014).
- 17 Berdyshev, E. *et al.* Dupilumab significantly improves skin barrier function in patients with moderate-to-severe atopic dermatitis. *Allergy* **77**, 3388-3397 (2022).
- 18 Lee, S. J., Kim, S. E., Shin, K. O., Park, K. & Lee, S. E. Dupilumab Therapy Improves Stratum Corneum Hydration and Skin Dysbiosis in Patients With Atopic Dermatitis. *Allergy Asthma Immunol Res* **13**, 762 (2021).
- 19 Sano, S. Psoriasis as a barrier disease. *Dermatologica Sinica* **33**, 64-69 (2015).
- 20 Yoshida, T., Beck, L. A. & De Benedetto, A. Skin barrier defects in atopic dermatitis: From old idea to new opportunity. *Allergology International* **71**, 3-13 (2022).
- 21 Bouwstra, J. A., Helder, R. W. J. & El Ghalbzouri, A. Human skin equivalents: Impaired barrier function in relation to the lipid and protein properties of the stratum corneum. *Adv Drug Deliv Rev* **175**, 113802 (2021).
- 22 Paton, C. M. & Ntambi, J. M. Biochemical and physiological function of stearyl-CoA desaturase. *Am J Physiol Endocrinol Metab* **297**, (2009).
- 23 Muller, P. Y., Milton, M., Lloyd, P., Sims, J. & Brennan, F. R. The minimum anticipated biological effect level (MABEL) for selection of first human dose in clinical trials with monoclonal antibodies. *Curr Opin Biotechnol* **20**, 722-729 (2009).
- 24 No, D. J., Amin, M., Bhutani, T. & Wu, J. J. A systematic review of active comparator controlled clinical trials in patients with moderate-to-severe psoriasis. *Journal of Dermatological Treatment* **29**, 467-474 (2018).
- 25 Orsini, C. *et al.* Line-field confocal optical coherence tomography: New insights for psoriasis treatment monitoring. *Journal of the European Academy of Dermatology and Venereology* (2023) DOI:10.1111/JDV.19568.
- 26 Csuka, E. A. *et al.* Reflectance Confocal Microscopy, Optical Coherence Tomography, and Multiphoton Microscopy in Inflammatory Skin Disease Diagnosis. *Lasers Surg Med* **53**, 776-797 (2021).
- 27 He, H. *et al.* Tape-Strip Proteomic Profiling of Atopic Dermatitis on Dupilumab Identifies Minimally Invasive Biomarkers. *Front Immunol* **11**, 565656 (2020).
- 28 He, H. *et al.* Tape strips detect distinct immune and barrier profiles in atopic dermatitis and psoriasis. *Journal of Allergy and Clinical Immunology* **147**, 199-212 (2021).
- 29 Bakker, E. *et al.* Biomarker Qualification at the European Medicines Agency: A Review of Biomarker Qualification Procedures From 2008 to 2020. *Clin Pharmacol Ther* **112**, 69 (2022).
- 30 Landeck, L., Kneip, C., Reischl, J. & Asadullah, K. Biomarkers and personalized medicine: current status and further perspectives with special focus on dermatology. *Exp Dermatol* **25**, 333-339 (2016).
- 31 van Zuuren, E. J., Fedorowicz, Z., Christensen, R., Lavrijsen, A. & Arents, B. W. M. Emollients and moisturisers for eczema. *Cochrane Database Syst Rev* **2017**, (2017).
- 32 Jackson, J. M., Alexis, A., Zirwas, M. & Taylor, S. Unmet needs for patients with seborrheic dermatitis. *J Am Acad Dermatol* **0**, (2023).
- 33 Renert-Yuval, Y. & Guttman-Yassky, E. New treatments for atopic dermatitis targeting beyond IL-4/IL-13 cytokines. *Annals of Allergy, Asthma & Immunology* **124**, 28-35 (2020).
- 34 Pammi, M., Aghaepour, N. & Neu, J. Multiomics, artificial intelligence, and precision medicine in perinatology. *Pediatric Research* **2022** **93**:2 **93**, 308-315 (2022).

## APPENDICES

SAMENVATTING IN HET NEDERLANDS

## VERKLARENDE WOORDENLIJST

*Enkele terugkerende termen die gebruikt worden in de Nederlandse samenvatting zijn hier uitgelegd, zodat deze snel kunnen worden opgezocht als ze voorbij komen. Deze zijn in de tekst rood en dikgedrukt.*

**Biologics:** therapeutische antilichamen met een specifieke werking.

**Biomarker:** een indicator van een biologisch proces waaruit de toestand van een individu (mede) kan worden afgeleid.

**Biosimilars:** goedkopere kopieën van de middelen die nu op de markt zijn.

**Ceramiden:** een groep moleculen die een groot deel uitmaken van de vetten in het stratum corneum. De specifieke klassen ceramiden worden vaak benoemd met een lettercode zoals "Cer[NS]".

**Ceramidesamenstelling:** de totale verhouding tussen de verschillende ceramideklassen.

**Constitutioneel eczeem:** in de volksmond gewoon eczeem genoemd en ook vaak aangeduid als atopisch eczeem.

**Endotypes:** verschillende types van dezelfde ziekte gekenmerkt door verschillen in de pathofysiologie.

**Farmacodynamiek:** wat het medicijn doet met het lichaam, bijvoorbeeld het remmen van processen waardoor de ziekte verdwijnt.

**Gerandomiseerde onderzoeken met controle-groep:** in het Engels 'Randomized Controlled Trials' waar deelnemers worden verdeeld tussen een groep die het onderzoeksmiddel krijgt en een groep die een placebo krijgt. Vaak weet de onderzoeker noch de deelnemer welk middel er aan de deelnemer gegeven wordt. Dan spreekt men van een 'dubbel-blind' onderzoek.

**Guselkumab:** een effectieve behandeling voor psoriasis.

**Huidequivalenten:** stukjes huid die kunstmatig zijn gekweekt in het laboratorium,

**Malassezia:** een gist die voorkomt op de vette zones van de huid en bijdraagt aan de ziekte Seborrhoïsch Eczeem.

**Microbioom:** alle micro-organismen zoals gisten en bacteriën die op een plek voorkomen.

**Multimodaal:** benadering vanuit verschillende aspecten.

**Organisatie van de stratum corneum vetten:** de vetten in het stratum corneum vormen op elkaar gestapelde lagen. Als we het hebben over hoe breed elke laag is en hoe dicht de vetten in zo'n laag naast elkaar liggen, spreken we over de organisatie. Als deze lagen smaller zijn en de vetten verder uit elkaar liggen neemt de huidbarrière af.

**Pathofysiologie:** het proces achter het ontstaan van de ziekte.

**Placebo:** nepmiddel.

**SCD-1:** afkorting voor het eiwit stearoyl-CoA desaturase-1 die onverzadigde vetzuren aanmaakt door een dubbele binding in het molecuul van een vetzuur zonder dubbele bindingen aan te brengen.

**Seborrhoïsch eczeem:** huidaandoening waar bij patiënten rode en schilferige plekken ontstaan op plekken waar de huid vettiger is, zoals bij de neusplooiën, wenkbrauwen en voorhoofd.

**Significant:** het woord significant wordt gebruikt om aan te tonen dat het zeer onwaarschijnlijk is dat een verschil, stijging of daling veroorzaakt is door toeval in plaats van bijvoorbeeld het effect van ziekte of een behandeling.

**Staphylococcus:** een bacterie die veelvuldig voorkomt op de huid. De soort *Staphylococcus aureus* wordt gezien als een mogelijke ziekteverwekker in constitutioneel eczeem.

**Stratum corneum:** de buitenste huidlaag, ook wel de hoornlaag genoemd, die zorgt voor de barrièrefunctie.

**Systeemdermatologie:** het bekijken van de ziekte als één geheel vanuit alle mogelijke aspecten.

**Trans-epidermaal waterverlies:** de hoeveelheid water die vanuit de huid naar buiten verdampst.

**Vroege fase klinisch geneesmiddelenonderzoek:** de eerste stappen in het onderzoeken van de veiligheid en werkzaamheid van nieuwe geneesmiddelen in kleine groepen gezonde vrijwilligers of patiënten.

Chronische inflammatoire huidziekten zijn aandoeningen waarbij een overdreven reactie van het immuunsysteem zorgt voor ontstekingen, ook wel inflammatie genoemd, van de huid. Deze groep huidaandoeningen, waar onder andere **constitutioneel eczeem**, **seborrhoïsch eczeem** en psoriasis onder vallen, treffen een groot deel van de bevolking.<sup>1</sup> Gelukkig kunnen deze ziekten tegenwoordig steeds beter worden behandeld. In het bijzonder psoriasis; hier heeft grondig onderzoek naar de achtergrond van de ziekte geleid tot nieuwe inzichten in de afwijkingen in het immuunsysteem die men daarna heeft weten te gebruiken om op aan te grijpen met zogenaamde **biologics**.<sup>2</sup> Dit zijn therapeutische eiwitten, in dit vakgebied vaak monoclonale antilichamen, die specifiek de processen kunnen stoppen die de overreactie in de huid veroorzaken. Deze middelen worden nu ook ontwikkeld voor **constitutioneel eczeem**. Hier wordt de ontsteking echter veroorzaakt door een ander deel van het immuunsysteem, waardoor de therapieën die voor psoriasis worden ontwikkeld hier onvoldoende werkzaam zijn.<sup>3</sup> Daarom wordt er voor de behandeling van **constitutioneel eczeem**, en andere inflammatoire huidziekten, nog steeds gebruik gemaakt van medicijnen die het immuunsysteem in zijn geheel remmen. Helaas leidt het gebruik van deze therapieën vaak tot bijwerkingen.<sup>4,5</sup>

Er is dus nog steeds een medische noodzaak voor patiënten met chronische inflammatoire huidziekten. Hiervoor moeten nieuwe medicijnen worden ontwikkeld. In de vroege stadia van geneesmiddelenontwikkeling waar nieuwe medicatie voor het eerst wordt toegediend aan gezonde vrijwilligers en patiënten, worden er nog vaak traditionele klinische uitkomsten gebruikt om in te schatten of een middel veilig en werkzaam is. In de dermatologie wordt vaak een schaal gebruikt van 0 tot 4 waarmee op het oog een inschatting gemaakt wordt hoe erg de huid is aangedaan door een ziekte. Anderzijds wordt er vaak gekeken of mensen de medicatie verdragen of juist bijwerkingen ervaren. Hierop baseert men of het zinvol is om de ontwikkeling van het kandidaat geneesmiddel door te zetten in grotere en duurdere onderzoeken. Uiteindelijk zal er een afweging gemaakt moeten worden tussen het voordeel dat een behandeling voor een patiënt oplevert en het risico op bijwerkingen die mogelijk kunnen optreden tijdens de behandeling.<sup>6</sup>

Het is echter mogelijk dat de effecten van het geneesmiddel tijdens de ontwikkeling niet optimaal worden vastgesteld. Dit kan komen doordat de dosering nog niet hoog genoeg is om een duidelijk effect te kunnen zien, maar ook doordat de uitkomsten erg variabel of niet gevoelig genoeg zijn.

Hierdoor kunnen onderzoekers onterecht besluiten dat het klinische ontwikkelingsprogramma moet worden stopgezet.<sup>7</sup> Er is echter een verschuiving gaande naar een rationelere manier van klinische geneesmiddelenontwikkeling waarbij doelgericht belangrijke farmacokinetische (wat doet het lichaam met de stof) en -dynamische kenmerken (wat doet de stof met het lichaam) van kandidaat geneesmiddelen worden geëvalueerd.<sup>8,9</sup> In de dermatologie kan deze doelgerichte benadering baat hebben bij een aanpak waar de ziekte als een geheel van alle mogelijke kanten wordt bekeken, de zogenaamde **systemendermatologie** methodologie. Hierin worden de, met het oog bepaalde, klinische bevindingen ondersteund door nieuwe objectieve uitleesmaten, zogenoemde '**biomarkers**'.<sup>7</sup> Voorbeelden van deze objectieve uitleesmaten zijn het analyseren van camerabeelden van de huid, het identificeren van immuuncellen in de huid maar ook het detecteren van huidvetten.

Het doel van dit proefschrift was om de ontwikkeling van klinische geneesmiddelen in een vroeg stadium te verbeteren door nieuwe meetmethoden te ontwikkelen en toe te passen. Deze kunnen, zonder de traditionele uitkomsten overboord te gooien, een rationele en datarijke klinische onderzoeken in een vroeg stadium mogelijk maken.

Dit proefschrift bestaat uit drie delen die de toegevoegde waarde van een datarijke aanpak voor vroege fase klinische geneesmiddelenontwikkeling illustreren. Het eerste deel beschrijft de karakterisering van **seborrhoïsch eczeem** met behulp van een **multimodale** benadering, oftewel een gelijktijdige benadering van de ziekte vanuit verschillende aspecten. Hierna wordt deze toegepast in een studie waarin een nieuw middel voor **seborrhoïsch eczeem** wordt onderzocht. In het tweede deel wordt verslag gedaan van een modelstudie in psoriasis waarbij verschillende complementaire technieken het vertrouwen in de klinische uitkomstmaten, die minder betrouwbaar zijn bij patiënten met een lage ernst van de ziekte, verhogen. In de laatste sectie wordt de **ceramidesamenstelling** van het **stratum corneum** gepositioneerd als een nuttige **biomarker** en een potentieel doelwit voor de optimalisatie van de huidbarrière. Tot slot worden in dit hoofdstuk kort de belangrijkste bevindingen van dit proefschrift beschreven en wordt een vooruitblik gegeven op de toepassing ervan in toekomstige vroege fase klinische geneesmiddelenontwikkeling van therapieën voor chronische inflammatoire huidziekten.

## **Deel 1 - Multimodale karakterisering van de huid van patiënten met seborrhoïsch eczeem.**

**Seborrhoïsch eczeem** is een chronische inflammatoire huidandoening die wordt gekenmerkt door de aanwezigheid van rode en schilferige huidplekken die voornamelijk voorkomen in gebieden waar er een verhoogde activiteit van de talgklieren is zoals het gezicht, de hoofdhuid en de bovenborst. Verschillende aspecten liggen ten grondslag aan het ontstaan van **seborrhoïsch eczeem**, maar er is veel nadruk op de aanwezigheid van de gist *Malassezia* op de aangedane huid.<sup>10</sup> Dit is echter een commensale gist, wat inhoudt dat deze ook voorkomt op de huid van mensen zonder **seborrhoïsch eczeem**. Dit betekent dat er inderdaad meerdere factoren bijdragen aan de totstandkoming van de ziekte.<sup>11</sup>

In hoofdstuk 2 wordt beschreven hoe het micro- en mycobioom, de barrièrefunctie van de huid en inflammatie samen bijdragen aan het klinische beeld bij **seborrhoïsch eczeem**. Hierbij werd gebruikt gemaakt van een **multimodale** benadering. Door eerst beelden te maken van de aangedane huid en zo de mate van roodheid en de morfologie van de huid vast te leggen, kon de aanwezigheid van een ontsteking duidelijk worden vastgesteld. Vervolgens werden het cutane **microbioom** en de barrièrefunctie gekarakteriseerd. Uit een mycobiële analyse bleek dat de gist *Malassezia* niet in verschillende hoeveelheden aanwezig was op aangedane huid in vergelijking met niet-aangedane huid, terwijl men denkt dat deze gist een belangrijke rol speelt in het ontstaan van de ziekte. Het **microbioom** van de aangedane huid vertoonde echter een verhoogde aanwezigheid van de bacterie *Staphylococcus*. Dit is een relevante bevinding gezien de ontstekingsbevorderende eigenschappen die worden toegeschreven aan *Staphylococcus aureus* bij andere huidziekten zoals **constitueel eczeem**.<sup>12</sup> Door de beperkte fylogenetische resolutie was het niet mogelijk de identificatie van het specifieke *Staphylococcus*-soort, zoals *Staphylococcus aureus* of *Staphylococcus epidermidis*, vast te stellen. Hierdoor kon er niet met zekerheid worden vastgesteld of specifiek *Staphylococcus aureus* verhoogd was of een andere soort *Staphylococcus*.

De huidbarrière functie werd gemeten aan de hand van het **trans-epidermale waterverlies**, oftewel de hoeveelheid water die vanuit de huid naar buiten verdampt. In de aangedane huid was een hoger **trans-epidermale waterverlies** dan in niet-aangedane huid. Dit duidt op een verslechterde barrière omdat de huid minder goed in staat is om het water tegen

te houden. Dit kon mogelijk ook worden toegeschreven aan het verhoogde **trans-epidermaal waterverlies** van de gezichtszones die vaak zijn aangedaan in **seborrhoïsch eczeem**, zoals de neusplooien waar er ook in gezonde mensen een relatief hoog waterverlies is.<sup>13</sup> Daarom werd de **ceramiden-samenstelling**, een bepaalde klasse van vetten, in het **stratum corneum** geanalyseerd. De vetten van het **stratum corneum** zijn belangrijk voor de barrièrefunctie, en veranderingen in de verhoudingen tussen deze vetten onderling kunnen zorgen voor een verslechterde barrière.<sup>14</sup> Uit de analyse bleek dat huidplekken met overmatig waterverlies gepaard gaan met veranderingen in de samenstelling van de ceramiden. Deze veranderingen waren vergelijkbaar met de veranderingen die eerder zijn waargenomen bij **constitutieel eczeem**, een ziektebeeld waarin de barrièrerverstoring al goed is gekarakteriseerd.<sup>15</sup> Het aantonen van de aanwezigheid van een verminderde huidbarrière in het ziektebeeld van **seborrhoïsch eczeem**, dat traditioneel vooral werd toegeschreven aan de aanwezigheid van Malassezia gisten, laat zien hoe een **multimodale** benadering nieuwe inzichten kan opleveren in de **pathofysiologie** en behandeling van ziektes.

Deze **multimodale** benadering werd ook toegepast in een **gerandomiseerd onderzoek met een controlegroep** waarin het antimicrobiële peptide omiganan werd onderzocht voor de behandeling van patiënten met milde-tot-matige **seborrhoïsch eczeem**. Het lag in de verwachting dat dit antimicrobiële middel de aanwezigheid van de bacterie Staphylococcus zou kunnen verminderen. Het was immers beschreven in hoofdstuk 3 dat er op de aangedane huid een **microbioom** aanwezig was dat niet in balans was, een zogeheten dysbiose, die gekenmerkt werd door een verhoogd aanwezigheid van Staphylococcus.

Het effect van topicale omiganan 1,75% gel tegenover placebo en ketoconazol 2,00% crème werd onderzocht. Ketoconazol is een topicaal antischimmelmiddel dat standaard wordt gebruikt bij de behandeling voor **seborrhoïsch eczeem** en diende als vergelijkend medicijn in dit onderzoek. Omiganan was veilig en werd goed verdragen, maar verminderde niet de ernst van de ziekte, bepaald aan de hand van klinische scores. Het had ook geen effect op de resultaten verkregen I) met beeldvorming, II) op door patiënten gerapporteerde effecten, III) op microbiële uitkomsten of IV) de integriteit van de huidbarrière wanneer deze werden vergeleken met de placebogroep. Daarentegen werd de werkzaamheid van ketoconazol bevestigd doordat klinische scores in vergelijking met placebo **significant** lager werden tijdens deze behandeling. Bovendien was er een uitgesproken **significante**

afname in de hoeveelheid Malassezia en een **significante** verbetering van de barrièrefunctie met een gelijktijdige normalisatie van **biomarkers** in de **ceramidesamenstelling** van het **stratum corneum**. Opmerkelijk is dat de overvloed aan Staphylococcus afnam ten opzichte van het begin in zowel de omiganan- als de ketoconazol- en placebogroep. Dit geeft aan dat de verhoogde hoeveelheid Staphylococcus niet samen lijkt te hangen met (veranderingen in) de ernst van de ziekte in de aangedane huid, aangezien een behandelingseffect niet alleen zichtbaar was bij patiënten die ketoconazol kregen. Dit nuanceert het belang van de verhoogde hoeveelheden Staphylococcus die in het onderzoek dat is beschreven in het vorige hoofdstuk waren vastgesteld. Deze studie toont echter de dynamiek van de barrièrefunctie tijdens de behandeling aan en laat hiermee het verband zien tussen de barrièrefunctie en de **ceramidesamenstelling** van het **stratum corneum**. Dit onderstreept het belang van barrière disfunctie bij **seborrhoïsch eczeem** verder. Uiteindelijk blijkt uit het onderzoek beschreven in dit hoofdstuk dat een **multimodale** benadering een hoge toegevoegde waarde kan hebben in onderzoek naar de **pathofysiologie** van een ziekte en dat behandelings-gerelateerde effecten hier zelfs nog verder aan kunnen bijdragen.

## **Deel 2 - Het belang van milde psoriasispatiënten voor vroege fase klinische geneesmiddelenontwikkeling, gebruik makend van een multimodale beeldvormingsbenadering**

Dit hoofdstuk gaat over een modelstudie bij chronische plaque psoriasis. Psoriasis is een veel voorkomende chronische inflammatoire huidziekte waar wereldwijd tot 3% van de bevolking aan leidt. Psoriasis heeft een aanzienlijke impact op de levenskwaliteit van patiënten, maar kan steeds beter worden behandeld met **biologics**.<sup>16,17</sup> In dit onderzoek werden milde en matig-tot-ernstige psoriasispatiënten gerandomiseerd tot een korte behandeling met **guselkumab** of **placebo**. **Guselkumab** is een zeer effectief middel voor de behandeling van matige-tot-ernstige plaque psoriasis. Het is een monoklonaal antilichaam gericht tegen het ontstekingseiwit interleukine-23, een belangrijke spil in psoriasis. **Guselkumab** bindt aan dit eiwit en voorkomt zo dat het een ontsteking kan veroorzaken. Hiermee wordt uiteindelijk de hele ontsteking in de huid weggenomen en verdwijnt de psoriasis.<sup>18,19</sup>

Uit de studies beschreven in hoofdstuk 4 blijkt dat onze groep van milde patiënten baat had bij een korte behandeling met **guselkumab**. Patiënten in deze groep, die tot 80% van alle psoriasispatiënten omvat, komen meestal niet

in aanmerking voor een behandeling met **biologics** gezien de hoge kosten die met deze behandeling gepaard gaan.<sup>20</sup> Onderzoekers hielden het echter voor mogelijk dat psoriasis permanent kon worden verholpen door mensen met een lichte ziekte ernst te behandelen met deze uiterst effectieve therapieën. In dit geval zou therapie met **biologics** ook kosteneffectief kunnen worden in deze populatie.<sup>21</sup> Immers, als er maar een paar injecties met **guselkumab** nodig zijn om te zorgen dat iemand geneest, is dit mogelijk een goedkope optie vergeleken met chronisch gebruik van medicatie en de bijkomende zorgverlening die hierbij komt kijken. Daarbij wordt ook voorkomen dat de ziekte zich in een later stadium uitbreidt en een behandeling van de ziekte met dure middelen alsnog noodzakelijk wordt. Een korte behandeling met een **biologic** zou hierdoor ook voor milde patiënten financieel aantrekkelijk worden. Helaas kregen alle patiënten in onze studie na het stoppen van de behandeling met **guselkumab** weer meer psoriasis. Desondanks duurde het soms langer dan 1 jaar na het geven van de laatste injectie voordat patiënten een terugval kregen, wat aantoont dat milde patiënten wel enorm profiteren van een korte behandeling met **guselkumab**. Het is mogelijk dat milde patiënten in de toekomst vaker in aanmerking kunnen komen voor een behandeling met **biologics** naarmate deze therapie goedkoper wordt, mogelijk door de ontwikkeling van **biosimilars** (goedkopere kopieën van de middelen die nu op de markt zijn) of door de verlenging van de tijd tussen het geven van opeenvolgende injecties waardoor er in totaal minder medicatie nodig is.<sup>22</sup>

Verzekerd van een duidelijk behandelings-effect, werd de reactie van deze milde patiënten op guselkumab verder gekarakteriseerd en vergeleken met die van matige-tot-ernstige patiënten die dezelfde therapie kregen. Dit is beschreven in hoofdstuk 5. Matige-tot-ernstige psoriasispatiënten kunnen tegenwoordig in de praktijk goed behandeld worden, onder andere met de guselkumab therapie die gebruikt wordt in de studies beschreven in dit proefschrift. Voor geneesmiddelenonderzoek is het echter belangrijk dat de ziekte duidelijk aanwezig is bij een patiënt voordat er een nieuw experimenteel middel toegediend wordt. Op die manier kan er worden aangetoond of het experimentele middel de psoriasis verminderd. Dit zou echter betekenen dat patiënten die nu hun ziekte goed onder controle kunnen houden eerst met hun medicatie moeten stoppen, waarna de ziekte kan terugkomen en patiënten weer kunnen deelnemen aan onderzoek. Dit legt een zware last op de patiënten en resulteert hierdoor in een daling van de hoeveelheid patiënten die deel kunnen en willen nemen aan onderzoeken. Daartegenover zou de deelname van milde patiënten een goed alternatief kan zijn. Deze patiënten

komen vaak niet in aanmerking voor dit soort goedwerkende behandelingen door de hoge kosten. Hoewel uit de studie beschreven in hoofdstuk 4 blijkt dat de behandeling met guselkumab effectief is bij milde patiënten, wordt het gebruik van klinische uitkomstmaten zoals de veelgebruikte Psoriasis Area and Severity Index (PASI)-score bij een lage ernst van de ziekte belemmerd door een lagere gevoeligheid.<sup>23</sup> Hierdoor kan het zo zijn dat de effecten bij milde patiënten niet goed kunnen worden opgepikt. Daarom werd een **multimodale** beeldvormings-toolbox toegepast om de waargenomen klinische effecten op een objectieve manier te ondersteunen. Met deze toolbox werd een psoriasisplek gevolgd met verschillende beeldvormingstechnieken, namelijk multispectrale beeldvorming, laser speckle contrast imaging en optical coherence tomography (zie afbeelding 1). Met multispectrale beeldvorming wordt het huidoppervlak vanuit meerdere kanten met verschillende kleuren licht beschenen waarmee een driedimensionaal beeld gevormd kan worden en de kleur van de huid goed kan worden bepaald.<sup>24</sup> In laser speckle contrast imaging wordt de huid beschenen met een near-infrarood laser en het licht dat van de huid terugkaatst wordt opgepikt door een detector. De doorbloeding van de huid zorgt ervoor dat het signaal verstoord wordt en een sterke mate van verstoring duidt op een hoge doorbloeding van de huid.<sup>25</sup> Tot slot werd de huid ook nog bekeken met optical coherence tomography. Hiermee wordt gevisualiseerd hoe de huid er onder de oppervlakte uit ziet en kan de dikte van de epidermis bepaald worden. Deze is vaak dikker in aangedane huid.<sup>26</sup>

De **multimodale** aanpak met verschillende cameras toonde, in overeenstemming met de **significante** afnames in de klinische scores, een significante vermindering in roodheid, significante verlaging van de ruwheid, significant verminderde doorbloeding en een verminderde epidermale dikte aan in de psoriasisplek. Al deze eigenschappen zijn verhoogd in de aangedane huid en duiden er dus op dat de huid zich geleidelijk herstelt. De objectieve beeldvormingstechnieken blijken hiermee waardevolle toevoegingen die de klinische scores, bepaald door artsen, konden verduidelijken en hielp onderbouwen. Bovendien bleek dat de klinische reactie op **guselkumab** bij milde patiënten vergelijkbaar is met de reactie van matige-tot-ernstige patiënten. Dit levert de mogelijkheid op om de populatie van milde psoriasispatiënten, die gemakkelijker te rekruteren is, op te nemen in toekomstige onderzoeken als een alternatief voor matige-tot-ernstige psoriasispatiënten en zou zo de ontwikkeling van **geneesmiddelen in een vroege fase** bij psoriasis kunnen versnellen.





Om het therapeutische gebied waarin de bepaling van het ceramide profiel zou kunnen worden toegepast af te bakenen, is in hoofdstuk 6 een systematische review en meta-analyse uitgevoerd waarin alle beschikbare literatuur over **ceramidesamenstellingen** in huidziekten is verzameld. Na het selecteren van artikelen die de uitkomsten direct vergelijken met de uitkomsten van gezonde vrijwilligers, bleek dat de ceramidesamenstelling van het **stratum corneum** bij **constitutioneel eczeem**, psoriasis, ichthyosis, xerosis, acne en palmoplantaire hyperkeratose veel van dezelfde veranderingen vertoonde; voornamelijk verminderde hoeveelheden CER[NP] en een verminderde gemiddelde lengte van de ceramide moleculen. Interessant genoeg was de aanwezigheid van de zeer korte ceramide CER[NSC34], een ceramide uit subklasse CER[NS] met een totale koolstofketenlengte van 34 atomen, consistent verhoogd in de aangedane huid van patiënten vergeleken met die van gezonde controles. Deze resultaten werden verder ondersteund door het uitvoeren van een meta-analyse. Hierin werden 31 **ceramidesamenstellingen** van gezonde controles en 68 **ceramidesamenstellingen** van verschillende huidziekten gecombineerd. Hieruit bleek dat de hoeveelheden van voornamelijk CER[NS], CER[NP] en CER[AS] veranderd waren bij **constitutioneel eczeem**, psoriasis, ichthyosis, palmoplantaire hyperkeratose en acne. De **ceramidesamenstelling** in de niet-aangedane huid van **constitutioneel eczeem** en psoriasis vertoonde een hoge mate van overeenkomst met die in gezonde controles. Hieruit blijkt dat de veranderingen in de **ceramidesamenstelling** van niet-aangedane **constitutioneel eczeem** die in de literatuur worden beschreven, niet zo éénzijdig zijn als de veranderingen die aanwezig zijn in de aangedane huid.

De mogelijkheid om met de **ceramidesamenstelling** een onderscheid te kunnen maken tussen de aangedane huid en niet-aangedane of gezonde huid werd vervolgens onderzocht in de eerdergenoemde psoriasisstudie beschreven in hoofdstuk 7. De resultaten vermeld in dit hoofdstuk komen goed overeen met de resultaten van de systematische literatuurstudie beschreven in hoofdstuk 6. De **stratum corneum ceramidesamenstelling** van de aangedane huid van psoriasis patiënten vertoonde **significant** verhoogde hoeveelheid CER[NS], CER[AS] en **significant** verlaagde hoeveelheid CER[NP] en CER[AP] vergeleken met de niet-aangedane huid en huid van gezonde controles. Daarnaast was de gemiddelde ketenlengte van ceramiden significant afgenomen en de hoeveelheid onverzadigde CER[NS], een CER[NS] ceramide met een extra dubbele binding in één van de staarten, en CER[NSC34]

significant toegenomen in de aangedane huid. Deze veranderingen hingen samen met de verslechterde barrièrefunctie die was bepaald via het **trans-epidermaal waterverlies**. Zoals beschreven in hoofdstuk 6 werden er geen noemenswaardige verschillen waargenomen tussen milde en matige-tot-ernstige patiënten. De **ceramidesamenstelling** werd ook onderzocht tijdens de behandeling met **guselkumab** of **placebo**. Er kon duidelijk onderscheid gemaakt worden tussen patiënten die **guselkumab** kregen en patiënten die placebo kregen. De samenstelling correleerde goed met afnamen in klinische ziekte-ernst en het **trans-epidermaal waterverlies**. Omdat de **ceramidesamenstelling** hetzelfde laat zien over tijd als de ziektelast, zou het bepalen van de **ceramidesamenstelling** als **biomarker** kunnen worden gebruikt. Dat het eveneens samen lijkt te hangen met de barrièrefunctie onderstreept dat een normale **ceramidesamenstelling** belangrijk is voor een goede huidbarrière.

De relatie tussen de verslechterde huidbarrière en veranderingen in de **ceramidesamenstelling** zoals gerapporteerd voor **constitutioneel eczeem**, **seborrhoïsch eczeem** en psoriasis staat waarschijnlijk ook in verband met de **pathofysiologie** van deze ziektes. Hiermee zou de huidbarrière een potentieel doel kunnen vormen voor nieuwe therapieën.<sup>31,32</sup> In hoofdstuk 8 wordt de mogelijkheid beschreven om specifieke delen in de lipidenaanmaak in de huid te beïnvloeden met behulp van *in vitro*, oftewel in het lab, gekweekte **huidequivalenten**. Hoewel **huidequivalenten** veel lijken op de menselijke huid, is de barrièrefunctie van deze **huidequivalenten** vermindert en vertoont de **ceramidesamenstelling** soortgelijke veranderingen als die worden waargenomen bij huidziekten, zoals besproken in hoofdstuk 6 waaronder een verhoogde hoeveelheid onverzadigde lipiden.<sup>33</sup> In een poging om deze hoeveelheid te verminderen werden deze modellen gekweekt met toevoeging van een remmer voor stearoyl-CoA desaturase-1 (**SCD-1**), het enzym dat verantwoordelijk is voor de omzetting van verzadigde vetzuren in enkelvoudig onverzadigde vetzuren.<sup>34</sup> Toevoeging van **SCD-1** remmer verminderde met succes de mate van onverzadiging in de vetzuren en ceramiden, maar deze was nog steeds hoger in vergelijking met de mate van onverzadiging in de normale menselijke huid. Bovendien bleef de **organisatie van de stratum corneum vetten**, die ook belangrijk is voor de barrièrefunctie van de huid en samenhangt met de aanwezigheid van onverzadigde vetten, vergelijkbaar met die van modellen zonder toevoeging van de **SCD-1** remmer. Ook de barrièrefunctie bleef vergelijkbaar met die van modellen waar geen **SCD-1** remmer aan was toegevoegd. Dat er ondanks

het remmen van **SCD-1** nog steeds enkelvoudig onverzadigde vetten aanwezig waren kan verklaard worden door een sterke verhoging van de aanmaak van **SCD-1** in de huid na toevoeging van de remmer. Een zekere mate van basisactiviteit van **SCD-1** blijft waarschijnlijk noodzakelijk voor vele andere biologische processen in de cel, zoals de aanmaak van onverzadigde lipiden die gebruikt worden voor celmembranen. Om te zorgen dat deze processen toch door konden gaan werd er waarschijnlijk aanzienlijk meer **SCD-1** aangemaakt om de remming teniet te doen. Hoewel de aanwezigheid van overgebleven enkelvoudig onverzadigde lipiden zou kunnen verklaren waarom er alleen een verwaarloosbare invloed op de barrièrefunctie was, zou het ook kunnen betekenen dat de barrièrefunctie van de huid van meer factoren afhankelijk is dan alleen de hoeveelheid onverzadigde vetten. Het zou bijvoorbeeld kunnen dat juist de **ceramidencompositie** en ketenlengte belangrijk zijn, of de hoeveelheid verzadigde vetten. Niettemin laat deze studie zien dat de veranderingen in de **ceramidesamenstelling** kunnen worden hersteld met behulp van een farmacologische interventie. In de toekomst zou de verminderde huidbarrière bij inflammatoire huidziekten mogelijk hersteld kunnen worden door het corrigeren van veranderingen in de vetten van het **stratum corneum**, wat uiteindelijk geïntegreerd kan worden in bestaande behandelingen om opvlammingen en terugvallen van de ziektes te voorkomen.

Samenvattend wordt in dit hoofdstuk beschreven dat veranderingen in de **ceramidesamenstelling** aanwezig zijn bij verschillende dermatologische aandoeningen, kunnen worden gebruikt als een nuttige **biomarker** ter ondersteuning van een **multimodale** aanpak van geneesmiddelontwikkeling en het een mogelijk aangrijpingspunt vormt voor nieuwe therapie.

## Perspectieven

### DE UITBREIDING VAN TOEKOMSTIGE VROEGE FASE KLINISCHE GENEESMIDDELENONDERZOEKEN MET EEN DATARIJKE AANPAK

De eindpunten in **vroege fase klinische geneesmiddelenonderzoek** bij patiënten lijken momenteel sterk op de eindpunten die gebruikt worden in **vroege fase onderzoek** in gezonde vrijwilligers. De eindpunten richten zich voornamelijk naar de veiligheid van een onderzoeksmiddel en proberen tegelijkertijd een geschikt toedieningsschema voor patiënten vast te stellen

op basis van **farmacodynamische** effecten voordat er wordt overgegaan op grotere groepen patiënten. Het selecteren van de optimale dosis wordt vaak gestuurd door het afwegen van ongewenste bijwerkingen met de afname van de ernst van de ziekte. Traditionele eindpunten zoals de Seborrheic Dermatitis Area and Severity Index of Psoriasis Area and Severity Index, zoals gebruikt in het onderzoek beschreven in dit proefschrift, worden echter in verband gebracht met een beperkte objectiviteit en gevoeligheid omdat ze visueel worden bepaald door artsen en categorisch zijn van aard. Het zou dus kunnen dat verschillende artsen de ziektelast verschillend inschatten. In combinatie met de mogelijkheid dat een waarneembare daling in ziektelast pas na een langere behandelingsperiode met het oog zichtbaar zou kunnen worden, is het mogelijk dat medicijneffecten over het hoofd worden gezien. Het gebruik van een **multimodale** benadering in onderzoek biedt de onderzoeker aanvullende resultaten die er aan bijdragen de behandelrespons bij patiënten objectief te bepalen. Het zou ervoor kunnen zorgen dat de ontwikkeling van kandidaat-geneesmiddelen mogelijk minder snel wordt afgebroken omdat het niet voldoende werkzaam lijkt, bijvoorbeeld omdat het onvoldoende hoog is gedoseerd om een breed detecteerbaar effect te bereiken. Daarnaast zou het implementeren van de technologieën die in dit proefschrift worden beschreven, kunnen helpen bij het bepalen van het 'minimaal verwachte biologische effectniveau' bij therapieën. Dit is de minimale dosis van een medicijn die een effect laat zien bij patiënten. Met deze aanpak zouden medicijnen die juist bijwerkingen vertonen doordat ze te sterk werken in plaats van bijwerkingen veroorzaken doordat, naarmate de dosis hoger wordt, andere processen dan het ziekteproces verstoord worden, tijdig kunnen worden opgemerkt. Dit kan het geval zijn bij **biologics** zoals gebruikt in het onderzoek beschreven in dit proefschrift die door hun specifieke werking eigenlijk voor weinig bijwerkingen zorgen.<sup>35</sup> Uiteindelijk kunnen de **biomarkers** die in dit proefschrift beschreven zijn de ontwikkeling van geneesmiddelen in de **vroege klinische fase** bevorderen door een solide basis te bieden voor het stap-voor-stap verhogen van de dosis en daarmee kunnen helpen bij de selectie voor de juiste doseringen voor latere fases van het onderzoek.

Naast de toepassing van dit platform in de vroege stadia van medicijnontwikkeling, kan een dergelijke benadering ook worden toegepast in de latere stadia om de respons tussen verschillende behandelingen te vergelijken. Voor patiënten met matige-tot-ernstige psoriasis zijn verschillende

**biologics** beschikbaar die allemaal een hoge mate van werkzaamheid vertonen. Om de meest gunstige therapie voor patiënten te vinden, zouden **gerandomiseerde** gecontroleerde fase III klinische onderzoeken kunnen worden uitgevoerd waarin nieuwe behandelingen worden vergeleken met de oude standaardbehandeling. Deze moeten echter vaak uitgevoerd worden met een zeer groot aantal patiënten.<sup>36</sup> In plaats daarvan kunnen technieken zoals gepresenteerd in dit proefschrift worden gebruikt om de respons van twee middelen ‘een-op-een’ te vergelijken in een kleinere groep patiënten, maar met de toevoeging van uitgebreidere meetmethodes die meerdere modaliteiten omvatten. Dit zou alsnog een goede mate van zekerheid geven voor deze nieuwe medicijnen. Bovendien zou het gebruik van deze aanpak om de gelijkwaardigheid van **biosimilars** aan te tonen, hun markttoegang kunnen versnellen. Dit zou hun ontwikkelingskosten kunnen verlagen wat belangrijk is om de prijs van deze therapieën laag te houden.

De metingen die beschreven zijn in de hoofdstukken van dit proefschrift zijn allemaal minimaal of niet-invasief van aard. Beeldvorming, wattenstaafjes of plakband laten geen blijvende sporen achter bij de proefpersonen waardoor ze intensief en herhaaldelijk gebruikt kunnen worden tijdens langdurige studies. Bovendien vormen ze een aanvullende reeks metingen die invasieve varianten zoals huidbiopten misschien zelfs kunnen vervangen. Optical Coherence Tomography, zoals gebruikt in dit proefschrift, zou artsen kunnen voorzien van een gedetailleerde en directe uitleesmaat over hoe de bovenste huidlagen er onder het oppervlakte uit zien.<sup>37,38</sup> Hoewel het hiermee niet mogelijk is om specifieke eiwitten en immuuncellen in de huid te bepalen, heeft de combinatie van tape stripping met technieken zoals sequencing (bepaling van welke genen er actief zijn) en proteomics (bepaling van welke eiwitten er aanwezig zijn) eerder aangetoond dat het mogelijk is om het specifieke immuun profiel van **constitutioneel eczeem** en psoriasis te detecteren in een mate die vergelijkbaar is met invasieve biopten.<sup>39,40</sup> Dit zou het gebruik van huidbiopten in de toekomst overbodig kunnen maken en voorkomen dat mensen nog lang littekens blijven houden na een onderzoek of diagnose. Bij **seborrhoïsch eczeem** zou een dergelijke benadering van groot belang zijn gezien de locatie van aangedane huid in het gezicht, waardoor het herhaaldelijk uitvoeren van biopten voor de monitoring van de ziekte uitgesloten is. Bovendien is het nog steeds niet duidelijk welk mechanisme in het immuunsysteem de grootste rol speelt in **seborrhoïsch eczeem**. Het is goed mogelijk dat deze grote gelijkenis vertoont met die van

**constitutioneel eczeem** en, indien bewezen, zou dit aanleiding kunnen zijn voor het starten van studies naar het gebruik van geneesmiddelen die al zijn goedgekeurd voor **constitutioneel eczeem** voor de behandeling van **seborrhoïsch eczeem**. Dit zou een kostenbesparend alternatief kunnen zijn voor omdat het gebruik van bestaande middelen goedkoper is dan de ontwikkeling van geheel nieuwe behandelingen.

Al met al is de toepassing van deze **multimodale** toolbox in dermatologisch onderzoek veelbelovend. Dit proefschrift biedt verschillende modaliteiten die verder ontwikkeld en gevalideerd kunnen worden om vervolgens gebruikt te kunnen worden in zowel medicijnontwikkeling als de klinische praktijk.<sup>41,42</sup>

## DE BARRIÈRE ALS MEDEVEROORZAKER VAN CHRONISCHE INFLAMMATOIRE HUIDZIEKTEN

De verminderde cutane barrièrefunctie wordt al langere tijd beschouwd als een verergerende factor voor **constitutioneel eczeem**.<sup>32</sup> Op basis van dit proefschrift zou een soortgelijke rol kunnen worden toegeschreven aan de verstoorde barrièrefunctie in **seborrhoïsch eczeem**. Bij **constitutioneel eczeem** worden vette zalven in hoge mate gebruikt met als doel de verstoorde huidbarrière te herstellen en de ziekte onder controle te houden.<sup>43</sup> Deze vette zalven, of emoliënten, worden echter niet vaak overwogen voor de behandeling van **seborrhoïsch eczeem**. Dit komt mogelijk door de veronderstelling dat het gebruik ervan overbodig zou zijn omdat er al een hoge productie van vetten is rondom de aangedane huid. Het blijkt dat gebruik van zalf de werkzaamheid van andere gelijktijdige gebruikte topicale therapieën verhoogt in **constitutioneel eczeem**, wat ook mogelijk zou kunnen zijn bij **seborrhoïsch eczeem**. Aangezien er nog steeds een medische noodzaak bestaat bij patiënten met **seborrhoïsch eczeem**,<sup>44</sup> zou het een haalbare en kosteneffectieve benadering kunnen zijn om de combinatie van bestaande medicatie voor **seborrhoïsch eczeem** met zalven te onderzoeken. Bovendien zou deze aanpak op meer huidziekten kunnen worden toegepast, aangezien de systematische literatuurstudie in hoofdstuk 6 laat zien dat de specifieke veranderingen in de **ceramidesamenstelling** van het **stratum corneum** in **seborrhoïsch eczeem** voorkomt in meer dermatologische aandoeningen. Hoewel dit een veelbelovend resultaat is, geeft dit review ook aan dat er over de **ceramidesamenstelling** in andere ziektebeelden dan **constitutioneel eczeem**, psoriasis en ichthyosis nog kennis ontbreekt.

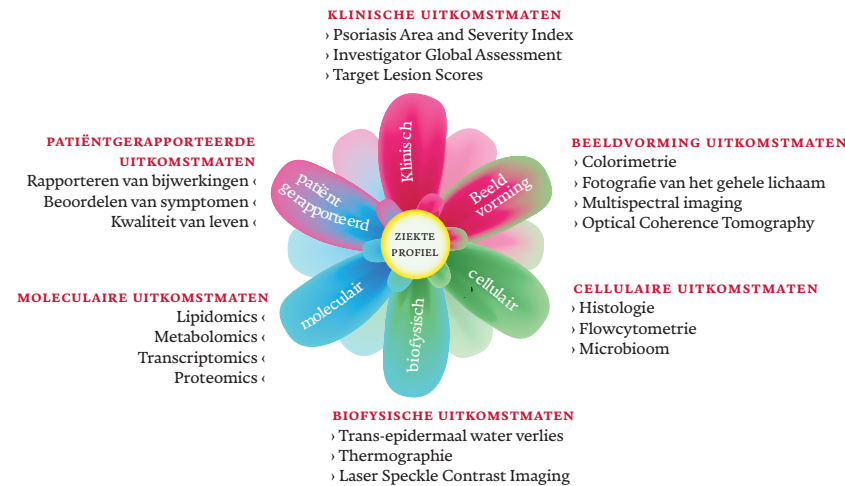
Voor bijvoorbeeld acne en hoofdroos is de **ceramidesamenstelling** nog niet onderzocht met de laatste technieken. Het toepassen van een uitgebreide analyse van de **ceramidesamenstelling**, zoals is uitgevoerd in hoofdstuk 7, zou een waardevolle aanvulling zijn voor deze ziektebeelden. Daarbij zijn er nog ziektebeelden waar de **ceramidesamenstelling** nog helemaal niet onderzocht is. Een grondige aanpak waarbij de **ceramidesamenstelling** van aangedane huid met de nieuwste technieken wordt vergeleken met dat van gezonde vrijwilligers meteen kan zorgen voor veel zekerheid over of de **ceramidesamenstelling** inderdaad veranderd is. Het daarbij vergelijken van de **ceramidenprofielen** van de aangedane en niet-aangedane huid, of de aangedane huid tijdens een behandeling, zou dit nog sterker maken. Het nauwkeurig karakteriseren van de **ceramidesamenstelling** van alle huidziekten zou de weg vrij kunnen maken voor het gebruik ervan als **biomarker** in klinische studies. Hoewel het platform dat in dit proefschrift is gebruikt uitgebreid is en een zeer hoge mate van detail gerechtvaardigd is voor het definiëren van de belangrijke verschillen tussen zieke en gezonde huid, blijft deze analyse duur en tijdrovend. Miniaturisatie van het proces zou nodig kunnen zijn voordat het op grote schaal kan worden toegepast als een klinisch onderzoeksinstrument. Op verschillende punten in het proces zouden verbeteringen doorgevoerd kunnen worden; I) er zou geprobeerd kunnen worden om het aantal stukjes plakband, waarmee de vetten van de huid af geharst worden, terug te brengen naar één enkel stukje waardoor de afname sneller kan gebeuren waardoor er minder tapes moeten worden verwerkt, II) er zou gekeken kunnen worden naar het ontwerpen van een kant-en-klare kit voor afname van deze vetten waardoor artsen, verpleegkundigen of patiënten zelf de afname kunnen doen en III) nadat de **ceramidesamenstelling** voor de eerste keer grondig is onderzocht, zou hierna alleen gekeken kunnen worden naar de veranderingen in het profiel die specifiek bij een ziekte voorkomen. Tezamen zou hierdoor de analyse vergemakkelijkt kunnen worden waardoor deze breed inzetbaar wordt.

### **HET GEBRUIK VAN SYSTEEMDERMATOLOGIE IN DE VROEGE FASE VAN GENEESMIDDELENONDERZOEK OM EEN BETER BEGRIP VAN DE ZIEKTE TE VERKRIJGEN**

De toegevoegde waarde van een **multimodale** benadering in de **vroege fase van geneesmiddelenonderzoek** voor het fundamentele begrip van ziektes wordt geïllustreerd in hoofdstuk 1. Hier zorgt het gelijktijdig onderzoeken van meerdere aspecten van dezelfde ziekte voor een kijk in de veelzijdige

**pathofysiologie** van **seborrhoïsch eczeem**. Door namelijk de ontsteking, de barrière en het **microbioom** binnen patiënten te vergelijken bleek er een duidelijke rol voor de huidbarrière weggelegd te zijn in deze ziekte. Het belang van een **multimodale** aanpak voor het onderzoek naar chronische inflammatoire huidziekten wordt benadrukt nu de eerste **biologics** die zijn ontwikkeld voor **constitueel eczeem**, niet zo effectief lijken te zijn als de biologics die zijn ontwikkeld voor psoriasis.<sup>45</sup> Het lijkt er op dat er meer aspecten bijdragen aan de totstandkoming van de ziekte waardoor het specifiek verhinderen van één enkel proces, of eigenlijk het verhinderen van één enkel proces in het immuunsysteem dat op zijn beurt voor een deel bijdraagt aan de ziekte, niet genoeg is voor het effectief behandelen van de ziekte. Een **multimodale** benadering van ziekten zou het mogelijk kunnen maken om verschillende **endotypes** van ziekten te bepalen.<sup>46</sup> **Endotypes** zijn verschillende types van dezelfde ziekte met belangrijke verschillen in de achterliggende ziekteprocessen. Hier zou een **multimodale** benadering noodzakelijk kunnen zijn. Het precieze **endotype** zou namelijk bepaald kunnen worden door specifieke veranderingen in bijvoorbeeld de samenstelling van de barrière, het immuunsysteem, het **microbioom** of juist een combinatie van deze aspecten. In de praktijk zou dit zich voor inflammatoire huidziekten uiteindelijk kunnen vertalen tot een behandeling waarbij meerdere delen binnen het immuunsysteem tegelijk moeten worden geremd, maar waarbij ook de verschillen in het **microbioom** worden aangepakt. Om dit te bereiken, zouden patiënten eerst als één geheel gekarakteriseerd moeten worden met behulp van een volledige **multimodale** aanpak waarbij niet specifiek wordt gekeken naar enkele aspecten, maar er ruimte is om nieuwe bevindingen te doen om zo alle factoren van de ziekte vast te leggen (afbeelding 3). Hieruit zou duidelijk kunnen worden wat een **endotype** definieert. Op zichzelf kunnen deze modaliteiten ook aanvullende informatie opleveren over de **pathofysiologie** van de ziekte. Met zo'n benadering wordt er ook een enorme hoeveelheid data gegenereerd. De integratie van al deze data met behulp van bijvoorbeeld machine learning en artificial intelligence zou deze berg data kunnen samenvatten in een enkele uitleesmaat; de verschillende **endotypes**. Deze data kan dan worden gebruikt in een patiëntgerichte aanpak, waar het **endotype** de basis vormt voor de keuze voor de behandeling waar die specifieke patiënt waarschijnlijk het best op zou reageren. Ook zou zo'n enkele uitleesmaat die opgebouwd is uit veel verschillende componenten gebruikt kunnen worden om te onderzoeken of een geselecteerde behandeling na verloop van tijd nog steeds de optimale keuze is voor een patiënt.<sup>47</sup>

**Afbeelding 3** Overzicht van de opbouw van een multimodale benadering. Bij elke aparte modaliteit, bijvoorbeeld de uitkomsten uit beeldvormingstechnieken, worden enkele voorbeelden van de technieken die hieronder vallen genoemd. Tezamen beschrijven alle modaliteiten de ziekten in groot detail.



## Algemene conclusie

Dit proefschrift beschrijft de toepassing van een **multimodale** benadering die gebruik maakt van veel verschillende **biomarkers** voor de ontwikkeling van geneesmiddelen voor chronische inflammatoire huidziekten. Het illustreert hoe men de kennis over de **pathofysiologie** van ziekten kan vergroten door gebruik te maken van veel verschillende data. Het laat ook zien dat zo'n aanpak een waardevolle toevoeging is om traditionele eindpunten die ingeschat worden door artsen te onderbouwen, zodat er met meer zekerheid een oordeel kan worden geveld over hoe werkzaam een nieuw middel is. Daarnaast laat het proefschrift de toepasbaarheid zien van de **ceramide-samenstelling** als **biomarker** in klinisch onderzoek, en bied dit een opzet om deze techniek ook te gebruiken bij andere inflammatoire huidaandoeningen of dermatologie in het algemeen. Uiteindelijk kunnen de bevindingen uit dit proefschrift worden geïmplementeerd in klinische studies, waar het een rationelere benadering van de effecten van geneesmiddelen tijdens de vroege klinische ontwikkeling in de dermatologie kan faciliteren.

## REFERENTIES

- Richard, M. A. *et al.* Prevalence of most common skin diseases in Europe: a population-based study. *Journal of the European Academy of Dermatology and Venereology* 36, 1088 (2022).
- Hawkes, J. E., Chan, T. C. & Krueger, J. G. Psoriasis Pathogenesis and the Development of Novel, Targeted Immune Therapies. *J Allergy Clin Immunol* 140, 645 (2017).
- Guttman-Yassky, E. & Krueger, J. G. Atopic dermatitis and psoriasis: two different immune diseases or one spectrum? *Curr Opin Immunol* 48, 68–73 (2017).
- A Comparison of Psoriasis Drug Failure Rates and Reasons for Discontinuation in Biologics vs Conventional Systemic Therapies. *Journal of Drugs in Dermatology* 13, 848–853 (2014).
- Pereyra-Rodriguez, J. J. *et al.* Short-term effectiveness and safety of biologics and small molecule drugs for moderate to severe atopic dermatitis: A systematic review and network meta-analysis. *Life* 11, 927 (2021).
- Willan, A. R., O'Brien, B. J. & Cook, D. J. Benefit-risk ratios in the assessment of the clinical evidence of a new therapy. *Control Clin Trials* 18, 121–130 (1997).
- Rissmann, R., Moerland, M. & van Doorn, M. B. A. Blueprint for mechanistic, data-rich early phase clinical pharmacology studies in dermatology. *Br J Clin Pharmacol* 86, 1011 (2020).
- Cohen, A. F., Burggraaf, J., Van Gerven, J. M. A., Moerland, M. & Groeneveld, G. J. The Use of Biomarkers in Human Pharmacology (Phase I) Studies. <https://doi.org/10.1146/annurev-pharmtox-011613-135918> 55, 55–74 (2015).
- Visser, S. J. de. A question based approach to drug development. *Doctoral Thesis* (Leiden University, 2003).
- Wikramanayake, T. C., Borda, L. J., Miteva, M. & Paus, R. Seboreic dermatitis—Looking beyond Malassezia. *Exp Dermatol* 28, 991–1001 (2019).
- Findley, K. *et al.* Topographic diversity of fungal and bacterial communities in human skin. *Nature* 2013 498:7454 498, 367–370 (2013).
- Geoghegan, J. A., Irvine, A. D. & Foster, T. J. Staphylococcus aureus and Atopic Dermatitis: A Complex and Evolving Relationship. *Trends Microbiol* 26, 484–497 (2018).
- Voegeli, R., Gierschendorf, J., Summers, B. & Rawlings, A. V. Facial skin mapping: from single point bio-instrumental evaluation to continuous visualization of skin hydration, barrier function, skin surface pH, and sebum in different ethnic skin types. *Int J Cosmet Sci* 41, 411–424 (2019).
- Bouwstra, J. A. *et al.* The skin barrier: An extraordinary interface with an exceptional lipid organization. *Prog Lipid Res* 92, 101252 (2023).
- Kim, B. E. & Leung, D. Y. M. Significance of Skin Barrier Dysfunction in Atopic Dermatitis. *Allergy Asthma Immunol Res* 10, 207 (2018).
- Langley, R. G. B., Krueger, G. G. & Griffiths, C. E. M. Psoriasis: epidemiology, clinical features, and quality of life. *Ann Rheum Dis* 64, iii8 (2005).
- Sbidian, E. *et al.* Systemic pharmacological treatments for chronic plaque psoriasis: a network meta-analysis. *Cochrane Database Syst Rev* 2017, (2017).
- Puig, L., Daudén, E., Cuervas-Mons, M., Novella, C. & Guisado, C. Persistence and effectiveness of guselkumab treatment in patients with moderate-to-severe plaque psoriasis in a non-interventional real-world setting: The SPRING study. *Journal of the European Academy of Dermatology and Venereology* 00, 1–11 (2023).
- Blauvelt, A. *et al.* Efficacy and safety of guselkumab, an anti-interleukin-23 monoclonal antibody, compared with adalimumab for the continuous treatment of patients with moderate to severe psoriasis: Results from the phase III, double-blinded, placebo- and active comparator-controlled VOYAGE 1 trial. *J Am Acad Dermatol* 76, 405–417 (2017).
- Papp, K. A. *et al.* Psoriasis Prevalence and Severity by Expert Elicitation. *Dermatol Ther (Heidelb)* 11, 1053 (2021).
- Eyerich, K. *et al.* IL-23 blockade with guselkumab potentially modifies psoriasis pathogenesis: rationale and study protocol of a phase 3b, randomised, double-blind, multicentre study in participants with moderate-to-severe plaque-type psoriasis (GUIDE). *BMJ Open* 11, (2021).
- Michielsens, C. A. J., van Muijen, M. E., Verhoef, L. M., van den Reek, J. M. P. A. & de Jong, E. M. G. J. Dose Tapering of Biologics in Patients with Psoriasis: A Scoping Review. *Drugs* 81, 349–366 (2021).
- Papp, K. A. *et al.* The Proposed PASI-HD Provides More Precise Assessment of Plaque Psoriasis Severity in Anatomical Regions with a Low Area Score. *Dermatol Ther (Heidelb)* 11, 1079–1083 (2021).
- Matias, A. R., Ferreira, M., Costa, P. & Neto, P. Skin colour, skin redness and melanin biometric measurements: comparison study between Antera® 3D, Mexameter® and Colorimeter®. *Skin Research and Technology* 21, 346–362 (2015).
- Linkous, C. *et al.* Applications of Laser Speckle Contrast Imaging Technology in Dermatology. *JID Innov* 3, 100187 (2023).
- Sattler, E., Kästle, R. & Welzel, J. Optical coherence tomography in dermatology. *J Biomed Opt* 18, 061224 (2013).
- van Smeden, J., Janssens, M., Gooris, G. S. & Bouwstra, J. A. The important role of stratum corneum lipids for the cutaneous barrier function. *Biochim Biophys Acta Mol Cell Biol Lipids* doi:https://dx.doi.org/10.1016/j.bbalip.2013.11.006.
- Kawana, M., Miyamoto, M., Ohno, Y. & Kihara, A. Comparative profiling and comprehensive quantification of stratum corneum ceramides in humans and mice by LC/MS/MS. *J Lipid Res* 61, 884 (2020).
- Berdyshev, E. *et al.* Dupilumab significantly improves skin barrier function in patients with moderate-to-severe atopic dermatitis. *Allergy* 77, 3388–3397 (2022).
- Lee, S. J., Kim, S. E., Shin, K. O., Park, K. & Lee, S. E. Dupilumab Therapy Improves Stratum Corneum Hydration and Skin Dysbiosis in Patients With Atopic Dermatitis. *Allergy Asthma Immunol Res* 13, 762 (2021).
- Sano, S. Psoriasis as a barrier disease. *Dermatologica Sinica* 33, 64–69 (2015).
- Yoshida, T., Beck, L. A. & De Benedetto, A. Skin barrier defects in atopic dermatitis: From old idea to new opportunity. *Allergy International* 71, 3–13 (2022).
- Bouwstra, J. A., Helder, R. W. J. & El Ghalbzouri, A. Human skin equivalents: Impaired barrier function in relation to the lipid and protein properties of the stratum corneum. *Adv Drug Deliv Rev* 175, 113802 (2021).
- Paton, C. M. & Ntambi, J. M. Biochemical and physiological function of stearyl-CoA desaturase. *AJP: Endocrinology and Metabolism* 297, E28–E37 (2009).
- Muller, P. Y., Milton, M., Lloyd, P., Sims, J. & Brennan, F. R. The minimum anticipated biological effect level (MABEL) for selection of first human dose in clinical trials with monoclonal antibodies. *Curr Opin Biotechnol* 20, 722–729 (2009).
- No, D. J., Amin, M., Bhutani, T. & Wu, J. J. A systematic review of active comparator controlled clinical trials in

- patients with moderate-to-severe psoriasis. *Journal of Dermatological Treatment* 29, 467–474 (2018).
- 37 Orsini, C. *et al.* Line-field confocal optical coherence tomography: New insights for psoriasis treatment monitoring. *Journal of the European Academy of Dermatology and Venereology* (2023) doi:10.1111/JDV.19568.
- 38 Csuka, E. A. *et al.* Reflectance Confocal Microscopy, Optical Coherence Tomography, and Multiphoton Microscopy in Inflammatory Skin Disease Diagnosis. *Lasers Surg Med* 53, 776–797 (2021).
- 39 He, H. *et al.* Tape-Strip Proteomic Profiling of Atopic Dermatitis on Dupilumab Identifies Minimally Invasive Biomarkers. *Front Immunol* 11, 565656 (2020).
- 40 He, H. *et al.* Tape strips detect distinct immune and barrier profiles in atopic dermatitis and psoriasis. *Journal of Allergy and Clinical Immunology* 147, 199–212 (2021).
- 41 Bakker, E. *et al.* Biomarker Qualification at the European Medicines Agency: A Review of Biomarker Qualification Procedures From 2008 to 2020. *Clin Pharmacol Ther* 112, 69 (2022).
- 42 Landeck, L., Kneip, C., Reischl, J. & Asadullah, K. Biomarkers and personalized medicine: current status and further perspectives with special focus on dermatology. *Exp Dermatol* 25, 333–339 (2016).
- 43 van Zuuren, E. J., Fedorowicz, Z., Christensen, R., Lavrijsen, A. & Arents, B. W. M. Emollients and moisturisers for eczema. *Cochrane Database Syst Rev* 2017, (2017).
- 44 Jackson, J. M., Alexis, A., Zirwas, M. & Taylor, S. Unmet needs for patients with seborrheic dermatitis. *J Am Acad Dermatol* 0, (2023).
- 45 Renert-Yuval, Y. & Guttman-Yassky, E. New treatments for atopic dermatitis targeting beyond IL-4/IL-13 cytokines. *Annals of Allergy, Asthma & Immunology* 124, 28–35 (2020).
- 46 Czarnowicki, T., He, H., Krueger, J. G. & Guttman-Yassky, E. Atopic dermatitis endotypes and implications for targeted therapeutics. *Journal of Allergy and Clinical Immunology* 143, 1–11 (2019).
- 47 Pammi, M., Aghaeepour, N. & Neu, J. Multiomics, artificial intelligence, and precision medicine in perinatology. *Pediatric Research* 2022 93:2 93, 308–315 (2022).

## CURRICULUM VITAE

Jannik Rousel was born on the 21<sup>st</sup> of October 1994 in Voorburg and grew up in Rijswijk. After graduating from the Lyceum Ypenburg in 2013, he started with his bachelor Bio-Pharmaceutical Sciences at Leiden University. During the last year of his bachelor, he performed an internship at the Division of Drug Delivery Technology, now the division of BioTherapeutics, of the Leiden Academic Centre for Drug Research in the skin research group of Prof. Dr. Joke A. Bouwstra. He would return here the following year for a more extensive internship as part of his master's degree in Bio-Pharmaceutical Sciences during which he investigated the skin barrier function of *in vivo* human skin models. Afterwards, Jannik performed an internship at Coriolis Pharma, Munich, on the functionality of polysorbates in therapeutic protein formulations under the supervision of Prof. Dr. Wim Jiskoot and Dr. Andrea Hawe. After completing his master's degree with honours, Jannik started his PhD as a clinical scientist at the Centre for Human Drug Research and Leiden Academic Centre for Drug Research under the supervision of Prof. Dr. Robert Rissmann and Prof. Dr. Joke A. Bouwstra focussing on systems dermatology with a special interest on the skin barrier function in inflammatory diseases. During his work in early-stage clinical trials at the Centre for Human Drug Research, Jannik was trained as a clinical pharmacologist.



## LIST OF PUBLICATIONS

### 2024

**Rousel J.**, Mergen C., Bergmans, M.E., Bruininx, L.J., de Kam, M.L., *et al.* Guselkumab treatment alleviates barrier dysfunction and normalizes the altered stratum corneum ceramide profile in lesional psoriasis. *Submitted.*

**Rousel J.**, Mergen C., Bergmans, M.E., Bruininx, L.J., de Kam, M.L., *et al.*, Lesional psoriasis is associated with alterations in the stratum corneum ceramide profile and concomitant decreases in barrier function. *Submitted.*

**Rousel J.**, Bergmans, M. E., Bruijninx, L.J., Lin, S., Niemeyer-van der Kolk, T., *et al.* A multimodal approach establishes mild psoriasis patients as suitable clinical trial participants with similar treatment responses compared to moderate-to-severe psoriasis patients in a blueprint for early-phase drug development. *Submitted.*

**Rousel J.**, Mergen, C., Schoones, J.W., Niemeyer-van der Kolk, T., van Doorn, M., *et al.* (2023). Similar alterations of the stratum corneum ceramide profile in atopic dermatitis, psoriasis and ichthyosis: results from a systematic review and meta-analysis., *The Journal of Investigative Dermatology* (2024), doi: <https://doi.org/10.1016/j.jid.2024.02.010>

### 2023

**Rousel J.**, Bergmans, M. E., van der Meulen, L. W. J., Pagan, L., de Bruin, D. T., *et al.* (2023). Guselkumab induction therapy demonstrates long-lasting efficacy in patients with mild psoriasis, results from a randomized, placebo-controlled exploratory clinical trial. *Journal of the American Academy of Dermatology*, 0(0), doi: <https://doi.org/10.1016/j.jaad.2023.09.071>

**Rousel J.**, Saghari, M., Pagan, L., Nádában, A., Gambrah, T., Theelen, B., *et al.* (2023). Treatment with the Topical Antimicrobial Peptide Omiganan in Mild-to-Moderate Facial Seborrheic Dermatitis versus Ketoconazole

and Placebo: Results of a Randomized Controlled Proof-of-Concept Trial. *International Journal of Molecular Sciences*, 24(18), 14315, doi: <https://doi.org/10.3390/IJMS241814315/>

**Rousel J.**, Nádában, A., Saghari, M., Pagan, L., Zhuparris, A., Theelen, B., *et al.* (2023). Lesional skin of seborrheic dermatitis patients is characterized by skin barrier dysfunction and correlating alterations in the stratum corneum ceramide composition. *Experimental Dermatology*, 00, 1–12, doi: <https://doi.org/10.1111/EXD.14952>

Nádában, A., **Rousel J.**, El Yachoui, D., Gooris, G. S., Beddoes, C. M., Dalglish, *et al.* (2023). Effect of sphingosine and phytosphingosine ceramide ratio on lipid arrangement and barrier function in skin lipid models. *Journal of Lipid Research*, 64(8), 100400, doi: <https://doi.org/10.1016/j.jlr.2023.100400>

Helder, R. W. J., **Rousel J.**, Boiten, W. A., Gooris, G. S., Nadaban, A., El Ghalbzouri, A., & Bouwstra, J. A. (2023). The effect of PPAR isoform (de)activation on the lipid composition in full-thickness skin models. *Experimental Dermatology*, 32(4), 469–478, doi: <https://doi.org/10.1111/EXD.14733>

### 2021

Helder, R. W. J., **Rousel J.**, Boiten, W. A., Gooris, G. S., Nadaban, A., El Ghalbzouri, A., & Bouwstra, J. A. (2021). Improved organotypic skin model with reduced quantity of monounsaturated ceramides by inhibiting stearyl-CoA desaturase-1. *Biochimica et Biophysica Acta (BBA) - Molecular and Cell Biology of Lipids*, 1866(4), 158885, doi: <https://doi.org/10.1016/j.bbali.2021.158885>

### 2020

Grabarek, A. D., Bozic, U., **Rousel J.**, Menzen, T., Kranz, W., Wuchner, K., *et al.* (2020). What Makes Polysorbate Functional? Impact of Polysorbate 80 Grade and Quality on IgG Stability During Mechanical Stress. *Journal of Pharmaceutical Sciences*, 109(1), 871–880, doi: <https://doi.org/10.1016/J.XPHS.2019.10.015>

**Organization of the stratum corneum lipids:** the lipids in the stratum corneum form layers stacked on top of each other. When we talk about how wide each layer is and how close the lipids in such a layer are positioned next to each other, we talk about their organization. If these layers are narrower and the lipids are further apart, the skin barrier decreases.

**Pathophysiology:** the process behind the development of the disease.

**Pharmacodynamics:** what the drug does to the body, for example, that they inhibit processes that make the disease disappear.

**Placebo:** fake drug that has no active substance.

**Randomized controlled trials:** Studies in which participants are divided between a group given the study drug and a group given a placebo. Often neither the investigator nor the participant knows which drug is given to the participant.

**SCD-1:** abbreviation for the protein stearoyl-CoA desaturase-1 that makes unsaturated fatty acids by inserting a double bond into the molecule of a fatty acid that has no double bonds.

**Seborrheic Dermatitis:** a skin condition where patients develop red and scaly patches in areas where the skin is oily, such as the nasolabial folds, eyebrows and forehead.

**Significant:** the word significant is used to show that it is highly unlikely that a difference, increase or decrease was caused by chance rather than, for example, the effect of disease or treatment.

**Staphylococcus:** a bacterium frequently found on the skin. The species *Staphylococcus aureus* is considered a possible pathogen in atopic dermatitis.

**Stratum corneum:** the outer layer of skin, also called the horny layer, which greatly contributes to the barrier function.

**Systems dermatology:** looking at disease as a whole from all possible aspects.

**Trans-epidermal water loss:** the constant flow of water that evaporates through the skin outward.

